IGM82-000-386
CNRC 26497

VOLUME 5/NO. 1/JANUARY 1984

POLYMER COMPOSITES

CONTENTS

1 Introductory Remarks/G. L. Bata

2 Editor's Note/L. A. Utracki, Guest Editor

3 R. SIMHA, R. K. JAIN, and S. C. JAIN/Bulk Modulus and Thermal Expansivity of Melt Polymer Composites: Statistical versus Macro-Mechanics

11 B. D. FAVIS, L. P. BLANCHARD, J. LEONARD, and R. E. PRUD'HOMME/The Formation of Coupling Agent Monolayers on the Surface of Mica

18 J. D. MILLER, K.-P. HOH, and H. ISHIDA/Studies of the Simulation of Silane Coupling Agent Structures on Particulate Fillers; The pH Effect

29 A. T. MUTEL and M. R. KAMAL/The Effect of Glass Fibers on the Rheological Behavior of Polypropylene Melts Between Rotating Parallel Plates

36 B. FISA and L. A. UTRACKI/Rheology of Mica-Reinforced Polyethylene Melts

44 L. A. UTRACKI and J. LARA/Extensional Flow of Mica-Filled Polyethylene

52 C. L. SWANSON, G. F. FANTA, and E. B. BAGLEY/Particle Flow and Sintering Processes in Extrusion

60 L. A. GOETTLER/Mechanical Property Enhancement in Short-Fiber Composites Through the Control of Fiber Orientation During Fabrication

72 D. McCAMMOND and P. A. NORTH/Deformation Design for Short-Fiber-Reinforced Thermoplastic

81 V. G. ZBORIL and D. A. HARBOURNE/Paper-Like Filled Polyethylene Films

88 S. NEWMAN and D. G. FESKO/Recent Developments in Sheet Molding Compound Technology

97 General Discussion

PUBLISHED BY THE SOCIETY OF PLASTICS ENGINEERS, INC.

POLYMER COMPOSITES

Published by the Society of Plastics Engineers

EDITOR—ROGER S. PORTER
c/o Polymer Science and Engineering
University of Massachusetts
Amherst, Mass. 01003

GUEST EDITOR—L. A. UTRACKI
c/o National Research Council Canada
Industrial Materials Research Institute
750 Bel-Air
Montreal, Quebec, Canada H4C 2K3

ASSOCIATE EDITOR—RICHARD E. BALL
c/o Western New England College
Springfield, Mass. 01119

ADVISORY BOARD

LAWRENCE J. BROUTMAN
Illinois Institute of Technology

LAWRENCE CESSNA
Hercules Inc.

ANTHONY T. DI BENEDETTO
University of Connecticut

NIKOLAY ENIKOLOPYAN
USSR Academy of Sciences

JOSEPH N. EPEL
Budd Company

DAVID H. KAELBLE
Arroyo Computer Center

JOHN L. KARDOS
Washington University

FREDERICK J. MCGARRY
Massachusetts Institute of Technology

L. NICOLAIS
University of Naples

R. BYRON PIPES
University of Delaware

N. S. SCHNEIDER
Army Materials and Mechanics Research Center

PUBLICATIONS COMMITTEE

D.W. RILEY, Chairman
Extrusion Engineers

R. P. BRADDICKS, JR.
Plastics Consultant

R. D. FORGER
Society of Plastics Engineers

J. C. HAARSMA
SIC Electric Co.

J. L. HULL
Hull Corporation

D. JESIOLOWSKI
Owens Illinois

M. A. MENDELSOHN
Westinghouse Electric Corp.

R. S. PORTER
University of Massachusetts

A. A. SCHOENGOOD
Society of Plastics Engineers

R. F. STAATS-WESTOVER
Bell Laboratories

G. R. THOM
Regal Plastics Company

A. M. VARNER
Moldflow USA, Inc.

A. E. WHITNEY, JR.
Goodyear Chemical

Copyright by the Society of Plastics Engineers, Inc., 1984. Reproduction in whole or in part without written permission is strictly prohibited.

Polymer Composites (ISSN 0272-8397) is published at 215 Canal St., Manchester, NH 03108. Address changes, undeliverable copies and orders for subscriptions should be sent to Circulation Manager, Society of Plastics Engineers, 14 Fairfield Dr., Brookfield Center, CT 06805. Published quarterly. Second class postage paid at Brookfield Center, Conn. and additional entry offices. Accepted at special postal rate provided in P.M. Sec. 132.122.

Neither the Society of Plastics Engineers, Inc., nor **Polymer Composites** is responsible for the views expressed by individual contributors either in articles published in **Polymer Composites** or in technical papers presented at meetings of the Society.

Subscription rates for 1984: SPE members, 1 year—$24. Nonmembers, 1 year—$50. Delivery outside North America, add $8 per year.

SOCIETY OF PLASTICS ENGINEERS, INC.
Business and Executive Offices, 14 Fairfield Dr., Brookfield Center, Conn. 06805

ROBERT D. FORGER
Publisher

GERALD D. NEAL
Circulation Manager

JANICE E. ALEXANDER
Production Manager

JOSEPH M. CASTAGNO
Copy Editor

OFFICERS OF THE SOCIETY

ROBERT J. SCHAFFHAUSER
President

WILLIAM C. KUHLKE
President-elect

RICHARD G. JOHNSON
First Vice President

GREG R. THOM
Second Vice President

JACQUES DE CRAENE
Vice President for International Affairs

JOHN R. KRETZSCHMAR
Secretary

BRUCE A. PETERSEN
Treasurer

ROBERT D. FORGER
Executive Director

POLYMER COMPOSITES is indexed by:—Chemical Abstracts—Engineering Index, Inc.

INTRODUCTORY REMARKS

The week before last, I had the opportunity to meet with Mr. Alex Williams, the Under Secretary—Research and Technology Policy Division of the Department of Industry of the United Kingdom while he was making a "tour d'horizon" of the Canadian scientific and technological community. In response to my questions, he indicated that the three major challenges he sees facing North American and particularly Canadian industry, are the need for a major effort in undersea technology on the continental shelf, an expanded effort to capitalize on the opportunities presented by composites and synthetic engineering materials, and an improvement in our ability to accelerate the translation of scientific knowledge to industrial practice. While ocean technology is not our immediate concern today, on the other two subjects Mr. Williams' vision coincides with ours.

Most practical engineering materials, with a notable exception of glasses, are composites. Metals and alloys, rubbers and semi-crystalline polymers are essentially low-aspect-ratio composites of crystals and amorphous regions, while wood and fibrous materials in general are composites with high aspect-ratio reinforcements. Our major problem however is the destruction of the aspect-ratio of the reinforcement in manmade composites by the mixing, blending, compounding, and forming processes we use. Avoiding this destruction results in excessive processing costs, which is only permissible in some specialty applications. The difference between what nature does and what we are trying to do is that nature grows its composites *in situ*, whereas we are trying to put the components together ourselves. Maybe our future efforts should be directed toward growing the reinforcement *in situ* in the finished article with appropriate grown-in-place orientations in the direction of the loading forces to which the article will be exposed.

Today, however, we are trying to face lesser problems looking at tasks which we are just learning to handle. Our central theme is the blending, compounding, and forming of essentially low-aspect-ratio-reinforcement composites. The blending and forming processes of composites represent the weakest links in the technological chain of reinforced plastics. Drs. Simha, Favis, and Ishida are going to look at interactions between the dispersed phase and the matrix, Drs. Utracki, Mutel, and Bagley will discuss the rheological behavior of these materials, Dr. Goettler will talk about compounding, whereas Drs. McCammond, Zboril, and Newman will treat the performance and application aspects of the finished product.

I am pleased to see the representatives of the speakers. They are evenly spread between industry, government, and academia. Half the speakers are from the US and the others from Canada. The fact that three of the eleven speakers are from the Industrial Materials Research Institute is of particular satisfaction to us considering our young age as an institution.

It is unfortunate that we had to limit participation due to space limitations. This is happily compensated for by the fact that we are reaching a wider audience through the pages of POLYMER COMPOSITES.

We are intent on continuing these series of mini-symposia in the field of polymer blends, plastic composites and mathematical modeling of processes. We also hope that future meetings can be accommodated in the lecture room of our new building. Our auditorium there will accommodate 200 people, which will permit us to have a broader interaction with our colleagues.

George L. Bata
Director
Industrial Materials Research Institute
National Research Council Canada

EDITOR'S NOTE

The sixth in the series, mini-symposium "Composites-'82" was held in Montreal on November 30, 1982. The following eleven papers presented during the meeting provide a cross section of the topics in the area of polymer composites, particularly those containing short fibers and flakes.

The annual series of the mini-symposia on mathematical modeling of plastics processing (February), polymer blends (April), and polymer composites (November), organized and sponsored by the Industrial Materials Research Institute of the National Research Council of Canada (IMRI-NRCC) in Montreal, is becoming a standard feature on the local calendar of meetings "to be attended." The popularity of these events is beginning to exceed the original goals as well as the physical means of the Institute, indicating the need for this type of communication.

The uniqueness of these meetings rests neither in the subject nor the level, but rather in the size and the composition of the audience; the meetings are small and the participation diverse enough to guarantee a vivid, uninhibited, and to-the-point interaction. The symposia tend towards the applied side, the discussions towards the exchange of ideas and experiences. It is our belief that one of the key requirements for proper development of science and technology is the free, continuous flow of information, a dialogue on concepts, and explorations between the members of the technical and commercial communities. The uniqueness of the symposia stems from providing an opportunity and a climate for such exchange.

The need for the dialogue exists not only in Canada. Benefitting from the generous help of Professor Roger S. Porter, who opened to us the pages of his prestigious journals, POLYMER ENGINEERING SCIENCE and POLYMER COMPOSITES, we are able to publish the proceedings, thus extending the reach of these symposia beyond the small group of participants. The flavor of the meetings can be gleaned from the transcript of discussions, printed after each article, as well as from that of the general discussion held at the end of each meeting. In all cases the editing has been kept at a minimum in order to preserve the tone of these encounters.

In two cases the "free-for-all" final discussions seem to be particularly valuable to the general readership. The symposium "Polymer Blends-1981" ended in discussion on terminology (See *Polym. Eng. Sci.*, 22, 137 (1982)). The current issue of proceedings of the "Composites-'82" is being closed with the discussion on the current problems of R/D and flow of information between the industrial, academic and governmental research groups. It seems that the present day economic difficulties result in lessening the industrial R/D effort and at the same time an increase of restriction on the exchange of technical information. Both these tendencies are clearly visible on the North American continent. If continued they will reinforce each other and lead to a loss of competitiveness of our industries.

L. A. Utracki
Guest Editor

Bulk Modulus and Thermal Expansivity of Melt Polymer Composites: Statistical versus Macro-Mechanics

ROBERT SIMHA, R. K. JAIN*, *and* S. C. JAIN**

Department of Macromolecular Science
Case Western Reserve University
Cleveland, Ohio 44106

Physical properties of composites as a function of filler content have been described in the past through models requiring the solution of macroscopic equations of motion for an elastic continuum or, on a more empirical level, by the assumption of various compositional averaging schemes. We discuss a model drawn from our molecular mixture theory. This allows us to avoid the formal problems attending concentrated suspensions and introduces molecular filler-medium interaction parameters. Comparisons with experimental material and empirical equations involving bulk modulus and thermal expansivity will be given. The theory opens the possibility of determining interfacial strengths from appropriate mechanical and thermal measurements and of predicting one set from another set of data.

INTRODUCTION

We have recently generalized a statistical thermodynamic theory of the liquid state (1) to multicomponent systems (2). The basis of this theory is a quasi-lattice model with volume- and temperature-dependent vacancies or free volume, derived by a minimization of the configurational free energy. The results can be presented in scaled form and the mixture treated formally as a homogeneous system with composition-dependent scaling parameters. In terms of this theory, binary mixtures of low- and high-molecular-weight components have been discussed (2,3). The quantities appropriate to the present concern are related to the equation of state (*PVT*) and are to be investigated as a function of composition, the interactions between the components, temperature, and pressure. From the *PVT* we directly obtain the bulk modulus (reciprocal isothermal compressibility) and the thermal expansivity.

We now wish to model a composite as a blend of a "soft" matrix and more or less rigid filler particles. These particles will be considered as giant chains in this treatment, differing from the matrix molecules by size and interaction parameters, including the flexibility parameter, to be defined below.

Conventional treatments are based on continuum mechanics, starting out with the analogy to the classical analyses of the viscosity of suspensions. These yield expressions for the shear modulus as a function of filler content and particle geometry. The difficulties characteristic of long-range interactions in concentrated media arise here also. Moreover, special ad hoc assumptions regarding the specifics of the interfacial layer must be introduced. Quantities such as the thermal expansivity are frequently discussed in terms of additivity assumptions.

In the second section, we recapitulate appropriate relationships. The third section illustrates the results, using a polyethylene melt as an example. Finally, the predicted thermal expansivities are compared qualitatively with a compilation of data on a variety of polymer-filler combinations. Moreover, we consider various empirical expressions in the literature, which relate the thermal expansion to the bulk moduli of the components.

RECAPITULATION OF GENERAL THEORY

The scaled equation of state for the homogeneous melt is (1):

$$\tilde{P}\tilde{V}/\tilde{T} = (1-\eta)^{-1} + (2y/\tilde{T})\,(y\tilde{V})^{-2}\,[1.011(y\tilde{V})^{-2} - 1.2045] \tag{1}$$

with $\eta = 2^{-1/6}\, y(y\tilde{V})^{-1/3}$, and the tildes indicating reduced quantities.

The vacancy fraction $1 - y$ is determined as a function of $\tilde{V}$ and $\tilde{T}$ by the minimization of the Helmholtz free energy, which yields the following relation for an s-mer:

$$(s/3c)\,[(s-1)/s + y^{-1}\ln(1-y)] = (1-\eta)^{-1}(\eta - 1/3) + (y/6\tilde{T})(y\tilde{V})^{-2}\,[2.409 - 3.033(y\tilde{V})^{-2}] \tag{2}$$

Here $3c$ is the number of effectively external degrees of freedom of the chain. In an s-mer, the flexibility parameter $3c/s$ will be of the order of unity for a flexible chain and $s \sim \infty$, where the important soft modes of motion are internal bond rotations. For a rigid chain, on the other hand, only external modes are active and the flexibility

* On leave from Rajdhani College, University of Delhi, New Delhi-110015, India.
** Present address: Hindu College, University of Delhi, Delhi-110007, India.

ratio will tend to zero. The coupled *Eqs. 1* and *2* represent the equation of state. The scaling parameters are defined by the intersegmental repulsions and attractions as follows:

$$V^* = N_A v^*/M_o \; ; \; P^* = E^*/(sv^*) \; ; \; T^* = E^*/S^* \quad (3)$$

Here V^* is a specific and v^* the intersegmental repulsive volume, with N_A and M_o Avogadro's number and the segmental molecular weight, respectively. The characteristic energy E^* for the s-mer equals $[s(z-2)+2]\epsilon^*$ and is determined by the intersegmental maximum attraction energy ϵ^* and the coordination number z of the lattice. Finally, the scaling entropy of the chain S^* equals kc, with k the Boltzmann constant. These definitions yield the relation

$$(P^*V^*/T^*)M_o = (c/s)R \quad (4)$$

For the high polymers of interest here, we have used the assignment $3c/s = 1$(1-4). *Equation 4* then relates M_o to the repeat unit of the n-mer by virtue of the relation $sM_o = nM_r$, once the scaling parameters have been obtained by the super-position of experimental and scaled theoretical isotherms and isobars. This, of course, presumes the quantitative adequacy of the theory, reflected in the essential constancy of the scaling parameters. Ample evidence for this in the high- as well as low-molecular-weight area has been presented in the literature (1, 2).

The numerical evaluation of the coupled *Eqs. 1* and *2* presents no difficulties. A convenient and highly accurate approximation in the limit $\tilde{P} \sim 0$, applicable to atmospheric pressure and facilitating matters further, has been shown to be (1):

$$\ln\tilde{V} = A + B \times \tilde{T}^{3/2} \quad (5)$$

A and B are functions of c and s. For $s \sim \infty$ and $3c/s = 1$, $A = -0.1034$, $B = 23.835$ in the range $0.95 \leq \tilde{V} \leq 1.40$. For other values of c, the solution of the exact equations, (*Eqs. 1* and *2*) can be fitted to *Eq. 5* with somewhat different numerical values. We note that an analogous relation representing the unreduced experimental volume-temperature data serves as an immediate diagnostic test of the theory and, if successful, yields V^* and T^*. Finally, a similar, even if more restrictive relation at elevated pressures, has been shown recently (3) to be valid. A and B then become functions of pressure.

Turning to multicomponent systems, we have shown that all the equations presented retain their validity, provided the pertinent parameters are redefined as proper averages. For a binary mixture of molar composition $x_1 = (1 - x_2)$, we have (2):

$$\langle s\rangle = x_1s_1 + x_2s_2 \; ; \; \langle c\rangle = x_1c_1 + x_2c_2 \; ; \; \langle M_o\rangle = (s_1x_1M_{o1} + s_2x_2M_{o2})/\langle s\rangle \quad (6)$$

The mole fractions appearing in *Eq. 6* are related to the weight fraction w_2 through the relation

$$x_1 = (1 - w_2)/[1 - w_2(1 - M_1/M_2)]$$

An important consequence of *Eq. 6*, combined with the generalization of *Eq. 4*, is this: When $\langle V^*\rangle$ and $\langle T^*\rangle$ have been extracted from dilatometric studies at atmospheric pressure, $\langle P^*\rangle$ can be computed and high-pressure information predicted without further recourse to experiment. It remains to specify the connection between the scaling parameters of homogeneous liquid and mixture. The result is:

$$\langle\epsilon^*\rangle\langle v^*\rangle^m = X_1^2\,\epsilon^*_{11}\,v^{*m}_{11} + 2X_1X_2\,\epsilon^*_{12}\,v^{*m}_{12} + X_2^2\,\epsilon^*_{22} \; ; \; m = 2, 4 \quad (7)$$

with the site fractions X_i defined by the mole fractions, viz.:

$$X_i = q_ix_i/\Sigma q_jx_j; \; q_i = [s_i(z-2)+2]/z \; ; \; i = 1, 2$$

Equation 7 and the generalized definitions of $\langle V^*\rangle$, $\langle T^*\rangle$, and $\langle P^*\rangle$ analogous to *Eq. 3* then provide the latter. Now the ϵ^*_{ii} and v^*_{ii} in *Eq. 7* are known from the appropriate studies of the pure components. This presumes, of course, that the presence of the second component does not alter the intrinsic interactions in the first component. This assumption does not necessarily affect the success of the theory for the blend, as we have recently shown in the instance of a particular polymer blend (3). However, we will have to make this assumption explicitly here, since the second component, that is, the additive, can not be studied separately, as in the case of a liquid mixture. Therefore, numerical assignments to the ratios $\epsilon^*_{22}/\epsilon^*_{11}$ and v^*_{22}/v^*_{11} are to be made. As to the cross interactions, the important quantity is the "adhesion" ratio $\epsilon^*_{12}/\epsilon^*_{11}$, where the index 2 refers to the filler. The variation of the excess properties of the composite with this ratio is the primary concern of this paper. The magnitude of the corresponding quantity v^*_{12}/v^*_{11} is less important and will be kept constant in what follows, as will the relative self interaction quantities. Division of the two *Eqs. 7* then yields $\langle v^*\rangle$; squaring of the first and division by the second provides $\langle\epsilon^*\rangle$.

From *Eqs. 1* and *2* there follows the expression for the reduced bulk modulus $\tilde{K} = [-(1/\tilde{V})(\partial\tilde{V}/\partial\tilde{P})_{\tilde{T}}]^{-1}$ with the result:

$$\begin{aligned}\tilde{K}\tilde{V}/\tilde{T} = {} & \tilde{P}\tilde{V}/\tilde{T} + (\eta/3)(1-\eta)^{-2} - (4y/\tilde{T})(y\tilde{V})^{-2} \\ & \times [1.2045 - 2.022(y\tilde{V})^{-2}] - \{(2\eta/3)(1-\eta)^{-2} \\ & + (2y/\tilde{T})(y\tilde{V})^{-2}[1.2045 - 3.033(y\tilde{V})^{-2}]\}^2 \\ & \times \{(4\eta/3)(1-\eta)^{-2} \\ & + (y/2\tilde{T})(y\tilde{V})^{-2}[9.099(y\tilde{V})^{-2} - 2.409] \\ & + (s/c)[y^{-1}\ln(1-y) + (1-y)^{-1}]\}^{-1} \quad (8)\end{aligned}$$

The thermal expansivity is from *Eq. 5* at atmospheric pressure:

$$\alpha = (1/V)(\partial V/\partial T)_P = (3/2)B(T/T^{*3})^{1/2} \quad (9)$$

Finally, the composition dependence of $\langle V^*\rangle$, $\langle T^*\rangle$, $\langle P^*\rangle$ is determined by the series of equations listed above. A least square fit of $\ln\tilde{V}$ computed with the aid of *Eqs. 1* and *2* for $\tilde{P} = 0$, provides the value of B for the mixture, as defined by *Eq. 5*.

RESULTS

Consider a melt of linear polyethylene. The equation of state of this polymer has been determined and the result successfully analyzed in terms of the theory de-

scribed (4). We obtain the following numerical values:

$$V^* = 1.1417 \text{ cm}^3/\text{g} \; ; \; T^* = 9772K \; ; \; P^* = 7478 \text{ bar} \; ; \; \epsilon^*_{11}/k = 325.7 \; K \; ; \; n_1/s_1 = 2.26$$

The last equation defines the segment as 2.26 methylene units. Assuming $n_1 = 2 \times 10^4$, the molecular weight M_1 of the matrix is 280, 540; the segmental molecular weight M_o in *Eq. 4* = 31.7 g/mole, and $s_1 = 8850$. A simple calculation yields for the ratio of chainlengths:

$$s_2/s_1 = (\rho_1 v^*_{11}/\rho_2 v^*_{22}) \, M_2/M_1$$

with ρ_2, ρ_1 the densities of the two components at a given temperature and pressure. From *Eqs. 6* and *3* one has:

$$<c> = c_1 \, [1 - x_2(1 - c_2/c_1)] \; ; <s> = s_1 \, [1 + x_2(s_2/s_1 - 1)]$$

$$<T^*> = T^*_1 \, (<\epsilon^*>/\epsilon^*_{11}) \times [1 + x_2(s_2/s_1 - 1)]/[1 + x_2(c_2/c_1 - 1)]$$

$$<V^*> = <v^*> <s> N_A/<M> \; ; <M> = x_1 M_1 \, [1 + (x_2/x_1) \, M_2/M_1]$$

$$<P^*> = P^*_1 \, (<\epsilon^*>/\epsilon^*_{11})/(<v^*>/v^*_{11}) \qquad (10)$$

To obtain $<\epsilon^*>$ and thence $<T^*>$ from *Eq. 7*, make the follow ing assignments:

$$s_2/s_1 = 4 \times 10^{12} \; ; \; \rho_2 = 2.7 \text{ g/cm}^3 \; ; \; \rho_1 = 0.77 \text{ g/cm}^3$$

$$v^*_{12}/v^*_{11} = 1.1 \; ; \; \epsilon^*_{22}/\epsilon^*_{11} = 5.$$

We simplify the procedure by assuming additivity for v^*_{12}, viz.:

$$v^*_{12} = \{[(v^*_{11})^{1/3} + (v^*_{22})^{1/3}]/2\}^3$$

Thus $<v^*>$, and $<\epsilon^*>$, and consequently $<T^*>$ and $<P^*>$ now follow from *Eq. 7* for a set of values of the adhesion ratio $\epsilon^*_{12}/\epsilon^*_{11}$. This, in addition to the composition, expressed as weight fraction w_2 or volume fraction v_2, is the significant parameter. The details of the magnitudes characterizing the filler are not too important, excepting the flexibility ratio. We begin with rigid particles, for which strictly according to the definition of c, $3c_2$ should equal 6. Moreover $3c_1 = s_1$ has been the usual assignment for flexible chains (1-4).

We begin with the bulk modulus, *Eq. 8*, expressed in *Fig. 1* as the reduced excess quantity

$$[K(w_2) - K(0)]/[K(0)v_2]$$

in analogy to the conventional description of viscosity measurements for suspensions. The maximal weight fraction here is about 30 percent, which should suffice to illustrate the desired results. Considering first atmospheric pressure, we observe a noteworthy result; that is, for an adhesion ratio close to unity, the limiting value, i.e., the intercept, is close to 2.5. This is the classical value for the intrinsic viscosity, derived by Einstein for a suspension of spheres. Beyond that, note the initial slope, marked by the dotted straight line for an adhesion ratio of 1.2. The result is 10.4, in the range of values obtained by several authors since the early work of Guth and Simha (5). The analogy between elasticity and hydrodynamic theory should strictly apply to the shear

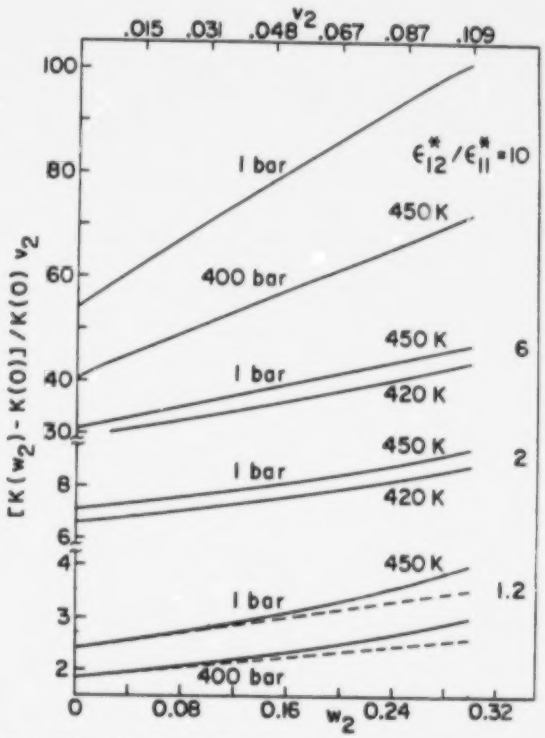

Fig. 1. Reduced bulk modulus ratio of composite as a function of weight (w_2) or volume (v_2) fraction of filler, different values of adhesion ratio, and of temperature and pressure for polyethylene melt. Dashed lines denote limiting slopes.

modulus, in the absence of special stress effects. The implication here would be Poisson ratios, which are weak functions of composition. However see Comment 3., p. 9. With increasing attractive filler-matrix interaction, the "intrinsic" bulk modulus ratio rises sharply, as seen in *Figs. 1-3*. In *Fig. 4*, it is shown that the infinite dilution increment is practically linear in the adhesion ratio $\epsilon^*_{12}/\epsilon^*_{11}$. This increment then is a measure of what in the context of viscosity is referred to as the effective hydrodynamic volume resulting from immobilization of solvent. Finally, with increasing temperature, the compressibility of the matrix increases sufficiently so as to increase the excess quantity exhibited, whereas an increment in pressure has the opposite effect.

A basic assumption underlying the generalization of *Eqs. 1* and *2* to multicomponent systems is the random placing of all molecular segments on the sites of the quasi-lattice. This may not represent an adequate assumption for sufficiently large values of the characteristic adhesion ratio. If so, it would tend to enlarge the value seen in the top range of compositions.

The foregoing results indicate a numerical similarity to those derived by the methods of hydrodynamics. A question which arises in the *molecular* hydrodynamics of suspensions is the effect of particle size, since the basic assumption is the treatment of the suspending medium as a continuum. It is of interest then to explore this element in the frame of our approach. Hence we reduce the ratio s_2/s_1 from the value of 4×10^{12} employed in

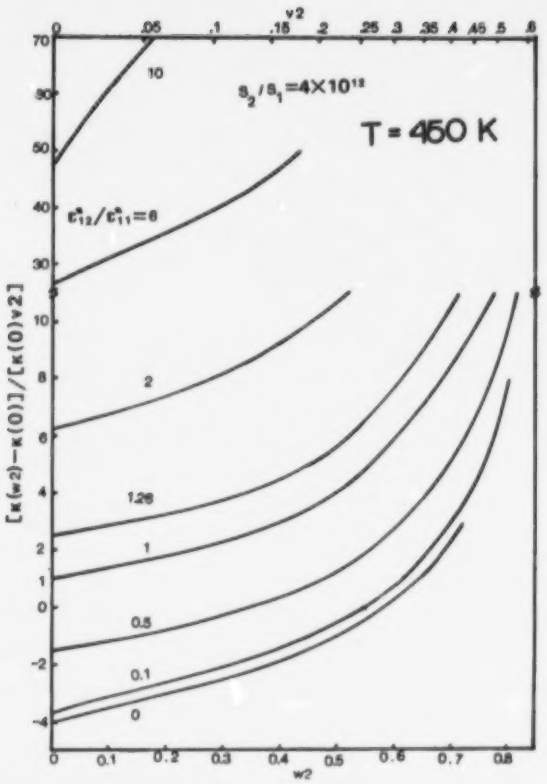

Fig. 2. Reduced bulk modulus ratio of composite as a function of weight (w_2) or volume (v_2) fraction, and different values of adhesion ratio at atmospheric pressure.

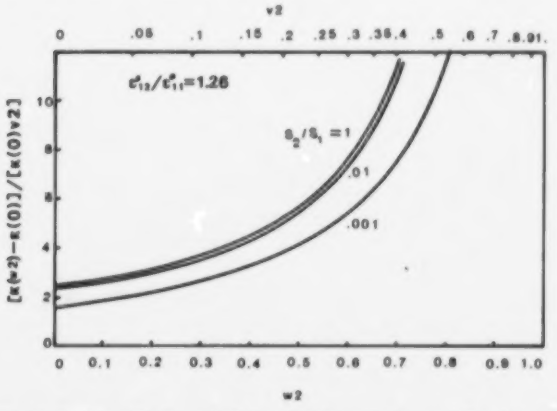

Fig. 3. Reduced bulk modulus ratio of composite as a function of weight (w_2) or volume (v_2) fraction for varying relative values of filler particle size (s_2/s_1) at atmospheric pressure.

Figs. 1 and 2 to 10^{-3} in *Fig. 3*. Only below 10^{-2} is a significant reduction in the original values noticeable. This independence on filler size extends to higher values of the adhesion ratio, not exhibited here. The effect is caused by a significantly constant free volume fraction $1 - y$ for a given volume fraction of particles, until sufficiently short chainlengths are reached.

The excess quantities discussed are the result of differences in essentially two quantities, namely the cross versus self interactions, and the differences in the

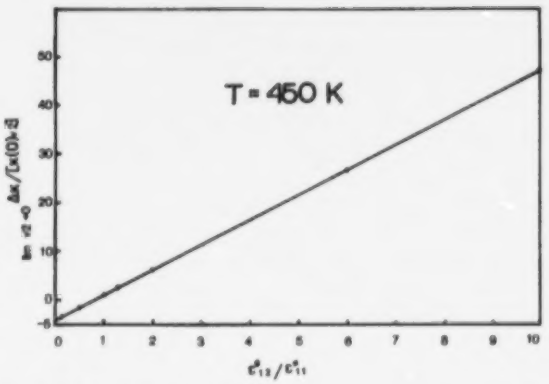

Fig. 4. Intrinsic bulk modulus increment as a function of adhesion ratio for polyethylene matrix.

flexibility parameter c's. Both affect the scaling temperatures and their averages. The former element has been displayed and we turn next to the latter in an attempt to model "soft" filler particles by considering the influence of the ratio

$$f = (c_2/s_2)/(c_1/s_1)$$

with $f = 0$ representing the condition for a rigid particle, as depicted in *Figs. 1-4*. *Figure 5* displays the results for 450K, 1 bar, and $\epsilon^*_{12}/\epsilon^*_{11} = 1.2$. The expected decrease is seen, with the limiting value of unity for the intercept at $f = 1$, and a practically linear dependence of this intercept on f. However, the effect is comparatively weak over the whole range of f-values. It appears that the curves are simply shifted with variations of f.

The second quantity to be computed over the same range of compositions and adhesion ratios is the thermal expansivity. We restrict ourselves to atmospheric pressure for purposes of illustration. Moreover, only rigid particles, $f \to 0$, will be considered. From *Eq. 9* we have for the normalized thermal expansivity:

$$\alpha(w_2)/\alpha(0) = [B(<s>)/23.8](T^*_1/<T^*>)^{3/2} \quad (11)$$

The numeric represents the value of B for the matrix, i.e., $s_1 \to \infty$, $3c_1/s_1 = 1$ (1), and $B(<s>)$ for the blend is

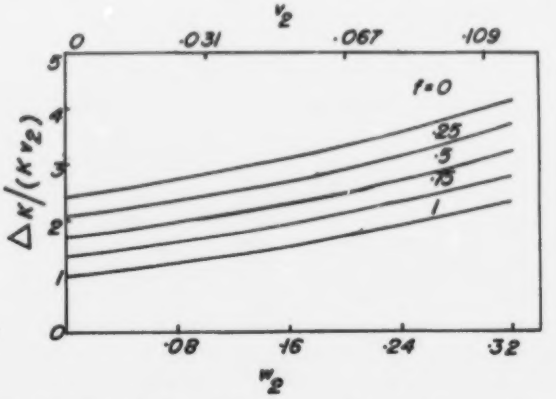

Fig. 5. Reduced bulk modulus ratio as a function of composition for different values of the flexibility parameter, see text, and polyethylene matrix; $f = 1$ rigid filler.

derived by means of a least square fit of *Eq. 5* to the theoretical equation of state, *Eqs. 1* and *2*.

The results are exhibited in *Figs. 6-8*. For $\epsilon^*_{12}/\epsilon^*_{11} \geq 4$, the decrease in the thermal expansion is pronounced indeed and, of course, far from any additivity rule. This is also clearly seen from the expression for the ratio of scaling temperatures, (see *Eq. 10*, combined with *Eq. 7*). When $\epsilon^*_{12}/\epsilon^*_{11} = 2$, the decrease is linear over a considerable range of w_2, which should, however, depend somewhat on the values selected for the other fixed parameters. The variation of the thermal expansion with filler content is essentially determined by the ratio $(T_1^*/<T^*>)^{3/2}$ in *Eq. 11*. When the adhesion ratio is reduced to a value of about 0.5 and less, maxima appear in α, as they do in the free volume fraction $1 - y$, illustrating the influence of the flexibility ratio c_2/c_1. *Figure 7* again indicates the absence of a size effect.

COMPARISON WITH EXPERIMENTAL DATA

Holliday and Robinson (6) have presented a compilation of thermal expansivities that encompasses a large number of matrix-filler pairs. The observations appear as dashed lines in *Fig. 6*, which define four bands. The theoretical curves below volume fractions of about 10 percent reproduce the general pattern, including the appearance of a maximum. We can only estimate adhesion ratios corresponding to the various bands. The

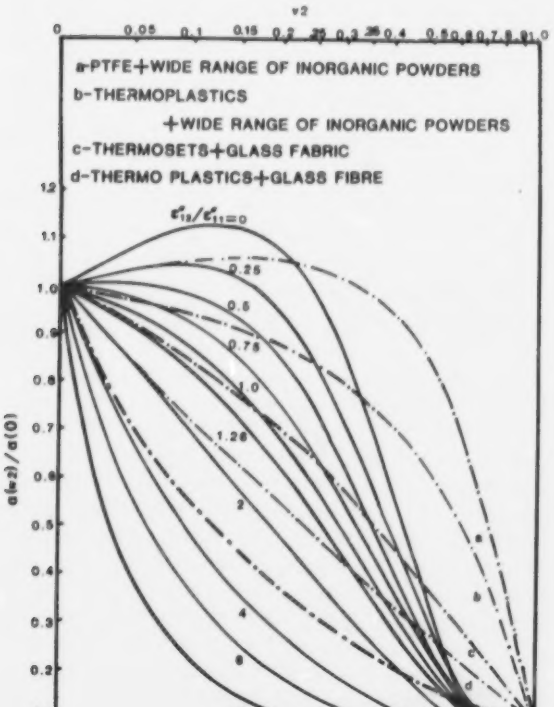

Fig. 6. Normalized thermal expansivity as a function of composition and different values of adhesion ratio for $s_2/s_1 = 4 \times 10^{12}$ at atmospheric pressure and T = 450K. The normalized block-diagrammatic form of data is shown by broken lines.

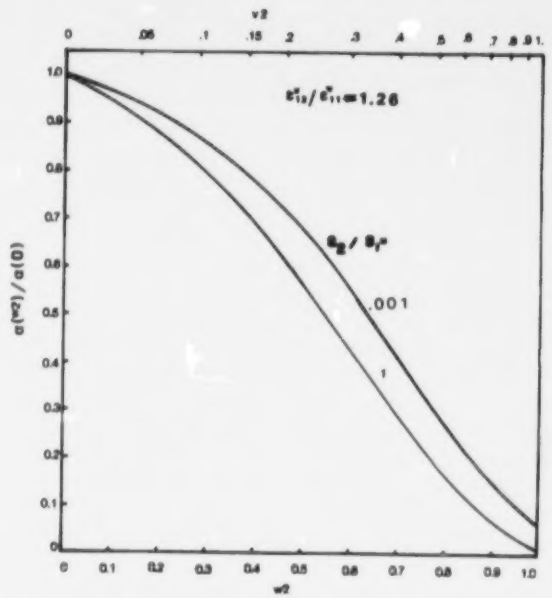

Fig. 7. Normalized thermal expansivity as a function of composition and different values of filler particle size at atmospheric pressure and T = 450K.

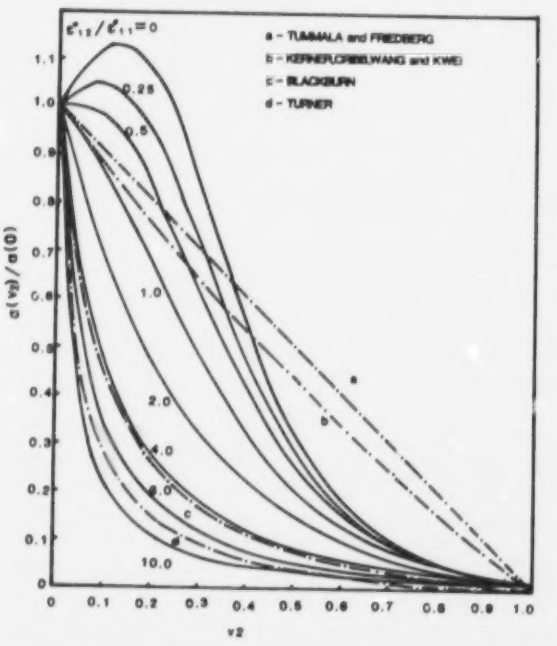

Fig. 8. Normalized thermal expansivity as a function of volume fraction of filler and different values of adhesion ratio for $s_2/s_1 = 4 \times 10^{12}$ at atmospheric pressure and T = 450K. Broken lines indicate various empirical relations.

steepest descent is ascribed to thermoplastic–glass-fiber combinations. At a volume fraction of 0.10, the characteristic expansivity ratio is 0.8. This corresponds in *Fig. 6* to an adhesion ratio of about 3 to 4. The slowest monotonic descent occurs for thermoplastics plus a "wide range of inorganic powders." These systems require adhesion ratios of less than unity. An intermediate

area between the two extremes cited refers to thermosets with glass fabric. The decrease for $v_2 \simeq 0.1$ suggests $\epsilon^*_{12} \simeq \epsilon^*_{11}$. Finally, there appears an extreme curve with a maximum at $v_2 \simeq 0.15$, which is to be characteristic of poly(tetrafluoroethylene) with a "wide range of inorganic powders," and $\epsilon^*_{12} < 0.5\ \epsilon^*_{11}$.

Strictly speaking, these comparisons should only be undertaken for matrices in the state of an equilibrium melt, and it is questionable which of the above systems satisfy this condition. In any case, a quantitative comparison of theory and experiment requires accurate measurements with well-defined systems of the type carried out in the past with polymer melts and glasses, and a properly modified theory in the instance of the latter.

We note in all instances a steeper decline in the expansivity ratio at elevated concentrations than is observed. We have no satisfactory explanation to offer. A clustering of filler particles with a concomitant "expulsion" of matrix layers, and gain in freedom of thermal motion could be involved, at least in the strong adhesion case.

COMPARISON WITH OTHER EQUATIONS

Several relations, connecting the thermal expansivity of a composite with the corresponding quantities for the components, have been proposed. They have been derived by macroscopic considerations, and are to be compared with our theoretical predictions. We begin with a recapitulation of these equations. Most of these refer to spherical particles. Kerner's equation (7) reads:

$$\alpha(v_2)/\alpha_1 = (1 - v_2)\ [1 - v_2\ \theta\ (1 - \alpha_2/\alpha_1)] + v_2\alpha_2/\alpha_1$$

with $\theta = (1/K_1 - 1/K_2)/[(1 - v_2)/K_2 + v_2/K_1 + 3/(4G_2)]$, where G_2 is the shear modulus and the subscript 2 refers to the filler. For glass spheres, we take a Poisson ratio ν_2 of 0.23 (8) and employ the relation

$$2G_2\ (1 + \nu_2) = 3K_2\ (1 - 2\nu_2)$$

The equation of Blackburn (9) is:

$$\alpha(v_2)/\alpha(0) = \frac{(3/2)\ (1 - \nu_2)\ (1 - v_2)\ (1 - \alpha_2/\alpha_1)}{(1 + \nu_2)/2 + (1 - v_2)\ (1 - 2\nu_2) + (1 - 2\nu_1)v_2(Y_2/Y_1)} + \alpha_2/\alpha_1$$

Young's moduli Y_2 and Y_1 are related to the other elastic constants by the equation

$$Y = 3K\ (1 - 2\nu)$$

The equation of Wang and Kwei (10) is:

$$\alpha(v_2)/\alpha(0) = 1 - v_2\ \theta\ (1 - \alpha_2/\alpha_1)$$

where $\theta = 3(Y_2/Y_1)\ (1 - \nu_1)/\{(Y_2/Y_1)\ [2v_2(1 - 2\nu_1) + (1 + \nu_1)] + 2(1 - v_2)\ (1 - 2\nu_2)\}$

The equation of Tummala and Friedberg (11) reads:

$$\alpha(v_2)/\alpha(0) = 1 - v_2\ \theta\ (1 - \alpha_2/\alpha_1)$$

where

$$\theta = [(1 + \nu_1)/2Y_1]\ [(1 + \nu_1)/2Y_1 + (1 - 2\nu_2)/Y_2]$$

The general equation of Turner (12) is:

$$\alpha(v_2)/\alpha(0) = [(1 - v_2)\ K_1 + v_2K_2(\alpha_2/\alpha_1)]/[(1 - v_2)K_1 + v_2K_2]$$

and Cribb (13)

$$\alpha(v_2)/\alpha(0) = \theta_1 + \theta_2(\alpha_2/\alpha_1)$$

with

$$\theta_1 = K_1(K_c - K_2)/[K_c(K_1 - K_2)]\ ;\ \theta_2 = K_2(K_1 - K_c)/[K_c(K_1 - K_2)]$$

The last expression requires an explicit knowledge of the composite's bulk modulus $K_c = K(v_2)$. The last two equations are not restricted to spherical inclusions. However to evaluate Cribb's result, we introduce Kerner's (7) relation for spheres, viz.:

$$K(v_2)/K_1 = \frac{(1 - v_2)/(3K_1 + 4G_1) + v_2(K_2/K_1)/(3K_2 + 4G_1)}{(1 - v_2)/(3K_1 + 4G_1) + v_2/(3K_2 + 4G_1)}$$

into the expressions for θ_1 and θ_2.

We now wish to apply the above series of expressions by evaluating all quantities except the Poisson ratios by means of our theroy. Thus we take $\nu_2 = 0.23$, as has already been stated, and ν_1 for polyethylene melt as 0.38 (8). *Equation 8* yields the bulk modulus $K_1 = 9074.3$ bar at 450K. For the filler, T^* is practically infinite, due to the extreme value of s_2 and the small c_2. Hence y in *Eqs. 1* and *2* tends to unity, and the equation of state reduces to the expression from cell theory. The result is

$$\tilde{K}_2 = 4.044/\tilde{V}^5 - \tilde{T}\eta/[3\tilde{V}(1 - \eta)^2] - \tilde{P}$$

This general equation reduces under the present conditions to the first term, since $\tilde{T} \to 0$, and $P = 1$ bar. Moreover $\tilde{V}_0 = 0.91616$. Finally $P^* = 340.0$ k bar and $K_2 = \tilde{K}P^* = 213.0$ k bar. Thence $G_2 = 140.3$ k bar, $Y_2 = 345.0$ k bar. For polyethylene we have $Y_1 = 6533.5$ bar and $G_1 = 2367.2$ bar. Substitution of these numbers into the relations listed yields the expansivity in *Fig. 8*, to be compared with the full lines derived from our theory. We note first that no maxima are reproduced by any of the macroscopic equations. Secondly, Blackburn's and Turner s equations closely correspond to our results for elevated adhesion ratios between 4 and 10. The other relations exhibit a considerably slower decay with increasing volume fraction of filler and are practically or nearly linear. Kerner's expression for the bulk modulus of the composite is practically linear up to $w_2 = 0.4$ and thereafter exhibits only a moderate rise up to $w_2 = 0.8$ or $v_2 \simeq 0.53$, and thus distinctly differs from the results in *Figs. 1* and *2*. This accounts for the comparatively slow decrease of $\alpha(v_2)$.

CONCLUSIONS

We have applied a molecular theory, formulated originally for liquid mixtures, to composites. In this theory,

explicit expressions for bulk modulus and thermal expansivity are obtained, and thus it is possible to predict one set of data from another. The relationships between these quantities and their temperature and pressure coefficients are explicitly defined by the equation of state of the composite. Treatments based on macroscopic theory and employing empiricism of various degrees discuss only mixing rules. One expects from a statistical theory the introduction of molecular characteristics and interaction parameters. We have considered here two parameters, namely the adhesion ratio between filler and matrix and the flexibility ratio of the filler. The emphasis in application has been on the former. In this manner the way is opened for the analysis of appropriate experimentation which relates surface treatment to macroscopic properties. Here we have offered only semiquantitative comparisons in two ways. One with a literature compilation of numerous data on thermal expansivity, the other with a series of equations involving bulk and shear moduli and thermal expansion coefficients. Significant differences from our results for various adhesion strengths appear, particularly at elevated filler contents. We note that the theory assumed the matrix to be an equilibrium melt. A generalization to glassy matrices requires certain modifications of the present theory. These have primarily to do with the partial freeze-in of the free volume fraction $1 - y$ in *Eq. 1* (1).

Considering the general issue of molecular versus macroscopic continuum theory, it is of interest that we reproduce the analog to the Einstein value for spherical suspensions, provided the excess of filler-matrix over matrix-matrix segmental attraction is small. Concerning the influence of size, no effect is observable, until one component exceeds the other in chain length by several orders of magnitude, when a reduction in the excess properties sets in. The important elements here are the free volume fraction and the flexibility parameter.

Macro-mechanics seeks to introduce explicitly the shape of the filler particle and so to also discuss orientation effects with elongated particles. This element is missing in our theory, and is characteristic of the lattice model in the form employed here. Specifically, the expression for the configurational entropy, arising from the mixing of lattice vacancies and chain segments, would require a modification, since this expression implies a spherical symmetry. Geometric asymmetry in a lattice model is naturally related to particle rigidity. We have accounted for dynamic rigidity by letting the flexibility parameter c_2/s_2 tend to zero, and covering subsequently a range of values in *Fig.* 5. However, conformational rigidity requires the revision of the entropy term referred to above and this remains to be introduced.

ACKNOWLEDGMENT

This work was supported by the National Science Foundation through Grant DMR 80-12232, Polymers Program.

REFERENCES

1. R. Simha and T. Somcynsky, *Macromolecules*, **2**, 342 (1969); R. Simha, *ibid.*, **10**, 1025 (1977).
2. R. K. Jain and R. Simha, *Macromolecules*, **13**, 1501 (1980).
3. R. K. Jain, R. Simha, and P. Zoller, *J. Polym. Sci., Polym. Phys. Ed.*, **20**, 1399 (1982).
4. O. Olabisis and R. Simha, *Macromolecules*, **8**, 211 (1975).
5. E. Guth and R. Simha, *Kolloid-Z.*, **74**, 266 (1936).
6. L. Holliday and J. Robinson, *J. Mater. Sci.*, **8**, 301 (1973).
7. E. H. Kerner, *Proc. Phys. Soc.*, **B69**, 808 (1956).
8. J. M. G. Cowie, "Polymers: Chemistry and Physics of Modern Materials," p. 226, International Textbook Company Ltd. (1973).
9. G. Arthur and J. A. Coulson, *J. Nuclear Mater.*, **13**, 242 (1964).
10. T. T. Wang and T. K. Kwei, *J. Polym. Sci.*, A2 **7**, 889 (1969).
11. R. R. Tummala and A. L. Friedberg, *J. Appl. Phys.*, **41**, 5104 (1970).
12. P. S. Turner, *J. Res. Nat. Bur. Stand.*, **37**, 239 (1946).
13. J. L. Cribb, *Nature*, **220**, 576 (1968).

ADDITIONAL COMMENTS

1. A question has been raised as to the particular definition for the characteristic segment of 2.26 methylene units. It will be recalled (see, for example, *Ref. 1*) that this follows from the particular assignment made to the flexibility ratio c/s for flexible high polymers. Thus, this should not be confused with the Kuhn segment, defined by conformational considerations of the single chain. Note also the qualitative consistency of the actual numerical value when viewed as part of a series of polymers with increasing structural complexity of the repeat unit, as discussed in the second of *Refs. 1*. That is, as the ratio n/s increases, the segment becomes increasingly smaller.
2. A further query concerns the selection of certain numerical assignments employed in our illustrations. First, regarding filler size effects, as shown in *Figs.* 3 and 7, the results are independent of the ratio s_2/s_1, over a wide range. While these observations are displayed only for one particular magnitude of the adhesion ratio, we indicate in the text the generality of these findings. The lattice model requires a decomposition of the filler into segments of equal size as those of the polymer. Thus the value of s_2 cited corresponds to a molecular weight M_2 of $s_2 \times 31.7$. With a density ρ_2 of 2.7 g/cm^3 as a representative value for a glass particle, this would correspond to the radius of a sphere of about 5 to 6 $\times 10^{-3}$ cm. Note also the comparatively low value of ρ_1 for our polyethylene melt. Finally, the additivity assumption for v^*_{12} is simply an arithmetic averaging of the radii of two spheres of different sizes. No particular significance needs to be attached to this, nor will it influence the results significantly.
3. Concerning the relation between Einstein's hydrodynamic result and the present considerations, we hereby revise some earlier conclusions. Macromechanics indicates that under the conditions yielding a factor of 2.5 for the shear modulus, the factor for the bulk modulus is 1. Figure 2. indicates that this is indeed the value derived for an adhesion ratio of unity. The important feature is the recovery of a result derived by continuum theory, from a molecular theory.

4. The pronounced differences in the normalized thermal expansivities compiled in *Ref. 6* are due, we believe, to the large differences in the matrix-filler interactions; see, for example, the teflon composite versus the thermoplastics combination. The authors do not offer any specific correlations. Such would require detailed considerations of well-defined systems which make adequate quantitiative comparisons between experiment and theory possible.

DISCUSSION

S. Newman. I am trying to understand this solvation layer you talk about. I presume it would be either an adsorbed layer or a layer of immobilized matrix, due to some sort of interaction with the surface. If I understood you correctly, this would essentially increase the effective volume fraction of the particle.

R. Simha. In the viscosity analogy we would say that the hydrodynamic volume is increased.

S. Newman. It would be more complicated, but would it be possible to treat this layer as a third phase whose properties differ from those of the continuous matrix and of the filler particle?

R. Simha. This was one reason to show at the end of my talk Frans Maurer's calculations, Dissertation, University, Duisburg, 1983, which explicitly treat the macromechanics of the three-phase system. In our frame I believe that a large value of the adhesion ratio should simulate the situation you enquire about. It will be of interest in this connection to extend the type of comparison shown in *Fig. 8* to moduli and three-phase situations. Moreover, the theory could be generalized, as you suggest. The formal expressions are already available in *Ref. 2*.

L. A. Goettler. It has been shown in rheological measurements that when the particle size is small enough, particle-particle interactive effects arise. I guess this would enter into your ϵ^*_{22}. Could this substantially affect your results and how could it be taken into account?

R. Simha. In the present model computations we have kept ϵ^*_{22} constant at $5 \times \epsilon^*_{11}$ and concentrated on displaying the results of varying the particle-matrix interaction. As far as actual particle agglomeration is concerned, size effects are insignificant, as is illustrated in *Fig. 3* and *7*. An enhancement of the interparticle attraction should act in the same direction as a decrease in adhesion ratio.

L. A. Utracki. You calculate what seems to be for the first time the analogue of an intrinsic viscosity below a value of 2.5. From the collection of compressibility and thermal expansivity data one can conclude that the potential system to prove this would be fluorinated hydrocarbons, e.g., Teflon, with inorganic particles. I think it should be an easy experiment to see whether the intrinsic viscosity is reduced below the Einstein value.

R. Simha. Yes. It should be recalled that a (partial) slip condition and a non-rigid particle yield values below 2.5. The usual hydrodynamic calculations assume the boundary condition of no relative velocity between particle and medium. A reduction of the adhesion ratio below unity should be equivalent to a change in this boundary condition. Recall however that our theroy deals with K. G remains to be computed.

S. Newman. You mean a system with non-wettable particles, as a case of non-adhesion? Take, for example, a fluorinated silicon oil and hard spherical glass particles.

L. A. Goettler. I believe Paul Han has shown somewhere that the viscosity was reduced when fillers were treated for non-wetting.

L. A. Utracki. I am not aware that intrinsic viscosities substantially below 2.5 have been reported. I know of values around 2, but this is almost within the error limits of 2.5. On another point: if I understand correctly, the theory is rigorous, i.e., no assumptions or fudge factors are introduced.

R. Simha. Beyond what already appears in the one-component theory and its generalization to mixtures.

L. A. Utracki. The same treatment should give you a description of multiphase immiscible polymer blends, such as polyethylene-polystyrene.

R. Simha. Yes, it has already been applied to miscible systems of low (*Ref. 2*) and high (*Ref. 3*) molecular weight.

The Formation of Coupling Agent Monolayers on the Surface of Mica

B. D. FAVIS

Conseil National de Recherche de Canada
Institut de Génie des Matériaux
750, rue Bel-Air
Montréal, Québec, Canada, H4C 2K3

and

L. P. BLANCHARD, J. LEONARD, *and* R. E. PRUD'HOMME

Groupe de Recherches sur les Macromolécules
Département de chimie et de génie chimique
Faculté des sciences et de génie
Université Laval
Québec, Québec, Canada, G1K 7P4

The interaction of very dilute solutions of a cationic vinylbenzyl silane (CVBS), a methacrylate functional silane (γ-MPS), and an isopropyl-tri-(dioctylpyrophosphato) titanate (IDT) with a mica surface has been studied by carbon analysis. For all three coupling agents the dependence of adsorption with time of treatment follows a step-like curve, where each step corresponds to a monolayer coverage on the mica. Under the operating conditions used it was noted that a particular monolayer is always completed before the next is started. The adsorption of γ-MPS was found to be very sensitive to the time allowed for hydrolysis of the silane, while the adsorption of CVBS was relatively independent of the hydrolysis time when it is varied from 0 to 5400 s. The results indicate that γ-MPS and CVBS near the mica surface form a dense structurally regular multilayer phase with the silane molecules oriented normal to the surface. IDT molecules occupy a surface area on mica which is characteristic of their branched nature.

INTRODUCTION

The use of mica in polymer composites has received considerable attention (1-3). When suitably delaminated and oriented within a polymer matrix, it is capable of imparting a high degree of reinforcement (4, 5). The Young's modulus of mica is twice that of glass fibers; the theoretical capacity of mica for reinforcement is thus more than evident. Mica is also advantageous in that it may be used at high loadings. It is relatively inexpensive and quite abundant.

Coupling agents are known to improve the properties of polymer composites especially in the wet state (6). The most commonly used ones are silanes. It is widely acknowledged that hydrolyzed silanes form covalent bonds with inorganic surfaces (see *Fig. 1*). Their effectiveness in mica-polymer composites has been shown by several authors. Boaira and Chaffey (7) found that a cationic vinylbenzyl silane and a dimethylaminoethyl methacrylate each improved the flexural properties of mica-reinforced polypropylene. Okuno and Woodhams

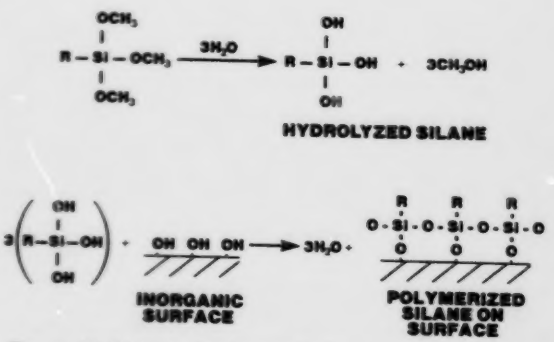

Fig. 1. Hydrolysis of silane followed by reaction with an inorganic surface.

(8) have shown that the addition of a cationic vinylbenzyl silane improved the tensile strength of mica-filled polypropylene, but had little effect on the flexural modulus.

In an earlier publication (9), aspects of the adsorption of a cationic vinylbenzyl silane (CVBS) were reported.

The results showed that its adsorption from aqueous solutions was dependent, in the lower concentration range, on the silane concentration. Adsorption was found to take place over a wide range of pH with the best treatment occurring at the lower pH values and the poorest at the higher pH values. The time dependence of the adsorption process followed a steplike curve where each step was equivalent with respect to the quantity of silane adsorbed. The regularity of the amount adsorbed per step and the calculated surface area occupied per molecule indicated that each step corresponds to a monolayer coverage. The magnitude of the surface area occupied per molecule was in the range expected for molecules oriented normal to the surface. The CVBS interphase on mica was therefore found to be a highly oriented, closely packed multilayer phase with the molecules oriented normal to the surface. The presence of steps, or plateaus, was taken as an indication that a particular monolayer was always completed before the next one was started and that there was a finite time required under the conditions used to initiate the adsorption of a given monolayer. This latter result was found to be analogous to a nucleation process which, once initiated, proceeded rapidly to the completion of the monolayer.

In this paper, additional data are presented for the adsorption of CVBS on mica, as are data for two additional coupling agents: γ-methacryloxypropyltrimethoxy silane (γ-MPS) and isopropyl-tri-(dioctylpyrophosphato) titanate (IDT). γ-MPS is a widely used organofunctional silane, which has been shown to be effective in bonding thermoplastics to particulate mineral fillers as well as to glass fibers (10, 11). Titanates have been shown to be capable of acting as coupling agents in polymer composites (12, 13) and allow high filler loadings in thermoplastics without adversely effecting the melt flow behavior.

The purpose of this paper is to compare three coupling agents with respect to their interaction with a mica surface.

EXPERIMENTAL

Mica

The mica used was of the Phlogopite variety supplied by Marietta Resources International Limited (trade name Suzorite mica). In these experiments, the 60 HK mica type was used, a designation whereby the value 60 corresponds to the average mesh size of the flakes and HK refers to its classification as being highly delaminated. Data for the characterization of this mica are presented elsewhere (9).

Coupling agents

Three coupling agents were examined in this study: a cationic vinylbenzyl silane, a methacrylate functional silane, and a titanate.

The cationic vinylbenzyl silane (CVBS) was obtained from Dow Corning Inc. (trade name Z-6032). Its molecular formula, shown in *Fig. 2*, is designated as N-β-(N-vinylbenzylamino) ethyl-γ-aminopropyltrimethoxy silane monohydrogen chloride (14).

The methacrylate functional silane (γ-MPS) was obtained from the Union Carbide Corp. (trade name A-174). Its molecular formula, shown in *Fig. 2*, is designated as γ-methacryloxypropyltrimethoxy silane (15).

The titanate used (IDT) was obtained from Kenrich Petrochemicals Inc. (trade name KR-38S) and its molecular formula, likewise given in *Fig. 2*, is designated as isopropyl-tri-(dioctylpyrophosphato) titanate (16).

Method of application and analysis

All of the mica treatment experiments involved a solution method: the silane experiments were carried out in aqueous solutions where the pH was adjusted with acetic acid, and the titanate treatments, in toluene. The silanes were hydrolyzed to silanols prior to the addition of mica and, unless otherwise indicated, the hydrolysis time was limited to 900 s at the end of which the mica was immediately added to the solution. This point was considered as time zero for the adsorption of coupling agent onto the mica. The suspension was continuously agitated and samples were removed at appropriate intervals to be filtered and washed on a Büchner filter. All of the experiments were carried out at a temperature of 23 ± 1°C.

The washed mica samples were later analyzed on a carbon hydrogen nitrogen analyzer (CHN), and the increase in carbon content due to the coupling agent treatment was determined. This enabled the calculation of the weight of silane adsorbed per unit weight of mica. Further details on the method are given elsewhere (9).

RESULTS

CVBS

Figure 3 shows results for the time dependence of CVBS adsorption onto mica at a pH of 3.2. This figure shows that the silane is adsorbed in discrete steps and that the process starts immediately from time zero. The correlation of the number of steps, or plateaus, with the quantity of CVBS adsorbed is given in *Fig. 4*. A similar step-like behavior and correlation of plateaus were observed at a pH of 5.5 and are reported elsewhere (9). A comparison of the adsorption kinetics of CVBS onto mica from more highly concentrated silane solutions at pH 5.5 is shown in *Fig. 5*. It is seen that the effect of concentration becomes important only after 500 s of treatment.

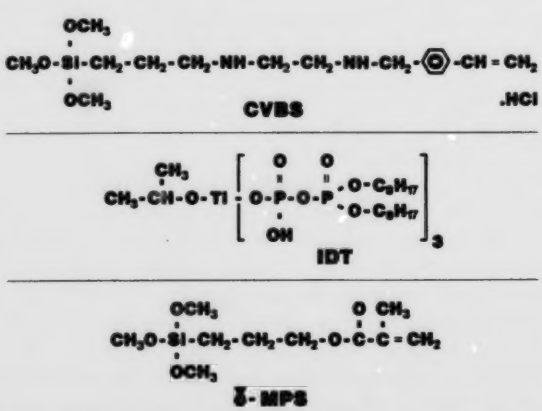

Fig. 2. Molecular formulas of the coupling agents studied.

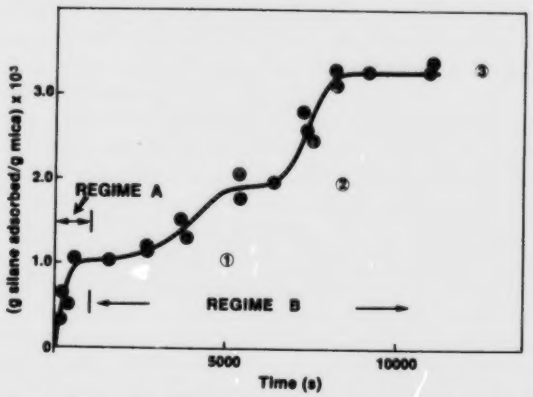

Fig. 3. Effect of treatment time on the adsorption of CVBS onto mica at pH 3.2. Initial concentration of silane in the treating solution was 0.025 g silane per 100 mL water. The weight ratio of silane to mica was 0.5 g silane per 100 g mica.

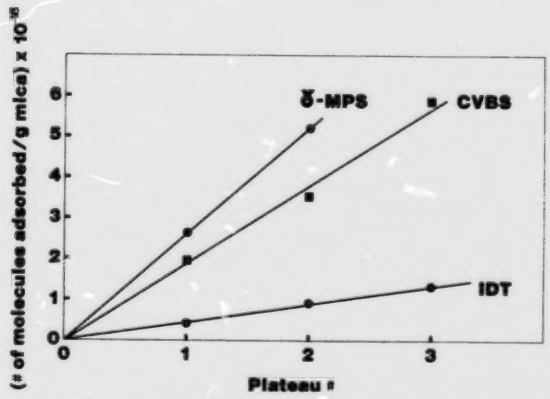

Fig. 4. Correlation of successive plateaus with the number of molecules adsorbed for CVBS, γ-MPS, and IDT.

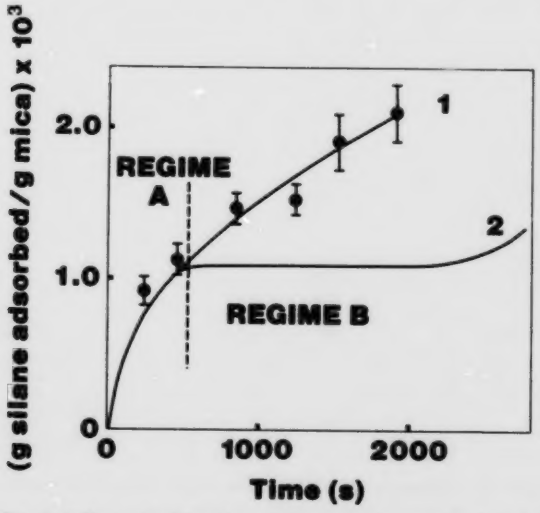

Fig. 5. Effect of adsorption: 1: from a concentrated CVBS solution (curve 1). Initial concentration of silane in the treating solution was 0.5 g silane per 100 mL water; the weight ratio of silane to mica was 10 g silane per 100 g mica. 2: Adsorption from a dilute solution is shown for comparison (curve 2). Initial concentration of silane in the treating solution is 0.025 g silane per 100 mL water; the weight ratio of silane to mica was 0.5 g silane per 100 g mica.

The time allowed for the hydrolysis of CVBS was varied to determine the importance of this parameter. Subsequently, the adsorption of this silane onto the mica, after 2700 s of treatment, was determined. The results obtained are shown in *Table 1* for hydrolysis times varying from 35 to 5400 s. It is observed that the amount of CVBS adsorbed remained relatively independent of the hydrolysis time.

IDT

Figure 6 shows the results of the effect of time of treatment on the adsorption of IDT onto mica. These data indicate similarities in the uptake of this molecule with that of CVBS. Titanate adsorption starts immediately from time zero and follows a step-like dependence with time. It is interesting to note that the two curves shown in *Fig. 6* (each run under the same operating conditions) superimpose up to the region of the first plateau. After this point, curve 2 reaches the second plateau more rapidly than curve 1. The ultimate value obtained for the second plateau by curve 2 is essentially the same as that obtained by curve 1. The correlation of the number of plateaus with the quantity of titanate adsorbed is given in *Fig. 4*.

γ-MPS

The time of treatment dependence of γ-MPS onto mica was studied at pH values of 3.5 and 5.5, the range most widely used for silane treatment. At the onset of the experiments, it was recognized that the adsorption process for γ-MPS is very sensitive to the time allowed for the hydrolysis process. The results given is *Figs. 7* and *8* therefore cover various hydrolysis times at pH values of 3.5 and 5.5.

The curves in *Fig. 7*, obtained with 300 and 1500 s hydrolysis times, tend towards plateau values and the latter shows the now well-recognized multiple-step behavior. Both curves in *Fig. 7b*, obtained under identical operating conditions, superimpose up to the first plateau region. However, as for the titanate, the approach to the second plateau takes place much later for curve 1. Both curves ultimately attain the same plateau value expressed in terms of the amount of silane adsorbed.

The adsorption of γ-MPS does not begin immediately at time zero. Rather, it is preceded by an induction period which is essentially the same for both 300 and 1500 s hydrolysis times (shown in *Fig. 7a* and *b*) if one includes the time for hydrolysis along with the time of treatment. When hydrolysis times were increased to 5400 s, no adsorption of γ-MPS onto the mica was observed to take place.

The behavior of γ-MPS at a pH of 3.5 is similar to that observed at a pH of 5.5 (see *Fig. 8*). the correlation

Table 1. Effect of Hydrolysis Time on the Adsorption of CVBS onto Mica

Hydrolysis time (s)	(g silane/g mica) $\times 10^3$
35	1.1
2700	1.1
5400	0.9

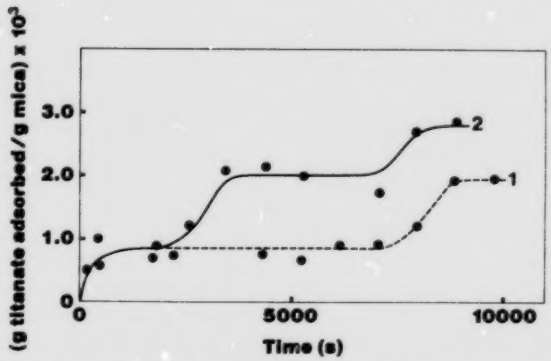

Fig. 6. Effect of treatment time on the adsorption of IDT onto mica from a toluene solution. Initial concentration of titanate in the treating solution was 0.025 g titanate per 100 mL toluene; the weight ratio of titanate to mica was 0.5 titanate per 100 g mica.

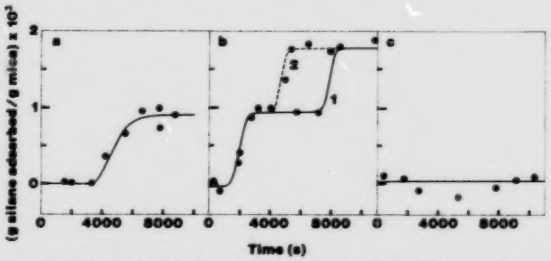

Fig. 7. Effect of hydrolysis time prior to the addition of mica on the adsorption kinetics of γ-MPS onto mica at pH 5.5 (a. 300 s hydrolysis, b. 1500 s hydrolysis, c. 5400 s hydrolysis). Initial concentration of silane in the treating solution was 0.025 g silane per 100 mL water; the weight ratio of silane to mica was 0.5 g silane/100 g mica.

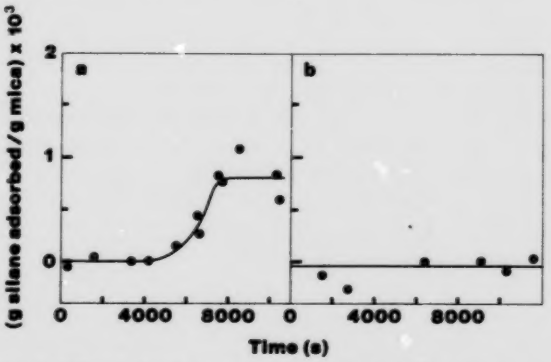

Fig. 8. Effect of hydrolysis time prior to the addition of mica on the adsorption kinetics of γ-MPS onto mica at pH 3.5 (a. 300 s hydrolysis, b. 5400 s hydrolysis). Initial concentration of silane in the treating solution was 0.025 g silane per 100 mL water; the weight ratio of silane to mica was 0.5 g silane per 100 g mica.

linking the number of plateaus to the quantity of γ-MPS adsorbed is given in *Fig. 4*.

DISCUSSION

Figure 6 illustrates that titanate molecules have a strong affinity for the mica surface since adsorption from a toluene solution starts immediately at time zero. *Figure 4* shows that there is an equal quantity of IDT adsorbed at each plateau, which indicates that, as with CVBS, each plateau corresponds to a monolayer coverage of titanate on mica.

The fact that no induction period occurs in the time zero region in *Fig. 6* differentiates this region from the rest of the curve. The immediate adsorption of IDT onto the mica near time zero is an indication of the rapid and highly favored interactions of this coupling agent with the mica surface. The rest of the curve in *Fig. 6* represents the multilayer adsorption region of titanate, where interactions are much less favored. The time required to initiate adsorption is therefore longer. The results illustrate the well-known principle that coupling-agent molecules have a stronger affinity for a silicate surface than for themselves. Similar behavior in this respect was noted for CVBS and the two corresponding regions are indicated as Regime A and Regime B in *Fig. 3*.

The average area occupied by a titanate molecule on mica was calculated from the number of molecules adsorbed per plateau and the surface area of the mica flake, 0.612 m^2g^{-1} (9). The calculated area, 1.43 nm^2 per molecule, is large compared to that for CVBS (*Table 2*) and is a reflection of the highly branched nature of IDT.

Figure 6 illustrates that the rise to the second or third plateau for IDT may occur at different times for experiments run under identical conditions. Such results would not be unexpected if a nucleation-like mechanism was necessary in order to initiate adsorption of a particular layer. Nucleation rates have been known to vary widely for the same system. They may be dramatically affected by the pressure of minute impurities.

Figures 7 and *8* show that the adsorption versus time curve for γ-MPS exhibits a behavior similar in many respects to that of CVBS and of IDT. Plateau behavior is observed with multiple plateaus evident for the 1500 s hydrolysis, pH 5.5 experiment. There is also an equal quantity of γ-MPS adsorbed per step, as shown in *Fig. 4*. It is interesting to note that γ-MPS exhibits an analogous behavior to that of IDT when considering the difference in induction times preceding the rise to the second plateau, as shown in *Fig. 7b*.

The average area occupied by a molecule of γ-MPS was calculated to be 0.24 nm^2 (*Table 2*). Stearic acid and iso-stearic acid on water, which are considered as classical examples of molecules oriented normal to a surface, occupy 0.20 nm^2 and 0.32 nm^2, respectively (17). The small area occupied by γ-MPS therefore indicates that, as for CVBS, the γ-MPS molecules are closely packed and oriented normal to the mica surface. This conclusion is supported by recent evidence from other studies. Ishida and Koenig have suggested that γ-MPS forms a structurally regular multilayer phase on E-glass fiber (18). These data were based on an observation by Fourier transform infrared spectroscopy of a high de-

Table 2. Calculated Surface Areas Occupied on Mica per Coupling Agent Molecule.

Molecule	Surface Area (nm^2)
CVBS	0.32
γ-MPS	0.24
IDT	1.43

gree of cross-linking between the adsorbed silanes. These authors again emphasized the likelihood of molecular organization by showing that a crystalline layer of phenylsilanetriol formed when it was adsorbed onto glass fibers (19). The dense nature of the polysiloxane interphase near the surface of glass fibers has been observed by Dibenidetto and Scola using ion-scattering spectroscopy (20).

It has been proposed that the structural regularity of a silane interphase is dependent on the concentration of silanetriol in solution and on the roughness of the inorganic surface (19). Solutions containing a high concentration of silanetriol can produce aggregates which may cause disorder in the adsorbed interphase. It is interesting to note the results obtained from a more highly concentrated solution of CVBS, as indicated in *Fig. 5;* the characteristic plateau for CVBS observed in dilute solution at approximately 1.1×10^{-3} gram silane/per gram mica is not apparent. Two explanations for this effect are possible: first, the plateau may exist, but the induction times are greatly reduced; or secondly, the second monolayer begins to adsorb before the first layer is completed. These results therefore indicate the possibility that adsorption from more highly concentrated silane solutions may lead to irregularities in the silane interphase.

It may also be noted from *Fig. 5* that the adsorption kinetics for forming the first monolayer (Regime A) did not change significantly whn adsorption was carried out from a more concentrated silane solution. The kinetics of formation of silane multilayers, however (Regime B), was concentration-dependent.

Rough surfaces such as silica can also introduce disorder in the silane phase to the point that multilayer formation is inhibited (21), whereas a smooth surface such as glass fibers adsorbs multilayers of silane. The results presented here are similar to those obtained with glass fiber in that silane multilayers were observed on mica. Mica is considered a classical example of a material that undergoes high basal cleavage forming planar nonporous surfaces.

As was mentioned in the experimental section, it was observed that the adsorption of γ-MPS onto mica was very dependent on the time allotted for hydrolysis of the silanes. *Figure 7* illustrates two effects which were noted. First, an induction period is required before the γ-MPS adsorbs onto mica (*Fig. 7a, b*); secondly, if the γ-MPS is left to hydrolyze for too long, no adsorption will take place at all under the conditions used (*Fig. 7c*). The former effect probably reflects a time dependence for the hydrolysis of the silane, while the latter is likely due to the instability of γ-MPS in aqueous solutions.

Shih and Koenig, by studying the SiO symmetric stretching mode of γ-MPS, have shown that the concentration of triol reached a maximum only after 30 minutes hydrolysis time and then started decreasing with time (22). Daley and Rodriguez (23) observed that γ-MPS, when catalyzed by acid, is completely hydrolyzed after approximately one hour. The latter authors also noted that the hydrolysis of γ-MPS was significantly slowed down in the presence of both acid and glass beads. In the present experiments, *Figs. 7a* and *7b* illustrate that, at a pH of 5.5, adsorption onto mica started after the silane had been hydrolyzed for approximately 3000 s. This value is obtained by adding the hydrolysis times prior to the addition of mica to the induction times reported in *Figs. 7a, b*. The similarities in this overall time period preceding adsorption for these two experiments indicate that the presence of mica does not significantly interfere with the hydrolysis of the silane.

Hydrolyzed organosilanes are known to undergo rapid condensation reactions through their silanol groups leading to the formation of dimers, trimers, and higher oligomers (24). These oligomers have been reported to be unsuitable as coupling agents. Such a phenomenon would explain the lack of adsorption onto mica in *Fig. 7c*. It is interesting to note in *Fig. 7b* that the adsorption of silane onto silane in the formation of multilayers continued long after 5400 s. These results suggest that it is specifically the formation of the first monolayer which is inhibited by long hydrolysis times.

The behavior of γ-MPS in water as shown in *Figs. 7* and *8* may be compared to that of CVBS (see *Table 1*). It can be seen that as the hydrolysis time is varied from 35 to 5400 s, very little difference is noted in the quantity of CVBS adsorbed onto mica (the mica was treated in silane solution for 2700 s). These two effects illustrate that, in contrast to γ-MPS, CVBS hydrolysis rapidly and is stable in water. Similar results for certain aminosilanes have been reported elsewhere and their extraordinary stability in aqueous solution is apparently related to an ability to form ring structures (25-27).

This study opens up certain areas of investigation. It has been suggested that one monolayer of coupling agent is not sufficient to obtain optimum bonding to the polymer (28). The data presented herein make it very conceivable to prepare mica samples treated with 1, 2, or 3 monolayers of coupling agent. A direct examination of the above hypothesis could therefore be tested.

Due to the low solution concentration of the coupling agent and the planar, non-porous nature of mica, the silanes formed a dense, multilayered structure with chains oriented normal to the surface. It would be interesting to test whether or not a dense organized structure of this type is beneficial in bonding to the polymer. If the penetration of the polymer into the silane interphase is important, for example, it is possible that a certain amount of disorder or irregularity may actually be desirable.

CONCLUSION

CVBS and γ-MPS, when adsorbed onto mica from very dilute aqueous solutions, have been found to form highly oriented, dense, multilayer structures. γ-MPS was further noted to be much more sensitive than CVBS to the time allowed for hydrolysis. IDT was demonstrated to have a strong affinity for mica, occupying a surface area which was characteristic of its branched nature. All three coupling agents studied, although of very different chemical compositions, exhibited a similar steplike dependence of adsorption with time of treatment.

ACKNOWLEDGEMENTS

This work was financed by the Industrial Materials Research Institute of the National Research Council of Canada (Contract No. 1SD81-00029).

The authors express appreciation to Mario Leclerc and Richard Voyer for assistance with the experimental work.

REFERENCES

1. M. Xanthos, G. C. Hawley, and J. Antonacci, Proc. 33rd Ann. Tech. Conf., Reinforced Plastics/Composites Div., SPI, Section 2-D (1978).
2. S. Newman and F. J. Meyer, *Polym. Compos.*, **1**, 37 (1980).
3. H. S. Katz and J. V. Milewski, "Handbook of Fillers and Reinforcements of Plastics," Ch. 20, Reinhold, Toronto (1978).
4. R. T. Woodhams, Canadian Patent 893163 (1972).
5. J. Lusis, R. T. Woodhams, and M. Xanthos, *Polym. Eng. Sci.*, **13**, 139 (1973).
6. R. B. Seymour, "Additives for Plastics," Ch. 6, Vol. 1, Academic Press, New York (1978).
7. M. S. Boaira and C. E. Chaffey, *Polym. Eng. Sci.*, **17**, 715 (1977).
8. K. Okuno and R. T. Woodhams, *Polym. Eng. Sci.*, **15**, 308 (1975).
9. B. D. Favis, L. P. Blanchard, J. Léonard, and R. E. Prud'homme, in press (*J. Appl. Poly. Sci.*).
10. S. Sterman and J. G. Marsden, Proc. 21st Annual Tech. Conf., Reinforced Plastics Div., SPI, Section 3-A (1966).
11. M. W. Ranney, S. E. Berger, and J. G. Marsden, Proc. 27th Annual Tech. Conf., Reinforced Plastics/Composites Div., SPI, Section 21-D (1972).
12. S. J. Monte and G. Sugerman, Proc. 31st Annual Tech. Conf., Reinforced Plastics/Composites Div., SPI, Section 6-E (1976).
13. S. J. Monte and G. Sugerman, Proc. 33rd Annual Tech. Conf., Reinforced Plastics/Composites Div., SPI, Section 2-B (1978).
14. Dow Corning Corporation, "Silane Coupling Agents," Technical Brochure (1981).
15. Union Carbide Corporation, "Organofunctional Silanes—A Profile," Technical Brochure (1981).
16. Kenrich Petrochemicals Inc., "Titanate Coupling Agents for Filled Polymers," Technical Brochure (1981).
17. H. E. Ries, *Sci. Am.*, **244**, 152 (1961).
18. H. Ishida and J. L. Koenig, *J. Colloid Interface Sci.*, **64**, 565 1978).
19. H. Ishida and J. L. Koenig, *J. Polym. Sci.*, **17**, 1807 (1979).
20. A. T. Dibenidetto and D. A. Scola, *J. Colloid Interface Sci.*, **64**, 480 (1978).
21. O. K. Johannson, F. O. Stark, G. E. Vogel, and R. M. Fleischman, *J. Compos. Mater.*, **1**, 278 (1967).
22. P. T. K. Shih and J. L. Koenig, *Mater. Sci. Eng.*, **20**, 137 (1975).
23. L. R. Daley and F. Rodriguez, *Polym. Eng. Sci.*, **9**, 428 (1969).
24. E. P. Plueddemann, Proc. 24th Annual Tech. Conf., Reinforced Plastics/Composites Div., SPI, Section 19-A (1969).
25. E. P. Plueddemann, Proc. 27th Ann. Tech. Conf., Reinforced Plastics/Composites Div., SPI, Section 11-B (1972).
26. H. Ishida, C. H. Chiang and J. L. Koenig, *Polymer*, **23**, 251 (1982).
27. C. P. Chiang, Ph.D. Thesis, Case Western Reserve University, Cleveland, Ohio (1981).
28. H. Ishida and J. L. Koenig, *Polym. Eng. Sci.*, **18**, 128 (1978).

DISCUSSION

L. A. Utracki: In *Fig. 7a, b,* you showed no adsorption of γ-MPS onto mica for about 60 min. You call that period "induction time." On the other hand, in *Figs. 7c* and *8b* you again have no adsorption—for longer times, to be certain—but now the explanation is different: a rapid condensation in solution. Do you have any evidence for the difference?

B. Favis: In *Fig. 7c,* we treated the mica for 3 hours and preceded that treatment with a 90 min. hydrolysis of the silane. Based on the results from *Fig. 7a, b,* there would be no particular reason why the adsorption should not occur immediately following the allotted hydrolysis period. This is the same system. The only explanation we have at the moment is that dimers, trimers, and tetramers were formed. γ-MPS is known to undergo rapid condensation reactions and these oligomers are not suitable as coupling agents.

H. Ishida: You have very low solution concentrations; I do not see why you should have any condensation.

B. Favis: Possibly you only require a small amount of condensation at these low concentrations in order to interfere with the process.

H. Ishida: I have a couple of questions. First, I do not see how the monolayers would be organized, head-to-tail, or head-to head? What tentative orientation would these layers have? I suppose you washed the samples before analyzing them? Why should all the layers remain? The second question is: did you consider the amino-silane getting into the layers of mica? Cations are known to penetrate into those layers, especially in alcoholic media, but it is also possible in aqueous systems as well.

B. Favis: In terms of your first question, you are asking what type of orientation do we have. The method used in this study is quantitative carbon analysis, essentially a gravimetric method. We have no way of knowing, therefore, whether the molecular orientation of the silane in a particular layer is head to head of head to tail. We would like to take samples treated with one, two, and three silane layers and observe the interactions by FTIR. Until then I don't think that we can really, with much confidence, speculate on the interactions. In reference now to your second point, I don't think this would be much of a problem. You have to consider that even if there is some entry in between the mica flakes, this should have come out in the surface area measurements and therefore we should be accounting for this effect.

H. Ishida: The effect I am speaking of could happen only in water or methanol in the presence of cations. Therefore, if you measure the surface area after treatment you should not obtain the same value.

B. Favis: This may be something that we should look at.

J. M. Charrier: I would like to comment on the question about the head-to-head or head-to-tail structure. I am not a chemist but if you had head-to-head versus head-to-tail orientations, would you see a difference in the formation of the next layer in terms of an induction time?

B. Favis: Yes, you would expect to see some differences in the induction time. This would be something that would be interesting to look at a little more closely. One would probably suspect that the interactions between the first and second monolayer would tend to have head-to-head orientation since you would then have an organic end compatible with another organic end.

J. M. Charrier: The next layer will be tail-to-tail?

B. Favis: Yes, you would expect, in that case, to see some differences in the induction period and even in the approach to the plateau. This being the case, we would perhaps even have to concentrate on the kinetics of adsorption from one plateau to the other.

J. M. Charrier: I found this a very interesting work and I am interested in some practical aspects of it. If you wanted to treat mica in an industrial context, could you briefly tell us what would be done and how difficult in terms of time or equipment this would be. As well, I heard some time ago that a certain silane is much more expensive than another, or that silanes are, in general, more expensive than other possible treatments. I suppose that the process itself is more costly. Do you have any comments? Would it really cost significantly more to deposit two layers of three layers, rather than just one layer? If so, would it be due to the cost of the silane or the extended duration of the process?

B. Favis: I will try to briefly give you a bit of background on how we go about commercially applying a silane. Our results presented here are all obtained using very dilute solutions. This is because our aim was to obtain fundamental relationships governing the interactions of silane with mica. In practice, however, a coupling agent is deposited on a surface like mica, as any other particulate mineral filler, using a dry blend method. In such a process, one can take a Henshel mixer, for example, place the filler in it and add, drop-wise, a solution of the coupling agent. One hopes for a statistical distribution of course. The basic problem in trying to work in that sort of system, and in turn to develop fundamental relationships, is why we studied treatments for dilute solution. If you are looking at the cheapest method, or the most rapid method of commercial treatment, this is not the way one would want to proceed.

L. A. Utracki: I agree that it is premature to talk about the structure of multilayers without having the documents from FTIR. This kind of research is extremely interesting but the discussion should be based on good experimental evidence. If you postulate hydrolysis and oligomer formation, this should be documented. It is not necessary to make these suppositions.

B. Favis: One of the things that we plan in the near future is to do some follow-up work on the GPC. We will actually hydrolyze the coupling agent, then analyze it by gel permeation chromatography to see if we can detect the presence of oligomers. Certainly, the work is ongoing.

Studies of the Simulation of Silane Coupling Agent Structures on Particulate Fillers; The pH Effect

JAMES D. MILLER, KA-PI HOH, *and* HATSUO ISHIDA

Department of Macromolecular Science
Case Western Reserve University
Cleveland, Ohio 44106

The molecular structure of γ-methacryloxypropyltrimethoxysilane (γ-MPS) deposited on the surfaces of particulate mineral fillers was modeled by adjusting the pH of an aqueous alcoholic solution of the silane in absence of a substrate. Hydrolyzates obtained from the solution were studied by gel permeation chromatography (GPC) and Fourier transform infrared spectroscopy (FT-IR) and found to be polymethacryloxypropylsilsesquioxanes whose configuration and molecular-weight distribution were dependent on the solution pH. In acidic environments (below pH 4) the polycondensation mechanism appeared to proceed in a selective manner to form polycyclic blocks which resemble a beaded chain following condensation between blocks. Under more neutral and basic conditions (at or above pH 4) the polycondensation mechanism resulted in polymethacryloxypropylsilsesquioxanes with the more equilibrated double chain ladder configuration. The molecular weight distribution of these structures was dependent on the stability of the silanol or the silanolate ion. Extremely high-molecular-weight and polydisperse polymethacryloxypropylsilsesquioxanes were generated at near neutral pH due to the formation of the double chain ladder configuration and the high silanol instablity in this pH range. The two different polymethacryloxypropylsilsesquioxane configurations were also observed on γ-MPS modified metal oxide substrates. The structures help explain some of the previously observed trends with respect to γ-MPS adsorption on particulate mineral fillers. In strongly basic environments the methacrylate function of γ-MPS partially hydrolyzes to form sodium carboxylate, and carbon dioxide is absorbed from the air and reacts to form sodium carbonate.

INTRODUCTION

The effectiveness of silane coupling agents in particulate-filled composites is dependent on the molecular structure of the silane molecules and their resulting interactions with both the filler particles and the matrix resin. Chemical reaction with the organofunctional groups of silane coupling agents is an accepted mechanism for the reinforcement of thermosetting resins; however, such reactions do not proceed rapidly in filled thermoplastics. Nonetheless, silanes are used successfully as coupling agents in many particulate filled thermoplastic systems (1-5). Plueddemann, *et al.* (6) have suggested that formation of interpenetrating polymer networks (IPN) at the interface is a possible mechanism for the reinforcement of filled thermoplastics by silane coupling agents. This is consistent with the known characteristics of the substituents involved; however, there is little experimental evidence for the occurrence of interpenetrating polymer networks beyond inference from the following experimental results. Plueddemann proposed that the uncured siloxane film deposited on the mineral surface acts as a lubricant and dispersing aid during initial mixing of fillers with the resin. At molding temperature, the siloxane is a partial solvent for the molten thermoplastic and, as the composite cools, the thermoplastic looses its solubility and separates as an interpenetrating phase with the siloxane at the interface. Some crosslinking may occur in the siloxane phase at mold temperatures; the addition of peroxides promotes this crosslinking, which may aid in trapping the dissolved thermoplastic phase (6). Gahde (1) demonstrated significant improvement in the mechanical properties of a methacrylate-functional silane-modified kaolin-reinforced polyethylene with homopolymerization of the silane at the substrate surface and without chemical grafting to the polyethylene, suggesting the importance of interpenetrating polymer

networks and orientation. Recently, Kaul, *et al.* (7) used an energy dispersive X-ray microscope (SEM-EDX) to monitor silicon atom concentration across the interface in a silane-modified γ-Al_2O_3/polyethylene joint. They concluded that interdiffusion between the coupling agent molecules and polyethylene occurs and is a function of the silane drying conditions.

Organofunctional silanes used as coupling agents in polymer composites consist of a single organic functionality and three alkoxy groups attached to a silicon atom. The alkoxy functionality is hydrolyzable in aqueous solutions and the resulting silanols may condense with each other and with substrate surface species. The molecular structure of polysilsesquioxanes, the polymeric species obtained from the hydrolysis and condensation of trifunctional silanes, have been studied in the past. The polycondensation reaction was found to follow rather simple and selective pathways resulting in structured polysilsesquioxanes.

The configuration of the adsorbed silane molecules in composite systems will determine the extent and effectiveness of the interpenetrating networks, which can be established in both thermoplastic and thermosetting composites. The molecular structure of the silanes will also contribute to the availability of the organic functionality to the resin molecules and the hydrothermal protection offered by the coupling agent. Therefore, the structure of organofunctional silanes used in composite materials is extremely important to the composite performance regardless of the precise reinforcement mechanism. A number of techniques have been employed to study the structure of organoalkoxysilanes in aqueous solutions. Plueddemann (8) used a combination of visual observation of solution stability, the Lentz technique (9) or silylation of the silanols, and H^1 NMR to study the hydrolysis and condensation reactions. It was concluded that the alkoxy groups hydrolyze rapidly in homogeneous solution to silanetriols, which condense slowly in a stepwise manner to complex siloxanols at a rate which is (i) decreased by the presence of MeOH; (ii) increased by a trace of F^- ions, (iii) decreased by dilution with water; (iv) strongly influenced by pH; and (v) only mildly dependent on the nature of the alkyl group, except for certain γ-substituted compounds.

In many other studies, the pH of the treating solution has also been observed to influence the structure of trifunctional silane coupling agents. It is believed that the pH of the silane treating solution and the ionic nature of the silane affect the rate of hydrolysis, the silanol stability and solubility in water, and the molecular-weight distribution of the condensation products. The solution pH along with the acid/base characteristics of the substrate surface should also affect the migration to and deposition on the filler surface and the nature of the interfacial chemical bond. Solution pH was suggested to be the largest factor for most silanes in determining the rate of hydrolysis and the rate of achieving solubility (10). The rate of silanol condensation in aqueous solution was also suggested to be largely determined by pH (11). Plueddemann demonstrated that under mildly acidic conditions (pH 3 to 5), alkoxysilanes hydrolyze rapidly, forming monomeric silanetriols, and condense slowly to form polymeric organic siloxanols. The rate of condensation was the slowest at pH 4 and very rapid in the range pH 7 to 9 (12). Similarly, the stability of silicic acid in water is a function of pH (13) with the silanol groups having a maximum stability at a pH of 2 to 3 and the rate of condensation to polysilicates the greatest at a pH of approximately 8.

The following experimental works cite examples of the pH influence on specific coupling agent systems. Kaas and Kardos (14) suggested that the condensation of neutral alkoxysilane coupling agents with glass and silica could be catalyzed by aliphatic amines. Greenlee reported that certain anions including nitrate, bromide, and phosphate act as adhesion promoters in room-temperature-cured silicone elastomers on aluminum and steel (15). The molecular structure of hydrolyzates of γ-aminopropyltriethoxysilane (γ-APS) is a function of pH and may affect the curing reaction between γ-APS and epoxies in composite materials (16). The amount of γ-APS adsorbed on a glass substrate surface is also influenced by the solution pH (17). Acid-base reactions have also been shown to be important to the alignment of silane coupling agents on filler surfaces (18), the condensation reaction of the hydrolyzed species (19, 20), the structure of physisorbed silane on the surface of particulate mineral fillers (20), the flexural strength of cationic silane modified polyester/silica castings and to a lesser extent for nonionic silane (21), and the nature of silane adsorption and desorption on the surface (20, 22).

We have recently reported that the structure and amount of physisorbed γ-methacryloxypropyltrimethoxysilane (γ-MPS) deposited on the surfaces of various particulate mineral fillers is a strong function of the acid/base characteristics of the substrate surface (20). This work details the simulation of the substrate pH effect on the molecular structure of deposited γ-methacryloxypropyltrimethoxysilane coupling agent by adjusting the solution pH in the absence of fillers. The system is characterized by Fourier transform infrared spectroscopy (FT-IR) and gel permeation chromatography (GPC).

EXPERIMENTAL

Silane coupling agent, γ-methacryloxypropyltrimethoxysilane (γ-MPS), was purchased from Petrarch Systems Inc., and hydrolyzed in an aqueous alcoholic solution (8 ml γ-MPS, 6 ml H_2O, 72 ml n-butanol) for one hour at room temperature. Samples of the solution were pH adjusted with dilute aqueous solutions of HCl and NaOH. The solutions were sealed for 12 hours at room temperature followed by exposure to an air stream for an additional 12 hours to drive off the alcohol. The samples were then allowed to stand in air at room temperature for a time sufficient to insure that further condensation would not take place. Particulate mineral fillers were treated with the aqueous alcoholic solution from an atomizer at a loading of 1 percent based on the weight of the filler. The filler samples were similarly sealed for 12 hours followed by exposure to the atmosphere for 12 hours and heating in air for 3 hours at 80°C.

A Fourier transform infrared spectrophotometer (Digilab FTS-20E) with a liquid-nitrogen-cooled mercury cadmium telluride (MCT) detector was used at a resolution of 2 cm^{-1} with coaddition of 200 scans. The spectrophotometer was purged with dry nitrogen to eliminate atmospheric water vapor. Polymethacryloxypropylsilsesquioxane samples were dissolved in tetrahydrofuran (THF) and cast as thin films on potassium bromide (KBr) plates. Solid, THF-insoluble precipitates obtained in a number of pH adjusted samples were ground with KBr and pressed into pellets. γ-MPS adsorbed on particulate mineral fillers was examined by diffuse reflectance Fourier transform infrared spectroscopy (DRIFT) using a Digilab DFR-100 diffuse reflectance attachment. DRIFT spectra were plotted according to the Kubelka-Munk function (23, 24).

A gel permeation chromatograph (GPC) consisting of a metering pump (Altex Model 110), two independent series of packed columns, and an ultraviolet detector at 254 nm (Beckman Model 153) were used to separate the oligomeric polymethacryloxypropylsilsesquioxane fractions. One series of columns was used to separate high molecular weight components in the range 8×10^6 to 500 g/mole and consisted of the following columns: 10^5Å μStyragel (Waters Associates), 10^4Å μSpherogel (Altex), 10^3Å Ultrastyragel (Waters Associates). The second series of columns was used to separate low molecular weight components of less than 10,000 g/mole and consisted of the following columns: 500Å μSpherogel (Altex), 100Å μStyragel (Waters Associates), and 100Å Ultrastyragel (Waters Associates). The mobile phase was tetrahydrofuran (THF) at an elution rate of 1 ml/min. The molecular-weight distribution of the polymeric silane was measured relative to near monodisperse polystyrene standards (Pressure Chemical Company).

RESULTS AND DISCUSSION

Figure 1 illustrates the chemical formula of γ-methacryloxypropyltrimethoxysilane (γ-MPS) and the generalized hydrolysis and condensation reactions to polymethacryloxypropylsilsesquioxane. Polysilsesquioxanes refer to monosubstituted siloxane polymers of the general form $(RSiO_{1.5})_n$. The polymethacryloxypropylsilsesquioxane samples deposited from pH-adjusted aqueous alcoholic solutions produce a variety of visually observable differences. Acidic environments in the range pH 1.30 to pH 5.30 produce homogeneous solutions of a clear viscous liquid whose viscosity increases with increasing pH. Products obtained under basic conditions above pH 8 are heterogeneous mixtures of a colored, cloudy, viscous liquid and a white or brown precipitate. Samples obtained from the hydrolyzed silane solutions adjusted to near neutral pH are rubbery solids. Attempts to dissolve the samples in THF confirmed that vastly different structures result from the pH influence. The samples obtained from acidic solutions and the viscous portion of samples obtained from basic solutions dissolved in THF in a matter of minutes; however, the solid precipitates obtained from basic solutions did not dissolve or swell in THF. The samples

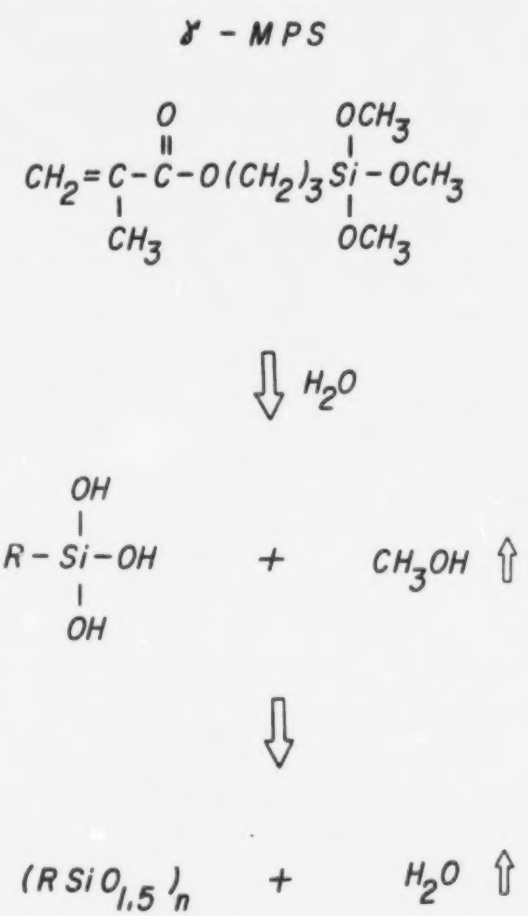

Fig. 1. Chemical formula of γ-methacryloxypropyltrimethoxysilane (γ-MPS) and the generalized hydrolysis and condensation reactions.

obtained from neutral solutions showed great resiliency to attack by THF and dissolution did not occur for a matter of days.

Figures 2 and *3* illustrate the molecular-weight distribution of the pH-adjusted polymethacryloxypropylsilsesquioxane samples fractionated by gel permeation chromatography (GPC) relative to near monodisperse polystyrene standards. The chromatograms show that the product of the hydrolysis reaction and subsequent drying of γ-MPS is a condensed polymethacryloxypropylsilsesquioxane with a molecular-weight distribution which is dependent on the pH of the solution. The pH of the aqueous alcoholic silane solution was adjusted after one hour of initial hydrolysis to simulate the treatment of particulate mineral fillers, since an effect of the filler surface is to impart long range acid/base characteristics to the deposited silane (20). The molecular-weight distributions in *Figs. 2* and *3* correspond closely with the observations made on a macroscopic level. In the acidic pH range, the average molecular weight of the condensed silane species increases with increasing pH. This is consistent with observed increase in viscosity over the same range. Chromatograms A, B, C, and D in *Fig. 2* exhibit a low-molecular-weight doublet with an

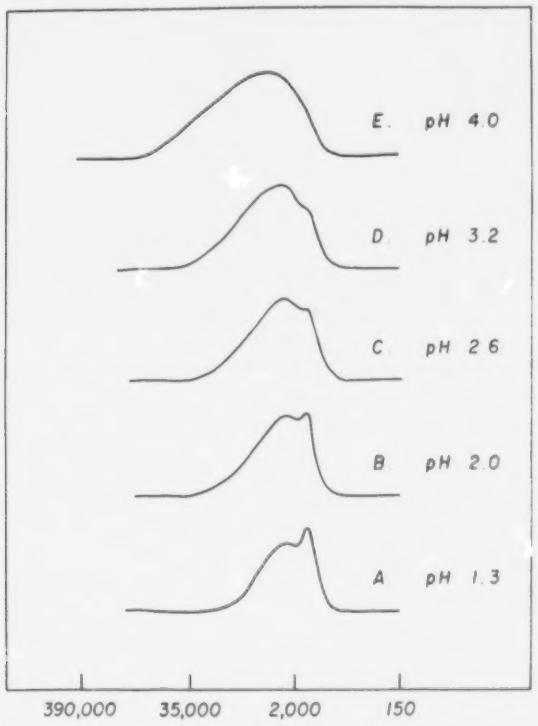

Fig. 2. GPC chromatograms of pH-adjusted polymethacryloxypropylsilsesquioxane: (A) pH 1.3, (B) pH 2.0, (C) pH 2.6, (D) pH 3.2, (E) pH 4.0.

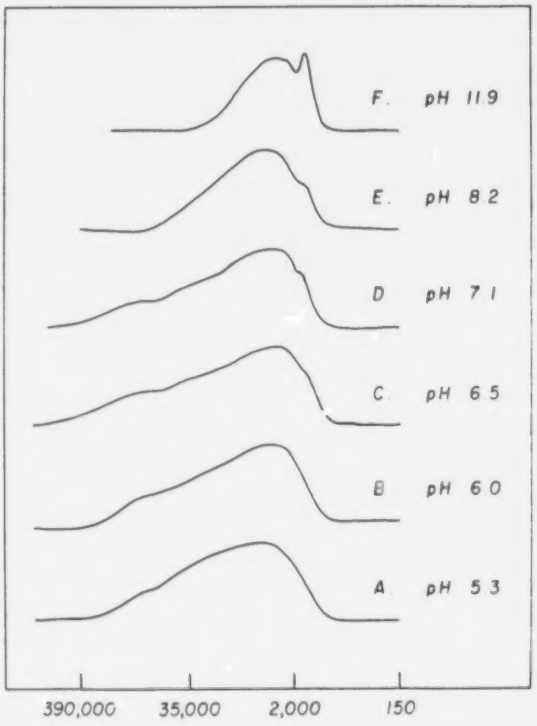

Fig. 3. GPC chromatograms of pH-adjusted polymethacryloxypropylsilsesquioxane: (A) pH 5.3, (B) pH 6.0, (C) pH 6.5, (D) pH 7.1, (E) pH 8.2, (F) pH 11.9.

increase in the relative intensity and polydispersity of the higher-molecular-weight peak with increasing pH. In chromatogram E, at pH 4.0, the rather sharp low-molecular-weight peak is no longer apparent and the molecular weight and polydispersity has increased significantly. Chromatograms A, B, C, and D in *Fig. 3* represent the polymethacryloxypropylsilsesquioxane samples adjusted to higher pH and exhibit a molecular-weight distribution similar to the sample at pH 4.0 in *Fig. 2* with the addition of a very high molecular weight and extremely polydisperse fraction. The largest contribution of the extremely high-molecular-weight fraction is observed in the sample at pH 6.5. This sample required the longest period of time to dissolve in THF. Chromatograms E and F in *Fig. 3* correspond to the samples adjusted to pH 8.2 and pH 11.9, respectively. They decrease in average molecular weight and polydispersity with increasing pH and exhibit a doublet which becomes well resolved at high pH. The rubbery solid samples of polymethacryloxypropylsilsesquioxane which are difficult to dissolve in THF were obtained at pH 6.0, 6.5, and 7.1. The precipitates obtained in the basic pH range are insoluble in THF and therefore were not submitted to GPC analysis. Although the calibration of the GPC chromatograms with monodisperse polystyrene is a helpful guide in evaluating the molecular weight and polydispersity of the polymethacryloxypropylsilsesquioxane samples, it cannot be taken as an indication of their actual molecular weight.

The molecular weight and molecular-weight distribution of the pH-adjusted polymethacryloxypropylsilsesquioxanes and their corresponding solubility in THF explains the previous observations made concerning γ-MPS-modified particulate fillers with different surface pH (20). Neutral surfaces promote the high-molecular-weight species. The moderately insoluble nature of these high-molecular-weight polymethacryloxypropylsilsesquioxanes results in little silane being able to be washed from a particulate filler surface by organic solvents both under experimental conditions (20) and in composite systems. As a result, on neutral surfaces the siloxane network is more widespread, and very little removable or physisorbed silane will exist. On acidic or basic fillers, this effect will be greatly reduced and the degree of physisorbed and chemisorbed silane will be more dependent on the nature of the interfacial bond.

A typical dry-blending treatment for the silane-modification of particulate fillers involves (i) spraying a small amount of an aqueous alcoholic solution of the coupling agent onto the filler surface after one hour of prehydrolysis; (ii) sealing the treated filler for 12 hours to insure uniform surface coverage by migration of the agent in the alcohol; and (iii) exposure of the filler to the atmosphere to drive off the alcohol. A similar procedure was undertaken in this work with the exception that instead of applying the treating solution to filler surfaces with different pH characteristics, the treating solution

was pH adjusted to model the surface effect. The molecular structure of the silane molecules during the course of the procedure was followed by gel permeation chromatography for samples adjusted to pH 3.6, pH 6.9, and pH 9.1 as seen in *Figs. 4*, *5*, and *6*, respectively.

Chromatograms A through E in *Figs. 4*, *5* and *6* correspond to samples withdrawn 1, 20, 40, 120, and 420 hours, respectively, after the initial 1-hour hydrolysis and pH adjustment. Chromatogram A is the polymethacryloxypropylsilsesquioxane species from the sealed aqueous alcoholic solution. Chromatogram B is the sample after most of the butanol has been driven off and chromatograms C, D, and E represent the polymethacryloxypropylsilsesquioxane structures with time after complete removal of the butanol. *Figure 4* illustrates that, at pH 3.6, the hydrolyzed γ-MPS quickly forms low-molecular-weight oligomers with rapid loss of the hydrolyzed monomer. The monomeric species is evident as the lowest-molecular-weight peak in chromatogram A of *Fig. 4*. The oligomers give sharp, well-defined peaks characteristic of selective polycondensation. Upon removal of the butanol, further condensation occurs, producing higher-molecular-weight species. The final polymethacryloxypropylsilsesquioxane condensation product at pH 3.6 is of a relatively low molecular weight and narrow dispersity. The same analysis simulating the reaction of hydrolyzed γ-MPS on the surfaces of neutral and basic particulate fillers is seen in *Figs. 5* and *6*. It is apparent that the polycondensation reaction at pH 6.9 and pH 9.1 is quite

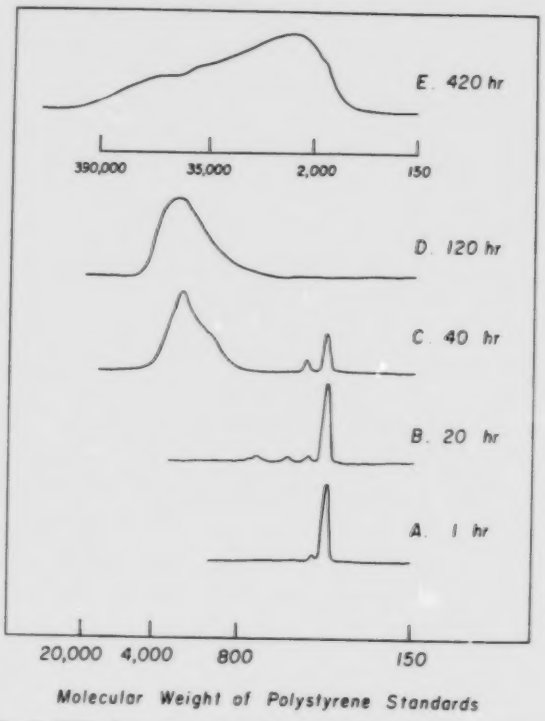

Fig. 5. GPC chromatograms of polymethacryloxypropylsilsesquioxane adjusted to pH 6.9 with time from pH adjustment: (A) 1 hr/in solution, (B) 20 hr/during drying, (C) 40 hr/dry, (D) 120 hr/dry, (E) 420 hr/dry.

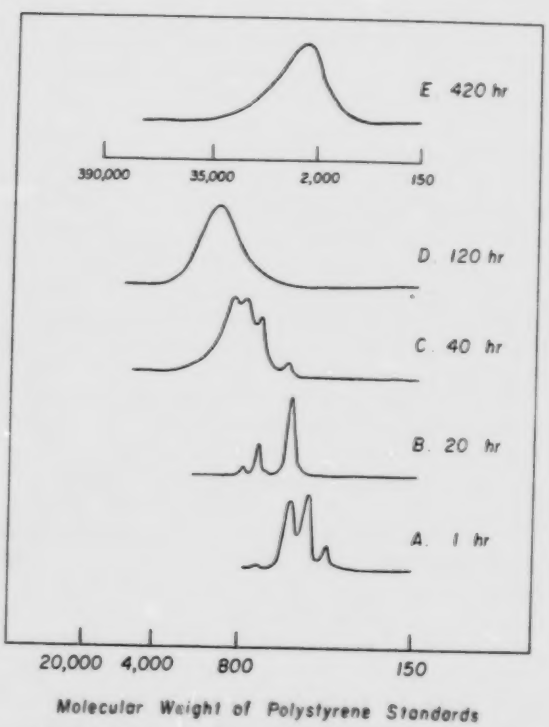

Fig. 4. GPC chromatograms of polymethacryloxypropylsilsesquioxane adjusted to pH 3.6 with time from pH adjustment: (A) 1 hr/in solution, (B) 20 hr/during drying, (C) 40 hr/dry, (D) 120 hr/dry, (E) 420 hr/dry.

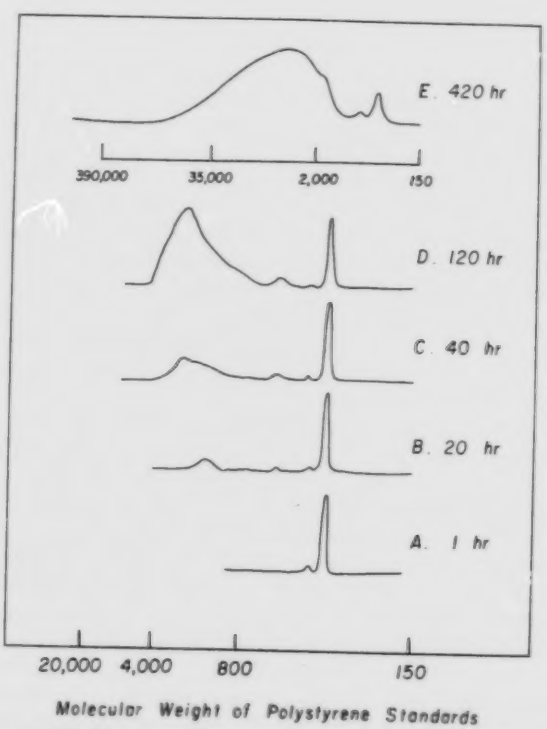

Fig. 6. GPC chromatograms of polymethacryloxypropylsilsesquioxane adjusted to pH 9.1 with time from pH adjustment: (A) 1 hr/in solution, (B) 20 hr/during drying, (C) 40 hr/dry, (D) 120 hr/dry, (E) 420 hr/dry.

different than at acidic pH. In *Fig. 5* at pH 6.9, the monomeric peak is predominant until complete removal of the butanol. Similarly, at pH 9.1 in *Fig. 6*, the monomeric species is predominant until complete removal of the butanol and remains significant even after 420 hours.

The samples obtained from neutral (pH 6.9) and basic (pH 9.1) solutions contain higher-molecular-weight and more polydisperse polymethacryloxypropylsilsesquioxanes than those from acidic solutions. From *Figs 5* and *6*, the mechanism of polycondensation appears to be very similar at pH 6.9 and pH 9.1, even though the molecular weight, polydispersity, and monomer content of the final products are different. At pH 3.6, the reaction path to polymethacryloxypropylsilsesquioxane appears to be dramatically different. The predominance of the low-molecular-weight oligomeric species and the apparent stability of certain configurations in solution as seen in chromatograms A, B, and C in *Fig. 3* suggest that, at acidic pH, cage-like polycyclic silsesquioxanes may be formed of the type suggested by Barry, *et al.* (25), Olsson (26, 27), Sprung and Guenther (28), and Brown (29-31).

Organofunctional silane coupling agents deposited on the surfaces of particulate mineral fillers and glass fibers are often cured at low temperatures. Temperatures in the range 80 to 120°C are typically used to ensure the complete condensation of hydrogen-bonded coupling agent silanols and coupling agent silanols hydrogen bonded with substrate surface silanols. *Figure 7* illustrates the effect of heat treatment on the polycondensation reaction as followed by gel permeation chromatography. Silane-modified fillers are typically heat treated shortly after removal of the solvent used to deposit the silane (20) and therefore, a similar method was used for the pH-adjusted bulk samples. Chromatogram A in *Fig. 7* is the unheated polymethacryloxypropylsilsesquioxane sample obtained from a pH-adjusted solution after removal of the alcohol by drying in air at room temperature. This chromatogram corrresponds to chromatogram C in Fig. 4. Chromatogram B represents the same sample after heat treatment in air at 80°C for 3 hours. Chromatogram C is the original sample after 170 hours with no elevated heat treatment. The similarity of chromatograms B and C in *Fig. 7* indicates that the effect of the heat treatment was simply to accelerate the same polycondensation reaction that occurred with time at room temperature. The same observation with respect to the effect of heat treatment on the intermolecular condensation of hydrolyzed γ-MPS was also seen for the samples obtained from solutions adjusted to other pH values. An analogous result might be assumed for the intermolecular reaction of hydrolyzed γ-MPS deposited on particulate fillers. However, since an effect of the substrate surface is to significantly reduce the effective concentration of neighboring coupling agent molecules (20), heat treatment may play a major role in overcoming this concentration barrier on the particulate filler surface.

Figure 8 illustrates the FT-IR spectra of the polymethacryloxypropylsilsesquioxanes obtained from pH-adjusted solutions in the antisymmetric Si-O-Si stretching

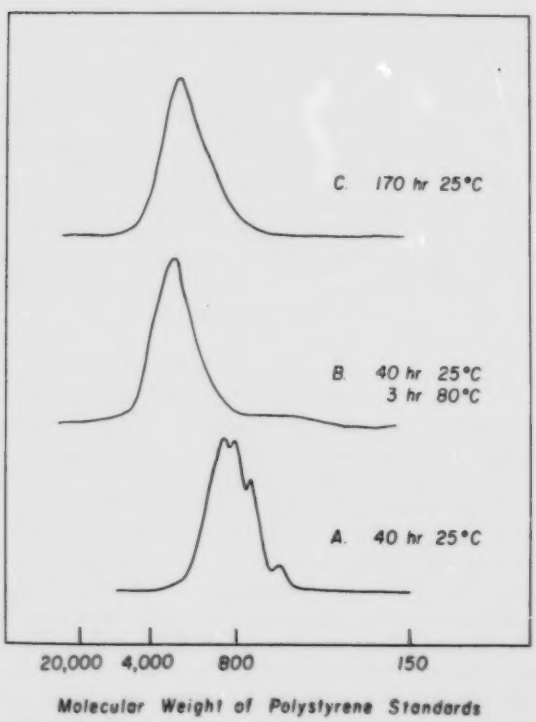

Fig. 7. GPC chromatograms of polymethacryloxypropylsilsesquioxane adjusted to pH 3.6 after (A) 40 hr at 25°C, (B) 40 hr at 25°C and 3 hr at 80°C, and (C) 170 hr at 25°C.

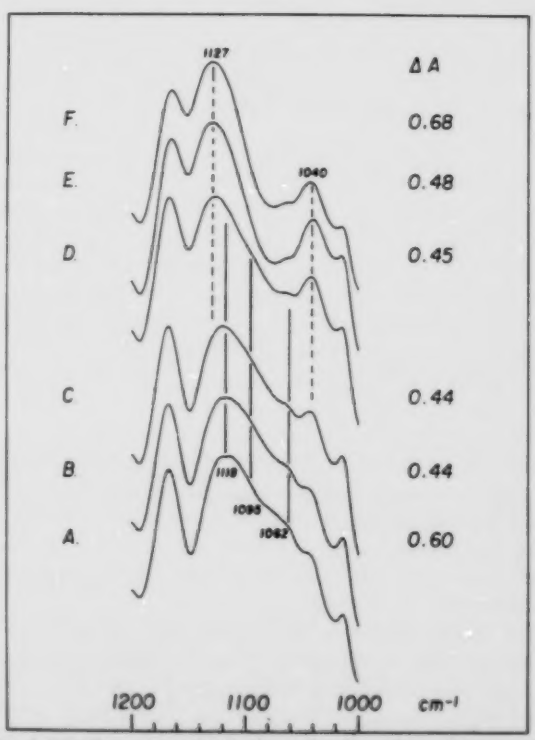

Fig. 8. FT-IR spectra of pH-adjusted polymethacryloxypropylsilsesquioxane: (A) pH 1.3, (B) pH 2.6, (C) pH 3.2, (D) pH 4.0, (E) pH 6.5, (F) pH 9.0.

region between 1200 and 1000 cm^{-1}. A rather sharp transition in the structures is noticeable between spectra C and D corresponding to the solutions adjusted to pH 3.2 and pH 4.0, respectively. Spectra A, B, and C correspond to a pH adjustment at or below pH 3.2 and consist of a strong broad band centered at 1118 cm^{-1}, a weak shoulder near 1095 cm^{-1}, and weak shoulders near 1062 cm^{-1} and 1040 cm^{-1}. Strong bands at 1127 cm^{-1} and 1040 cm^{-1} and a weak band near 1064 cm^{-1} are observed in spectra D, E, and F for the solutions adjusted to pH 4.0 and higher. If the polymethacryloxypropylsilsesquioxanes were of indefinite, highly random structures, a broad siloxane band covering the entire 1150 to 1000 cm^{-1} range might be expected (32). However, the infrared spectra in *Fig. 8* suggest that the structures are relatively ordered and the differences in the infrared absorption bands of the pH-adjusted samples suggest that two dissimilar polysilsesquioxane species form as a function of pH. Analysis of the pH-adjusted condensates of γ-MPS by the Si-O-Si antisymmetric stretching vibrations is complicated by the presence of methacrylate fingerprint bands. The interpretation is also made difficult by the distribution of specific condensation products which occur and are not easily separable.

It has been suggested and confirmed that the condensation mechanism of hydrolyzed trihalosilanes and trialkoxysilanes is relatively selective and the products are highly ordered silsesquioxanes. Crystalline precipitates of polyphenylsilsesquioxane were first obtained by Barry, *et al.* (25) and shown to be the caged pentacyclic octamer (26, 27). Brown reported a variety of polycyclic caged structures and a very high-molecular-weight soluble double chain polymer obtained from the base catalyzed equilibration of polyphenylsilsesquioxane (29, 31). *Figure 9* depicts the idealized structures of the two general types of polysilsesquioxane configurations as characterized and suggested by Brown (33). The vertices in each structure represent a trifunctional silicon atom with an Si-O-Si linkage along each axis. The organofunctional group is omitted. Structure A is referred to as a beaded chain configuration of cubical octamers or polycyclic caged blocks. Structure B is the linear double chain or ladder configuration.

The polymethacryloxypropylsilsesquioxane structure obtained from solutions adjusted to pH 3.2 and below, spectra A, B, and C in *Fig. 8*, may be attributed to the acid-catalyzed non-equilibrative linkage of polycyclic caged blocks to resemble an irregularly branched string of beads as suggested by Brown (31). The polysilsesquioxane product in spectra D, E, and F of *Fig. 8* formed from solutions at pH 4.0 and above may be assumed to be the double chain ladder structure similar to the stereoregular cis-syndiotactic double chain polyphenylsilsesquioxane obtained by Brown, *et al.* (29). Extensive work by Brown (31) suggested that hydrolysis of phenyltrichlorosilane in aqueous toluene produced a condensate with a distribution of chain lengths in the randomly connected "beaded chain" structure. The infrared spectrum of this species consisted of Si-O-Si antisymmetric stretching vibrations at 1060(msh), 1095(wsh), 1120(s), and ~1150(sh) cm^{-1}. These results are very similar to spectra A, B, and C in *Fig. 8* obtained for polymethacryloxypropylsilsesquioxane adjusted to pH 3.2 and below. Molecular-weight determination of fractionated polyphenylsilsesquioxanes suggested that two major fractions exist of the average composition $T_{21}(OH)_3$ or $T_{22}(OH)_4$ and $T_{62}(OH)_{10}$ where T represents a trifunctional unit of siloxane structure (31). *Figures 2* and *3* illustrate that the assumed bead-like polymethacryloxypropylsilsesquioxane structures have a significantly lower molecular weight than the structures obtained at pH 4.0 and above and consist of two major fractions. This lower molecular weight is entirely expected for a beaded chain structure with incomplete interpolycyclic block condensation (33).

Alkali-equilibrated condensates of phenyltriethoxysilane in aqueous acetone produce polyphenylsilsesquioxanes, which gave X-Ray diffraction patterns indicative of the cis-syndiotactic double-chain high polymer (31). Similar linear double chain phenylsilsesquioxanes were obtained by Brown with a procedure resembling the one used in this work. The infrared spectrum of this species showed two Si-O-Si antisymmetric stretching bands centered near 1130 cm^{-1} and 1045 cm^{-1} (29). The band near 1045 cm^{-1} was attributed to the antisymmetric stretching Si-O-Si in-phase chain vibration of the ladder-type structure. This was confirmed by demonstration that rearrangement of the ladder-type prepolymer to low-molecular-weight caged structures occurs in solution. During this rearrangement, there was a sharp decrease and eventually a complete loss of the 1045 cm^{-1} band representing a cleavage of the polymer chains (29). The polymethacryloxypropylsilsesquioxane condensates obtained at pH 4.0 and above from aqueous alcoholic solution show similar bands at 1127 and 1040 cm^{-1} in spectra D, E, and F of *Fig. 8*. These bands are slightly shifted from their corresponding positions in polyphenylsilsesquioxane but are comparable in shape and intensity, suggesting that double chain ladder-type structures of polymethacryloxypropylsilsesquioxane were formed from solutions at pH 4.0 and above. Intrinsic viscosity measurements of the alkali-equilibrated polyphenylsilsesquioxanes typically gave values which corresponded to weight average molecular weights of 28,000, 41,000, and 60,000 with an M_w/M_n of 1.4 by osmometry (29). This corresponds to an average molecular

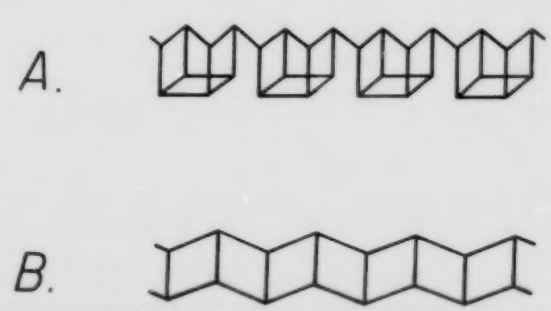

Fig. 9. Idealized molecular structures of polysilsesquioxanes in the (A) beaded chain configuration and the (B) double chain ladder configuration as suggested by Brown (33).

size of 158 phenyl-T units (29) and is significantly higher than that observed for the beaded chain structure. Similarly, the GPC chromatograms in *Figs. 2* and 3 illustrate that higher molecular weight and more polydisperse structures were obtained when the ladder type polymethacryloxypropylsilsesquioxanes were formed from solutions at pH 4.0 and above.

Each pH-adjusted polymethacryloxypropylsilsesquioxane prepared in this work could be expected to consist of some distribution of beaded chain and double chain ladder products. This is reflected by the presence to some degree of bands assigned to both configurations in all the infrared spectra in *Fig. 8*. This occurrence is most evident in spectra C and D in *Fig. 8* since these samples represent the transition between the two proposed structures. The band at 1040 cm^{-1} is assigned to the double chain ladder structure but this band also appears less intensely in spectra A, B, and C, which are attributed to the beaded chain configuration. Similarly, the band near 1062 cm^{-1} in spectra A, B, and C also appears weakly in spectra E and F and more strongly in spectrum D near the transition pH. Intermediate structures to the beaded chain and double chain ladder configurations may include hybrid structures in which cage-like groups are fused onto the ends of a short ladder polymer chain (33). This type of configuration may be partially responsible for the presence of absorption bands characteristic of both the bead and ladder structures seen throughout the pH range in *Fig. 8*. Without fractionation of the components the infrared spectra of the pH-adjusted polymethacryloxypropylsilsesquioxane samples are expected to consist to some degree of a variety of products and configurations.

Additional support for the presence of these pH-dependent structures is seen by reexamining the initial condensation products of hydrolyzed γ-MPS in *Figs. 4* through 6. In *Fig. 4* at pH 3.6, the polycondensation mechanism appears to be proceeding through well-defined steps presumably from the silanetriol to the diol, to the cyclic tetrol, to the caged octol, and finally to intermolecular condensation products forming linked caged octamers as suggested by Brown (31). In *Figs* 5 and 6 at higher pH, the polycondensation mechanisms appear to be very similar to each other, and yet remarkably different from the polycondensation at an acid pH. The relative amount of low-molecular-weight cage-like structure is very small and the hydrolyzed monomer predominates until the butanol is completely removed. These conditions are similar to the slow precipitation from an equilibrated condensate (28, 29) and presumably give relatively high polymers with the double chain ladder configuration.

The configuration of silane coupling agent molecules on the surface of fiber and particulate reinforcements used in polymer composites is of great practical and scientific interest. The silane solutions were pH adjusted to model the effect of the substrate surface and *Fig. 10* demonstrates the ability to observe the configurational differences on the substrate surface. *Figure 10* shows the diffuse reflectance Fourier transform infrared (DRIFT) spectra of γ-MPS deposited on

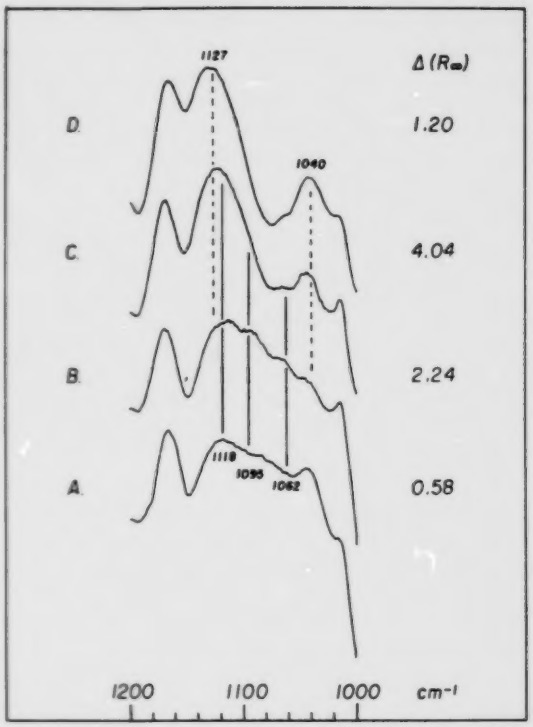

Fig. 10. DRIFT spectra of polymethacryloxypropylsilsesquioxane on the substrate surface; (A) calcium oxide, (B) antimony oxide, (C) nickel oxide, (D) lead oxide.

four metal oxides from a natural pH treating solution. Spectrum A indicates the presence of a mixture of the two configurations on the surface of calcium oxide. Spectrum B shows predominantly the beaded chain polymethacryloxypropylsilsesquioxane configuration on the surface of antimony oxide. Spectrum C and D indicate presence of the linear double-chain ladder structures on the surfaces of nickel oxide and lead oxide, respectively. The nickel oxide and lead oxide examples follow the trend observed in the pH-adjusted samples since the aqueous slurry pH values for these metal oxides are 7.0 and 10.0, respectively (20). The antimony oxide sample has an aqueous slurry pH of 4.4, which is greater than the pH of the configurational transition observed in *Fig. 8*. Therefore, we might expect the double chain ladder structure; however, spectrum B in *Fig. 10* shows that the beaded chain configuration is observed. The aqueous slurry pH value may not be an extremely precise measure of the pH effect imposed by the substrate surface. There may also be a concentration or mobility limitation imposed on the coupling agent molecules by the substrate. With this consideration and the apparent existence of weak bands at 1127 cm^{-1} and 1040 cm^{-1} indicating a distribution of structures, the result is not surprising. More unexpected results were obtained on calcium oxide. Calcium oxide has a high aqueous slurry pH of 12.4 and therefore, the ladder structure would be suggested. However, as seen in spectrum A of *Fig. 10*, a mixture of the two configurations appears to exist due to the presence of bands in the 1100-1050 cm^{-1} range along with a strong band at 1040 cm^{-1}. A possible

explanation for the presence of the caged structure on basic calcium oxide is that the substrate has a relatively high specific surface area resulting in an effective decrease in silane concentration. Thus, the polycondensation may become kinetically controlled, favoring the beaded chain configuration. Similarly, cage-like polycyclic polyphenylsilsesquioxanes were obtained from alkali-equilibrated solutions when the concentration was very dilute (29). The formation of specific polysilsesquioxane configurations is a complex function of a number of factors including the solution pH, concentration, solvent, temperature, silane type, and substrate characteristics. The previous explanations must be investigated further but suggest the possibility of controlling the molecular configuration of silane coupling agents on the particulate mineral surface to obtain desired effects.

The stability of silanols is known to be a strong function of pH. *Figure 11* depicts silanol stability as a function of pH in the polymethacryloxypropylsilsesquioxane samples obtained from pH-adjusted solutions. Silanol stability was measured as the integrated area of the silanol OH band from 3700 to 3250 cm^{-1} and normalized by the carbonyl absorbance near 1700 cm^{-1}. The curve is consistent with previous observations of silanol stability (34), indicating maximum but limited stability at pH 2 to 3, minimum silanol stability in the range pH 6 to 8, and complete stability as silanolate ions at high pH. If the condensation mechanism of hydrolyzed organosilanes was a completely random, non-selective process, then we would expect a molecular-weight distribution that inversely parallels the silanol stability. Secondly, if only a single molecular configuration was obtained through polycondensation, we would also expect the molecular weight of the polymethacryloxypropylsilsesquioxanes to inversely follow the silanol stability as a function of pH. These trends, however, are not observed. At low pH, where the condensation product resembles the string of polycyclic caged beads, the molecular weight of the polymethacryloxypropylsilsesquioxane increases with increasing silanol stability. This might at first seem to be an anomaly, and yet, decreased silanol stability may favor lower molecular weight products because the increased reactivity of the silanols preferentially results in more complete cyclization rather than linear intermolecular linkage. Once the double chain ladder structure is formed, above pH 4.0, the decrease in silanol stability results in an increase in molecular weight because the closed caged structures which limit molecular weight do not occur. Therefore, the negative and positive slopes of silanol stability as a function of pH in *Fig. 11* reflect the transition between the beaded chain and double chain ladder configurations. At high pH, the molecular weight of the polymethacryloxypropylsilsesquioxane condensation products begins to decrease because the silanolate ions tend to be stable and unreactive. The silanolate ion concentration increases with increasing pH.

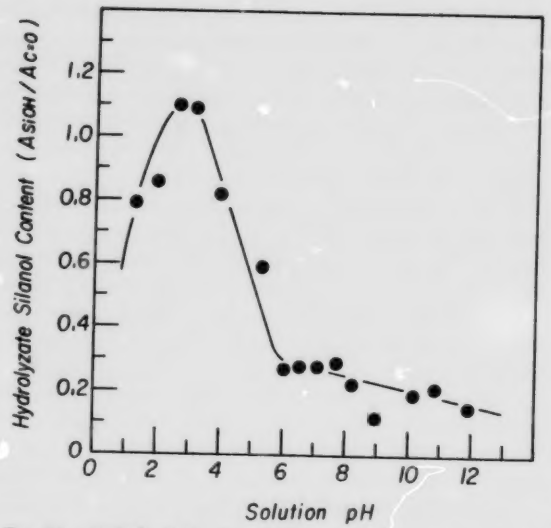

Fig. 11. γ-MPS hydrolyzate silanol content as a function of pH adjustment. Hydrolyzates prepared by drying in air at room temperature.

Tetrahydrofuran (THF) insoluble precipitates were formed in the pH adjusted polymethacryloxypropylsilsesquioxane samples above pH 7.7. The precipitates were of sufficient concentration to be easily collected in the samples above pH 10.2. Fourier transform infrared spectroscopy shows the precipitates to consist of two sodium salts. *Figure 12* is the infrared spectrum of the precipitate found in the polymethacryloxypropylsilsesquioxane samples obtained from solutions adjusted to pH 10.2 and pH 10.8, and can be identified as sodium carboxylate characterized by strong CO_2^- antisymmetric and symmetric stretching vibrations at 1550 cm^{-1} and 1420 cm^{-1}, respectively. The sodium carboxylate is the result of the base catalyzed hydrolysis of the ester to an acid and an alcohol according to the following equation:

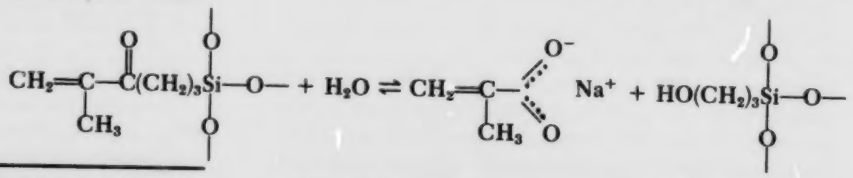

The result is similar to that obtained by Boerio, *et al.* (35) in their study of silane-modified copper mirrors, with the exception that the carboxylate species was observed only at low pH. This discrepancy may be explained since any methacrylic acid formed by acidic hydrolysis is probably volatile enough to evaporate during drying. On the other hand, the hydrolysis products obtained during basic hydrolysis and by Boerio (35) on copper can form non-volatile salts. In the polymethacryloxypropylsilsesquioxane samples adjusted to pH 11.9 and pH 12.5, a second precipitate was also identified spectroscopically as sodium carbonate. *Figure 13* is the infrared

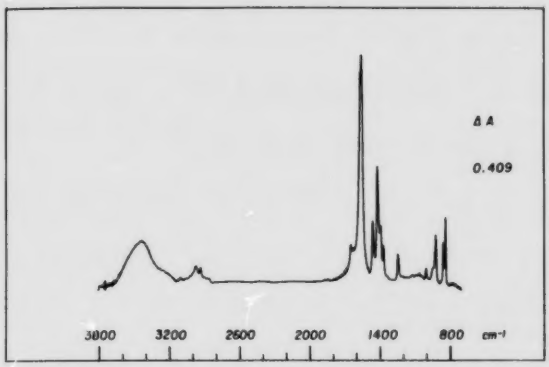

Fig. 12. FT-IR spectrum of sodium carboxylate obtained as a precipitate from pH-adjusted polymethacryloxypropylsilsesquioxane.

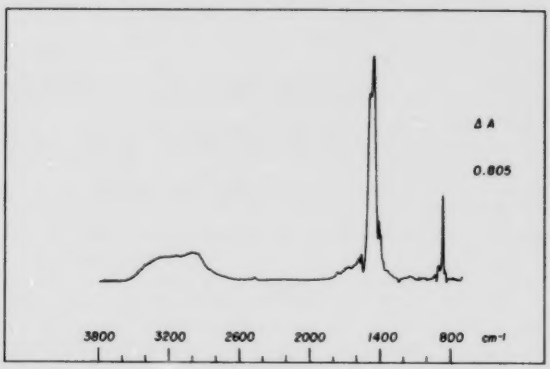

Fig. 13. Ft-IR spectrum of sodium carbonate obtained as a precipitate from pH-adjusted polymethacryloxypropylsilses quioxane.

spectrum of sodium carbonate obtained by digital subtraction of the sodium carboxylate spectrum, since the precipitates separated at pH 11.9 and pH 12.5 were mixtures of the two species. The sodium carbonate is presumably formed by the absorption of CO_2 from the air (36).

Hydrolysis of the methacrylate functionality should be catalyzed by both acid and base although no apparent precipitate was formed under acidic conditions. This may be due to the evaporation of methacrylic acid as mentioned previously. The significance of the methacrylate hydrolysis is its role on the particulate filler surface. In this work only a small amount of carboxylate or carbonate species was observed on any filler surface by DRIFT. It is probable that deposition from aqueous solution would result in a significantly greater amount of sodium carboxylate formation. Plueddemann (21) observed a substantial decrease in the flexural strength of polyester castings of a methacrylate silane modified silica when the silane was applied from an aqueous solution with a pH greater than 10. A significant amount of the hydrolysis products was first obtained in this experiment at a pH that corresponds exactly with the initial onset of strength reduction observed by Pleuddemann. Although a number of factors may explain this decrease in strength, it is reasonable to assume that a significant degree of methacrylate hydrolysis would result in a loss in mechanical performance, since the hydrolyzed methacrylate functionality cannot form extensive organic networks through polymerization of the C═C group.

CONCLUSION

The molecular structure of γ-methacryloxypropyltrimethoxysilane deposited on particulate mineral fillers can be modeled by obtaining the hydrolyzates of a pH-adjusted aqueous alcoholic silane solution. The polycondensation reaction to polymethacryloxypropylsilsesquioxane was found to be rather selective similar to other polysilsesquioxanes. The configuration and molecular-weight distribution of the polymethacryloxypropylsilsesquioxane was dependent on the solution pH.

Fourier transform infrared spectroscopy (FT-IR) and gel permeation chromatography (GPC) indicate that, in acidic environments below pH 4, hydrolyzed γ-MPS condenses to a polymethacryloxypropylsilsesquioxane in the form of caged polycyclic blocks, which resemble a beaded chain following condensation between blocks. In more neutral and basic environments, at or above pH 4, the polycondensation mechanism results in the more equilibrated double chain ladder configuration.

These differing molecular configurations of polymethacryloxypropylsilsesquioxane were also observed on the surfaces of particulate metal oxides. The molecular structure of γ-MPS deposited on the surfaces of particulate mineral fillers as controlled in part by the pH nature of the filler should have implications with respect to composite performance. Adsorption and desorption phenomena, availability of the organic functionality, establishment of interpenetrating polymer networks, and hydrolytic stablity may all be affected by the configurational changes in the adsorbed polymethacryloxypropylsilsesquioxane.

ACKNOWLEDGMENT

The authors are grateful for the fellowship of J. D. Miller provided by Owens-Corning Fiberglas Corporation.

REFERENCES

1. J. Gahde, *Plaste u Kautschuk*, **22**, 626 (1975).
2. E. P. Plueddemann, *Proc. 27th Ann. Tech. Conf., Reinf. Plastics/Composites Div.*, SPI, Section 2-B (1972).
3. W. T. Collins and J. L. Kludt, *Proc. 30th Ann. Tech. Conf. Reinf. Plastics/Composites Div.*, SPI, Section 7-0 (1975).
4. M. A. Lutz and K. E. Polmanteer, *Coatings Tech.*, **51**, 33 (1979).
5. E. P. Plueddemann, in "Polyelectrolytes and their Applications," A. Rembaum and E. Seleguy, eds., p. 119, D. Reidel Pub. Co., Dortrecht-Holland (1975).
6. E. P. Plueddemann and G. L. Stark, *Proc. 35th Ann. Tech. Conf., Reinf. Plastics/Composites Inst.*, SPI, Section 20-B (1980).
7. A. Kaul, N. H. Sung, I. Chin, and C. S. P. Sung, *Proc. 37th Ann. Tech. Conf., Reinforced Plastics/Composites Inst.*, SPI, Section 2-E (1982).
8. E. P. Plueddemann, *Proc. 24th Ann. Tech. Conf., Reinf. Plastics/Composites Div.*, SPI, Section 19-A (1969).

9. C. W. Lentz, *Inorg. Chem.*, **3**, 574 (1964).
10. M. R. Rosen, *Coatings Tech.*, **50**, 70 (1978).
11. O. K. Johannson, F. O. Stark, G. E. Vogel, R. M. Lacefield, R. H. Baney, and O. L. Flaningam, in "Interfaces in Composites," ASTM STP 452, p. 168, (1969).
12. P. W. Erickson and E. P. Pleuddemann, in "Composite Materials, Vol. 6," E. P. Plueddemann, ed., Academic Press, New York (1974).
13. R. C. Merrill and R. W. Spencer, *J. Phys. Colloid Chem.*, **54**, 506 (1950).
14. R. L. Kaas and J. L. Kardos, *32nd ANTEC*, SPE, paper 22 (1976).
15. T. W. Greenlee, in "Adhesion Science and Technology, Vol. 9A," L. H. Lee, ed., Plenum Press, New York (1975).
16. S. Naviroj, J. L. Koeing, and H. Ishida, *Proc. 37th Ann. Reinf. Plastics/Composites Inst.*, SPI, Section 2-C (1982).
17. S. Naviroj, J. L. Koenig, and H. Ishida, *J. Macromol. Sci.-Phys.*, **B22**, 291 (1983).
18. E. P. Plueddemann, *Proc. 25th Ann. Tech. Conf., Reinforced Plastics/Composites Div.*, SPI, Section 13-D (1970).
19. E. P. Plueddemann, *Proc. 24th Ann. Tech. Conf., Reinforced Plastics/Composites Div.*, SPI, Section 19-A (1969).
20. H. Ishida and J. D. Miller, *Proc. 38th Ann. Tech. Conf. Reinforced Plastics/Composites Inst.*, SPI, Section 4-E (1983).
21. E. P. Plueddemann and G. L. Stark, *Mod. Plast.*, **92**, 74 (1974).
22. R. D. Kulkarni and E. D. Goddard, *Proc. 35th Ann. Tech. Conf. Reinforced Plastics/Composites Inst.*, SPI, Section 20-E (1980).
23. P. Kubelka and F. Munk, *Z. Tech. Phys.*, **12**, 593 (1931).
24. P. Kubelka and F. Munk, *J. Opt. Soc. Am.*, **38**, 448 (1948).
25. A. J. Barry, W. H. Daudt, J. J. Domicone, and J. W. Gilkey, *J. Am. Chem. Soc.*, **77**, 4248 (1955).
26. K. Olsson, *Arkiv. Kemi*, **16**, 209 (1960).
27. K. Olsson and C. Grönwall, *Arkiv. Kemi*, **17**, 529 (1961).
28. M. M. Sprung and F. O. Guenther, *J. Polym. Sci.*, **28**, 17 (1958).
29. J. F. Brown, Jr., L. H. Vogt, Jr., and P. I. Prescott, *J. Am. Chem. Soc.*, **86**, 1120 (1964).
30. J. F. Brown, Jr. and L. H. Vogt, Jr., *J. Am. Chem. Soc.*, **87**, 4313 (1965).
31. J. F. Brown, Jr., *J. Am. Chem. Soc.*, **87**, 4317 (1965).
32. D. R. Anderson, in "Analysis of Silicones," A. Lee Smith, ed., J. Wiley, New York (1974), p. 279.
33. J. F. Brown, Jr., *Am. Chem. Soc. Org. Plast. Chem. Preprints*, **25**, 311 (1965).
34. E. P. Plueddemann, priv. commun., Sept. 1982.
35. F. J. Boerio and S. Y. Cheng, *J. Colloid Interface Sci.*, **68**, 252 (1979).
36. S. Culler, H. Ishida, and J. L. Koenig, *J. Colloid Interface Sci.*, **96**, 69 (1983).

DISCUSSION

P. D. McLean: What happens when you bake these to say 150°C?

H. Ishida: Heat treatment is a very interesting part. We expected that upon heating, the structure will change completely, but this is not the case. The structure of silane would be maintained as long as the starting pH is the same. The heating enhances only the rate at which the final structure is formed, the structure predetermined by the initial pH. You will not change from bead-like to ladder-like structure by the heat treatment.

L. A. Utracki: The very large molecules of silane, which are becoming physically attached to the filler particles, are they the proper structures to bind with the matrix? Upon a heat treatment, do you change either the structure of the binding ability effectiveness of silane or not?

H. Ishida: If you have a large molecule, physically adsorbed, by heat treatment you may increase the chemisorption. This will depend on the nature of the filler particle. Unreacted, floating around Si-OH groups may react with the chemically adsorbed silane molecules. Even though covalent bonds will prevent solvent wash of the newly attached outside layers, I do not believe that such a poor chemical linkage can be helpful for filler-matrix interactions, which is essential to improved properties of the composites. It is understood that for a reinforcing mechanism you must have the first layer very tightly, chemically bonded to the filler particle, the second physically adsorbed outside layer of silane particles, and then loosely, but chemically bonded intermediate layer. The matrix molecules penetrate the two outside layers down to the tightly bonded one, forming a sort of inter penetrating network, reinforcing the poorly connected silane molecules. In this case you may expect a good reinforcing effect. In other words, you want to have a loose, chemically bonded to the surface silane layer. I do not think that a discussion of higher or lower hydrophobicity of silane molecules as a measure of its effectiveness has any meaning at all.

The Effect of Glass Fibers on the Rheological Behavior of Polypropylene Melts Between Rotating Parallel Plates

A. T. MUTEL *and* M. R. KAMAL

Department of Chemical Engineering
McGill University
3480 University Street
Montreal, Quebec, Canada
H3A 2A7

The Rheometrics mechanical spectrometer has been employed in the parallel plate mode to study the rheological behavior of pure polypropylene resin and melts filled with 10, 20, 30, and 40 percent by weight glass fibers. Steady-state shear data show that, for loadings above 20 percent fiber, increasing fiber loading leads to an increase in viscosity of the melt. The effect of increasing fiber content becomes smaller at higher shear rates. For the same loading range, fiber addition increases the first normal stress difference, and the effect of fiber loading becomes smaller with increasing shear rate. At 10 percent loading, the viscosity of the filled polymer melt is lower than that of the pure resin melt. These results require further confirmation.

Strain sweeps employing dynamic measurements in conjunction with the parallel plate mode of the Mechanical Spectrometer were carried out. In general, it was found the dynamic properties are strain dependent. Steady shear data employing the cone-and-plate mode were not repeatable.

INTRODUCTION

The technological importance of thermoplastics reinforced with glass fibers has increased considerably in the recent decade due to the enhancement achieved in the mechanical and thermal performance of fiber-reinforced plastics composites. However, in spite of this fact, only a few significant and dependable studies of the melt-flow behavior and rheological properties of these materials have appeared in the literature. Most of the data reported have been obtained by using capillary rheometry and the cone-and-plate mode of the mechanical spectrometer (2, 11). Han (1) obtained steady shear viscosity by using a slit rheometer. Maschmeyer and Hill (2, 3) measured steady shear viscosity of glass-fiber-filled silicone oil in the shear rate range of 10^0 to 10^4 s^{-1} by using a capillary rheometer, with capillary diameters of 1/4 and 1/8 inch (fiber length 0.01 inch). Czarnecki and White (4), White *et al.* (5), and Chan *et al.* (6) made use of the Rheometrics mechanical spectrometer in the cone-and-plate mode to measure the steady shear viscosity and principal normal stress difference of fiber filled polymer melts in the shear range of 10^{-2} to 10^1 s^{-1}. Chan, *et al.* (6), Oyanagi and Yamaguchi (7), Crowson, *et al.* (8), Crowson and Folkes (9), and Charrier and Rieger (10) measured steady shear viscosity of fiber-filled polymer melts by using capillary rheometry in the shear rate range of 10^1 to 10^4 s^{-1}. Almost all data, except Charrier and Rieger, show that addition of fibers increases the steady shear viscosity compared to the pure resin, with an increasing effect by increasing loading.

The increasing effect of fibers on shear viscosity is more pronounced at low shear rates and decreases with increasing shear rate and almost vanishes after the shear rate of 10^2 ins/s^{-1}. Fiber length was found to be an important parameter for the shear viscosity, although there are some contradictory data published (9). Contradictory results may be attributed to the difficulties in controlling fiber-length distribution. The principal normal stress difference was found to be increased by the addition of fibers, with the effect increasing with increasing loading. The few results available show a nonlinear dependence on shear rate, while the relation is linear when plotted against shear stress. No dynamic test data for fiber-filled polymer melts have been reported.

The aim of the present study is to investigate the steady and dynamic rheological properties of glass-fiber-filled polypropylene melt by using a Rheometrics mechanical spectrometer. Both cone-and-plate and parallel plate modes of operation are employed.

EXPERIMENTAL

Materials

Polypropylene (PP) formulations filled with 0, 10, 20, 30, and 40 percent by weight glass fiber supplied by the Fiberfill Division of Dart Industries were used in the

experiments. The compound was available in the form of pellets with fiber lengths of the order of 3 mm and a diameter of 10 μm. Fiber lengths were reduced after compression molding to prepare the specimens for testing in the mechanical spectrometer, showing a broad distribution between 300 and 2000 μm. The material was compression molded into disc shaped specimens with a diameter of 12.5 mm and a thickness of 2.0 mm at 220°C and 25,000 psi. Molding time was approximately one minute.

Apparatus

A Rheometrics Mechanical Spectrometer was used for steady shear and dynamic measurements in the concentric parallel plate and cone-and-plate modes. Both diameters of the plate and cone were 12.5 mm. Cone angle was 0.4 rad and the parallel plate gap was 1.0 mm. The shear stress, τ_{12} ($\dot{\gamma}$), was calculated from the measured torque, T, and the principal normal stress difference, N_1 ($\dot{\gamma}$), from the measured thrust, F, according to standard procedures. The parallel plate viscosity data were obtained without making any corrections for the variability of the shear rate in the gap.

RESULTS

Steady Shear Experiments

Steady shear results obtained from cone-and-plate experiments were not repeatable. Material easily leaked out of the gap between the cone and plate and exhibited degradation. If the dimensions of the gap (~ 50 μm) and the fibers (diameter ~ 10 μm and maximum length around 2.5 mm) are considered, it is clear that considerable wall effect and initial orientation effects will be present. Accordingly, it was decided to carry out the experiments in the parallel plate mode, with a gap of 1 mm. Moreover, the relaxation time for the material after the adjustment of gap thickness was around five minutes for the parallel plates, while it varied between 45 and 60 minutes for the cone-and-plate measurements. The time that the polymer was exposed to high temperature was about ten times longer for the cone-and-plate case, which cause the degradation of the polymer.

Plots of steady shear viscosity, η, as a function of shear rate, $\dot{\gamma}$, measured in the parallel plate mode for pure PP and various loadings of glass fibers are shown in *Fig. 1*. The reported lines represent averages of five measurements at each shear rate. Percent deviation from the average increases with increasing loading; for 40 percent glass fibers, average deviation is around 15 percent, while that for pure resin is 4 percent. All compositions show shear thinning behavior, as expected. Addition of fibers increases the shear viscosity for the same shear rate and the effect increases with increasing loading, except for the case of 10 percent fiber addition. Shear viscosity values for 10 percent glass fiber in PP are always lower than for pure resin. Also, the effect of fibers on viscosity decreases with increasing shear rate.

The dependence of the first normal stress difference, measured by parallel plates, on shear rate is shown in *Fig. 2* for different loadings. Fiber addition increases the first normal stress difference, and the effect increases

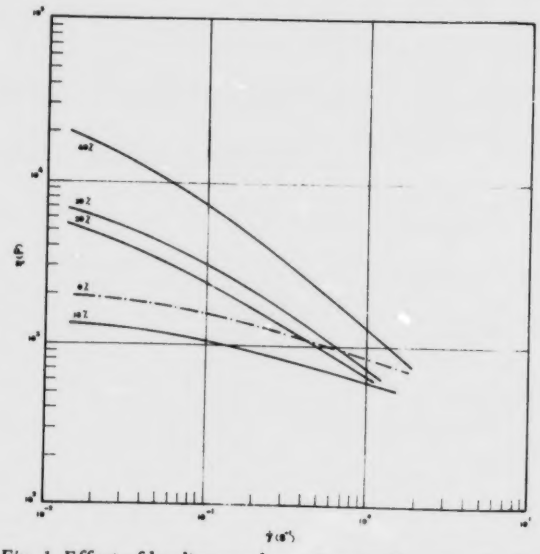

Fig. 1. Effect of loading on shear viscosity functions for fiber-filled PP melt at 250 C.

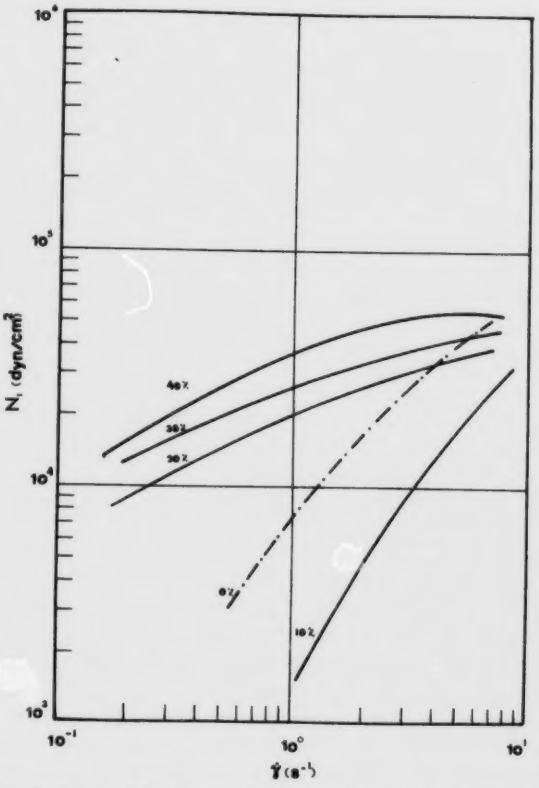

Fig. 2. Effect of loading on first normal stress difference as a function of shear rate for glass-fiber-filled PP melt at 250 C.

with increasing loading, except for the case of 10 percent fiber content again. The effect of loading decreases with increasing shear rate, and the first normal stress difference becomes equal to, even lower than, that of the pure resin.

White, *et al.* (5) observed a linear relation between the first normal stress difference and shear stress. Ac-

cordingly, for the results of this work, first normal stress difference was plotted against shear stress. Although a linear dependence of the first normal stress difference on shear stress was observed for pure PP and 10 percent filled PP, the relation is non-linear for higher loadings (*Fig. 3*).

In *Fig. 4*, the principal normal stress coefficient is plotted against shear rate for various loadings. The relation is linear for loadings higher than 10 percent, but it is non-linear for pure PP and 10 percent filled PP.

Dynamic Measurements

Dynamic tests were carried out only with the parallel plate mode. Strain sweep tests were made to determine the linear viscoelastic range. *Figures 5* and *6* show the dependence of storage modulus, G', and complex viscosity, η^*, on strain. Although pure PP has a wide linear viscoelastic range (5 to 50 percent strain), all of the fiber-filled formulation exhibit strain dependence of the measured properties in the strain range considered (5 to 95 percent). Strain sweep experiments were repeated at lower frequencies with 20- and 30-percent filled PP to observe the effect of frequency on strain dependence, at lower frequencies. *Figures 7* and *8* show the effect of frequency for 20- and 30-percent filled PP. For 20-percent filled PP, there is no effect of strain on the dynamic properties for strain levels above 50 percent at a frequency of 1 cycle per second. For 30 percent loading, a strain-independent region is observed at frequencies of 0.5 and 0.1 radian per second.

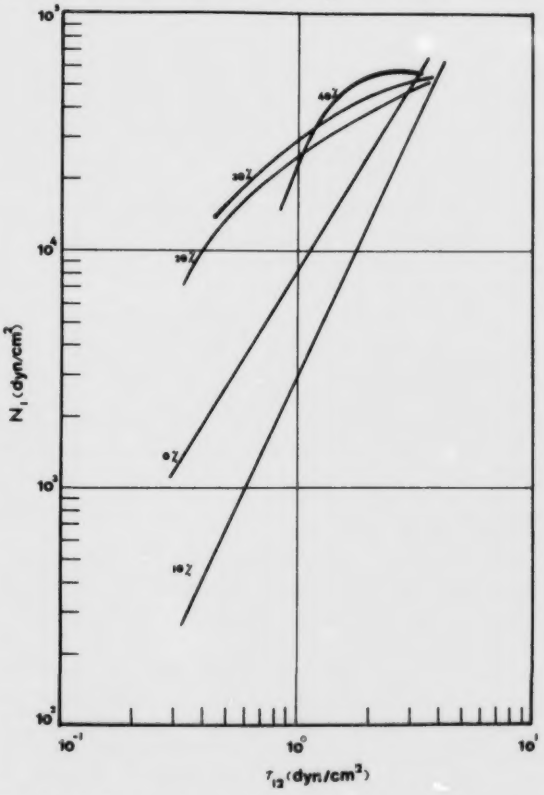

Fig. 3. Effect of loading on first normal stress difference as a function of shear stress for glass-fiber-filled PP melt at 250 C.

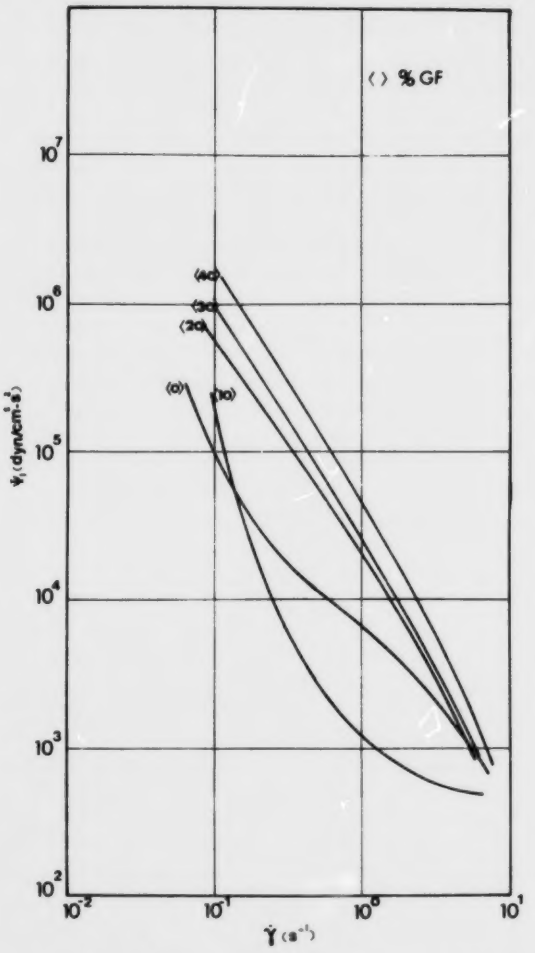

Fig. 4. Effect of loading on first normal stress difference coefficient, Ψ_1, as a function of shear rate, $\dot{\gamma}$, for glass-fiber-filled PP melt at 250 C.

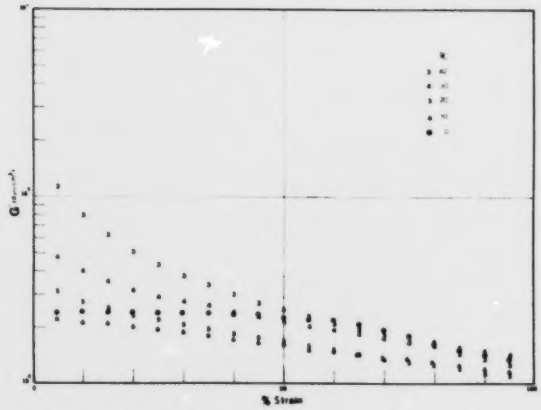

Fig. 5. Effect of loading on storage modulus, G', as a function of strain, γ, for glass-fiber-filled PP at 250 C.

Frequency sweep results for pure PP are shown in *Fig. 9*. Repeatability for the data is within 5 percent. At high frequencies, surface deformations increase deviations from the average.

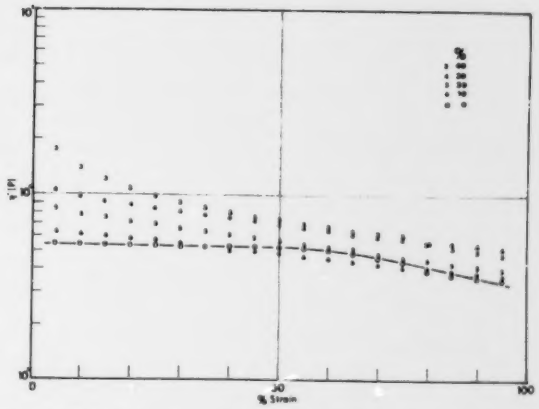

Fig. 6. Effect of loading on complex viscosity, η^*, as a function of strain, γ, for glass-fiber-filled PP melt at 250 C.

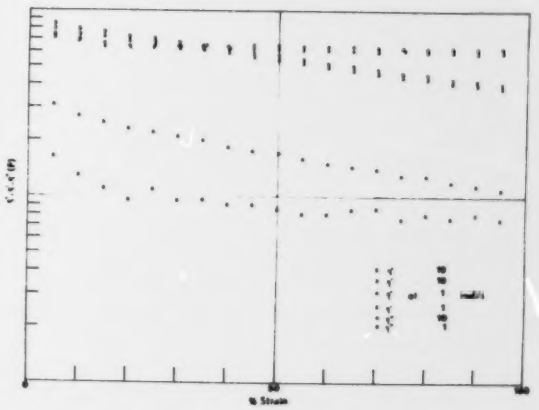

Fig. 7. Effect of frequency on dynamic properties as a function of strain for PP 20 percent glass fibers at 250 C.

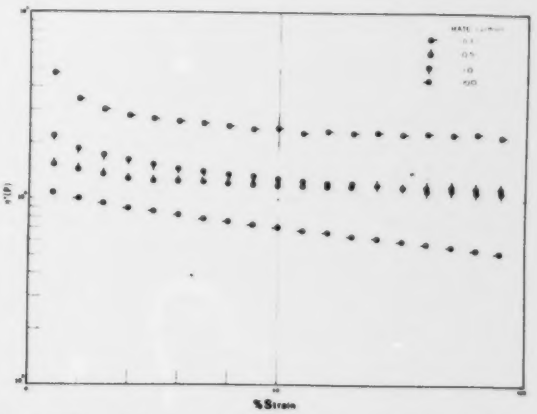

Fig. 8. Effect of frequency on complex viscosity, η^*, as a function of strain, γ, for PP 30 percent glass fibers at 250 C.

DISCUSSION

Steady Shear Measurements

Dependence of steady shear viscosity on shear rate is consistent with earlier results of other workers in the sense that viscosity is increased by filler addition and

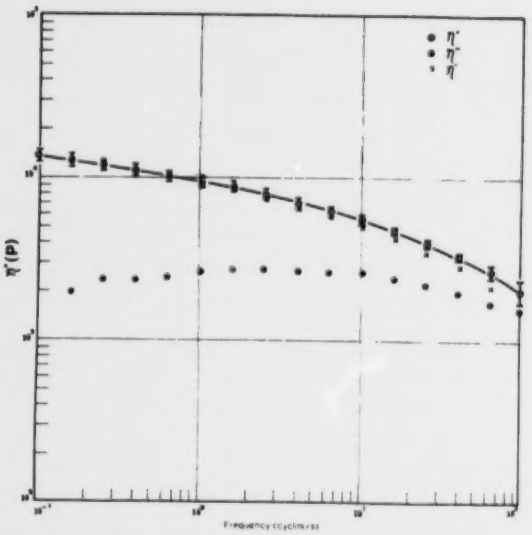

Fig. 9. Dynamic properties, η^*, η', and η'' as a function of frequency for pure PP melt at 250 C.

that the effect of fillers on viscosity increases with increasing loading and decreases with increasing shear rate (except 10 percent fiber addition). The increasing effect of fibers on viscosity is explained by the increased viscous dissipation due to shearing between fibers and particle/particle interactions. However, no convincing explanation has been proposed for the decrease in this effect with increasing shear rate. Our results for 10-percent fiber addition show a reverse effect. Addition of 10-percent glass fibers decreases the viscosity at the same shear rate. The same decreasing effect is observed for the first normal stress difference with 10-percent fiber addition, while, at higher loadings, the first normal stress difference is increased relative to the pure resin. A totally different effect for 10-percent fiber content when compared with higher loadings is clearly observable in plots of first normal stress difference, N_1, against shear rate and shear stress, and principal normal stress coefficient against shear rate.

A variety of factors might contribute to reducing viscosity at 10-percent loading. One factor might be the degradation of the resin during processing and testing. This possibility is currently under investigation. Another factor might be due to the plasticizing influence of some coupling agents. In fact, Chaffey (12) has made similar observations where the addition of low concentrations of solid particles have contributed to lowering the viscosity of the melt.

There seem to be two competing mechanisms influencing the rheological behavior of fiber-filled polymer melts. One is the rupture and partial destruction of polymer chain entanglements by the shearing action between the fibers and by fiber motion, which decreases the viscous dissipation and elastic effects caused by polymer chain entanglements. The other is the increased viscous dissipation due to hydrodynamic interaction between fibers, particle/particle interactions, and fiber/fiber entanglements. The first factor is dominant at low fiber loadings, because, at low concentra-

tions, particle/particle interactions and fiber entanglements are not considerable. However, at high loadings, particle interactions and especially fiber entanglements play a significant role. High shear rates disrupt the fiber entanglements and cause fiber breakage, which reduced particle/particle interactions (particle/particle interaction probability is directly related to particle length).

A complicating factor in the parallel plate measurements is flow instabilities and material loss from the gap at higher shear rates. Melt instabilities and material loss have been observed in the present experiments at shear rates above 1 s^{-1}. Accordingly, the data are not reported for shear rates above 1 s^{-1}.

Earlier workers generally used either capillary or cone-and-plate rheometry. In cone-and-plate, the gap between the cone and plate (~50 to 100 μm) is of the same order of magnitude as fiber diameter and much smaller than fiber length. Accordingly, motion of the fibers is restricted. Thus, cone-and-plate data would probably be influenced by wall effect. On the other hand, fibers rotate around their axes and translate end-to-end in the gap between parallel plates, as observed visually. Entanglements of fibers and disruption of polymer chain entanglements are less likely.

In capillary flow, fibers are aligned in the flow direction parallel to capillary walls, as a result of converging flow at the entrance of the capillary. The velocity profile is blunt for power law fluids, especially suspensions, in the capillary. Shearing takes place in a narrow region close to the wall. The core part passes through almost unsheared. The net effect is to restrict the motion of fibers and reduce the rupture and partial destruction of polymer chain entanglements. Therefore, hydrodynamic interaction among fibers is the dominant mechanism. At low shear rates, a zero shear viscosity region is usually observed in conjunction with most polymer melts. A zero shear viscosity was observed for pure polypropylene and 10-percent filled material, but at higher loadings, no zero shear viscosity was observed for the shear range employed.

Dynamic Measurements

Dynamic measurements show a strong dependence of dynamic properties on strain for the filled polymer melts at a frequency of 10 radians per second, although pure resin dynamic properties show strain-independent behavior over a broad strain range. This is not surprising since, as predicted by various theoretical models, fiber orientation, which influences rheological properties, is strongly affected by strain.

It is seen in *Fig.* 5 that the elastic storage modulus is increased considerably at low strains with the addition of fibers. The effect of fibers is very pronounced in the case of 30 and 40 percent loadings. The effect is restricted to strains below 15 percent and 20 percent loading. Again, the storage modulus for 10 percent loading is lower than that of the pure resin. At high strains, the values for storage modulus for 30 and 40 percent loadings are almost the same as those of the pure resin. For 10 and 20 percent loadings, the modulus is slightly lower than that of the pure resin. These results suggest that elastic energy is used for the reorientation of fibers in the composite at low strains. The effect of fibers on elastic energy storage diminishes as a stable equilibrium orientation is approached.

Data on complex viscosity (*Fig.* 6) show that the addition of fibers increases viscous dissipation in the melt. The complex viscosity at 30 and 40 percent loadings is higher than that of the pure resin, throughout the strain range employed. At 10 and 20 percent loadings, complex viscosities are higher than those of the pure resin for strains below 40 percent. The difference diminishes between 40 and 90 percent strain levels.

Figures 7 and 8 show the effect of frequency on η', η'', and η^* for 20 and 30 percent loadings. It is seen that, at a frequency of 10 radians per second, η'' decreases with increasing strain over the whole range of strains covered. However, at a frequency of 1 radian per second, η'' decreases with increasing strain initially and levels off above a strain of 20 percent. These results suggest that, at frequencies of 10 radians per second and higher, the experimental time is shorter than the characteristic time associated with formation of a stable structure in the system.

The other two dynamic parameters, η' and η^*, exhibit values that are very close to each other. The strain dependence of these two functions is similar to that of η''. For strains greater than 40 percent, values of η' and η^* at 10 radians per second become lower than those observed at 1 radian per second. However, below 40 percent strain, η' and η^* values observed for 10 radians per second are higher than those for 1 radian per second, which may be the result of increased viscous and elastic dissipation during fiber structure reorientation.

The results shown in *Fig.* 9 suggest that increasing the frequency leads to a larger contribution of the elastic component, η'', to the overall complex viscosity, η^*. The overall effect of increasing frequency, especially at strains above 40 percent, is to lower the effective viscosity of the system, η^*. These observations are in agreement with the types of behavior observed with pure melts, except in the low strain range, where increased elastic contributions and viscous dissipation suggest that properties are highly dependent on the transient structure of the system.

CONCLUSIONS

Parallel plate rheometry has been employed to study the steady shear viscosity and normal stress behavior of glass-fiber-reinforced polypropylene melts at shear rates between 0.01 and 1.0 s^{-1}. Fiber loadings between 10 and 40 percent were included in the study. For fiber loading above 10 percent, both the viscosity and normal stress at a given shear rate are increased by increasing the fiber loading. The effect of fiber loading diminishes at higher shear rates. These results are in agreement with the findings of other workers. At 10 percent loading, both the shear viscosity and normal forces appear to be lower than in the pure resin. It is necessary to confirm this observation, which should be significant, if confirmed. Dynamic shear measurements reflect the

importance of fiber orientation as indicated by the strain dependence of the dynamic parameters, especially at low strains. These measurements suggest that the elastic contribution to the complex viscosity increases with shear rate.

ACKNOWLEDGMENTS

The authors would like to acknowledge financial support from the following organizations: Engineering Mechanics Department of General Motors Corporation, Natural Sciences and Engineering Research Council of Canada, and Ministère de l'Education of the Government of Quebec. Discussions with Dr. J. M. Charrier from the Chemical Engineering Department at McGill University were also helpful.

NOMENCLATURE

F	force on the plate, grams.
G'	storage modulus, dynes per cm^2.
G''	loss modulus, dynes per cm^2.
H	gap between plates, mm.
N_1	principal normal stress difference, dynes per cm^2.
R	radius of plates, mm.
T	torque, grams.
τ_{12}	shear stress, dynes per cm^2.
γ	strain.
$\dot{\gamma}$	strain rate, s^{-1}.
θ	shearing angle, radians.
ω	frequency, radians per second.
η^*	complex viscosity, dynes/cm^2
η'	dynamic viscosity, dynes/cm^2
η''	imaginary part of complex viscosity, dynes/cm^2

REFERENCES

1. C. D. Han, C. Sandford, and H. J. Yoo, *Polym. Eng. Sci.*, **18**, 849 (1978).
2. R. O. Maschmeyer and C. T. Hill, ACS Organic Coat. and Plast. Chem., 166th Meeting of the ACS, Chicago, Ill, Aug. 27-29, 1973.
3. R. O. Maschmeyer, and C. T. Hill, *Trans. Soc. Rheol.*, **21** 195 (1977).
4. L. Czarnecki, and J. White, *J. Appl. Polym. Sci.*, **25**, 1217 (1980).
5. J. L. White, L. Czarnecki and H. Tanaka, *Rubb. Chem. Technol.*, **53** 823 (1980).
6. Yu Chan, J. L. White, and Y. Oyanagi, *J. Rheol.*, **22**, 507 (1978).
7. Y. Oyanagi, and Y. Yamaguchi, *J. Soc. Rheol. Jap.*, **3**, 64 (1975).
8. R. J. Crowson, M. J. Folkes, and R. F. Bright, *Polym. Eng. Sci.*, **20**, 925 (1980).
9. R. J. Crowson, and M. J. Folkes, unpublished.
10. J. M. Charrier, and J. M. Rieger, *Fibre Sci. Technol.*, **7**, 161 (1974).
11. T. T. Tee, and C. Y. Yap, *SPE ANTEC Techn. Papers*, **24**, 262 (1978).
12. C. E. Chaffey, Proc. 2nd World Congress of Chemical Engineering, **6**, 301 (1981).

DISCUSSION

E. B. Bagley: I am very pleased to see that you used a parallel plate rheometer. I would like to make a general comment—it is a very appropriate rheometer to study the heterophase systems. I have a series of questions: (1) did you look into the effect of sample thickness in parallel plate mode?

A. T. Mutel: Yes. Below 0.5 (mm) the results were irreproducible—we have been using fibers of the length 0.3 to 1.0 (mm). However we found that for thicknesses above 0.8 mm to 1.2 mm, the results were very reproducible.

E. B. Bagley: The second question: For PP, your flow curve does not reach the Newtonian region. Your results are typical for a system which is changing because of temperature instability, degradation, etc. My question is: to what extent are you certain the 10 percent viscosity drop for composites below that of pure PP is not due to degradation?

A. T. Mutel: We have made time sweeps for these materials and there was no degradation within the normal experiment time, i.e., about 15 minutes. Our time sweeps were for about 1 hour and the response was stable.

M. E. Ryan: Can you be absolutely certain that the PP is the same at 0 percent as at 40 percent glass fiber?

A. T. Mutel: We are assuming this. The PP used at 0, 10, and 20 percent comes from the same batch.

M. R. Kamal: We should really emphasize that in this work we are looking for an optimum experimental technique, rather than detailed characterization of the material. We do not wish to stand very strongly behind the fact that 10 percent goes below PP. What we shall do after selecting the technique is to go to more controlled resins, fill them ourselves or have control over how they are filled with the glass and select the coupling agent that we need. I should add another point that Mr. Mutel did not mention. Our ultimate objective is to model the rheological behavior of these materials, via the most accurate measurements of the rheological properties, so that we can find the constitutive relations which will describe the flow. This is part of an effort toward modeling a commercial process, like injection molding of fiber-filled PP and similar materials.

S. Newman: I do not want to dwell on this 10 percent. It looks a little strange and it may very well be that in the blending/compounding there was a molecular-weight degradation, which may have exceeded the effect of addition of 10 percent of filler. It is very hard to understand and accept this 10 percent behavior. Because of the fiber orientation effect, it may make a difference if you do your frequency sweep from low to high frequency versus sweeping from high to low. I wonder if you did the measurements in one or in both directions and if this made a difference?

A. T. Mutel: With these materials it takes about 10 minutes to reach a steady value. For this reason we took one data point per sample. There was no frequency sweep.

R. Simha: In the light of what Professor Kamal said, it is probably premature to ask the question. Can you say anything about the relationship for a given system, about the static and dynamic moduli or viscosities?

What often is done is to accept the relationship developed for the static situation automatically to the complex modulus. Can anything in this direction be gleaned from your results at this stage?

A. T. Mutel: As shown in the text of the manuscript, there is reasonable agreement between dynamic and steady shear measurements.

S. Newman: The comparison would have to be done for static and dynamic moduli in shear.

R. Simha: Indeed.

A. T. Mutel: That has been the case in our work.

A. Ishida: What effect do you see in fiber/fiber interaction? At what fiber loading do you start seeing the interactions? At 20 percent?

A. T. Mutel: Much less than that.

L. A. Utracki: You can see this already at about 5 volume percent. Obviously the value depends on the aspect ratio.

A. Ishida: Do you know what the surface treatment of these fibers was?

A. T. Mutel: No.

L. A. Goettler: The level at which the interaction occurs must depend on the fiber length. You said that the length varied from 0.3 to 3 (mm). Was that the distribution in a given sample?

A. T. Mutel: Yes. You start with 3 (mm) fibers, but during the sample preparation they break so you get fibers of the length anywhere from 0.3 to 3.

L. A. Goettler: Is it a uniform or weighted toward one end distribution?

A. T. Mutel: Fairly uniform.

Rheology of Mica-Reinforced Polyethylene Melts*

B. FISA and L. A. UTRACKI

Industrial Materials Research Institute
National Research Council of Canada
75, boul. De Mortagne Boucherville,
Québec, Canada J4B 6Y4

Seven samples of HDPE containing 0, 2, 5, 10, 25, 40 and 60 weight percent of mica were prepared on a roll mill at 200°C. The samples were tested at T = 150, 170, 190 and 210°C for a wide range of rate of deformation from 10^{-2} to 2×10^{4} s^{-1}. Both capillary and rotational rheometers were used. The samples were found to be thermally stable. The results indicate that η, G', and G'' increase with mica content for the whole range of deformation rates. The relaxation time spectrum for the sample containing 60 weight percent of mica showed a particulate contribution. The zero shear viscosity was discussed in terms of suspension theories.

INTRODUCTION

The mica group of minerals is characterized by a nearly perfect cleavage of the monoclinic sheet-like crystals of the approximate formula (1): $KMg_3AlSiO_{10}(OH,F)_2$. Ground and classified mica flakes are being used in plastics, either alone or with other reinforcing fillers such as glass fibers. The main purpose of mica is to enhance the stiffness, reduce the warpage, gas diffusivity, and thermal expansion, as well as to improve the chemical resistance (1, 2). The most important parameter related to the reinforcing effect of mica is the flake aspect ratio, p, i.e., the flake diameter divided by the flake thickness. High aspect ratios are desirable to maximize the mechanical properties of mica-reinforced plastics. It follows that attrition of mica flakes during processing is detrimental. Reduction of p was observed not only during extrusion of filled polypropylene (PP) (3) but even during dry blending with poly(vinyl chloride) (4).

Another important factor which strongly affects the ultimate properties of the mica-containing materials is the flake orientation (5), determined by the rheology and processing. Properties such as tensile strength, modulus of elasticity, flexural modulus, impact strength, and permeability can be improved by proper flake orientation. Like other fillers, mica is frequently surface-treated with various coupling agents. The treatment improves the filler dispersion in the resin and enhances the mica-polymer interaction.

The rheology of filled polymer melts has been receiving increased attention. Two recent reviews provide an excellent overview (6, 7). In particular, it is worth mentioning the work by Okuno and Woodhams (3), who studied the flow of mica-filled PP in the range of the shear rate, $\dot{\gamma}$, from 4 to 15 s^{-1}(5). The authors reported that flake degradation as well as orientation took place. White, *et al.* (8) reported steady state flow data of polystyrene containing 20 weight percent different fillers, including mica. Similarly, as reported for glass-fiber-filled polymer melts (9, 11), the mica-composites also did not show the yield phenomenon. Chaffey, *et al.* (12, 13) studied the effect of the sizing agent on flow and the mechanical properties of mica-filled polypropylene. Here also yield has not been observed.

The objective of the present work is to study the rheological behavior of mica-filled polyethylene over a broad range of shear rates, frequencies, filler concentrations and temperatures.

EXPERIMENTAL

Materials

The high-density polyethylene, HDPE, used in this study was an injection grade having a density ρ = 0.955 (g/ml) and the melt index, MI = 14 (g/10 min). The mica was a commercial silane-treated phlogopite (Suzorite 200NP). The average aspect ratio, p, for this grade is reported to be about 35 (1).

Preparation of the samples

The materials were blended using a laboratory roll mill (Brabender, Model PM2000) with rolls heated to 200°C. After the resin had melted, the mica was added gradually. The total mixing time was 15 minutes. All the mixing parameters—roll speed, gap between rolls, total sample volume—were kept constant for all compositions from 0 to 60 weight percent of mica. After compounding, the material was granulated in a laboratory granulator. For the dynamic-mode tests the samples were compression-molded at 170°C for 8 minutes into 5 cm diameter, 2 mm thick discs. The composition of the samples is given in *Table 1*.

*Based on the presentation given at the symposium on Rheological Properties of Polymers, held during 65th CIC Chemical Conference, Toronto, May 31 through June 2, 1982.

Table 1. Characteristics of the HDPE/Mica Samples

Sample No.	Mica Content nominal c(wt%)	Mica Content measured[a] ϕ(vol. fract.)	Flake diameter, d, (μm)	ΔE_η, (ω = 10) (kcal/mol)
1	0	0.0000	113	4.30
2	2	0.0062	107	—
3	5	0.0152	104	4.43
4	10	—	—	4.50
5	25	0.0818	94	4.20
6	40	0.1532	91	4.24
7	60	0.2910	92	(4.98)

NOTE: (a) calculated from pyrolytically determined mica content assuming density of phlogopite ρ = 2.83 and ρ(PE, 150°C) = 0.781 (g.ml).

Rheological measurements

The Rheometrics mechanical spectrometer Model 605 (RMS) was used in the dynamic mode with the 5 cm diameter plates. Initially, each sample was tested at constant frequencies, ω = 1 and 10 rad/s to verify the strain, γ, dependence of the storage, G', and loss, G'', moduli. On the basis of these tests all the experiments were performed at γ = 35 percent. Then the thermal stability of the samples was examined again at ω = 1 and 10. The remaining procedures were identical to those described previously (14).

The Instron capillary rheometer (ICR) was used to measure viscosity at shear rates between 1 and $10^4\,s^{-1}$. A series of capillaries of various lengths and diameters were used (*Table 2*). The results were computed using the Bagley and Rabinowitsch corrections (15, 16).

Gel permeation chromatography, GPC

Waters Associates GPC Model 150C equipped with five μ-Styragel columns (500, 10^3, 10^4, 10^5, 10^6, Å) operating at 135°C with 1, 2, 4 trichlorobenzene (TCB) as solvent was used. Polymer solutions were prepared by heating 0.1 g of the sample in a solution of 0.1 g of 1, 1, 3tris-(5-tertbutyl-4-hydroxy-2-methylphenyl)-butane and 0.lg of dilaurylthiodipropionate (stabilizers) in 100 ml of TCB at 145°C for about 100 minutes. The data were evaluated using Waters Model 130 Data Module with the sixth version of the program (17). The instrument was calibrated using 26 standard polystyrene samples dissolved in TCB at 135°C. There was no attempt to obtain either the absolute molecular weights or the branching index of the polyethylenes.

Particle size analysis

The particle size distribution of mica powder was determined using the HIAC-PA720 particle size analyzer equipped with the CMH-300 sensor. The polyethylene/mica granules were pyrolyzed in an oven at 450°C for about 15 minutes. The resulting mica powder was suspended in demineralized and filtered water at a concentration of about 0.004 g/l. The suspension was then analyzed for particle size distribution. The complete description of this technique including the calibration procedure used for mica powder will be described elsewhere (18).

Table 2. List of ICR Capillaries.

N°	Length (cm)	Diameter (cm)	L/D
1	5.10	0.127	40
2	1.27	0.127	10
3	0.63	0.127	5
4	0.13	0.127	1
5	2.54	0.076	33
6	0.038	0.076	0.5

Scanning electron microscopy, SEM

The Suzorite 200NP mica and its compounds with HDPE were observed under SEM-JEOL Model JSM-35CF. The samples were gold-coated using Technics Hammer V high vacuum metalization chamber.

RESULTS AND DISCUSSION

A SEM-photograph of mica is shown in *Fig. 1A*. There is a very broad distribution of flake size and shape (viz. *Fig. 2*). The volume average flake diameter of the original material was determined as d_v = 113 μm. It is known (19) that the flow properties of non-uniform particulates correlate with the "volume-to-surface" or in the polymer nomenclature, the z-average diameter, d_z; its value was calculated as d_z = 65 μm. Taking the latter value and assuming the flake thickness to be independent of

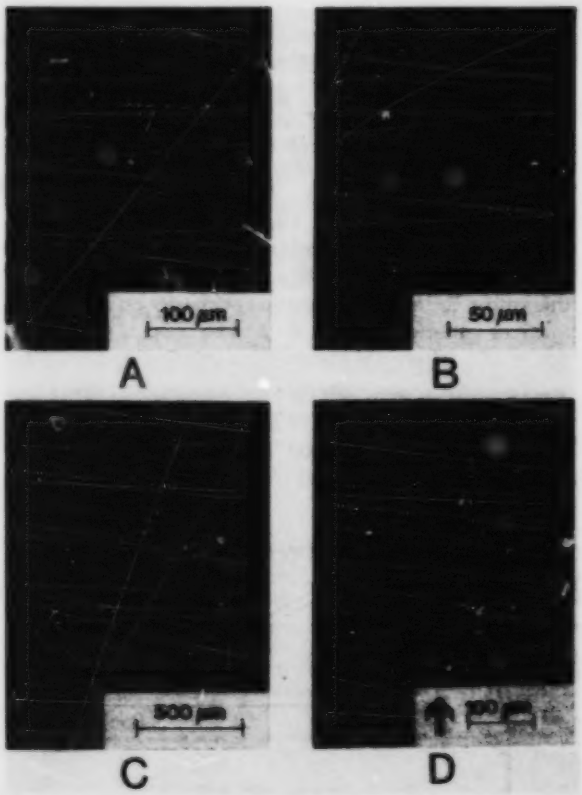

Fig. 1. Morphology of mica and mica/HDPE extrudates at 190°C. 1A. Mica as received. 1B. Surface texture of a sample containing 60 percent mica extruded with a 0.076 cm diameter capillary L/D = 33, $\dot{\gamma}$ = 212 s^{-1}. 1C. Same as 1B, at lower magnification. 1D. Longitudinal section of a sample containing 25 percent mica; 0.076 cm diameter capillary, L/D = 33, $\dot{\gamma}$ = 183 s^{-1}. The arrow indicates the flow direction.

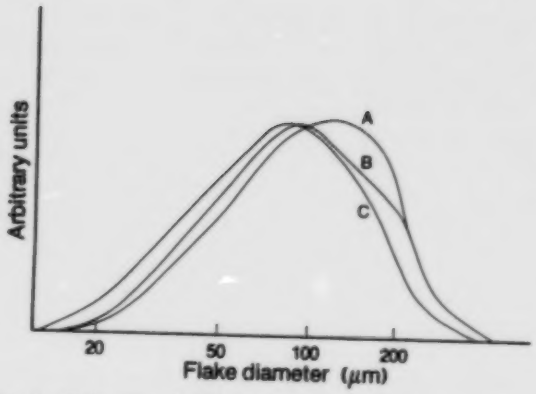

Fig. 2. Flake size distribution curves. A. Virgin mica. B. Extracted from sample with 2 percent mica. C. Extracted from sample with 60 percent mica.

the size (only a small, systematic change of thickness with d_v was observed), the rheologically important aspect ratio was computed as $p_s = 20.2$.

It can be seen in *Table 1* and *Fig. 3* that the attrition of flakes increases with the mica content. The data can be fitted to the growth function:

$$d_v = \alpha_0/(1 - \alpha_1 \exp\{\alpha_2 \phi\}) \quad (1)$$

with the following values of the parameters: $\alpha_0 = 92$ μm $\alpha_1 = 0.18584$ and $\alpha_2 = 30$; the standard error of fit is: $s = 0.8$ percent.

The significance of the exponential term falls below 3 percent at the flake overlap concentration, $\phi_c = 0.06$: i.e., while at low ϕ, the attrition sharply increases with concentration at and above ϕ_c it reaches its maximum and constant value. This may suggest that under the constant processing conditions (constant temperature, T, rate of shear, $\dot{\gamma}$, and compounding time, t), as used in this study, the attrition depends primarily on the probability of particle collision, P. At low concentration $P \propto \phi^2 x = \phi^{8/3}$, where x is the collision crossection area (19),

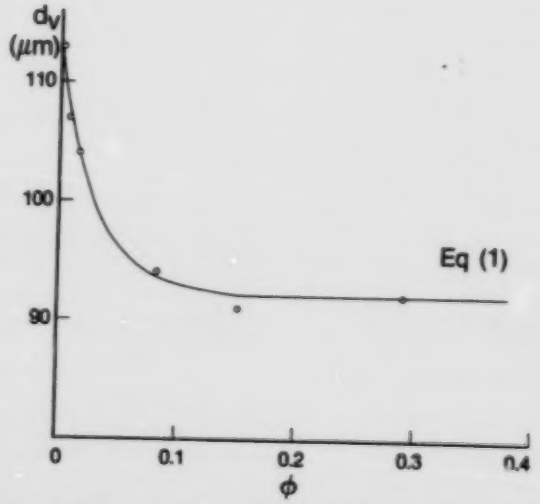

Fig. 3. Volume average diameter of mica flakes, d_v, after processing versus the mica volume fraction, ϕ; curve – Eq 1.

while at $\phi > \phi_c$, $P \simeq 1$. To determine the mechanism, the effect of all parameters,—ϕ, T, $\dot{\gamma}$, t, the flakes diameter and their distribution will have to be studied. It is interesting to see in *Fig. 2* that attrition first affects the largest particles.

It was reported (4) that attrition has a small effect on the flow of mica-filled polypropylene. However, since it reduces the aspect ratio, which in turn governs the mechanical properties (20), the attrition should be minimized. The data of *Fig. 3* illustrates the difficulties encountered in dispersing the micas; despite high fluidity of the HDPE, (MI = 14) and high T used during compounding (200°C), about 20 percent reduction in d_v and p did occur.

The surface texture of an extruded polyethylene strand is shown at two different magnifications in *Fig.1B* and *1C*. A considerable surface roughness, due to mica flakes protruding from beneath the surface, is visible. The roughness, present in all HDPE/mica samples, is particularly pronounced at high mica content. Knutsson *et al.* (21) have reported that in glass-fiber-filled polycarbonate melts, the surface roughness was decreasing with $\dot{\gamma}$, probably as a result of increased fiber orientation in the extrudate. For our HDPE/mica system, the roughness was found to be independent of $\dot{\gamma}$. The roughness is most likely due to a very large difference in HDPE density (about 25 percent!) between the ambient and extrusion temperatures.

A photomicrograph of a longitudinal cross section of an extruded strand containing 25 percent mica shown in the *Fig. 1D* illustrates the orientation of the mica flakes in the shear field. The flakes are preferentially oriented in the flow direction throughout the sample. This observation is at variance with that reported by Okuno and Woodhams (3), who, working with mica-filled polypropylene, observed a more complex flow pattern; in the center of the extrudate, the orientation was predominately perpendicular to the flow direction, becoming gradually parallel in the region close to the surface. It should be noted that Okuno and Woodhams used a die with a diameter about 10 times larger than those used in this work and L/D = 9. It is possible that under these conditions, an equilibrium orientation was not reached at the exit of the die.

In *Fig. 4* the result of strain, γ, scan for HDPE is shown. It is apparent that while the loss modulus, G'', and the complex viscosity, η^*, are independent of γ within the range of 5 to 70 percent, the storage modulus continuously changes with γ. The decrease of all the three functions at $\gamma > 70$ percent is related to the sample loss, while the initial decrease in G' is an artifact of the measurements, caused by the non-relaxed condition of the sample; the scan in the reverse direction from $\gamma = 65$ to 0 percent as well as a slower scans with 1 percent step (not 5 percent as in *Fig. 4*) both demonstrate this quite convincingly.

In *Figs. 5* and *6*, the G'' versus γ dependence for HDPE/mica samples (c = 0, 2, 5, 10, 25, 40 and 60 weight percent) at 170°C and at $\omega = 1$ and 10 rads/s, respectively is shown. It is apparent that at the strain $\gamma =$ 35 percent, used in this work, linear response is ob-

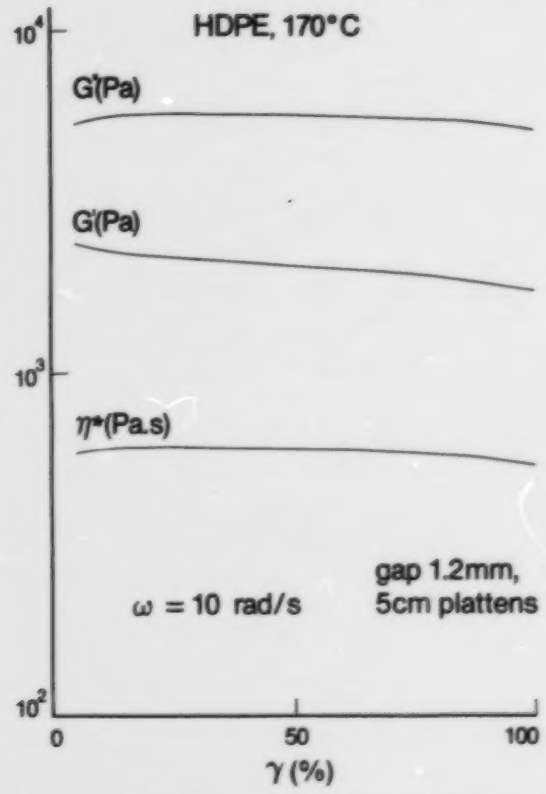

Fig. 4. Storage modulus, G', loss modulus, G", and complex viscosity, η, versus strain, γ, for neat polyethylene at 170°C and at a frequency, ω = 10 rad/s.*

tained only for the samples containing $c < 10$ percent of mica. The deviation from linearity increases with c, ω, and γ.

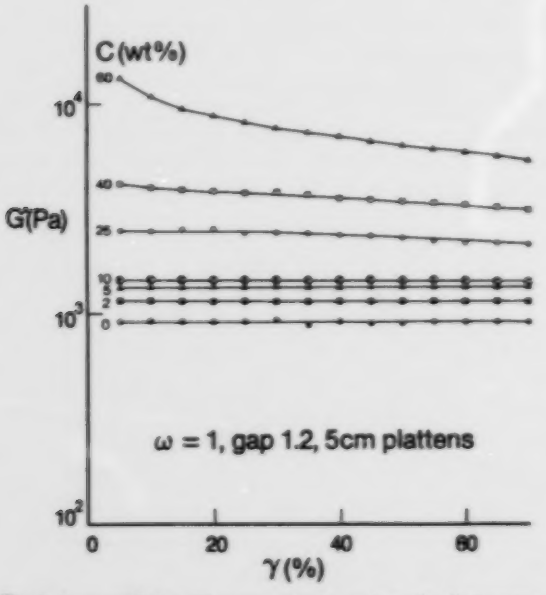

Fig. 5. Loss modulus, G", versus strain, γ, for polyethylene/mica samples at 170°C and ω = 1 rad/s; the numbers indicate mica content in weight percent.

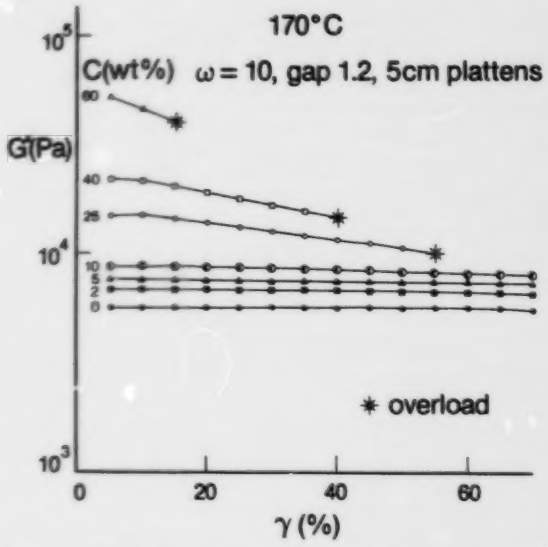

Fig. 6. Loss modulus, G", versus strain, γ, for polyethylene/mica at 170°C and ω = 10 rad/s; mica content (weight percent) is indicated.

The thermal stability of HDPE is illustrated in *Fig. 7*; at 210°C the resin is stable only up to 10 minutes. Exposure for longer times causes a very slight increase of G'' and η^* but quite a significant increase, by 85 percent, of G'. It seems that some crosslinking is taking place. To test this hypothesis, the GPC of the HDPE at various stages of processing and measurements was taken. The results, reported in *Table 3*, do not indicate any increase of molecular weights, rather a slight decrease (within the range of experimental error of GPC, ±6 percent of M_z is observed. The most likely explanation of the G' increase for HDPE is the surface effect.

In *Fig. 8* the time variation of G' is shown. It can be seen that addition of mica prevents the increase of signal observed for the neat resin. The initial decrease of signal for 40 and 60 percent samples is due to flake alignment and not to degradation. The HDPE/mica composites are thermally stable at $T < 210$°C for $t < 30$ min.

In *Fig. 9* the values of η' taken at $\gamma = 10$ percent and at $\omega = 1$ and 10 (rads/s) for two samples $c = 5$ and 40

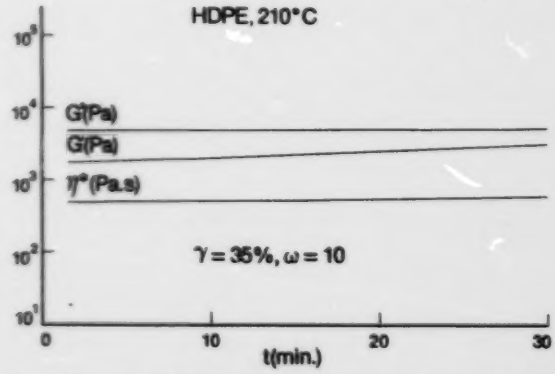

Fig. 7. Rheological functions, η, G', and G" versus time for polyethylene at 210°C.*

Table 3. Gel Permeation Chromatography of Polyethylene Sample Treated as Indicated

	A	B	C	D
	Virgin resin	15 min. on roll mill at 200°C	B+8 min. in press at 170°C	C+30 min. in RMS at 190°C
$M_n \cdot 10^{-4}$	3.6	4.0	3.8	3.8
$M_w \cdot 10^{-4}$	12.2	13.1	12.4	12.4
$M_z \cdot 10^{-4}$	39.7	39.4	38.3	35.8

percent of mica are shown. Excepting the 60 percent sample, for which a serious non-linearity was observed, all the remaining samples, at both frequencies, showed the same value of the activation energy of viscous flow; $\Delta E_\eta = 4.5 \pm 0.5$ kcal/mol (viz. *Table 1*). In these Arrhenian plots, there was no indication of any change of the mechanism of flow in the full range of c and T.

The viscosity-shear rate curves for compositions containing 0, 25, and 60 percent of mica are shown in *Fig. 10*. The data were obtained from rotational and capillary rheometers at 190°C. In all cases an excellent superposition of data from both instruments was observed, indicating that the viscosity of mica-filled polyethylene is instrument independent. This has been observed with other filled melts (8, 21). Experimental points obtained with different diameter dies fall on the same curves, i.e., wall effects such as wall slip or particle migration (14, 22, 23) are not significant.

Figure 10 also shows that at shear rates between 10^{-2} and 10^4 (sec^{-1}) the viscosities increase with the filler content; the difference between filled and unfilled compositions becomes smaller at high shear rates. While these results were to be expected, it is worth noting that at high $\dot{\gamma}$, viscosities lower than those of unfilled resin were reported for silane-treated mica-filled polypropylene (12) and titanate treated $CaCO_3$-filled polyethylene and polypropylene (24). These effects were attributed to an improved filler dispersion promoted by the coupling agent (24). Such behavior may also be caused by (i) either the shear degradation of the matrix polymer or that caused by the coupling agent, or (ii) inter-layer slip phenomenon caused by the incompatible filler coupling agent.

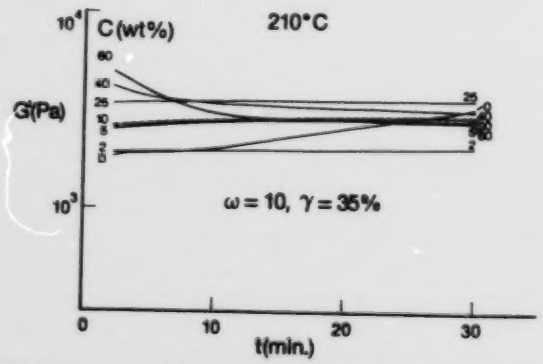

Fig. 8. Storage modulus, G', of polyethylene/mica versus time at 210°C mica concentration is marked.

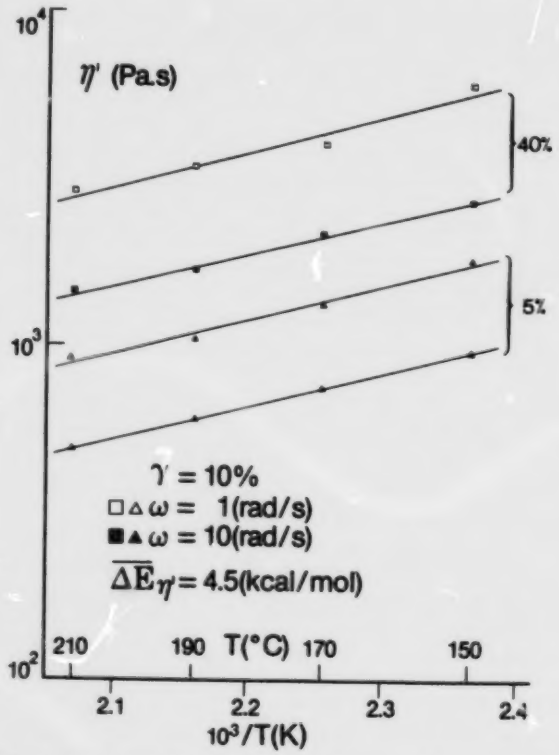

Fig. 9. Arrhenius plot for two samples containing 5 and 40 weight percent mica at γ = 10 percent and at two frequencies: ω = 1 and 10 rad/s.

In *Figs. 11* and *12*, η' versus ω and G' versus ω, respectively, at 170°C are shown. For concentrations of mica $c < 40$ weight percent there does not seem to be any sign of yielding; the behavior of the 60-percent-sample will be discussed later. It is worth recalling that also for polystyrene containing 20 volume percent of mica (i.e., $c = 41$ weight percent) the yield was not observed at rates down to $\dot{\gamma} = 10^{-2}$ (8).

Useful information about the structure of viscoelastic bodies can be gained by studying the relationship between the real and imaginary parts of complex rheological functions (25). One such example is shown in *Fig. 13*, where the imaginary part of complex viscosity,

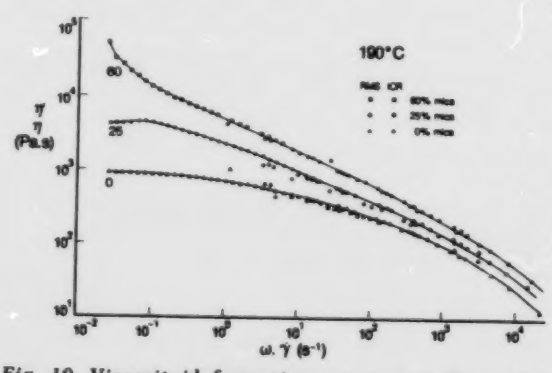

Fig. 10. Viscosity/deformation rate curves for samples containing 0, 25 and 60 weight percent mica at 190°C (RMS and ICR data).

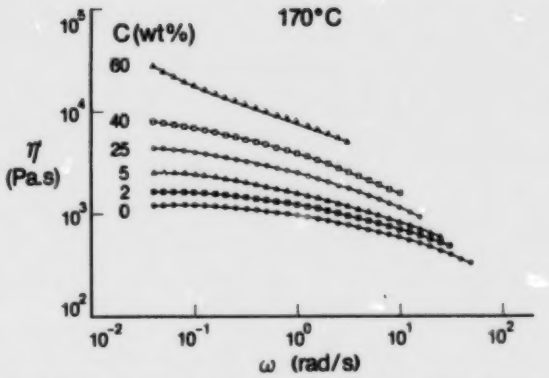

Fig. 11. Dynamic viscosity, η', of HDPE/mica samples at 170°C. Numbers refer to the mica content.

η'', is plotted as a function of dynamic viscosity, η'. For systems without a change of structure, a semicircular pattern is expected with $\eta' = \eta'' = 0$ at $\omega \rightarrow \infty$ and $\eta' = \eta'_o$, $\eta'' = 0$ at $\omega \rightarrow 0$. Up to and including 40 percent mica, curves of approximately semicircular shapes are obtained. The increasing diameter of the semicircles is related to the increase of the relaxation time of the system (25). The graph allows for an approximate calculation of the zero shear viscosity $\eta_o = \lim_{\omega \to 0} \eta'$. These values are listed in *Table 4*.

In *Table 4* the second set of η_0 is computed (26) from G'' via the relaxation spectrum $H(\lambda)$:

$$\eta_0 = \int_0^\infty H(\lambda) d\lambda; \quad \lambda = \sqrt{3}/\omega \qquad (2)$$

where

$$H(\lambda) = (2/\pi) G''(\omega) [1 - d\ln G''(\omega)/d\ln\omega] \qquad (3)$$

or

$$H(\lambda) = -(2\omega^2/\pi)(d\eta'/d\omega)$$

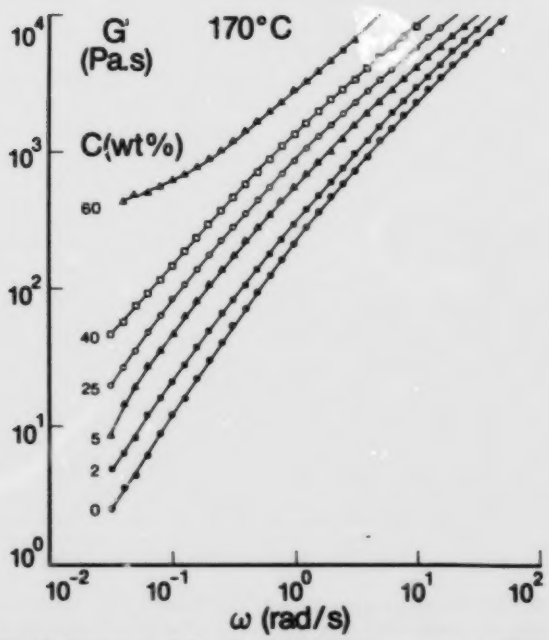

Fig. 12. Storage modulus, G', of HDPE/mica samples at 170°C. Numbers refer to the mica content.

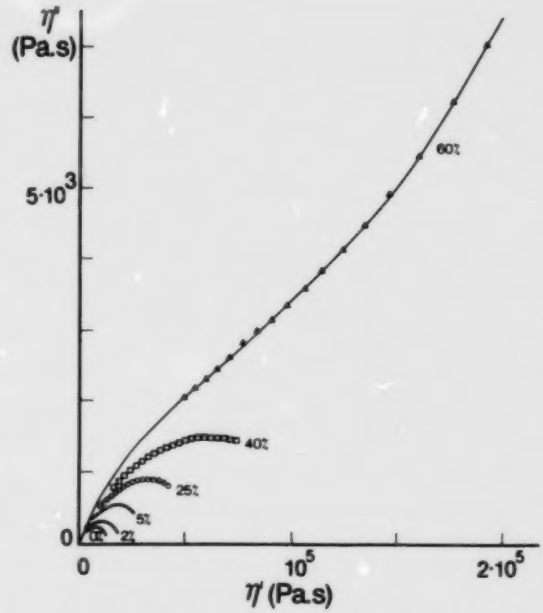

Fig. 13. Imaginary part, η'', of complex viscosity plotted as a function of dynamic viscosity, η', at 170°C. Numbers refer to the mica content.

The derivative in *Eq 3* was determined graphically. Examples of H(λ) spectrum are shown in *Fig. 14*. It has been observed that at 170°C addition of up to 40 weight percent of mica broadens the relaxation spectrum. For the sample containing 60 percent of flakes the spectrum is composed of two parts: (i) for lower relaxation times, λ, the polymer spectrum broadened by interactions with mica, is observed; (ii) at $\lambda > 17$ s, the mica flakes contribution is clearly seen. A phenomenon, similar in nature, was reported on Onogi and Matsumoto (6) for high strain (γ = 80 percent) measurements of polystyrene solution containing 20 weight percent of spherical particles.

The data presented in *Figs. 10* through *14* indicate that of all the samples, the one containing 60 percent of mica behaves in an odd fashion. An explanation of this behavior can be found in (*Figs. 5* and *14*) the non-linear type of viscoelastic deformation. The "yield-like" behavior observed in *Figs. 10* through *12* does not indicate yielding but rather the influence of the flake-to-flake interaction at low deformation rates. By the same token,

Table 4. Zero Shear Viscosities of HDPE/Mica Samples at 170°C.

Samples N°	φ	$\eta'_o \times 10^{-4}$ (Poise) (A)	(B)	η_r
1	0.0000	1.22	—	1.00
2	0.0062	1.71	—	1.40
3	0.0152	2.49	2.20	2.04-1.80
4	0.0316	2.62	3.60	2.15-2.95
5	0.0818	5.32	6.45	4.36-5.29
6	0.1532	9.2	11.8	7.54-9.67
7	0.2910	—	>40	>33

NOTE: (A) from the relaxation spectrum.
(B) from η'' vs η' plot.

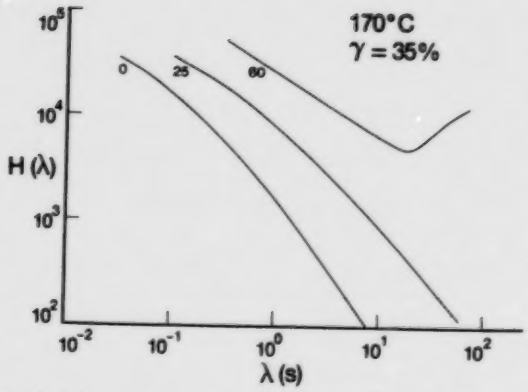

Fig. 14. Relaxation spectra of samples containing 0, 25 and 60 weight percent mica calculated from G" versus ω by means of Eq 3.

it is impossible to try any extrapolation of these curves to zero deformation rate. Also, the relaxation spectrum is very incomplete and it is impossible to predict its form (6). From the expected symmetry of η'' versus η' plots, one may speculate that $\eta_0 > 4 \cdot 10^5$ Poise. The measurements of this sample at lower ω and γ are being carried out.

Turning now to the η_0 versus ϕ dependence, it is convenient to discuss it in terms of the zero-shear suspension viscosity. For low concentration of elipsoids of rotation Simha (27) wrote:

$$\eta_r = \eta_0/\eta_0(\text{medium}) = 1 + a_1 \phi \qquad (4)$$

where

$$a_1 = (14/15) + \frac{p^2}{5}\left[\frac{1}{3(\ln^2 p - 1.5)} + \frac{1}{\ln p - 0.5}\right] \qquad (5)$$

Equation 5 for $p_z = 20.2$ gives $a_1 = 51.6$—the value used to calculate the solid line curve in *Fig. 15*. The broken line represents the η_r versus ϕ relation of the hard sphere suspensions (see, e.g., *Ref. 7*). The calculated flake overlap concentration, ϕ_c, is also marked. The observed agreement in *Fig. 15* between the experimental data points and the prediction of *Eqs. 4* and *5* was not expected for $\phi > \phi_c$. Most likely it is due to compensation of effects. At $\phi = \phi_c$ the flakes must change the packing order from the random to ordered. Such a change of packing must depress η_0. On the other hand. at $\phi > \phi_c$, higher interactive terms should be added to the power-series *Eq. 4*. Compensation between these two contributions is most likely responsible for the observed linearity. It is worth noting that η_0's as computed from $H(\lambda)$ are lower than those estimated from the η'' versus η' plot. Looking at the $H(\lambda)$ spectra (*Fig. 14*) it may in fact be expected that these curves, representing only parts of the spectrum, should yield too small values of η_0 on integration.

Frequently the zero-shear viscosities of solutions or suspensions are presented in a semi-logarithmic plot. Lingard and Whitmore (28) reported that the viscosity of glass-fiber suspension may be approximated by the empirical dependence:

$$\ln \eta_r = 8.52\phi \qquad (6)$$

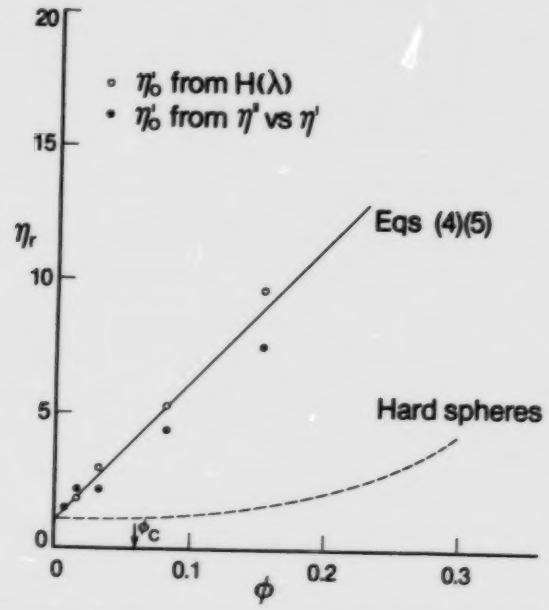

Fig. 15. Relative viscosity, η_r, versus volume fraction, ϕ. The points were determined either from $H(\lambda)$, using Eq 2 or from h" versus η' plot, Fig. 13. The solid line curve was calculated using Eqs 4 and 5. For comparison, dependence for suspension of hard spheres (e.g., Ref. 7) is shown (broken line). The flake overlap concentration, ϕ_c, is also marked.

This relation, along with the data of *Fig. 15* are presented in *Fig. 16*. Since the constant slope in *Fig. 16* indicates constant hydrodynamic volume of the suspended particles, V_h, it can be seen that for HDPE/mica systems two values of V_h are required—a large one below, and a smaller one above ϕ_c; the first value $V_h(\phi < \phi_c) = a_1 = 51.6$, whereas the second $V_h(\phi > \phi_c) = a_1 = 8.5$. For the randomly rotating disc, the ratio of the

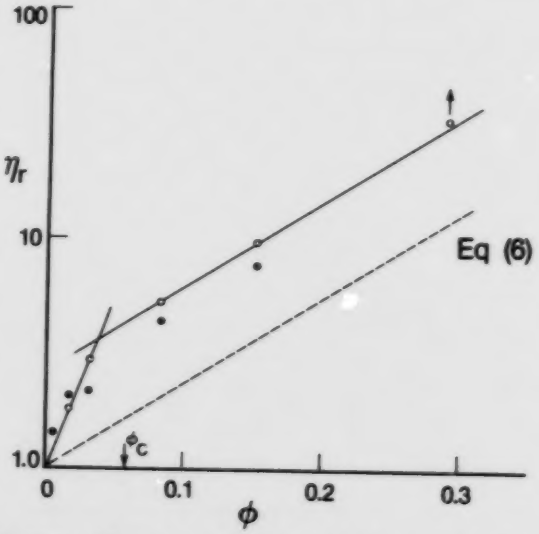

Fig. 16. Semi-log presentation of data from Fig. 15. The broken line was calculated from Eq 6, the solid lines represent the behavior below and above ϕ_c with intrinsic viscosities of 51.6 and 8.5, respectively.

occupied to actual volume is $2p/3$, i.e., 13.5 for the Suzorite 200NP. If the ratio of $V_h's$ is the same, than at $\phi > \phi_c$ the occupied volume is more than twice as large as the actual one, indicating significant amount of flakes movement.

CONCLUSION

It was found that even the relatively mild method of dispersing surface-coated mica in a low viscosity polymer melt, causes a significant amount of attrition. The prepared compositions were thermally stable at $T \leq 210°C$ for at least 30 min. The activation energy of viscous flow was determined as 4.5 ± 0.5 kcal/mol, independent of composition and only slightly dependent on the test frequency. In dynamic testing at $\omega = 10$(rad/s) a strain sensitivity increasing with concentration was observed. However, only the sample containing 60 weight percent of mica showed a non-linear viscoelastic response in its dynamic functions. In all cases, the values of η, G', and G'' increased with concentration in a full range of $\dot{\gamma}$ or frequency.

The relaxation time spectrum was found to broaden and shift to longer time values with increase of mica content. Only for the sample containing 60 percent of filler was a two-part spectrum computed—for shorter relaxation times the polymer part predominates while at longer times that of the mica flakes becomes more important. This may provide an explanation for surprisingly good correlation between the dynamic viscosity, η', measured at $\gamma = 35$ percent, and the steady state capillary viscosities η. The latter parameter was found to be independent of the capillary diameter as well.

The zero shear viscosity, η_0, determined by two different methods, indicates a sharp change in flow mechanism near the critical flake overlap concentration $\phi_c = 0.05$ to 0.06. Below this value, a flow of randomly tumbling particles follows Simha's prediction; above this value a drastic reduction of the intrinsic viscosity (from 51.6 to 8.5) was observed. For $\phi \leq 0.16$ (or up to 40 weight percent of mica), the relative viscosity of the composites seems to follow a simple linear dependence.

REFERENCES

1. R. T. Woodhams and M. Xanthos, "Handbook of Fillers and Reinforcements for Plastics," H. S. Katz, J. W. Milewski Eds., p. 333, Van Nostrand Reinhold Co., (1978).
2. M. Xanthos, *Plas. Comp.*, **2**, 19 (1979).
3. K. Okuno and R. T. Woodhams, *Polym. Eng. Sci.*, **15**, 308 (1975).
4. P. Bataille and T. V. Bui, *Polym. Compos.*, **2**, 8 (1981).
5. I. Lee, S. Turner, and R. T. Woodhams, *Polym. Compos.*, **3**, 212 (1982).
6. S. Onogi and T. Matsumoto, *Polym. Eng. Rev.*, **1**, 45 (1981).
7. L. A. Utracki and B. Fisa, *Polym. Compos.*, **3**, 193 (1982).
8. J. L. White, L. Czarnecki, and H. Tanaka, *Rubber Chem. Technol.*, **53**, 823 (1980).
9. Y. Chan, J. L. White, and Y. Oyanagi, *J. Rheology*, **22**, 507 (1978).
10. R. J. Crowson, M. J. Folkes, and P. F. Bright, *Polym. Eng. Sci.*, **20**, 925, 934 (1980).
11. B. A. Knutsson, K. B. Abbas, and J. L. White, *Rheology*, **3**, 83, (1980).
12. M. S. Boaira and C. E. Chaffey, *Polym. Eng. Sci.*, **17**, 715 (1977).
13. V. P. Juskey and C. E. Chaffey, *Can. J. Chem. Eng.*, **60**, 334 (1982).
14. L. A. Utracki, A. M. Catani, G. L. Bata, M. R. Kamal, and V. Tan, *J. Appl. Polym. Sci.*, **27**, 1913 (1982).
15. R. W. Whorlow, "Rheological Techniques," Ellis Harwood Ltd, Chester, England, (1980).
16. L. A. Utracki and M. M. Dumoulin, *SPE ANTEC Tech. Papers*, **28**, 51 (1982).
17. L. A. Utracki and M. M. Dumoulin, *ACS Org. Coat. Plastics Div. Preprints*, **48**, (1983).
18. B. Fisa, B. D. Favis, and B. Sanschagrin, Powder Techn., submitted.
19. L. A. Utracki, *J. Coll. Interf. Sci.*, **42**, 185 (1973).
20. G. A. McFarren, T. F. Sanderson, and F. G. Schappell, *Polym. Eng. Sci.*, **17**, 46 (1977).
21. B. A. Knutsson, J. L. White, *J. Appl. Polym. Sci.*, **26**, 2347 (1981).
22. L. A. Utracki, Z. Barkerdjian, and M. R. Kamal, *Trans. Soc. Rheology*, **19**, 173 (1975).
23. L. A. Utracki, Z. Barkerdjian, and M. R. Kamal, *J. Appl. Polym. Sci.*, **19**, 481 (1975).
24. S. J. Monte and G. Sugerman, *Poly.-Plast. Technol. Eng.*, **17**, 95 (1981).
25. J. M. Pierrard, "La rhéologie," B. Persoz Ed., Masson Ltée Cie, Paris (1969).
26. J. D. Ferry, "Viscoelastic Properties of Polymers," J. Wiley and Sons, New York, 2nd Ed., (1970).
27. R. Simha, *J. Chem. Phys.*, **13**, 188 (1945).
28. P. S. Lingard and R. L. Whitmore, *Chemeca*, **11** (1970).

Extensional Flow of Mica-Filled Polyethylene

L. A. UTRACKI *and* J. LARA

National Research Council of Canada
Industrial Materials Research Institute
75, boul. De Mortagne Boucherville,
Québec, Canada J4B 6Y4

Extensional flow of mica-filled high density polyethylene was studied at 150°C in a Rheometrics elongational rheometer. The constant strain-rate mode at a rate of 10^{-3} to 1.0 s^{-1}, and the constant stress mode were used. The mica content was 0, 25, 40, and 60 weight percent. In both testing modes, the steady state elongational viscosities were obtained; those for the filled samples were about ten to twenty times larger than the shear viscosity at corresponding (low) rates of deformation.

INTRODUCTION

In 1906, Trouton (1) measured extensional viscosities, η_e, of tar, pitch, and wax, finding $\eta_e \simeq 3\eta_0$, where η_0 is the zero shear viscosity. It took 32 more years before η_e for polymer melts was determined (2). The modern methods of η_e measurements have been developed during the last 30 years. For a review of the subject see, e.g., Petrie and Dealy (3). The rheological properties, including uniaxial extensional flow, of particulate-filled polymer melts were recently reviewed by Utracki and Fisa (4).

In the present paper we want to distinguish the steady state elongational (or extensional) viscosity:

$$\eta_e = \sigma_{11}/\dot{\epsilon}, \tag{1}$$

(where $\dot{\epsilon} = d\epsilon/dt = (dL/dt)/L$, L is the sample length at time t, σ_{11} is the extensional stress, and $\dot{\epsilon}$ is the rate of elongation) from its time-dependent homologue $\eta_e^t = \sigma_{11}^t/\epsilon$. In the study of elongational flow of filled polymers there are two phenomena of particular interest: (i) the magnitude of the yield stress, and (ii), the Trouton ratio:

$$R_T^0 = \lim_{\dot{\gamma},\, \dot{\epsilon} \to 0} \eta_e/3\eta \tag{2}$$

An extensive amount of work on elongation flow of filled polymers was published by White, *et al.* (5, 6). Melts filled with short glass fibers, GF, and submicron particulates of carbon black, CB, calcium carbonate, $CaCO_3$, and titanium dioxide, TiO_2, were investigated. The authors reported that for the particulate-filled systems the ratio of the extensional yield stress to the shear yield stress:

$$\sigma_{11,y}/\sigma_{12,y} = 1.73$$

in agreement with the von-Mises criterion (equivalent to a critical distortional strain energy of a particle-particle gel-like structure).

It should be remarked that the phenomenon of yielding is subject to interpretation. In a strict sense, the yield indicates the existence of a solid-like behavior for $\sigma_{ij} < \sigma_{ij,y}$ and a liquid-like one above this limit. Origins of the phenomenon may vary, but a tri-dimensional structure must always be postulated, i.e., for systems with the yield:

$$\lim \sigma_{ij} \neq 0$$
$$\dot{\gamma}_{ij} \to 0$$

Recently, for suspension of rigid particles of poly (styrene-co-divinyl benzene) in polystyrene solution, Onogi and Matsumoto (7) noted that yield is an artifact of interparticle structures having long relaxation times; at low and decreasing rates of deformation, $\dot{\gamma} < 10^{-2}$, the authors observed that σ_{12} tends toward zero.

While the above described experiment does not negate existence of the yield phenomenon, it clearly demonstrates the necessity for careful measurements at very low rates of deformation in order to ascertain correct interpretation of the multi-phase flow data. It is also of interest to note that only the attractive particle-particle interactions (7) were responsible for the apparent yielding; the repulsive ones did not lead to this behavior. The suspensions with inter-particle structures behave as a Newtonian liquid with η_0 usually much larger than that of the suspending medium. A similar observation was recently made by M. C. Williams (8) regarding the very low velocity creep behavior of block polymer solutions, as well as by one of the authors regarding the low rate of shear behavior of explosive emulsions (9). It seems that in numerous multiphase fluids, there are different ranges of the rate of deformation where the stress, σ_{ij}, remains proportional to the velocity of deformation $\dot{\gamma}_{ij}$; the uppermost Onogi's plateau at the lowest rates (below the "yielding" strain rate zone), the upper Newtonian region usually determined via subtraction of yield stress, and finally the lower Newtonian region observed at a very high range of deformation rates. If constancy of the ratio, $\sigma_{ij}/\dot{\gamma}_{ij}$ indicates a stable structure, then in multiphase systems few of these are possible: one dominated by inter-particle interactions,

the other behaving like an oriented suspension in a Newtonian liquid, and finally the one dominated by flow of the continuous phase. It is worth recalling that the two upper plateau regions followed by the power-law flow zone were recently reported for shear flow of poly(ethylene terephthalate)/poly(amide-6,6) blends (10).

One should expect that such effects of structural changes will show up also in elongational flow, though not necessarily at the same rate of deformation as in shear. For small-diameter particles, yield is easily observed (viz. e.g., *Ref. 4*). The reason for this is the immobilization of a liquid layer adjacent to the particle, which increases its occupied volume fraction. For elongated or plate-like particles, the interactions are affected by orientation. GF-filled polymer melts showed the yield in extension but not in shear (5).

For both Newtonian and non-Newtonian single-phase liquids, the Trouton ratio $R_T^0 = 1$ (4, 11); for Newtonian liquids containing ϕ-volume fraction of particles with an aspect ratio p, Batchelor wrote (12):

$$R_T^0 = 1 + 4\phi p^2/9 \ln(\pi/\phi) \qquad (3)$$

Weinberger and Goddard (13) observed that after addition of $\phi = 0.013$ of GF with $p = 57$ to a Newtonian liquid: (i) the yield was not observed, (ii) the shear viscosity increased by 8 percent, and (iii) $R_T^0 = 3.3$, to be compared with 3.42 calculated from *Eq 3*. Similarly, Mewis and Metzner (14), for a suspension of GF in a low-molecular-weight polybutene ($\phi = 0.001$ to 0.01 and $p = 280$ to 1260), found R_T^0 varying from 19 to 261 in agreement with *Eq 3*. Nakajima (15) reported that for poly(butadiene-co-acrylonitryle) containing 40 phr of FEF carbon black the η_e versus $\dot{\epsilon}$ parallels the 3η versus $\dot{\gamma}$ dependence over a wide range of rates of deformation, and $R_T \doteq 2$ (R_T is defined as a ratio of $\eta_e/3\eta$ at $\dot{\epsilon} = \dot{\gamma}$ and T = constant.).

EXPERIMENTAL

Materials. Commercial injection-molding-grade high-density polyethylene, HDPE, prepared by the gas phase process with a density $\rho = 0.955$ g/ml, and melt index MI = 14 g/10 min was characterized by gel permeation chromatography using a Waters Sci. GPC-150C instrument at 135°C with 1,2,4-trichlorobenzene, TCB, as a solvent. The four columns (10^3, 10^4, 10^5, and 10^6 Å) were calibrated using 24 polystyrene, PS, standard samples in TCB at 135°C. The results are listed in *Table 1*. To prevent oxidative degradation of HDPE, 0.1 weight percent of antioxidants (Topanol CA, Nonox DLTDP; 50:50) was added to TCB.

Suzorite 200NP, phlogopite-type mica was used in the studies (16). The volume average diameter of the flakes was 113 μm and the aspect ratio $p = 35$. The material was commercially surface treated with a silane coupling agent. For more information, see (17).

The materials were blended on a Brabender two-roll mill at 210°C for 15 min. The samples containing nominally 0, 25, 40, and 60 weight percent of mica were prepared (see *Table 2*). The effect of compounding on molecular weights of HDPE is shown in *Table 1*. In the table the third row refers to the sample collected after blending and subsequent rheological RMS testing, the fourth to the sample immersed in Dow 200 silicon oil. In the last row the standard deviation of the measurements is given. For rheological testing the blends were granulated and molded.

Table 1. Results of GPC Characterization of HDPE.[1]

No.	Sample	$M_n \cdot 10^{-3}$	$M_w \cdot 10^{-3}$	$M_z \cdot 10^{-3}$	M_w/M_n
1	original	36	122	397	11.0
2	compounded[2]	38	124	383	10.2
3	measured[3]	38	124	358	9.4
4	oil[4]	30	72	270	9.0
	GPC error (±)	1.3	4.4	40	1.2

[1] M_n, M_w, and M_z indicate number, weight and z-average molecular weight, respectively.
[2] 15 min at 210°C on roll mill, ground and compression molded for 7 min at 190°C.
[3] Compounded as in (2) then sheared in RMS for 30 min at 190°C.
[4] After 2 hrs at 150°C in Dow 200.

Table 2. Characteristics of HDPE/Mica Composites.

Sample No.	Mica Content nominal w(wt%)	Mica Content actual[a] ϕ	R_T^0 Eq 3	Observed R_T at $\dot{\epsilon}$ = 0.04 s^{-1}
1	0	0.000	1.00	1.0
2	25	0.0982	4.42	3.4
3	40	0.1812	8.66	5.0
4	60	0.3342	18.98	6.7

[a] Calculated from pyrolytically determined mica content assuming density of phlogopite ρ = 2.83 and that of HDPE ρ = 0.781 g/ml.

Rheological measurements. The shear properties of the samples at 150°C were determined in the dynamic and steady state mode using the Rheometrics mechanical spectrometer, RMS Model 605, and the Instron capillary rheometer, ICR. Details of these measurements are published separately (17). The extensional properties were determined in the Rheometrics extensional rheometer, RER. The instrument, well-described in the literature (18, 19), was used in constant elongation rate, $\dot{\epsilon}$, and constant extensional stress, σ_{11}, modes. The samples were transfer molded under vacuum, annealed, and then affixed with epoxy (overnight curing) to the aluminum ties. Prepared in this manner, specimens did not show any shape change on immersion in hot ($T \leq$ 190°C) silicone oil. For the test the samples were mounted in the instrument and immersed in silicone oil (Dow 200 for sample 1, Dow 710 for samples 2 and 3, and Dow 1265 for sample 4) at 150°C. The test started after a 7-to-10-minute-long temperature-equilibration period. To evaluate the effect of the initial residence time, t_R, the samples were kept in the silicone oils at 150°C for a period of up to 30 min; for $t_R < 10$ min the subsequently measured η_e^t was only slightly affected, but for $t_R > 10$ min the effect was quite pronounced. During the longer term t_R-study outside the RER, the following results were obtained: (i) in poly(dimethyl siloxanes) (Dow 200, 210H) a degradative weight loss $\Delta w = 0.2$ to 0.3 weight percent per hour was observed, (ii) in poly(methyl phenyl siloxane) (Dow 710) the samples swelled up to the equilibrium of 6 to 7 weight percent in 10 to 12 hours, and (iii) in the fluorosilicone oil (Dow 1265) the samples were not affected at least for $t_R < 4$ hours.

During the measurements in RER the maximum temperature difference, as read by three thermocouples placed at different heights in the sample chamber, did not exceed 0.2°C. For each sample the uniformity of the cylindrical sample diameter was verified at three different heights; in all cases the average diameter was found to be: $d = 5.54 \pm 0.05$ mm. The sample length used in this study was $L_0 = 21.0 \pm 0.5$ mm.

RESULTS

The extensional viscosity, η_e^t, at constant strain rate versus total strain $\epsilon = \dot{\epsilon}t$ for the four samples listed in *Table 2* is presented in *Figs. 1-4*. The reproducibility of η_e^t results is shown in *Fig. 5*. Here 11 samples of HDPE from two transfer-molding preparations are stretched at $\dot{\epsilon} = 0.3\ s^{-1}$ and at 150°C. The value of the maximum viscosity is: $6500 < \eta_e$ (Pa.s) < 7200. The residence time of the lower curve was 50 percent lower than for the others. Investigation of the origin of this difference led to discovery of non-trivial effects of the commonly used silicone oils, Dow 200 and Dow 710. While addition of antioxidants could reduce the (small) degradative effect of the first oil by about 50 percent, no solution was found to prevent PE swelling in the second. However, in spite of these effects η_e was obtained (See *Figs. 1-4*) and the data from $\dot{\epsilon}$ = const. and σ_{11} = const. (different t_R's) agreed within the range of experimental error. There is some indication that at low rates of straining, i.e., for long testing times, the swelling does reduce the maximum strain, ϵ_r (see *Fig. 2*).

The experimental error of the measurements was ± 6 percent. However, it was found that the total noise level of the instrument is nearly constant, independent of sample and $\dot{\epsilon}$; it amounts to ± 0.04 percent of the nominal reference spring constant value. For the neat polymer at $\epsilon = 10^{-2}\ s^{-1}$, this translates into ± 20 percent of the signal noise, which leads to a greater experimental uncertainty of low rate of elongation data, especially for unfilled HDPE. Because of the instrument limitation, we were also unable to determine η_e for that sample in the constant stress mode.

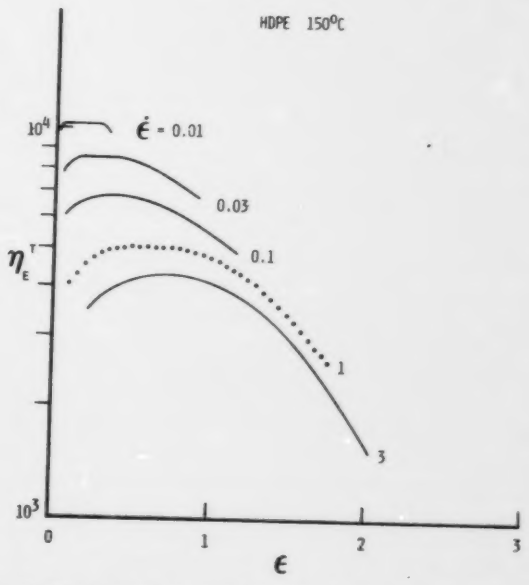

Fig. 1. Constant strain rate elongational viscosity η_e^t at 150°C versus strain ϵ for HDPE.

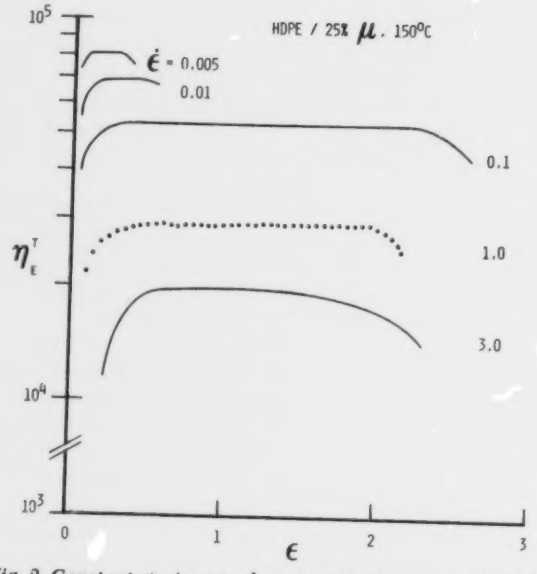

Fig. 2. Constant strain rate elongational viscosity η_e^t at 150°C versus strain ϵ for HDPE containing 25 weight percent of mica.

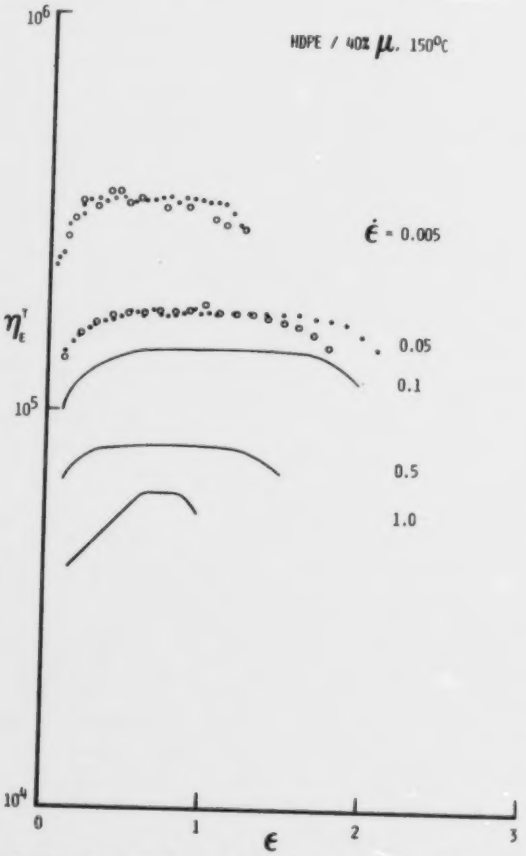

Fig. 3. Constant strain rate elongational viscosity η_e^t at 150°C versus strain ϵ for HDPE containing 40 weight percent of mica.

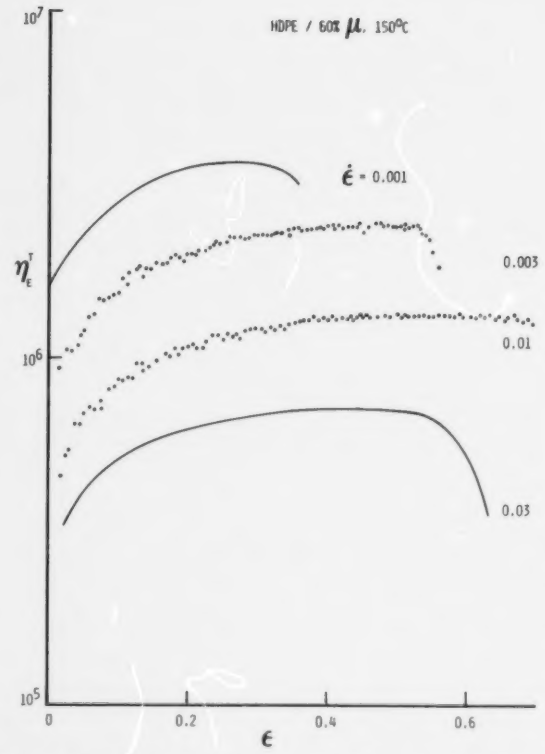

Fig. 4. Constant strain rate elongational viscosity η_e^+ at 150°C versus strain ϵ for HDPE containing 60 weight percent of mica.

It can be seen in *Figs. 1-4* that for all four samples there is no superposition of data taken at different strain rates. The viscosity, η_e^+, increases with a decrease of $\dot{\epsilon}$. The sample-to-sample reproducibility of data is good as illustrated in *Fig. 3* for samples tested at $\dot{\epsilon} = 0.005$ and $0.05\ s^{-1}$. The plateau level, η_e, is well established, indicating that the asymptotic equilibrium conditions have been achieved. The values of the plateau, identified with η_e, are listed in part A of *Table 3*.

In *Figs. 6* and *7*, examples of results at constant extensional stress, σ_{11}, are presented for samples No. 2 and No. 3, respectively. It can be seen that within 3 s, the stress reaches a steady value and stays constant for about 40 s. During most of this time the strain increases linearly, allowing calculation of $\dot{\epsilon}$ and in effect the equilibrium value of η_e; these are listed in Part B of *Table 3*.

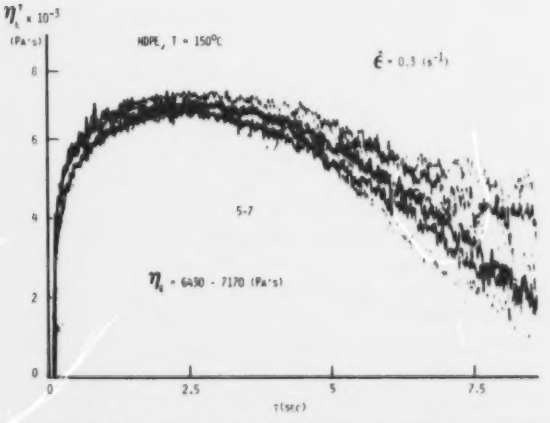

Fig. 5. Test of reproducibility: 11 samples of HDPE measured at 150°C and $\dot{\epsilon} = 0.3\ s^{-1}$. Plateau: $\eta_e = 680 \pm 37$ Pa.s.

Table 3. Elongational Viscosity, $\eta_e \cdot 10^{-3}$ for HDPE/Mica Composites at 150°C.

$\dot{\epsilon}(s^{-1})$	η_e for sample No. 1	No. 2	No. 3	No. 4
A: $\dot{\epsilon}$ = const.				
3.0	4.13	19.58	—	—
1.0	4.95	29.27	61.8	—
0.5	4.13	32.64	81.6	—
0.3	6.80 ± 0.37	—	—	
0.1	6.52	53.25	142.	—
0.5	5.91	58.57	176.	—
0.03	8.39	—	—	719.
0.01	10.18	68.59	270.	1330.
0.005	—	80.62	346.	—
0.003	—	—	—	2400.
0.001	—	98.50	380.	3600.
B: σ_{11} = const.				
0.164		41.7		
0.148		47.3		
0.108			115.	
0.042		59.1		
0.035			193.	
0.030		65.6		
0.013		73.0		
0.011				1068.
0.0096				1041.
0.0093			268.	
0.0073				1216.
0.0018				2780.

The results of extensional and shear mode testing of samples No. 1-4 are compared in *Figs. 8-11*, where $\eta_e/3$ versus $\dot{\epsilon}$ (from *Table 3*) and η' versus ω [from (17)] are plotted. The η' is the real part of the complex viscosity determined at a strain $\gamma = 35$ percent and frequency ω. Two observations can be made: (i) only for neat polymer the Trouton ratio, $R_T = 1$, (ii) for the other samples $R_T = 3$ to 7 (here R_T is taken at $\dot{\epsilon} = \omega = 0.04$, i.e., at the overlapping rates of deformation). This is also illustrated in *Fig. 12*, where $\eta_e/3$ at $\dot{\epsilon} = 0.1$ and η' at $\omega = 0.1$ are plotted versus the volume fraction of mica, ϕ. The broken line is drawn according to the empirical relation:

$$\ln \eta_r = 8.52\phi \qquad (4)$$

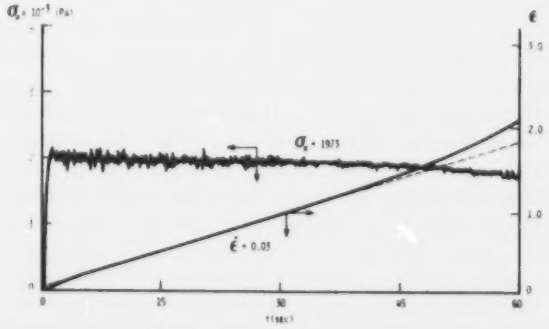

Fig. 6. Stress and strain versus time traces for HDPE containing 25 weight percent of mica tested at 150°C in a constant stress mode.

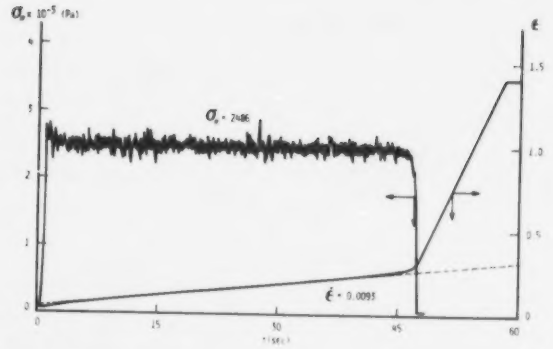

Fig. 7. Stress and strain versus time traces for HDPE containing 40 weight percent of mica tested at 150°C in a constant stress mode.

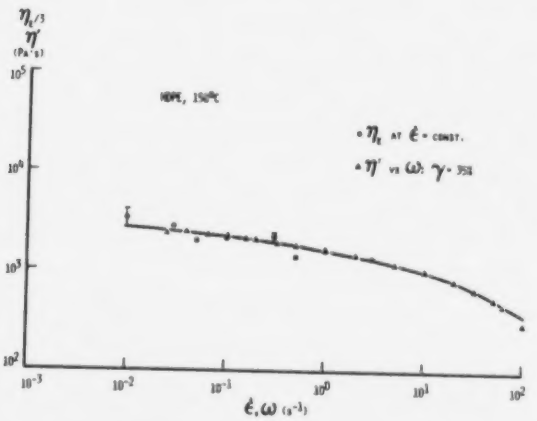

Fig. 8. Comparison of equilibrium elongational with dynamic viscosity at the same rate of deformation HDPE at 150°C.

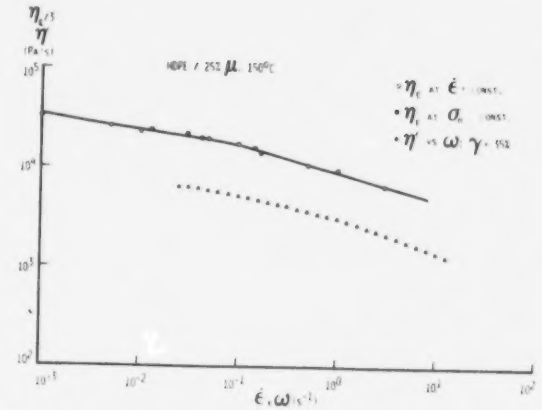

Fig. 9. Comparison of equilibrium elongational with dynamic viscosity at the same rate of deformation HDPE with 25 weight percent of mica at 150°C; constant strain rate and constant stress data are shown.

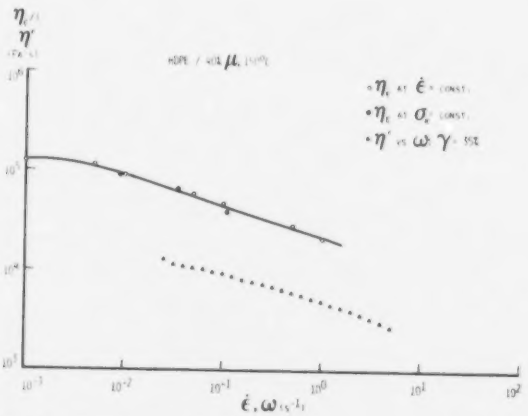

Fig. 10. Comparison of equilibrium elongational with dynamic viscosity at the same rate of deformation HDPE with 40 weight percent of mica at 150°C; constant strain rate and constant stress data are shown.

established (20) for suspensions of GF with $p = 37.8$ ($\eta_r = \eta/\eta_0$, where η_0 is the zero-shear viscosity of HDPE); for details, see (17).

DISCUSSION

The data in *Table 1* demonstrate that there is no sign of the thermal degradation in the molten state even after 52 min exposure at $T > 190$°C. However, the resin immersed in the Dow 200 silicone oil becomes more sensitive to degradation, even at 150°C. Since addition of antioxidants slows down this process, the degradation mechanism, most likely, is radical. As FTIR did not show any oil penetration into the sample but a presence of degradation products in the oil, the process must involve a progressive attack of the radicals either generated in the oil or activated in the surface layer on the sample.

In spite of all precautions, the melt compounding was seen to reduce the average mica flake size from 113 to 92 ± 2 μm (17).

In what follows, the results of the extensional testing will be compared with those obtained in the oscillatory mode at strain of $\gamma = 35$ percent. Previously the latter data were found to follow the capillary viscosity results (17), indicating that at these strains the flow behavior of the mica-filled HDPE resembles that of the steady state capillary one.

The results obtained for the mica-filled HDPE are in qualitative agreement with those reported (5) for GF-filled polymer melts. In both cases, for neat polymer $R_T^0 = 1$, whereas in the presence of a filler R_T increased with its concentration and decreased with the deformation rate. The values of R_T reported in *Table 2* are lower than those observed for GF ($R_{T,max} = 7$ to 10). There are three reasons for this: (i) the higher deformation rates at which R_T for mica-filled melts was calculated; (ii) the lower mica aspect ratio; and (iii) the smaller effect of the disc-shape than rod-shape particles of the same aspect ratio, p, on the flow properties of suspensions.

In the previous study of flow of plastisol (9), it was observed that for a polydispersed system, the volume-to-surface diameter, d_{vs}, gives the best correlation. Since there is little variation of flake thickness with its diameter, the aspect ratio can be taken as proportional to the latter parameter; i.e., $p = 20.2$ for the original and $p = 16.5$ for the compounded micas. The values of R_T^0 listed in *Table 2* were computed from *Eq 3* using the latter

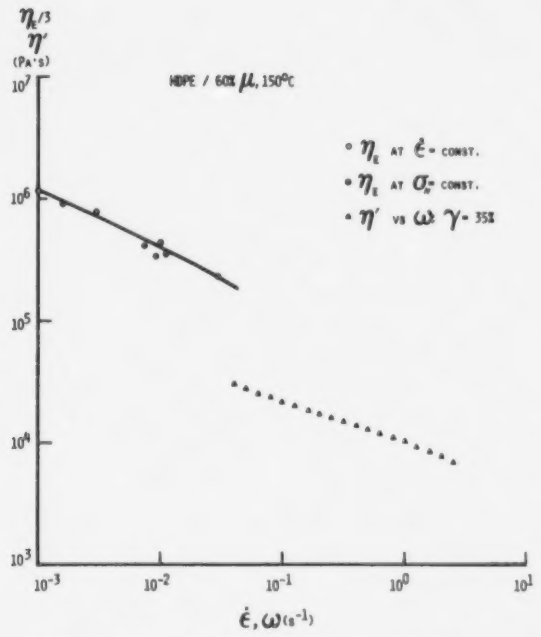

Fig. 11. Comparison of equilibrium elongational with dynamic viscosity at the same rate of deformation HDPE with 60 weight percent of mica at 150°C.

value of p. It can be seen that the experimented R_T taken at $\omega = \dot{\epsilon} = 0.04$ are lower. The difference $(R_T^0 - R_T)$ clearly increases with concentration, ϕ. In all fairness,

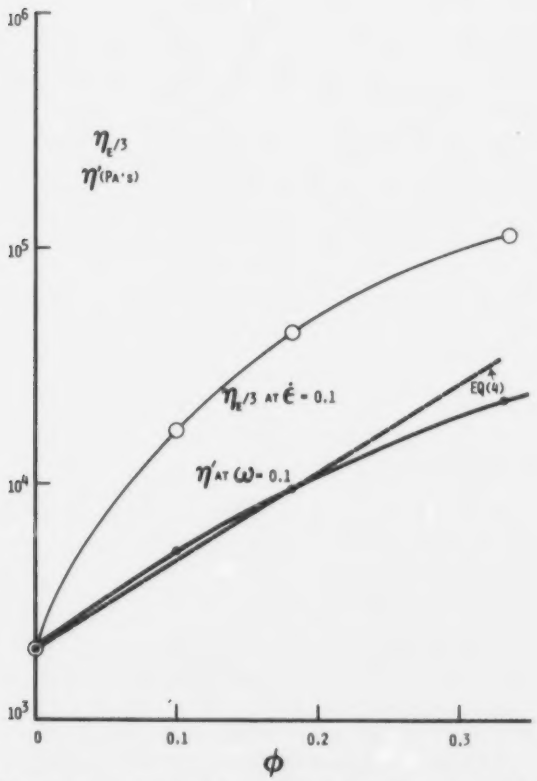

Fig. 12. Concentration dependence of elongational and dynamic viscosity; see text.

Eq 3 should not be used for comparison with the experimental data. In its derivation Batchelor assumed the continuous phase to be a Newtonian liquid. While stretching the filled specimens, the overall deformation rate $\dot{\epsilon}$ is significantly lower than that affecting the continuous phase; only at much lower rates of strain may the liquid experience shear rates comparable to those of the Newtonian region. This may also explain why there is no leveling off of the η_e for the experimentally accessible $\dot{\epsilon}$. Furthermore, for all samples but HDPE the η' versus ω plots do not show the Newtonian plateau. Clearly lower rates of deformation data are needed for any meaningful comparison with *Eq 3*.

It is of interest to examine the shape of the curves in *Figs. 1-4*. It is apparent that addition of 25 or even 40 weight percent of mica to HDPE results in a better control of melt flow, especially in the middle range of $\dot{\epsilon}$. If the melt strength is related to the maximum value of ϵ, then addition of mica which causes an increase of ϵ_c from about 1 to 2 or 2.5 is advantageous. For samples containing 60 weight percent of mica the maximum strain is low, $\epsilon_c < 0.7$ In addition, it can be seen that it takes a relatively long time for η_e^t to reach its equilibrium value; the flakes are highly hindered in their ability to align with the stress. Calculation shows that for flakes of $\rho = 20.2$ the onset of hindrance occurs at $\phi_c = 0.05$ or about 16 weight percent (assuming uniform flake size); for poly-dispersed flakes, this critical value is a function of the distribution function.

It is of great interest to note in *Figs. 9* to *11* the excellent agreement between the η_e determined from constant stress and that from constant strain rate experiments. This agreement, observed previously for polymer melts (17, 21), has not been reported for filled polymers. Because of the different time/stress history in these tests, one should not *a priori* expect the agreement. The agreement for sample Nos. 2 and 3 is particularly gratifying; as mentioned previously, these were tested in Dow 710 oil, which swells polyethylenes. The agreement may be taken as an indication that: (i) the observed η_e^t plateau does represent the equilibrium, η_e, and (ii) that the oil does not seriously affect the short time results.

Finally, in *Fig. 12* the low deformation rate (0.1 s^{-1}) viscosities $\eta_e/3$ and η' are shown. The broken line represents *Eq 4* derived for GF suspensions. Coincidence of our η'-data with predictions of *Eq 3* is apparent. On the other hand, the tendency of both the functions $\eta_e/3$ and η' to increase less rapidly with ϕ at higher concentration is a surprising observation for these samples. There may be three reasons for this behavior: (i) η_e and η' are taken at non-zero rate of deformation, (ii) the flakes can rotate only at $\phi < \phi_c = 0.06$—above ϕ_c the effective occupied volume, and the viscosities increase less rapidly with ϕ, and (iii) there is an effect of attrition on p. Calculations (4, 17) indicate that the zero shear viscosity η_o of sample No. 4 should be at least 10 times larger than the measured η' at $\omega = 0.1$ rad/s.

The latter information also means that in the tested samples, the yield was not observed. This is in spite of the low frequency upturn of the flow curve of

sample No. 4; even the highest recorded value of η' is about on decade lower than what the zero shear viscosity of suspension theories would predict.

CONCLUSIONS

The elongational flow of mica-filled HDPE was measured. It was found that at least down to $\dot{\epsilon} = 10^{-3}\ s^{-1}$ there is no leveling-off of the η_e versus $\dot{\epsilon}$ curves. The Trouton ratio, $R_T = \eta_e/3\eta'$ was found to increase with mica content up to the value of 6.7 for samples containing 60 weight percent of mica; i.e., the η_e-enhancing effect is smaller then that of glass fibers. It was also observed that addition of less than 40 weight percent of mica improved the melt strength of HDPE.

REFERENCES

1. F. T. Trouton, *Proc. R. Soc.*, **A-77**, 426 (1906).
2. E. Jenckel and K. Ueberreiter, *Z. Phys. Chem.*, **182A**, 361 (1938).
3. C. J. S. Petrie and J. M. Dealy, "Proceed. 8th Intl. Congress Rheology," G. Astarita, G. Marrucci and L. Nicolais Eds., vol. 1, 177, Plenum Press, New York (1980).
4. L. A. Utracki and B. Fisa, *Polym. Compos.*, **3**, 193 (1982); see also L. A. Utracki, "Proceedings AICHE Meeting," Los Angeles, Vol. 14-19, 1982; Paper No 7a.
5a. J. L. White and H. Tanaka, *J. Appl. Polym. Sci.*, **26**, 579 (1981).
5b. H. Tanaka and J. L. White, *Polym. Eng. Sci.*, **20**, 949 (1980).
5c. Yu Chan, J. L. White, and Y. Oyanagi, *J. Rheology*, **22**, 507 (1978); ibid., **24**, 500 (1980).
6. Y. Ide and J. L. White, *J. Appl. Polym. Sci.*, **22**, 1061 (1978).
7. S. Onogi and T. Matsumoto, *Polym. Eng. Rev.*, **1**, 45 (1981).
8. M. C. Williams, priv. commun.
9. L. A. Utracki, unpublished.
10. L. A. Utracki, A. M. Catani, G. L. Bata, M. R. Kamal, and V. Tan, *J. Appl. Polym. Sci.*, **27**, 1913 (1982).
11. V. S. Au-Yeung and C. W. Macosko, *J. Rheology*, **25**, 445 (1981).
12. G. K. Batchelor, *J. Fluid Mech.*, **46**, 813 (1971).
13. G. B. Weinberger and J. D. Goddard, *Int. J. Multiphase Flow*, **1**, 465 (1974).
14. J. Mewis and A. B. Metzner, *J. Fluid Mech.*, **62**, 593 (1974).
15. N. Nakajima, *Rubber Chem. Technol.*, **53**, 1088 (1980).
16a. R. T. Woodhams and M. Xanthos in "Handbook of Fillers and Reinforcements for Plastics," H. S. Katz and J. V. Milewski Eds., Ch. 20, Van Nostrand Reinhold Co. (1978).
16b. M. Xanthos, *Plast. Comp.*, **2**, 19 (1979).
17. B. Fisa and L. A. Utracki, *Polym. Compos.*, **5**, 36 (1984).
18. H. Münstedt, *J. Rheology*, **23**, 421 (1979).
19. V. S. Au-Yeung and C. W. Macosko, *Mod. Plastics*, **58**, 84 (1981).
20. P. S. Lingard and R. L. Whitmore, *Chemeca*, 11 (1970).
21. e.g. see: H. M. Laun, and H. Münstedt, *Rheologica Acta*, **15**, 517 (1976); V. S. Au-Yeung, C. W. Macosko, and V. R. Raju, *J. Rheology*, **25**, 445 (1981).

DISCUSSION

E. B. Bagley: You said that the upswing of viscosity on lowering the rate of deformation should not be taken as an indication of yield. For the sample containing 60 wt % of mica the upswing was clearly visible. Do you have yielding there or not? Can you elaborate?

L. A. Utracki: I do not think that the upswing is necessarily related to yielding. Neither do I think that we observed the yield phenomenon in the dynamic and extensional flows of the composites; at least the evidence is non-conclusive. In multi-component systems, the situation is particularly complex. For fiber-filled melts at the rates of deformation down to 0.001 J. L. White, et al. (see ref. 5c of the paper) did not see yielding in shear but in extension. On the other hand, yielding was observed in almost every system containing small filler particles. Onogi and Matsumoto demonstrated that in order to show "apparent" yield the suspended particles must have strong attractive inter-particle interactions. In other words, the yielding phenomenon is not always present in filled systems. One may approach this problem another way, asking: "what should the zero shear viscosity be for a given concentration?" There are numerous semi-empirical equations which allow this parameter to be computed. For our PE-mica systems, I calculated that the viscosity should be about 10 times higher (for 60% mica sample) than the maximum value determined experimentally. This means that on increase of ω the flow curve at $\omega \simeq 10^{-2}$ falls from the Newtonian plateau to the observed values. The rapid decrease of η' from the (expected) plateau may be due to flake orientation on shearing. The only way we can unequivocally identify yielding is to do a very slow rate measurement. We plan to characterize these samples at $\dot{\gamma} > 10^{-5}$, using the Rheometrics System-4.

S. Newman: Perhaps you can clarify this for me. The G'-data also flattened out at low frequencies. This is usually taken to suggest yield. Could you comment on the G' plateau for the 60% concentration.

L. A. Utracki: You may have a plateau for different reasons. First, you may have a stable structure and the elastic response is constant within a certain range of frequency; e.g. a rubbery plateau as for a lightly crosslinked polymer. However, you may also generate a plateau by a sort of "slip" mechanism. For liquids G' should increase with frequency. But if the liquid structure undergoes a systematic change with ω (a sort of shear ordering) the increase may be significantly slower. I believe that this is what we see for the 60%-sample. The "secondary G'-plateau" indicates a transitory structure. According to Onogi and Matsumoto the level of the plateau should depend on strain.

R. Simha: When one looks at viscosity of highly concentrated systems under finite deformation, there is always one element which has to be taken into account, and that may account for your results; that is the change in the radial distribution, if it was a spherical particles system, or in the configurational distribution function for non spherical ones—a change under the influence of shear. This is actually the basis for a treatment of viscosity of pure liquids which we have known since Kirkwood and it is also important when one deals with suspensions. This is the point I wanted to make. I also have a question. You seem to have passed a transition region be-

tween 40 and 60 wt % mica. Did you comment on why it should occur at such a high concentration? You have elongated particles—is this an orientation effect? If so, it should be visible at a lower concentration; one should not have to go to between 40 and 60% to see it.

L. A. Utracki: We calculated that the particle overlap concentration is around 5 vol. %. Plotting the relative viscosity: $\eta_r = \eta'/\eta'(PE)$, when η' is taken at the lowest rate of deformation, as a function of the particles volume fraction for a full series of mica-HDPE samples we could compare the results with the theoretical predictions. First, for $\phi < 0.05$ your equation (R. Simha, *J. Chem. Phys.*, 13, 188 (1945)) for ellipsoids of rotation gave excellent agreement. For these low concentrations we used the aspect ratio $p = 20.2$. Around the critical overlap concentration $\phi_c = 0.05$ the viscosity increase with concentration slows down. For concentrations above 20 wt % of mica, initially the data could be well-fitted to a simple exponential equation with the intrinsic viscosity of 8.5. As the concentration increased, so did the difference between the predicted and observed viscosity. For the sample continuing 60 wt % of mica the calculated η_r was about 10 times higher then measured. The reason, as I said before, is most likely due to the shear orientation of flakes even at these low frequencies. There is the transition due to flakes orientation, as you expected, for $\phi \simeq \phi_c = 0.05$. The observed difference in dynamic behavior between the 60 wt % sample and the others is due to the fact that with this sample we are deep into a strain-dependent zone of deformation, where the relaxation spectrum is quite complex with contribution from both the matrix and the filler. This behavior, in my opinion, should not be interpreted from the zero-shear properties point of view.

Particle Flow and Sintering Processes in Extrusion

C. L. SWANSON, G. F. FANTA, *and* E. B. BAGLEY

Northern Regional Research Center,
Agricultural Research Service,
US Department of Agriculture,*
Peoria, Illinois 61604

The flow mechanism of particulate polymers during processing is reviewed. The extrusion of starch-g-poly(methyl acrylate) polymers is a good example of this type of processing, since graft copolymers retain their granular appearance and do not melt, even at high temperature, due to the rigid starch matrix. The formation of a continuous plastic by extrusion is accomplished by the sintering of heat-deformed granules in the high-pressure zone of the extruder die. Photomicrographs confirm this mode of formation. Plots of flow rate through the extruder die versus pressure in the die are presented. Tensile strengths and percent elongation of extruded specimens are not greatly affected by variations in flow rate. The equilibrium moisture content (about 5 percent) of starch-g-poly(methyl acrylate) plasticizes the starch component and thus reduces the operating pressure in the die. Tensile strengths, however, are unaffected by the presence of equilibrium moisture. Final traces of residual acid (resulting from initiator solution) are difficult to remove from starch-g-poly(methyl acrylate), and prolonged heating of the graft copolymer in the presence of this acid results in polymer degradation.

INTRODUCTION

The decreases of viscosity, η, of polymer molecules with increasing shear rate, $\dot{\gamma}$, is a phenomenon of fundamental significance in polymer processing. A functional relationship between η and $\dot{\gamma}$, which is in general agreement with experiment, can be derived based on the concept that a polymer molecule in a shear field rotates at an average angular velocity $\dot{\gamma}/2$. As a monomer unit or segment of the rotating polymer chain rotates about the center of gravity of the molecule it experiences sinusoidally alternating tension and compression. Energy losses occurring during this deformation can be analyzed in detail and quantitative expressions relating η to $\dot{\gamma}$ can then be derived as described extensively in the literature and numerous books on polymer flow (1-3).

This approach to analyzing the non-Newtonian flow behavior of polymer systems is particularly appealing when applied to relatively isolated molecules in solution. It is more surprising that the functional dependence of viscosity on shear rate predicted for the dilute solutions can be carried over into concentrated systems, including polymer melts. In these concentrated systems, effects due to factors such as chain entanglement would be expected to complicate the analysis and it is not as self-evident, as it is in the dilute systems, that the basic concept is correct. For such reasons, the reptation model of Doi-Edwards to describe the motion of polymeric molecules is gaining acceptance.

Regardless of how the behavior of polymer molecules in the melt should be described, there is a class of materials to which the simple model of a particle rotating in a shear field should be applicable. This was emphasized by Bueche (1) referring to comments by Pao (4, 5) and work of Boyd (6) as follows:

"Another approach to this problem has been taken by Pao, the essence of whose theory is as follows. He considers the rotating body to be a piece of matter having the same retardation spectrum as the gross polymer. The rotating object need not be reduced to molecular terms, it can just as well be a minute particle of polymer. The relation between the frequency response of the polymer and its response to shear rate is completely obvious in a qualitative way. The polymer particle is clearly undergoing oscillatory distortion, and it will evidence the dynamic viscosity one would predict for an oscillating applied force and the agreement between theory and experiment is relatively good."

A question now arises as to whether any systems of any practical importance exist where this consideration is important. The answer is yes and the purpose of this paper is to review some of these systems and to indicate some of the properties and behavior that could be of significance in the processing of certain types of composites.

* The mention of firm names or trade products does not imply that they are endorsed or recommended by the U.S. Department of Agriculture over other firms or similar products not mentioned.

PREVIOUS WORK

The rheological unit in raw elastomers

In an ingenious paper in 1955, Mooney and Wolstenholme (7) showed that for raw elastomers, subjected to continuous shear, groups of molecules would "move and rotate essentially as elastic solid bodies." By placing a rubber soluble dye along a plane parallel to the plane of shear, they observed that dye was transferred across the shear planes "just as ink is transferred by a series of inking rollers on a printing press" (*Fig. 1*) (7). The average size of these flow units ranged from 1 to 35 μm. The results indicated that the elastomer flow units are close packed with a negligible volume of liquid material between them.

The authors also discussed the irregularities, thickness variation, and surface quality of calendered sheets with reference to the existence of these large flow units.

Poly(vinyl chloride) extrusions

Twelve years after the postulation of "supermolecular flow units" by Mooney and Wolstenholme, Berens and Folt (8) showed that such flow units could be identified and played a major role in determining melt flow behavior of poly(vinyl chloride) (PVC). They found in extrusion studies that pronounced differences in apparent viscosity, post-extrusion swelling, and extrudate roughness could not be correlated with molecular weight, molecular-weight distribution, or other parameters of molecular structure. Through the use of electron microscopy to examine fracture surfaces of molded or extruded PVC samples, they demonstrated that resin particles, as formed during polymerization, had maintained their identity and shape during melt flow processes.

Berens and Folt went on to argue that melt flow occurs largely by rolling and slipping of the polymer particles past each other and that the flow behavior is characterized by a relatively low apparent melt viseosity and a low degree of extrudate swelling.

In a subsequent paper, the authors discussed the effects of additives (9), comparing 2000 Å PVC latex having relatively "clean" surfaces with other preparations to which various laurates had been added. They concluded that a major role of calcium soaps and other lubricants in PVC was to preserve the contribution of a particle flow process by providing an increased resistance to loss of particle identity. Temperature of extrusion, too, had a significant effect on the flow mechanism. From fracture studies, Berens and Folt showed that the identity of PVC particles is largely lost when the melt is pressed, milled, or extruded at >200°C. At this temperature, rapid molecular interdiffusion of PVC particle boundaries occurred, and, as expected, the characteristic particle-slippage flow process behavior is obscured or eliminated by the high-temperature treatment.

In a later study of particle-size effects on flow of emulsion PVC, Berens and Folt (10) examined in more detail the flow rate, post-extrusion swell, and extrudate appearance as functions of temperature and pressure. Both particulate and molecular flow processes were observed and the relative importance of these two modes of flow varied with conditions. Particle slippage was favored by large particle size, high molecular weight, and low temperature as well as by the shear stress level. Apparent viscosity, swelling, and roughness were minimized when particle flow predominated.

The effect of temperature is well illustrated in *Fig. 2* taken from Berens and Folt (*Fig 4* of *Ref. 10*) where the extrudate diameter is plotted as a function of shear rate in the temperature range 170 to 210°C. Normally such data for polymer melts is given as die swell, B, the ratio of extrudate diameter, D, to die diameter, D_o, i.e., as $B = D/D_o$. For many thermoplastics, B is in the range from just over 1 to as high as 5, depending on die length to diameter ratio, polymer molecular weight, shear rate, and shear history. For the PVC sample of *Fig. 2*, the value of B is only about 1.06 at 170° and reaches only about 1.12 even at 200°C. Only at 210°C does the die swell begin to approach normal behavior for a thermoplastic melt, reaching about 1.27. The functional rela

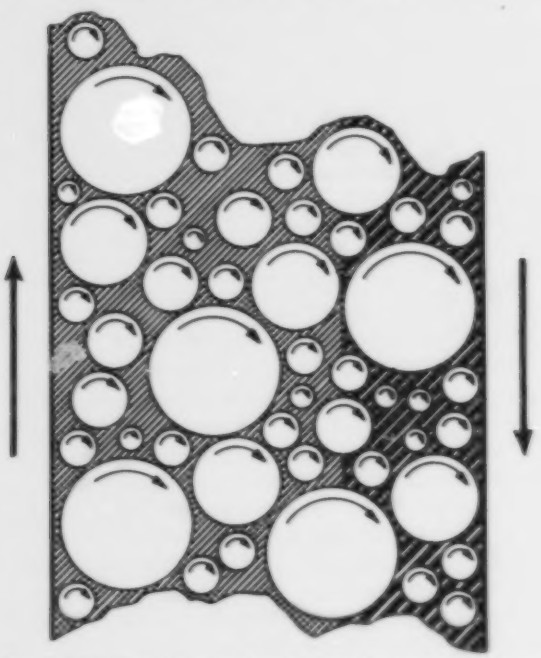

Fig. 1. Rotation of supermolecular particles under shear stress. (from Mooney and Wolstenholme, Ref. 7)

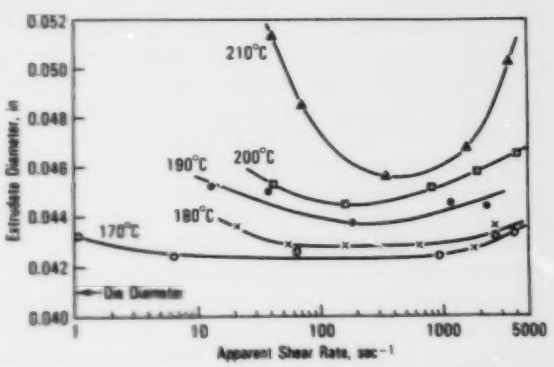

Fig. 2. Diameter of PVC extrudate as functions of shear rate and temperature (from Berens and Folt, Ref. 10).

tionship shown for B-$\dot{\gamma}$ at 210° is most unusual since normal thermoplastics show B increasing monotonically with increasing shear rate. The rise in B with $\dot{\gamma}$ at the higher shear rates suggests that shearing the granules promotes particle fusion and hence favors the onset of polymer melt flow at the molecular level, in contrast to the particulate flow so evident at the lower temperatures and shear rates where the particulate properties of the material predominate.

The commercial importance of PVC has resulted in other, more recent papers, examining morphological changes in PVC products during processing as well as effects of additives. Attention is drawn to the work of Krzewki and Collins (11, 12) on additives and their effect on fusion; Krzewki and Collins on effect of processing variables on fusion (13); Fahey (14) on morphological progression and elasticity development during extrusion of PVC; and by Fahey (15) on compaction testing to examine lubrication and fusion characteristics of PVC compounds. Among these papers, attention should be drawn particularly to Krzewki and Collins (13) and the sequence of electron micrographs showing progressive particulate fusion as processing temperature rises from 120 to 140, 160, and 210°C.

Particle deformability and particulate flow mechanism

In considering PVC particulate flow, Berens and Folt tend to emphasize the particle slippage aspects. Mooney and Wolstenholme emphasized that the particles move and rotate as elastic bodies. The particle deformability is clearly of major significance in determining the details of the material response to a given shear stress. If the particles are rigid, flow will not occur at all above certain volume fraction levels. Thus for a system consisting of, say, close packed spherical particles, flow can only occur if they can deform in such a way that they can slip past each other. The viscosity level observed in such systems will then depend on the ease with which this particle deformation/relative motion can occur.

The basic principle involved is illustrated in *Fig. 3* (16). Here the viscosity of a corn starch dispersion is shown as a function of shear rate as a function of cooking time. A 25 percent starch (dry basis, db) dispersion as originally mixed in water has a relatively low viscosity. After 15 min at 65°C, however, the granules have swollen enough so that the volume fraction of starch granules has increased to give a viscosity level around 600 centipoise (cp). However, within a shear rate range of about 10 to 100 s^{-1} the dispersion is dilatant. The shear stress level is still relatively low and the particles still relatively rigid at the stresses applied. After 30 min at 65°C, the particles have swollen still more, are softer, and more deformable. The increased softening of the particles coupled with a higher shear stress level due to the increased viscosity at the higher volume fraction levels, eliminates the dilatancy. After 75 min the particles are fully swollen. They occupy a larger volume fraction in the dispersion than they do after shorter heating times. Consequently, the viscosity has reached a maximum and the shear stresses acting on the particle are at maximum levels. Since the swollen particles are also softer or more deformable in this highly swollen state, the flow curve now obeys a power-law relationship indistinguishable from the response that would be expected for a polymer solution or melt. Nevertheless, at 65°C, the system consists only of a concentrated dispersion of deformable particles suspended in water at a concentration of nearly 100 percent. Very little free water exists between the particles. Equivalent behavior is shown for wheat starch (17).

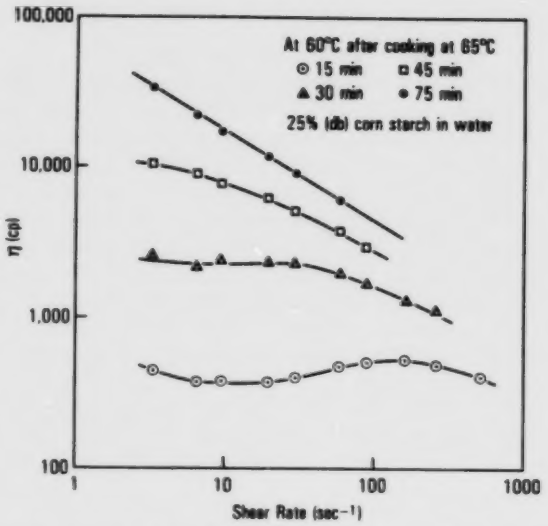

Fig. 3. Viscosity of starch dispersions as functions of shear rate and temperature (from Bagley and Christianson, Ref. 16).

As might be expected, particulate systems can show yield points (18). Yield points will occur in particulate systems because minimum shear stress levels would be expected to be necessary to overcome frictional effects as well as to deform the particles enough so that flow can actually occur. These basic concepts have been exam ined in detail in a series of papers on closepacked dispersions of deformable particles in which the particles are polyelectrolyte gels (19-23). On dispersing in water, the particles swell as much as two thousand times. The viscosity reaches very high levels as the volume fraction of the gel in the dispersion approaches unity, and the flow curves show the same power-law relation as seen in *Fig. 3* for the starch dispersions. The gel systems also showed yield points.

By controlling the crosslinking and hence the particle modulus different viscosity levels can be achieved as shown in *Fig. 4* from *Ref. 21*. Here the viscosity at 100 sec^{-1} is plotted against CQ, where C (g dry polymer per cm^3 of water) is the concentration of the gel particles in water and Q (g swollen gel per g of dry polymer) is the equilibrium swelling that the gel particle undergoes in water, which, of course, depends on the ionic strength for these polyelectrolyte gels. The quantity CQ is then approximately a volume fraction at $CQ \leq 1$ since Q is very large, in the range 100 to 1000. Above $CQ = 1$, water is in deficit and the particles are not fully swollen.

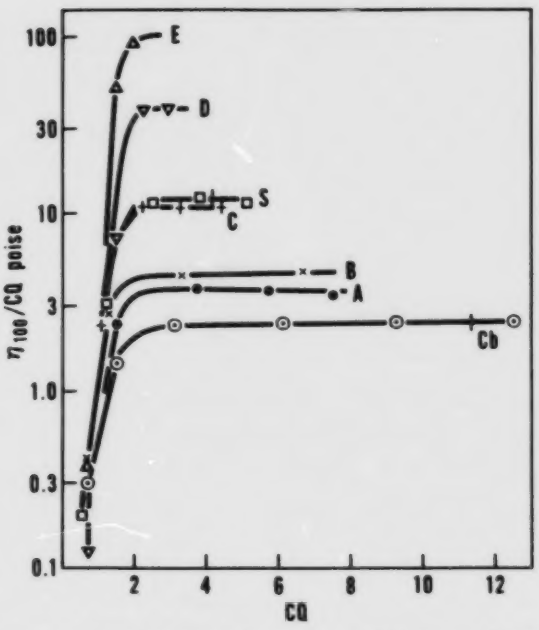

Fig. 4. Reduced viscosity function (η_{100}/CQ) versus CQ for starch (S), Carbopol 941 (Cb), and a series of hydrolyzed starch-g-poly(acrylonitrile) polymers (A-E) during a series of isotonic dilutions. η_{100} is measured at $\dot{\gamma} = 100\ sec^{-1}$, C is concentration (g/g), and Q is the equilibrium swelling ratio (g swollen gel/g polymer). Initial concentrations were: S, 1.5 percent; Cb, 1.23 percent; and A-E, 1.0 percent (from Taylor and Bagley, Ref. 21).

Extrusion behavior of some particulate systems

The flow properties of particulate systems are thus seen to depend on the volume fraction occupied by the particles, the deformability of the particles, and the frictional properties of the particles. The actual behavior in an extruder will depend on the shear stress levels reached and the ease with which the particles can respond, either by slipping or by deforming.

a. Consider the extrusion behavior of soy flakes at relatively low temperatures, 30 to 50°C. These irregularly shaped flakes, when extruded through tubes, show a pressure at the die-entry that is essentially constant, or decreases, with output rate from the extruder (24). The compacted soy particles are moving by a plug flow mechanism where the output rate-rpm relation can be computed knowing only the coefficient of friction of the dough on the metal of the extruder barrel and die. Shear stresses large enough to cause flow are not generated before slip occurs. At higher temperatures, ~ 100°C, the system particles do flow and the material behaves as do normal viscoelastic fluids, presumably because the water more effectively plasticizes the particles at the higher temperature, rendering the particles softer and more deformable.

b. Another system for which plug flow was believed to occur is described by Bagley, *et al.* (25). In an attempt to use starch as a rigid filler for thermoplastics, thermoplastic polymers were grafted onto the rigid starch filler. The objective was to provide a "coupling agent" on the granule surface compatible with the thermoplastic matrix. Surprisingly, extrusion of the grafted filler mixed with a thermoplastic polymer matrix led to very poor quality extrudates. It was found, in fact, that the grafted filler alone, without any thermoplastic matrix, extruded perfectly well. The material exited from the extruder die with no die swell but with excellent physical properties. Because there was no die swell it was thought that the materials were flowing as a plug (as with the soy doughs) and that at the pressures and temperatures encountered in the die that the powder sintered to form a good final product, the properties of which related to the glass-transition temperature of the grafted thermoplastic. Thus a starch-polystyrene graft copolymer gives a sintered extrudate which is rigid at room temperature while a starch-poly(methyl acrylate) graft polymer gives a very flexible sintered extrudate.

In this paper, we report preliminary results from extrusion of cornstarch-g-poly(methyl acrylate) (CSgMA). We examine the reproducibility of extrusion, the tensile properties and structure of the extrudates, and the pressure-output rate relationship to gain insight into the processes involved in extrusion of these materials.

MATERIALS AND METHODS

Materials

Globe 3005 corn starch (11 percent moisture) was from CPC International. Methyl acrylate was from Polysciences, Inc., and was used as received. Ceric ammonium nitrate was certified A. C. S. grade from Fisher Scientific.

Graft polymerization

The pilot scale graft copolymerization was conducted in an enclosed 10 gallon jacketed reactor constructed of 316 stainless steel. Reactants were stirred vigorously throughout the polymerization. The reactor was charged with 21 liters of distilled water and 2.1 kg (db) of starch. It was then heated to 35°C and held there for 1-1/2 h while sparging the reaction chamber with nitrogen. Methyl acrylate (4.2 kg) was added in one portion followed at 10 min intervals by four 315 ml portions of ceric ammonium nitrate initiator solution (0.2 M in 1 N HNO_3). An exotherm after the third addition of initiator briefly raised the reaction temperature to 42°C. The graft copolymer was recovered by filtration 1-3/4 h after the last addition of initiator, resuspended in water and neutralized to pH 7 by addition of 1 N NaOH. The pH decreased to 6.5 overnight and was readjusted to 7.0. The material was then washed with water three times. The major portion of the product was dried at 35°C in a forced draft oven to a moisture content of 5.1 weight percent and then ground to pass a 12-mesh screen. Yield of this portion of product (polymer A) was 3956 g (db). It contained 66 weight percent grafted and homopolymer PMA as calculated from weight loss after removal of starch by treatment with $NaIO_4$ and then with $NaOCH_3$ in methanol. $\bar{M}_w$ and $\bar{M}_n$ values determined by Gpc were 710,000 and 271,000, respectively, for the PMA polymer recovered. Some residual acid was trapped in product A and was released during extrusion, so that the pH of an aqueous slurry of the extrudate was near 3.5.

Homopolymer was removed from one portion of the wet product by extracting four times with acetone. The yield was 918 g (db), of homopolymer-free graft copolymer (polymer B). $\bar{M}_w$ and $\bar{M}_n$ of grafted PMA was 773,000 and 378,000, respectively. Another portion of wet product was neutralized by soaking overnight in pH 7 Beckman buffer, and was then washed and air-dried (yield 927 g, polymer C). Extrudates of this product were free of residual acid.

Extrusion

Polymers were passed through a 3/4-in. Laboratory Sample Batch Extruder (C. W. Brabender Instruments, Inc.) with L/D ratio of 20 to 1 and a 3 to 1 compression ratio screw. The extruder was driven by a variable speed Brabender Plasticorder. Extrudates exited from a slit die (1 by 0.020 in.) heated to 140°C. The inlet zone of the extruder was maintained at 90°C and the exit end of the extruder was held at 140°C. Pressure was measured with a transducer mounted just upstream of the die entrance.

Physical testing

Tensile strengths were measured as reported earlier (26). Particle sizes were determined by Coulter Electronics, Inc., with a Coulter Counter. Samples were examined and photographed in a Hitachi ISI scanning electron microscope. Specimens were mounted on aluminum specimen stubs with silver paint and coated with a 200 Å layer of gold-palladium (60-40) alloy. Electron microscope gain voltage was 11 KV.

RESULTS AND DISCUSSION

Typical starch-g-PMA extrudates are smooth surfaced, translucent, leathery ribbons (*Fig. 5*). Their ultimate tensile strengths (UTS) are about 21 MPa and are fairly insensitive to the percentage of PMA (50 to 70 percent) grafted to the starch. Tensile strengths are little affected by changing the flow rate through the extruder die, since as flow rate values increased from 3 to 28 g/min there was only a very slight increase in the tensile strengths (*Table 1*). Percentage elongation is also relatively unaffected by the flow rate.

Five samples of the starch-g-PMA copolymer A (see Materials and Methods) containing 5.1 percent moisture were extruded under the same conditions to establish the reproducibility of extrusion data. Relative standard deviation for pressure in the extruder die was 2.9 percent or less at flow rates that were varied from 3 to 12 g/min by changing the rpm of the extruder. At extruder speeds of 20 rpm and above, flow rate and pressure fluctuated moderately at constant temperature during prolonged extrusion so that replicate measurements were necessary to establish the mean values of flow rate and pressure. Flow rate values are more constant at lower rpm. The variable flow rate values are probably related to the particular screw-die configuration used and might not be observed with production extruders.

Since graft copolymer particles do not melt at temperatures below the decomposition temperature of starch

Fig. 5. Extrudates of starch-g-PMA.

(about 180°C), one might expect a plug flow mechanism for extrusion of these graft copolymers in the absence of a lubricating matrix of ungrafted polymer. In analogy with the behavior of rigid particulate soy material in extrusion it had thus been expected that the pressure drop through the die would be independent of output rate. As *Fig. 6* shows, however, this is not the case. The pressure increases in a regular fashion with increasing throughput rate. Calculations of apparent viscosities as a function of shear rate show that the material obeys a power-law relation with the viscosity values dropping from about 6×10^4 Pa.s at 50 s^{-1} to about 10^4 Pa.s at 300 s^{-1}. Lack of adequate quantities of material preclude more extensive study of the viscosity behavior at this time. Graft copolymer B that had been freed of homopolymer, produced a curve similar to *Fig. 6*. Likewise, extrusion behavior was unaffected by adding 5 phr of Acryloid K-125 processing aid (Rohm and Haas). Viscous flow can take place if starch granules are permeated with PMA to the point where hydrogen bonding, which nor-

Table 1. Tensile Properties of Starch-g-PMA Extrudates

Flow rate (g/min)	Screw RPM	UTS (MPa)	Elongation (%)
3.79	8.6	20.1	232
5.13	13.3	19.8	200
7.32	20.0	20.5	219
12.59	40.0	20.6	233
18.11	60.0	20.5	236
18.94	80.0	20.8	238
27.03	140.0	20.9	275
27.65	100.0	21.6	252

Polymer C (see Materials and Methods). Pumping screw (3/1 compression ratio).

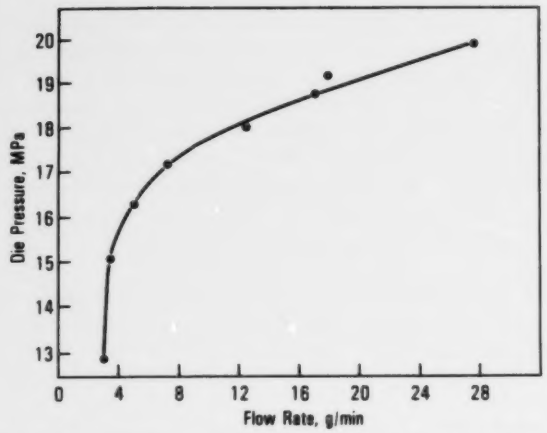

Fig. 6. Die pressure versus flow rate for starch-g-PMA (polymer C).

mally inhibits granule deformation, has been weakened to the point where the granules will flow under heat and pressure. More systematic studies are needed, however, to confirm the flow mechanism.

Ungrafted corn starch granules were shown by Coulter Counter measurement to have a median diameter of 8.57 μm. After grafting to a 67 weight percent PMA level, the measured median particle diameter increased about 59 percent to 13.66 μM. Within the experimental error, this is equal to the diameter predicted by adding the volume of grafted PMA (density 1.07 $g \cdot cm^{-3}$) to the volume of a median sized granule of starch (density 1.50 $g \cdot cm^{-3}$). Although we cannot rule out surface grafting, granules of polymer are most likely grafted throughout most of the granule interior. Polyacrylonitrile grafted to granular starch at high levels of addition has been shown by electron microscopy to penetrate to the center of the granules (27).

Photomicrographs of extruded specimens of starch-g-PMA disclose granule-sized fused particles with easily discernible boundaries (*Fig. 7*). All extrudates disintegrate on standing in solvents for PMA, although the graft copolymer particles are insoluble. Thus a particulate structure (formed via pressure fusion of heat softened particles) persists throughout the extrusion process. Specimens that have been stressed to failure apparently separate between particles, as shown in *Fig 8*.

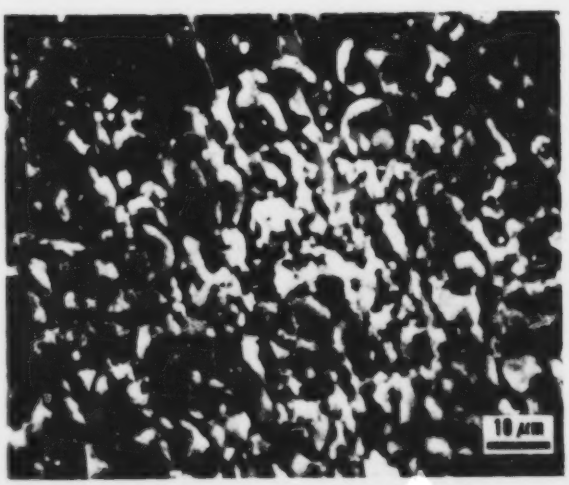

Fig. 7. Scanning electron photomicrograph of specimen of extruded starch-g-PMA (polymer C). Sample photographed at 1000 times.

Since the starch portion of the graft copolymers is plasticized by water, the moisture content of the copolymer influences the pressure required for extrusion. The copolymers normally contain about 5 percent moisture when in equilibrium with ambient air. If dried at low temperature under vacuum, almost all this moisture can be removed from the graft copolymer, and the subsequent extrusion develops higher pressures (*Fig. 9*). The

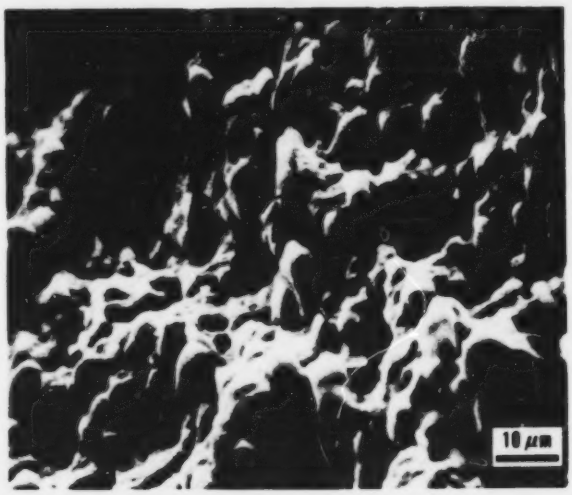

Fig. 8. Scanning electrophotomicrograph of fracture zone of tensile test specimen of extruded starch-g-PMA (polymer C). Sample photographed at 1000 times.

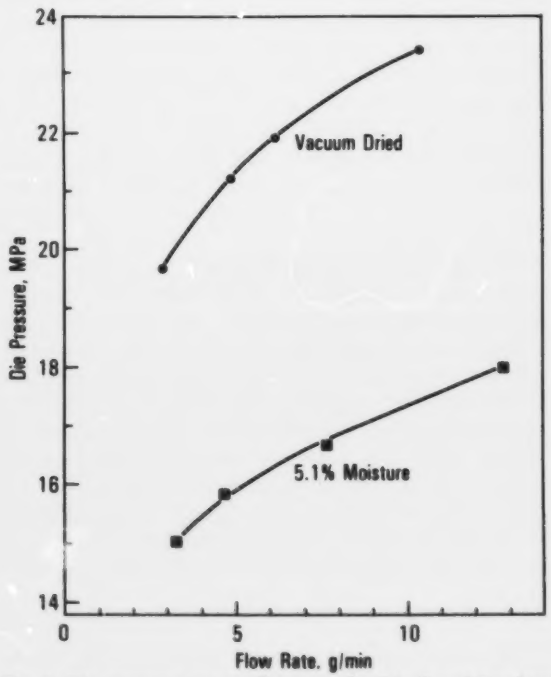

Fig. 9. Die pressure versus flow rate for "dry" and "ambient moisture" starch-g-PMA (polymer A).

increase in pressure with flow rate suggests that even dry graft copolymers are exhibiting viscous flow.

Apparent viscosities and shear rates can be calculated from equations that take into account the geometry and dimensions of the die, the die pressure, and the rate of extrusion. Dried copolymer A has a calculated apparent viscosity of 88,200 Pa.s, while viscosities of copolymers A and C were both 63,100 Pa.s at 50 s^{-1} shear rate.

Drying the starch-*g*-PMA copolymer had little effect on the physical properties of the extrudate. Tensile strengths were 19.5 and 19.6 MPa for dry and ambient moisture extrusion while elongations were 199 and 190 percent, respectively.

Heating the graft copolymer in the presence of acid (e.g., the residual acid present in starch-*g*-PMA that has not been completely neutralized during preparation) may hydrolyze the starch portion to oligosaccharides and sugars and also hydrolyzes some of the methyl acrylate ester linkages. Heating polymer A for 20 h at 103°C reduced $\overline{M}_w$ of the PMA moiety from 710,000 to 48,800 and $\overline{M}_n$ from 271,000 to 16,900. The heating increased water solubles from 0 to 36.2 percent and acetone solubles from 4 to 58.6 percent. Infrared spectra indicate that all fractions contain both carbohydrate and synthetic polymer segments. Tensile strength and percent elongation are decreased by prolonged heating. However, the short duration heating during extrusion does not appreciably degrade tensile properties, although $\overline{M}_w$ and $\overline{M}_n$ are reduced to 673,000 and 188,000, respectively.

CONCLUSION

Evidence from electron microscopy suggests that powdered starch-*g*-PMA copolymer retains a particulate structure during continuous extrusion, although the relationship between pressure and flow rate is typical of that for viscous flow; the mechanisms remain to be confirmed. Our work thus provides another example of the superparticle flow described by Mooney, Folt, *et al.* (7-10). Although the graft copolymer does not melt, it appears to flow under heat and pressure. The extrusion may be closely related to low-temperature extrusions i.e., plug flow of PVC, as discussed by Folt and coworkers (8-10).

The necessity for careful neutralization of the copolymer before drying has also been demonstrated. Very small amounts of residual acid in the copolymer decrease tensile strength and elongation when the copolymer is heated. Thus the life expectancy of articles fabricated from incompletely neutralized starch-*g*-PMA might be reduced. However, carefully controlled degradation could lower melt viscosity and enhance compatibility with other thermoplastic materials.

Properties of extrudates are little affected by changing the extrusion rate so long as sufficient pressure and kneading are available to fuse thoroughly the particles of copolymer. Ambient moisture in the graft copolymer reduces the pressure required for extrusion without an appreciable effect on tensile properties of the extrudate.

Additional work is needed to determine the effects of die and barrel temperature, die geometry, particle size, mastication, partial hydrolysis of the starch, and similar variables on the extrusion behavior of these graft copolymers.

ACKNOWLEDGMENT

We gratefully acknowlege the efforts of Robert Fecht (chemical analysis and physical testing), Robert Burr (extrusions), and Frederick L. Baker (electron microscopy).

REFERENCES

1. F. Bueche, "Physical Properties of Polymers," Interscience Publishers, John Wiley and Sons, New York (1962).
2. S. Middleman, "The Flow of High Polymers," Interscience Publishers, New York (1968).
3. Chang Dae Han, "Rheology in Polymer Processing," Academic Press, New York (1976).
4. Y. H. Pao, *J. Appl. Phys.*, **28**, 591 (1957).
5. Y. H. Pao, *J. Chem. Phys.*, **25**, 1294 (1956).
6. R. H. Boyd, *J. Appl. Phys.*, **29**, 453 (1958).
7. M. Mooney and W. E. Wolstenholme, *J. Appl. Phys.*, **25**, 1098 (1955).
8. A. R. Berens and V. L. Folt, *Trans. Soc. Rheology*, **11**, 95 (1967).
9. A. R. Berens and V. L. Folt, *Polym. Eng. Sci.*, **8**, 5 (1968).
10. A. R. Berens and V. L. Folt, *Polym. Eng. Sci.*, **9**, 27 (1969).
11. R. J. Krzewki and E. A. Collins, *J. Vinyl Technol.*, **3**, 116 (1981).
12. R. J. Krzewki and E. A. Collins, *J. Macromol. Sci.-Phys.*, **B20**, 465 (1981).
13. R. J. Krzewki and E. A. Collins, *J. Macromol. Sci.-Phys.*, **B20** (4), 443 (1981).
14. T. E. Fahey, *J. Macromol. Sci.-Phys.*, **B20**, 415 (1981).
15. T. E. Fahey, *J. Macromol. Sci.-Phys.*, **B20**, 319 (1981).
16. D. D. Christianson and E. B. Bagley, *Cereal Chem*, **60**, 116 (1983).
17. E. B. Bagley and D. D. Christianson, *J. Text. Studies*, **13**, 115 (1982).
18. E. B. Bagley and D. D. Christianson, *Staerke*, **35**, 81 (1983).
19. E. B. Bagley and N. W. Taylor, *J. Polym. Sci., Symp. No. 45*, 185 (1974).
20. N. W. Taylor and E. B. Bagley, *J. Polym. Sci., Polym. Phys. Ed.*, **13**, 1133 (1975).
21. N. W. Taylor and E. B. Bagley, *J. Appl. Polym. Sci.*, **21**, 113 (1977).
22. N. W. Taylor and E. B. Bagley, *J. Appl. Polym. Sci.*, **21**, 1607 (1977).
23. N. W. Taylor and E. B. Bagley, *J. Appl. Polym. Sci.*, **23**, 1897 (1979).
24. B. K. Jasberg, G. C. Mustakas, and E. B. Bagley, *J. Rheology*, **23**, 437 (1979).
25. E. B. Bagley, G. F. Fanta, R. C. Burr, W. M. Doane, and C. R. Russell, *Polym. Eng. Sci.*, **17**, 311 (1977).
26. C. L. Swanson, G. F. Fanta, R. G. Fecht, and R. C. Burr, in "Renewable Resources for Polymer Applications," C. E. Carraher and L. H. Sperling, eds., p. 59 Plenum, New York, (1983).
27. G. F. Fanta, F. L. Baker, R. C. Burr, W. M. Doane, and C. R. Russell, *Staerke*, **25**, 157 (1973).

DISCUSSION

S. Newman: Many years ago I did something that appears to be very similar, but with a different approach to making the materials. You took starch and grafted thermoplastics on to it. What I had done was to emulsion polymerize a spherical particle (could either be a low T_g acrylate of some kind or something which can be cross

linked) and then, by continuing the polymerization process, by shifting to a new monomer, e.g. a non-crosslinkable monomer, I could produce what I call a graded particle. A rigid core of hard or crosslinked material was essentially coated in the emulsion polymerization; a system which was very much like yours. It could be processed, could be molded, a perfectly nice material. In fact, ultimately I did use it in a powder coating system. If you have a sintering system you can make a powder coating.

E. B. Bagley: Glad to hear that. If you have any references I would like to have them.

S. Newman: Several patents by myself and some articles in *J. Polym. Sci.*

L. A. Utracki: Ed, I am a little bit confused because on the one hand, you are indicating that your grafted particles show a viscous, not a plug flow, but on the other hand you are comparing it to PVC particulate flow, which is known to be plug flow.

E. Bagley: This question gets to the heart of the issue. Consider any system of close-packed particles. If the system is sheared, the particle deformability and the stress level should be the critical parameters. If the particles are effectively rigid, at the stresses applied, you may get slip and plug flow as in the extrusion at low temperatures of soy dough. The particles could alternately slip and slide past each other in a complex cooperative fashion as discussed by Berens and Folt. If the particles are easily deformable (e.g., the hydrolyzed starch-polyacrylonitrile graft copolymer) the particles will be strained in a cyclic way in this cooperative particle motion to give a response indistinguishable from that seen in normal polymer melts and solutions as discussed by Bueche. The figure showing the viscosity response of the starch granule dispersions illustrates some of the changes in rheological response as the stress level changes and the particle deformability is altered.

L. A. Utracki: It seems that SEM could give you the answer if you have skin core structure which one may expect to observe as a result of a plug flow.

E. B. Bagley: We are using the SEM and optical microscopy to examine specific systems and I agree that this can be most informative.

R. Simha: If I understand you correctly, Ed, you do have a particle to which are tied flexible molecules. Have you studied the molecular weight of these, and the modes of attachments? They must be influenced by the flow. It depends on how the flexible chain goes onto the particle. If it were to be sticking out you would have to fight the entanglements as you shear, whereas if they are lying down there is no question of entanglements and there is more or less only the coating effect.

E. B. Bagley: The molecular weights and modes of attachment have been studied in the starch graft systems. The starch can be removed chemically and the grafted synthetic polymer can be characterized. In only one situation am I certain of the effects which you ask about. This is the hydrolyzed starch-polyacrylonitrile where the polyelectrolyte character seems to prevent any interactions between the swollen gel particles. This is truly a situation where no entanglements exist but the viscosity and normal stress dependence on shear rate are qualitatively indistinguishable from the response of the polymer solution or melt.

S. Newman: Would not the entanglement depend on the molecular weight of the grafts?

E. B. Bagley: Yes, but also, as remarked by Professor Simha, on how the flexible chain goes into the particle.

Mechanical Property Enhancement in Short-Fiber Composites Through the Control of Fiber Orientation During Fabrication

LLOYD A. GOETTLER

Rubber Chemicals Division
Monsanto Polymer Products Company
260 Springside Drive
Akron, Ohio 44313

The mechanical properties of plastics and elastomers reinforced by short fibers are generally dictated by the selection of matrix and reinforcement. However, the high tensile properties attainable in these systems through laboratory processing techniques are frequently not obtained in conventional fabrication operations. To gain a wider latitude in meeting economic and performance constraints, the control of composite structure in the fabrication step should not be overlooked. Tool geometry and processing conditions can be manipulated specifically to control the fiber orientation distribution in the product. A study of fiber orientation in composite compounds during flow through runners, gates, and dies leads to recommendations for optimizing the directional strength and stiffness according to a kinematic model. Performance data on parts fabricated from various short-fiber composite materials bear out these projections.

INTRODUCTION

The incorporation of fillers and reinforcing particles into a polymer produces a microscopically inhomogeneous material, whose properties are more dependent upon processing techniques and conditions than are the usual unfilled polymers. The sensitivity increases with the degree of reinforcement. In many cases, the composite properties are dominated by the structure of the fabricated part, rather than by the properties of the constituent materials.

Reinforcement by the use of fibers, particularly glass fibers, predominates in the reinforced plastics industry. Such short-fiber-reinforced polymers can offer some of the property advantages of continuous fiber reinforcement combined with economical flow processing that is amenable to the large-scale production of composite hardware.

An analysis for the tensile behavior of short-fiber composites usually begins with the strength and modulus equations. These equations point out the dependence upon reinforcement concentration and aspect ratio alone (in addition to the constituent properties). However, implicit in these equations is the assumption that the fibers are well aligned in the stress direction, which is extremely difficult to attain in short-fiber composites. Futhermore, if the dispersion of fibers is incomplete, cracks may easily propagate parallel to the fiber orientation regardless of the stress direction. Finally, composite failure may occur through molding flaws, or the presence of excessive voids. Even the interface strength may be subject to the processing conditions. Thus, the full picture is considerably more complicated than the idealized equations of composite mechanics indicate.

Not only is the fabrication operation an essential step in the production of a fiber-reinforced part, so that its effects are unavoidable, but it can be used as a tool to impart a special desired morphology. The proper processing environment must be diagnosed, implemented, and controlled to diminish or turn to advantage the unavoidable consequences, and to impart a desirable material structure. In the current state of the art, the latent capabilities of flow processing have yet to be fully exploited. The structures of short-fiber composites are usually neither manipulated nor controlled (although there is evidence of increasing development interest in this area (1-3)). The resulting fabrication process, though still economically attractive, represents an inefficient use of the discontinuous fiber reinforcement.

The purpose of this paper is to describe the effects of flow on composite structure and how these can be optimized to fit the geometry and application of the fabricated part. Any practical fabrication step utilizing short-fiber reinforcements will involve the flow of a suspension of the fibers in either a matrix resin, precursors of it, or a preliminary suspending medium used to establish the composite structure prior to resin infiltration. The first relates to the molding of reinforced thermoplastics, the second to reinforced thermo-

sets molded in a B-staged condition prior to crosslinking, and the last to pre-pregging techniques.

The aspects of composite structure that determine composite properties apply in general to any resin system. The specific examples of processing-property relationships derived from studies with glass-fiber-reinforced nylon and epoxy will also be relevant to other composites.

MATRIX DEPENDENCY

First consider under what conditions the role of composite structure can be minimized. By utilizing well-dispersed fibers of shorter length, tensile properties are less directional and show a greater dependency on the characteristics of the matrix.

Reinforcements are coated with a coupling agent, usually a silane, to augment adhesion to the polymer. With thermosetting resins, actual covalent bonds may be formed by silanol bridges between the surface of the reinforcement and the polymer. However, physical forces (hydrogen bonding, polar forces) usually predominate, and the function of the binder coating is to make the surface more compatible with the polymer. Some data in *Table 1* show the variation in tensile strength that can be expected among a variety of injection-molded thermoplastic resins reinforced with 16 volume percent (30 weight percent) discontinuous glass fiber. By subtracting from the composite strength a term for the contribution of the matrix, a quantity is obtained which represents the reinforcement afforded by the fibers. *Figure 1* shows that the fiber reinforcement so defined is a linear function of the dielectric constant, a measure of the polarity of the matrix, for the wide range of polymers listed in *Table 1* (7). No such simple relationship is evident for the tensile strengths of the unfilled polymers, as shown in *Fig. 2*.

FIBER LENGTH AND COMPOSITE STRUCTURE

As long as the aspect ratio of glass fiber exceeds about 200, the full stiffness and strength benefit of the short fiber will be realized. With thermosetting molding compounds processed through a plunger molding machine, it is not difficult to maintain that value. More care is required when a reciporcating screw is used with thermoplastics.

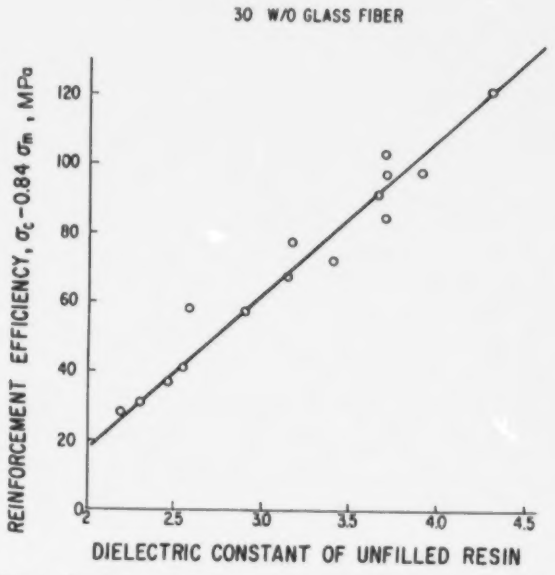

Fig. 1. Dependence of composite strength on matrix polarity.

However, there is still some benefit to be gained from fiber length in thermoplastic composites, even with the well-bonded, ductile nylon 6 matrix. Data reported in *Table 2* show fiber length and concentration effects for the injection moldings of a tensile bar using both ram and reciprocating screw machines. The latter produced more extensive fiber damage, which tended to eradicate the differences in fiber length of the molding compounds. The longitudinal fiber alignment induced by the constricted neck section of the tensile cavity, which will be explained more fully in a subsequent section, is seen to yield exceedingly high tensile strength and modulus properties in the ram moldings of the long fiber compounds.

The gradual reduction in the length of a graphite fiber by repeated moldings in the ram machine is shown in *Table 3* in comparison with glass fiber attrition in both ram and screw machines. The protection afforded the fibers of being segregated into bundles is evident in the epoxy data. Of course, some degree of dispersion must be obtained during the molding operation to produce reinforcement of the molded part. It appears that

Table 1. Tensile and dielectric properties of 16 volume percent short glass fiber/thermoplastic composites.

Polymer	Tensile Strength, MPa			Dielectric Constant at 60 Hz
	σ_c, Composite	σ_m, Matrix	$\sigma_c - .84\sigma_m$	
Nylon 6-6	183 [4]	74	120	4.3
Nylon 6	162 [4]	70	103	3.7
Nylon 6-10	148 [4]	60	97	3.9
ABS	134 [4]	44	97	3.7
PET	152 [5]	73	91	3.65
Acetal copolymer	136	61	84	3.7
Polycarbonate	130 [4]	63	77	3.17
PVC	113 [4]	49	71	3.4
Polysulfone	127 [4]	72	66	3.14
PPO	126 [6]	81	58	2.58
SAN	122 [4]	77	57	2.9
Polystyrene	88 [4]	56	41	2.55
Ionomer	60	28	36	2.45
Polyethylene (HD)	63	38	30	2.3
Polypropylene	55 [4]	32	28	2.2

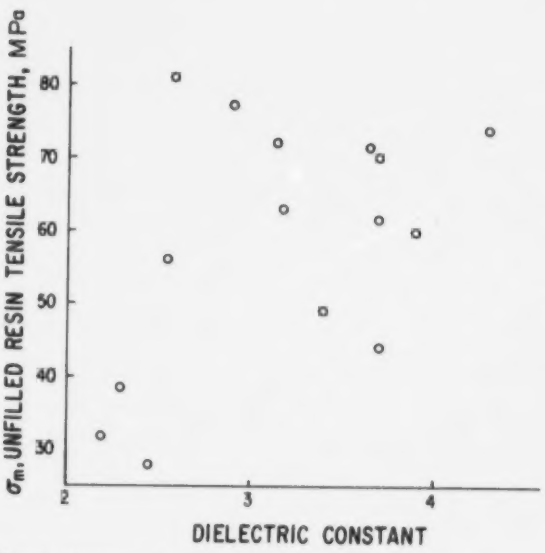

Fig. 2. Absence of polarity effect in unfilled polymers.

attrition in the screw machine will not reduce the mean fiber aspect ratio below about 20. Above this limit, the residual fiber length depends upon the initial length in the feed material.

With thermosetting matrices, tensile strengths are substantially lower when the fiber length is short (like that in injection-molded RTP). For example, in a glass fiber epoxy composite, the tensile strength drops from 210 to 55 MPa as the fiber length is reduced from 6.4 to 1.6 mm or less. In such systems, for which the matrix has a low (< 1.0 percent) elongation to failure, long fibers are required, and there is a greater need to control fiber orientation.

The best structure for an aligned discontinuous fiber composite comprises long fibers that are well dispersed in the molding compound. Unfortunately, this type of structure is very difficult to obtain. In producing a high dispersion, the fibers are invariably broken. For this reason, the fibers in most commercial molding compounds of the long fiber type are formed into bundles of 100 to 200. If the long fiber length can be preserved during the molding operation, the resulting molding will contain weak shear planes, causing off-axis failure. Composite performance will be keyed to the orientation of these planes. Thus, both fiber length and fiber orientation are critical.

FIBER ALIGNMENT TECHNIQUES

There are two different methods for attaining aligned discontinuous fiber moldings. Either an oriented mat or strand may be impregnated with resin and the resulting prepreg compression molded, or a molding compound may be aligned and fabricated in a single step, as in injection molding.

Although several processes have been developed for pre-aligning fibers before they are infiltrated with resin (8-10), the most perfect fiber alignment in short-fiber composites can only be obtained by tedious methods of hand lay-up of well-oriented, highly elongated grains of resin-coated fibers. These could be prepared, for example, by the method of Takano (11), who added an immiscible epoxy resin to a suspension of clusters of individual fibers in a Couette flow field. The composites made by hand-laying such elongated grains not only excel in precision of alignment (± 7°), but also are unique in simultaneously affording high degrees of fiber wet-out, dispersion, and end overlapping. The

Table 2. Comparative tensile properties for nylon 6 composite moldings.

Type of Molding Machine	Fiber Conc. (vol/o)	Fiber Length* mm	Tensile Strength, MPa	Young's Modulus, GPa	Ultimate Elongation, percent
Recip. Screw	30.4	8.9	191	13.0	2.5
	23.1	8.9	193	12.1	2.4
	23.1	.3	154	11.0	2.5
Ram	30.4	8.9	282	17.6	2.2
	23.1	8.9	210	12.3	2.0
	23.1	.3	170	11.3	2.3

* in molding compound

Table 3. Fiber damage in injection molding

Type of molding	Material	Passes through Molding Machine	Volume-mean aspect ratio	Remarks
Ram	Thornel 50 in Polycarbonate	0	1060.	
		1	108.	
		2	42.	
		3	32.	
Ram	glass fiber in epoxy	0	260	
		1	250	highly bundled
		1	133	dispersed
Recip. Screw	glass fiber in Nylon 6	0	25	
		1	19	
Recip. Screw	glass fiber in polypropylene	0	47	
		1	41	
Recip. Screw	glass fiber in Nylon 66	0	19	
		1	19	

values of tensile strength and modulus reported in *Table 6* for this method can be attributed to the large percentage (about 40 percent) of the fibers that are fractured in a tensile failure, compared, for example, to almost none in conventional injection moldings.

Exact alignment techniques are more difficult to apply for thermoplastic composites. The high-molecular-weight resins must either be melted, or solution coated onto the fibers. The latter is preferable because of the high viscosity of the thermoplastic melts. However, precautions must be taken for solvent removal. Tensile properties parallel to the fiber direction for highly aligned melt—or solvent—impregnated thermoplastic composites are competitive with thermosetting systems.

The best resin-reinforcement contact in a thermoplastic system can be obtained when the two are combined before polymerizing the resin. Then, viscosity of the monomer is in the centipoise range. In addition, void elimination is enhanced, and high fiber loadings with less fiber damage are possible. For example, composites prepared by polymerizing ϵ-caprolactam (nylon 6) around a highly aligned array of glass fibers display high tensile strength and elongation to failure in the transverse direction. The tensile strength of 83 MPa, equal to that of the matrix, and an elongation of 2.0 percent achievable at 30 volume percent fiber content, are unknown for other nonelastomeric polymer systems. In contrast, a typical brittle epoxy reinforced with fibers transverse to the stress direction breaks at 0.5 percent strain and about 55 MPa tensile stress. With such a material, classical design limits for laminated structures could be surpassed.

CONTROLLED FIBER ORIENTATION (IN MOLDING)

Geometry

The only practical, economical, large volume methods for producing aligned short-fiber composites are those in which the fiber alignment is generated directly in the final fabrication step of the composite. These all involve flow through channels and encompass both continuous (extrusion) and intermittent (injection and transfer molding) processes. The latter are the most important to the reinforced plastics industry and the former to the rubber industry.

Shear flow with a high-viscosity matrix resin through uniform channels or the elongational forces in flows through converging/diverging channels will produce orientation of the fibers and anisotropic properties which, if not controlled, may be detrimental to the performance of the extruded or molded part. For example, the transverse strength of an epoxy composite containing 50 volume percent 3mm E-glass fiber is typically only 1/6 of the longitudinal strength. A similar reduction obtains for the elastic modulus. If left uncontrolled, unfavorable orientation patterns may cause the loss of 75 percent of the potential stiffness. But, by manipulating geometry, processing conditions, and material composition, it is possible to turn this orientation effect to advantage by aligning the fibers into the direction of maximum load.

A myriad of geometrical shapes can be encountered in a mold design. Five basic right prisms that differ in form relative to the gate placement are given in *Fig. 3*. Many straight sections can be approximated by one of these arrangements. However, a complete study of the effects of cavity geometry on fiber orientation would have to involve the gate size relative to the cavity dimensions, nonparallel wall sections, and curved channels, including bends and tees. If the effect of each of these sections on the orientation in the molding compound entering the section were known, the complete orientation distribution in a molded part could be synthesized by joining the necessary elements together to at least approximate the overall geometry. Alternately, it may be possible to compute the complete fiber orientation distribution function *a priori* even in complex flows by numerical calculations based on a finite element approach (12).

Here we treat Type I elements of different entrance configurations, which occur frequently not only as a part component, but also as the runner system of a mold or the flow channel of an extruder. A qualitative consideration of some other geometries encountered in flow molding is given by Woebcken (13).

Experimental Procedure

The molding compounds used were composed of an epoxy resin of the epichlorohydrin/bisphenol A type (Epon 828, Shell Chemical Company) that was cured with methylenedianiline at 30 phr and reinforced with chopped E-glass fiber (240 fibers per bundle, epoxy-compatible silane finish). They were prepared by heating the resin and hardener together at 60°C for about 30 minutes and then rapidly impregnating the glass with the mixture in a sigma-blade blender. Upon standing

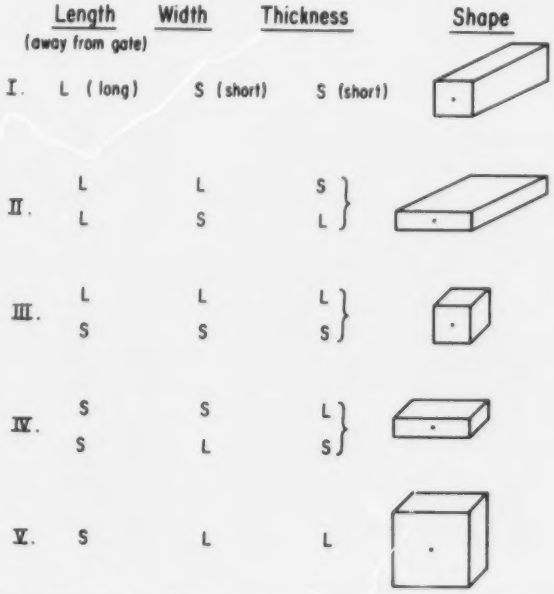

Fig. 3. Possible straight channel geometries relative to the gate position.

overnight at room temperature, the resin advanced to a non-tacky B-stage with about 45 percent of the epoxide groups reacted, which could then be easily molded.

Pieces were transfer molded on a 62-ton plunger press at a relatively low temperature of 95°C to minimize resin cure while the cavity was filling. Fill rate was controlled by adjusting the ram travel speed through a flow control valve on the hydraulic line. The flow and fiber orientation patterns could then be analyzed under conditions of constant viscosity. A high exotherm that developed within the molding following the latent period produced a full cure with 30 minutes.

Orientation Effects

The bar geometry depicted in *Fig. 4* is typical of many conventionally end-gated moldings. Three views of a typical molding are shown in *Fig. 5*. Carbon black can be added to some grains of the feed to make the orientation easily visible. No orientation can be observed on the outer molded surfaces, but about 1 mm must be ground away to make a pattern visible. The cross-section view (x_1 plane) shows a somewhat concentric pattern that results from the biaxial stretching of the material as it flows through the gate, which will be described below. A lack of symmetry in the x_1 and x_3 planes may be caused by the asymmetric position of the gate near the top of the mold. Otherwise, the orientation in the core region should be strictly concentric.

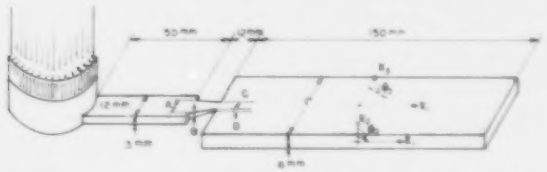

Fig. 4. Geometry for plunger molding of 3 mm glass-fiber-reinforced epoxy bars.

a. x_1 = constant

b. x_3 = 0

c. x_2 = 0

Fig. 5. A typical end-gated bar molded from glass-fiber-reinforced epoxy.

Some aggregation of fibers occurs in the molded sample. The fibers in the molding compounds are in the form of bundles to give a dense material and to allow initial flow to take place without fiber breakage and plugging of orifices. This clumping, in addition to the stranding that is produced by flow through a small gate, gives rise to a grainy structure. There is no evidence, however, of large-scale fiber-resin separation that would be manifested as a variation in fiber content of the molding. No variation in fiber loading occurs along the length of the bar.

In the diverging flow that occurs as the cross-section broadens from the gate to that of the bar cavity, the fibers become oriented perpendicular to the streamlines of flow. This fiber rotation has been shown dramatically (14) by reversing the gate section to produce a gradual channel expansion. The resulting orientation is primarily across the bar, but when the change in the cross-sectional area is abrupt the streamlines extend as spokes of a wheel from the point of gate attachement, giving rise to a component of longitudinal orientation near the wall. This could be subsequently enhanced by shear at the wall. The change in orientation from the gate to the cavity occurs over a region of about 13 mm. The overall structure of the bar, then, is a transversely oriented core surrounded by a longitudinally oriented skin.

This mechanism of buckling, biaxially stretching to fill the cavity cross-section, and distortion of the resulting hermispheric shell by shear at the wall, is one of the mechanisms for the production of transverse orientation in the core of a molding. The other occurs at the vent end of the mold where the material that was initially freely squirted into the empty mold cavity is finally compressed to fill out the cross-section. In this compaction the material is folded back on itself. This produces an end-effect region of exceedingly transverse orientation (because there is no shear) that extends back about 25 mm from the end of the mold.

Contours of constant θ_1, the polar angle around the flow axis, are shown in *Fig. 6* as a function of position across the cross-section normal to the flow direction.

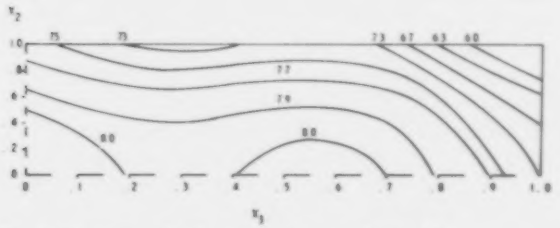

Fig. 6. Contours of polar angle in an end-gated bar.

When $\theta_1 = 90°$, the orientation is completely transverse. The values represented are the means of the distribution in θ_1 over different fibers at each point in the molding. The polar angle θ_1 about the x_1 (flow) axis is related to the planar angles ϕ_2 and ϕ_3 projected into the orthogonal longitudinal x_2 and x_3 planes for each fiber according to

$$\tan^2 \theta_1 = \text{ctn}^2 \phi_2 + \text{ctn}^2 \phi_3 \qquad (1)$$

The mean is obtained as the first moment of the bivariate distribution in ϕ_2 and ϕ_3 by considering that these variables are independent and normally distributed:

$$\bar{\theta}_1 (x_2, x_3) = \int_0^\pi \theta f(\theta)\, d\theta$$

$$= \int_{-\infty}^{\infty} \int_{-\infty}^{\infty} \tan^{-1} [(\text{ctn}^2 \phi_2 + \text{ctn}^2 \phi_3)^{1/2}] \, n(\phi_2)\, n(\phi_3)\, d\phi_2 d\phi_3, \qquad (2)$$

where $f(\theta)$ is the probability function of the polar angle θ and $n(\phi_2)$, $n(\phi_3)$ are the normally distributed probability functions of the planar angles ϕ_2 and ϕ_3. The normal distributions of the planar angles are characterized by a mean and standard deviation, each measurable and calculable as a function of spatial position within the molding.

Except for end effects within 25mm of the ends of the molding, it was found that the dependence on the x_1 coordinate measuring distance of flow is not significant. *Figure 6* shows that the orientation in the end-gated bar, which required a considerable amount of flow to form, is almost completely transverse. Such a condition results from the lack of shear deformation in long-fiber molding compounds. Only at the corners of the bar does the orientation deviate substantially from the transverse pattern set up by the expanding flow from the runner into the cavity.

Although processing (molding) conditions have an influence on the orientation distribution (14), only limited changes are possible. The longitudinal skin could be made larger, but a transversely oriented core still persists. Orientation can best be controlled by integrating converging and diverging sections into the mold design, and selectively placing the gating to produce the desired flows. In particular, a high degree of longitudinal alignment results when a converging flow, caused by a reduction in cross-section, is incorporated into the mold design. *Figure 7* shows how this converging flow completely removes the transversely oriented core. Only in this manner can a low mean fiber orientation $\bar{\bar{\theta}}_1 = \int\int_A \bar{\theta}_1\, dA$ be attained to produce a high longitudinal stiffness. The angle about the flow direction assumed by 75 percent of the fibers can be reduced from 45 degrees with conventional gating to less than 20 degrees. Tensile strength and modulus in the direction of flow then increase from 50 to 185 MPa and 10 to 25 GPa, respectively, in a 40 volume percent glass fiber epoxy composite.

Fig. 7. Fiber reorientation into the flow direction through a converging flow.

Analysis of Orientability

The orientability of different molding compounds and the mechanical tensile properties that result from orienting fibers into the flow direction can be studied in a converging conical channel preceding a uniform rod. The converging channel could be either incorporated into the runner system or made an integral part of the molded piece. The similarity to the die geometry of plastics extruders is also evident. Such a geometry is shown in *Fig. 8*.

Depending upon the viscosity of the suspending fluid (*i.e.*, polymer matrix), fiber suspensions at concentrations exceeding five volume percent fiber (5 v/o) exhibit either a Bingham or a pseudoplastic behavior. The former occurs when the resin viscosity is either very low or very high (15), depending perhaps on the state of fiber orientation, and comprises a plug flow through uniform channels with all shear occurring in a thin (<0.5 mm) layer of pure resin at the wall (16). In this condition, which applies in general to thermosetting matrices, there is no effect of shearing flows on the fiber orientation distribution. As the viscosity moderates (or at lower fiber lengths and concentrations), the fiber core begins to shear at its edges, giving a flatly curved velocity profile corresponding to a pseudoplastic fluid with a very low flow index (17). Since thermoplastic matrices typically have viscosities in the middle range of 10^4 to 10^5 poise at their processing temperature, some shear orientation of fibers into the direction of flow will occur near the walls.

However, the predominant mechanism for aligning fibers is through an elongational flow field.

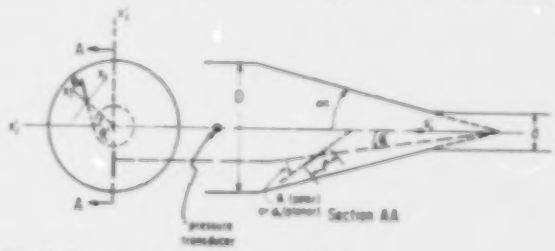

Fig. 8. Converging channel geometry.

Takserman-Krozer and Ziabicki (18) relate the rotation of a rigid ellipsoid in very dilute suspension to an extentional velocity gradient in uniform extension

$$\dot{\theta}_1 = \frac{3}{4}\lambda\left(\frac{dv_1}{dx_1}\right)\sin 2\theta_1 \tag{3}$$

$$\dot{\phi}_1 = 0 \tag{4}$$

where

θ_1 is the co-latitude and ϕ_1 the longitude in a spherical coordinate system based on x_1 as the polar axis.

λ is a shape coefficient $(r^2 - 1)/(r^2 + 1)$ related to the eccentricity, r, of the ellipsoid. It approaches unity for both rods and ellipses when the particle axis ratio exceeds 10.

v_1 is the axial velocity component, being negative in converging flows.

The assumption that the particles are rigid is valid for short glass fiber composites. However, particle interactions in highly loaded composites (>10 v/o fiber) play a large role in determining orientation behavior and cannot be neglected.

A rheological model developed by Erickson (19) for transversely isotropic fluids extends the applicability of *Eq. 3* by allowing λ to be a phenomenological material parameter that is not tied to the particle shape but may assume values both greater and less than unity. The degree of fiber interaction, which depends upon the physical constitution of the system, including fiber length and concentration, determines the value of λ. Since large values of λ result in faster fiber rotations and a higher degree of alignment, it is called the "orientability" parameter.

Since concentrated, long-fiber suspensions are resistant to shear deformation, this can be neglected in the flow analysis. Then, since v_θ and v_ϕ are identically zero, the continuity equation in spherical coordinates reduces to:

$$\frac{1}{x_1}\frac{\partial}{\partial x_1}(x_1^2 v_1) = 0 \tag{5}$$

The radial velocity component must be independent of ϕ by symmetry, and since there is no shear, it is independent of θ as well. Thus, *Eq. 5* may be integrated to

$$v_1 = \frac{C}{x_1^2} \tag{6}$$

The integration constant C is related to the volumetric flow rate, Q, by the macroscopic material balance

$$Q = \int v_1\, dA \tag{7}$$

$$= 2\pi \int_0^\alpha x_1^2\, v_1 \sin\theta\, d\theta \tag{8}$$

so that

$$v_1 = \frac{Q}{2\pi x_1^2 (1 - \cos\alpha)} \tag{9}$$

Equation 3 can now be integrated by evaluating $\dot{\theta}_1$ as the derivative following the motion:

$$\dot{\theta}_1 = v_1 \frac{d\theta_1}{dx_1} \tag{10}$$

and substituting for dv_1/dx_1 by differentiating *Eq. 9*; there results

$$\frac{\tan\theta_1}{\tan\theta_1^\circ} = \left(\frac{A}{A^\circ}\right)^{3\lambda/2}. \tag{11}$$

where superscript ° relates to the initial position,

A is the local cross-sectional area of the channel

θ_1 (A) is the local angle between the fiber axis and its streamline, which can be interpreted either as the changing orientation taken on by a single fiber as it traverses the channel or the axial variation in orientation displayed at any one instant by different fibers all following the same flow path through the channel.

A°/A is an effective draw ratio.

Thus, orientation is primarily dependent on the amount of elongational strain imposed. Some typical changes in θ_1 predicted by this equation are illustrated in *Fig. 9*.

Since λ is always positive, a tighter axial alignment is produced as the ratio of the cross-sectional area of the rod to that of the enlarged upstream section is reduced. The highest rate of rotation of the fibers occurs when they are aligned at 45 degrees to the streamline. An initial transverse 90 degree orientation represents an unstable state of equilibrium. Similarly, the approach to absolute alignment along the streamline is also very slow. Proper design of convergence would allow for reasonably good alignment without going to excessively large area changes. In a mold design, the small outlet diameter would conform to the dimensions of the molded part, but the larger upstream area that would be required for orientation could pose an economic burden in terms of mold cost, machine capacity, and material loss unless it, too, could be incorporated into the part. Applications to extrusion are self-evident.

The value of λ may be determined from a logarithmic plot of *Eq. 11*, or its derivative

$$\tan\phi_2 = C x_1^{3\lambda} \tag{12}$$

where ϕ_2 is the projection of θ_1 on a plane containing the axis

x_1 is the axial displacement along the cone.

C is a constant of proportionality.

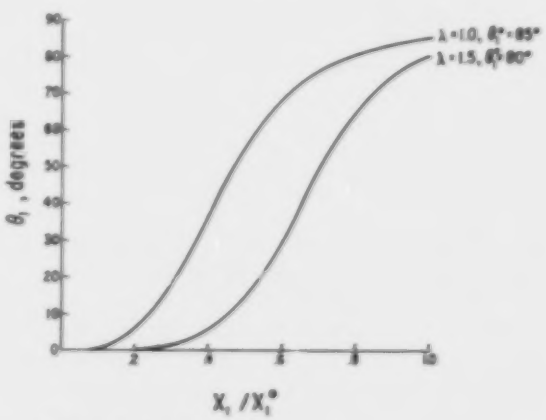

Fig. 9. Typical variations in θ_1.

Such a determination is illustrated in *Fig. 10*, where two sets of data for different initial orientations are compared. Theoretical analyses of fiber rotations in dilute solutions predict λ to be approximately unity. This has been verified experimentally in a low volume fraction composite (20). However, in the highly concentrated suspensions of 20 to 50 v/o of 3 to 6 mm long fibers generally encountered in the molding industry, the fiber-fiber interactions cause it to be reduced.

Of the variables which may be expected to influence the fiber orientation, the area reduction ratio is the most important since that variable appears explicitly in the mathematical model for θ_1. All of the other parameters might be important through their possible effect on the orientability parameter, λ. These include geometric factors (channel dimensions relative to fiber size and convergence angle), processing-controlled rate and pressure parameters, and material characteristics (viscosity, fiber concentration, fiber aspect ratio).

It should be noted that the flow rate, Q, and matrix viscosity, η, are likely combined in their effect through the Reynolds Number, indicating that they act through an inertial effect. The limiting of flows in polymer processing to low Reynolds Numbers suggests that inertial effects are not important and consequently that these are not important variables. An exception might be in the gate to an injection mold cavity, or when viscoelastic effects predominate.

Results

The orientability parameter is found to vary with the mobility of the fibers in the flowing melt. Thus, it is lower for long (≥ 6 mm) fibers that can tangle. It is higher for lower concentrations of fibers, and when the flowing suspension contains some voidage. For thermoset premix, at least, the orientability factor is not affected by small changes in matrix viscosity. These data are summarized in *Table 4*. A slight dependence on elongation rate occurs when the suspension is not fully compacted during flow (21). The angle of convergence of the die has no effect on fiber orientability.

Tensile properties of rods flow-molded from premix epoxy molding compound are summarized in *Table 5*. As the rod diameter decreases, the stretching of the fluid flowing into the rod cavity increases, causing an improvement in the degree of fiber alignment. However, maximum possible alignment is limited to an average polar angle of about 20 degrees to the flow axis. Flow disturbances, perhaps due to the intermittent nature of the flow (22), disrupt the orientation patterns when the extension rate is too high, so that fiber orientation and the mechanical properties of the rod are not predictable from *Eq. 11*. Such oscillations are illustrated in *Fig. 11*. The maximum attainable stiffness with this material is represented by a Young's modulus of 24.8 GPa, and a strength of 186 MPa. A fiber length of 3 mm has been found to be optimum for maximizing the degree of fiber alignment.

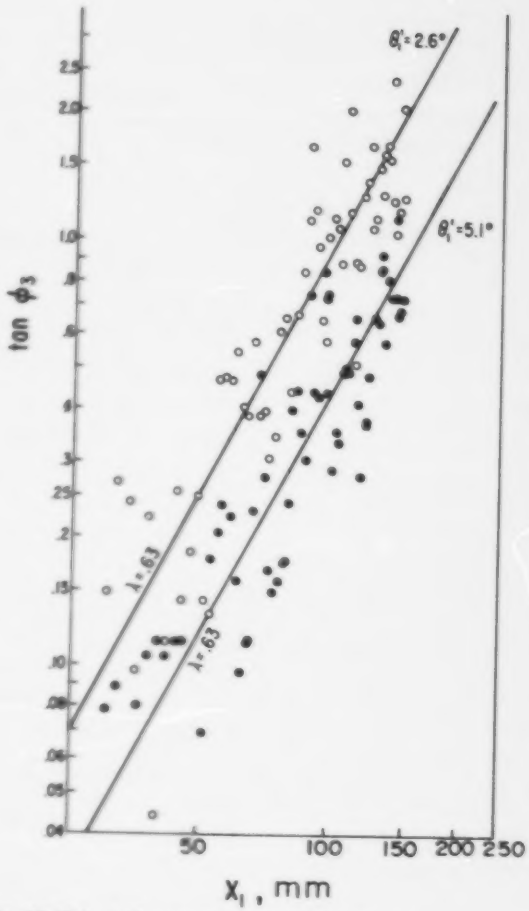

Fig. 10. Orientation measurements fit to Eq. 12.

With thermoplastic resins, the contribution of shear might aid in improving fiber alignment. Takano (23) has

Table 4. Determinations of the orientability parameter: glass fiber in epoxy

Fiber length, mm	Fiber concentration, v/o	Type of flow	λ
3	25	Compacted	.8
3	40	Compacted	.5
3	40	Opened	.7
6	40	Opened	.6
<1.5	35	Either	.25

Table 5. Tensile properties of molded rods: 3mm glass fiber, Epon 828 epoxy resin. (λ = 0.7)

Rod Diameter, mm	A°/A	Mean Fiber orientation degrees		Young's Modulus GPa		Tensile strength, MPa
		predicted	actual	predicted	actual	
12	6.3	32.4	29.5	16.4	17.7	110
9	11.1	19.1	21.2	26.6	23.4	183
6	25.0	8.4	25.7	30.7	19.4	145

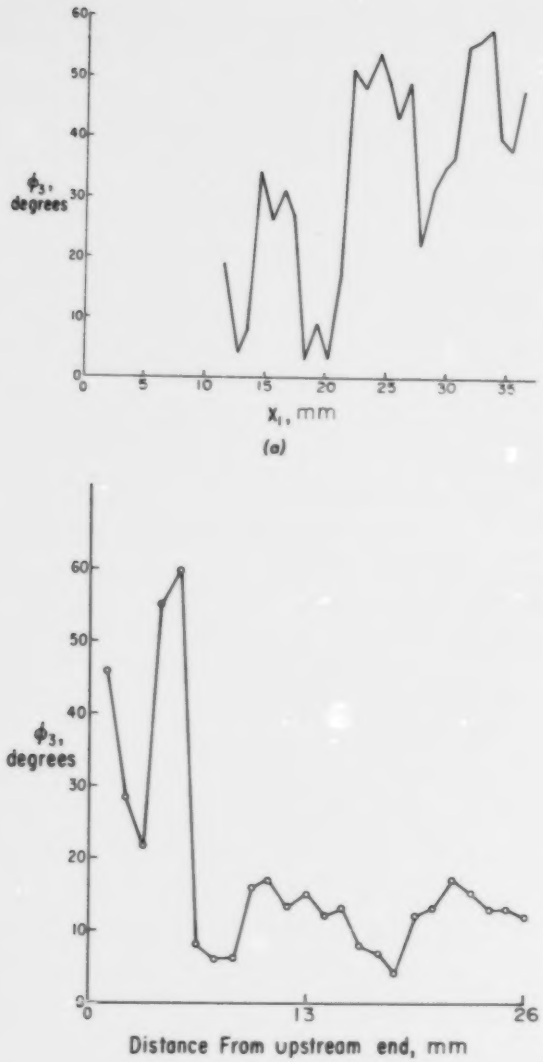

Fig. 11. Oscillations in the axial orientation profile a) In the converging cone and b) In the attached 9.5 mm rod for 40 v/o 3-mm glass fiber in epoxy.

reported improvements in orientability when the matrix viscosity in a fiber suspension is such that some level of shear occurs in elongational flows. However, Modlen (24) has shown that the concurrent shear in an elongational flow has comparatively small effect on the fiber orientation distribution. An additional effect in the injection molding of thermoplastics is that alignment would also be favored by the buildup of a frozen skin of shear-aligned material at the cold wall during flow.

The tensile properties attained by this controlled transfer molding technique, in which the fibers are preferentially aligned into the applied stress direction, are compared with the more common end-gated configuration conventionally used in molding, along with other methods, in *Table 6*. By comparison with *Table 2*, similar stiffness levels are obtained by injecting long-fiber reinforced nylon through the elongational flow field leading into the small neck of the tensile specimens used. However, tensile strength is higher by virtue of the superior matrix performance of the nylon polymer.

EXTRUSION

Extrusion can be used as a means of prepreg manufacture for obtaining some degree of fiber alignment with either thermoplastic or thermosetting matrices (in the B-stage). By the proper design of the converging channel of the extruder die, orientation distributions in which the average fiber deviation from the axis is about 20 degrees have been produced with an epoxy resin. This is about the same degree of fiber orientation as was obtained in transfer molding, which is not surprising since the fiber orientation is obtained by converging flow in either case. Again, strength is limited by cleavage breaks that occur around fiber agglomerates. Data are reported in *Table 6*.

By proper design of the extruder die, extrusion may also be used to produce continuous profiles in which the fibers are turned transverse to the extrusion direction. Such fiber orientation may be useful, for example, for transverse stiffening of a flat profile. One commercially important application, however, is the hoop reinforcement of an extruded tube (25). Monsanto Company has developed proprietary extruder die technology for this purpose (26, 27). The market has been the reinforcement of rubber hose with treated short cellulose fibers. This product contains agents for dispersion and bonding to elastomers. Since the mean aspect ratio of these fibers is in excess of 75 to 1, they provide a high degree of reinforcement and can be efficiently aligned to

Table 6. Comparison of methods for aligning short glass fibers in epoxy

Process	Fiber Content, v/o	Avg. Fiber Angle, Degrees	E GPa	Tensile Strength MPa
Conventional Injection molding	40	40-60	10.3	48
Controlled molding (this work)	40	19	26.9	190
Hand lay-up of extruded prepreg.	40	20	24.1	230
	57	20	34.5	240
Hand lay-up of encapsulated grain	57	7	39.3	310

impart high property levels. However, the dies are also operative with other matrices, such as thermoplastics reinforced with cellulose fiber (28) or glass fiber (see *Table 7*).

It has been shown that fibers flowing as a suspension in a matrix vehicle respond to elongated flow fields according to *Eqs. 3-11*. In these extrusion dies, which induce normal velocity gradients in the flows, the deposition of the fibers in the transverse plane is dependent upon the relative magnitudes of the gradients dv_2/dx_2 and dv_3/dx_3. The degree of circumferential fiber orientation is proportional to a power of the ratio of outlet and inlet radii (R_2/R_1) in a die whose channel expands along a conical contour, like that shown in *Fig. 12*. If the channel thickness W also increases, either alone or in conjunction with the conical expansion, the radial fiber orientation is enhanced according to the same function of the ratio of outlet to inlet channel thicknesses. For cellulose fibers in rubber at 10 v/o, the orientability parameter $\lambda \sim 0.9$

Instead of measuring fiber angles, the degree of fiber orientation is interpreted in terms of a mechanical anisotropy: in Young's modulus, strain induced by solvent swellings, or hose growth under hydrostatic loading. *Table 7* shows the effects of die geometry. Note that swelling strain, the only convenient measurement of radial fiber orientation, varies inversely to the degree of directional reinforcement.

In a hose, the expanding mandrel die imparts equally constrained hoop and axial growth under pressure, as well as an enhanced burst strength that is related to the diameter expansion in the die and to the degree of fiber reinforcement in the stock. See *Fig. 13*.

Radial fiber orientation can be accomplished by placing an obstruction in the flow channel. Radial orientation is important for dimensional stability in solvent immersion. The solvent swell data of *Table 7* indicate that circumferential reinforcement is related to the radius expansion in the die, whereas the degree of radial reinforcement is a function of the channel width expansion. Axial reinforcement is inversely related to the overall area expansion, A_2/A_1, which is the product of the radius and thickness ratios.

CONCLUSION

Matrix and reinforcement selection are important to property development in short-fiber composites. The shape and stiffness of the latter determine the extent to which the stress load can be relieved from the matrix. On the other hand, the matrix and the interface also influence the ultimate properties. Only when these are optimized can the full reinforcing potential of the fibers be realized.

FIBER ORIENTATION WITH A CONICALLY EXPANDING DIE

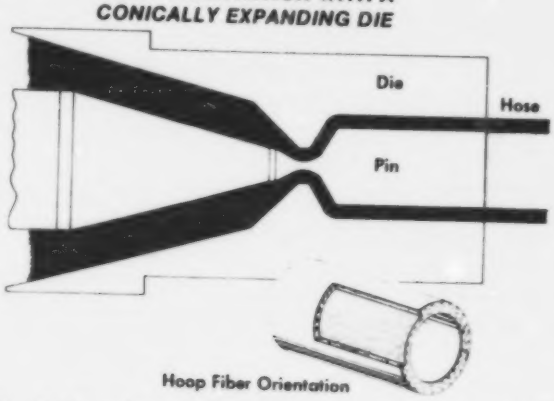

Fig. 12. Expanding extrusion die for generating a circumferential orientation of the reinforcing fibers.

In practical fabrications of short-fiber composites, structural parameters that are altered by the flow dictate performance. These involve the shape or disposition of the reinforcing phases and the condition of the interface. Close control over these factors can only be maintained at the expense of processing economics. However, in long-fiber composites, fiber orientation is the predominant criterion, and it can be manipulated to a significant extent through the formulation, tool geometry, and processing conditions.

The conditions for optimum fiber orientability are:

1. Fiber aspect ratio sufficiently high that hydrodynamic forces will act to cause fiber rotation, but small enough to minimize bending and tangling. For a 12 μm diameter fiber, 3 mm is optimum.
2. Low fiber concentration and low compaction during flow to provide high rotational mobility.

In injection molding of glass-fiber-reinforced epoxy, tensile strength can be increased more than threefold from 50 to 185 MPa, and Young's modulus from 10 to 25 GPa by instituting the proper control of fiber orientation. However, fabrication processing cannot give average alignments better than 15 to 20 degrees from the flow direction. This may limit the utility of the process for making high-performance parts, but wide opportuni-

Table 7. Anisotropy in extruded tubes

$\frac{R_2}{R_1}$	$\frac{W_2}{W_1}$	$\frac{A_2}{A_1}$	Young's Modulus, MPa		% Swell		
			Hoop	Axial	Hoop	Radial	Axial
A. Cellulose fiber-reinforced rubber (20w/o)							
2	1	2	39	41	—	—	—
4	1	4	50	18	—	—	—
2	2	4	30	17	—	—	—
1.0	1.5	1.5	—	—	17	18	2
1.0	4.5	4.5	—	—	12	6	13
3.0	1.5	4.5	—	—	6	12	13
B. Glass-fiber-reinforced polypropylene (20w/o, 9.5mm)							
4	1	4	680	415			
C. Glass-fiber-reinforced polypropylene (40w/o, 0.6mm)							
4	1	4	960	1040			

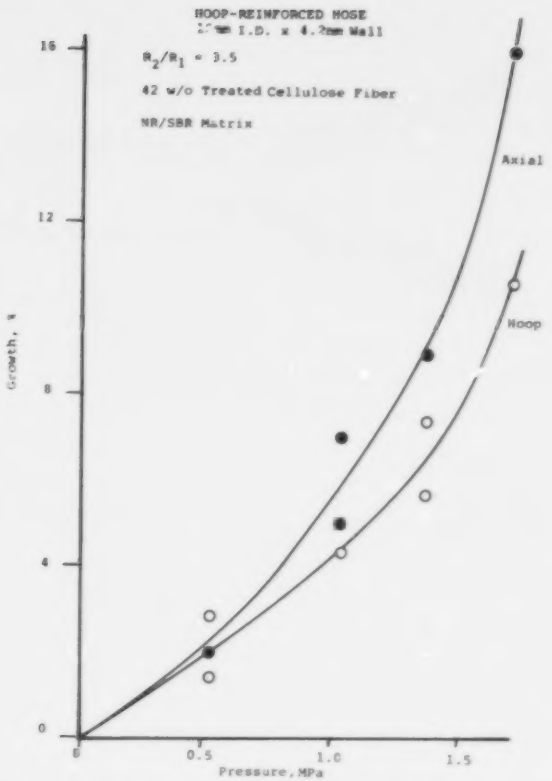

Fig. 13. Growth characteristics of a rubber hose reinforced with circumferentially oriented short cellulose fibers under a static pressure loading.

ties exist for property improvement in the commercial molding industry, where high volume production is also an important factor.

REFERENCES

1. M. J. Folkes, and D. A. M. Russell, *Polymer*, **21**, 1252 (1980).
2. F. J. Lockett, *Plastics Rubber Process.*, **5** (3-4), 85 (Sept.-Dec. 1980).
3. P. F. Bright, and M. W. Darlington, *Plastics Rubber Process. Applications*, **1**, 139 (1981).
4. J. D. Crabtree, and D. Pickthall, in "Advances in Polymer Blends and Reinforcements," Institution of the Rubber Industry, conference at Loughborough, Leicestershire, England, Sept. 1969.
5. A. F. Emmett, SPE Retec, Akron, Sept. 1970.
6. A. C. Bernardo, *SPE J.*, **26**, 39 (1970).
7. L. A. Goettler, T. B. Lewis, and L. E. Nielsen, *Am. Chem. Soc., Div. Polym. Chem. Polym. Prepr.*, **14**, 436 (1973).
8. N. J. Paratt, *Composites*, 25 (Sept. 1969).
9. G. E. G. Bagg, M. E. N. Evans, and A. W. H. Pryde, *Composites*, **97** (Dec. 1969).
10. R. L. Mehan, *J. Compos. Mater.*, **4**, 90 (1970).
11. M. Takano, "Rheology of Rod-like Particles in Viscous Media, Part I. Formation of Composites from Single Fibers," AD 849-285, Feb. 1969.
12. W. C. Jackson, F. Folgar, and C. L. Tucker III, "Prediction and Control of Fiber Orientation in Molded Parts," A.I.Ch.E. Annual Meeting, Los Angeles, Nov. 1982.
13. W. Woebcken, *Modern Plastics*, **40**, 146 (Dec. 1963).
14. L. A. Goettler, *Modern Plastics*, **48**, 140 (April 1970).
15. L. A. Goettler, "Effects of Matrix Characteristics in the Processing of Short Fiber Composites," in J. C. Seferis and L. Nicolais, eds, "The Role of the Polymeric Matrix in the Processing and Structural Properties of Composite Materials," Plenum Press, New York, 1983, p. 289.
16. J. Bell, *J. Compos. Mater.*, **3**, 244 (1969).
17. R. J. Crowson, and M. J. Folkes, *Polym. Eng. Sci.*, **20**, 934 (1980).
18. R. Takserman-Krozer, and A. Ziabicki, *J. Polym. Sci.*, **A1**, 491 (1963).
19. J. L. Ericksen, *Kolloid Z.*, *173*, 117 (1960).
20. L. Nicolais, L. Nicodemo, P. Masi, and A. T. DiBenedetto, *Polym. Eng. Sci.*, **19**, 1046 (1979).
21. L. A. Goettler, "Molding of Oriented Short Fiber Composites III. Rate Effects on Fiber Alignment in Convergent Channels," AD 779907, May 1974.
22. G. G. Stankoi, E. B. Trostyanskaya, N. Kazanskii, V. V. Okorokov, and O. Ya. Milchasenok, *Soviet Plastics*, **47** (Sept. 1968).
23. M. Takano, Monsanto/Washingtoon Univ. ARPA/ONR Report, "Rheology of Rod-like Particles in Viscous Media."
24. G. F. Modlen, *J. Mater. Sci.*, **4**, 283 (1969).
25. L. A. Goettler, R. I. Leib, and A. J. Lambright, *Rubber Chem. Technol.* **52**, 838 (1979).
26. L. A. Goettler, and A. J. Lambright (to Monsanto Company), U.S. 4,056,591 (Nov. 1977).
27. L. A. Goettler, and A. J. Lambright (to Monsanto Company, U.S. 4,057,610 (Nov. 1977).
28. L. A. Goettler, *Polym. Compos.*, **4**, 249 (1983).

DISCUSSION

M. Ryan: You showed several slides of fiber orientation made visible by etching. In one of them you showed a section across the thickness where the fiber seems to be oriented transverse to the thickness direction. I was a little surprised that this pattern was not consistent with the orientation in the horizontal plane. Coulc you comment on that?

L. A. Goettler: The gate used was sufficiently small so the flow expanded in both the vertical and horizontal planes. However, since the gate was located at the upper edge of the cavity the expansion in the thickness direction was not symmetric, and the resulting orientation profile was distorted.

Q. Samak: When you discussed the function for evaluating the orientation, you said that the point average value for theta is calculated on the basis of experimental measurements. How did you do that?

L. A. Goettler: We made experimental measurements of the two planar orientation angles in orthogonal planes. If you know the projections of a single fiber onto these two planes, you can calculate its polar angle directly. Here we are trying to get an average distribution over many fibers. I have characterized the local average projected planar orientation angle as a function of spatial position in both orthogonal planes parallel to the flow. I then know these average planar orientations at any point in the bar. I also measured the local individual fiber orientation distributions directly, using a higher magnification. Thus, I know the spread of the distribution in fiber angles about the local means in each of these planes. Then I went through an averaging technique, *Eq. 2*, in which I assumed a normal distribution for the angles around those means and thereby calculated the mean polar angle at each point.

Q. Samak: What do you actually measure experimentally?

L. A. Goettler: Experimentally, I am measuring the projections of the fiber angles on two orthogonal planes. When this is done, I can mathematically combine those to obtain the polar angle. The measurements are effectively done over many fibers.

Q. Samak: You have a graph showing that the Young's modulus was independent over flow rate. Is that for any viscosity? What are the limitations for the validity of this figure?

L. A. Goettler: About 40 to 1000 poise was the viscosity range of the epoxy covered in that graph. I do not think that this experiment was comprehensive enough to be able to generalize the results. In very slow flows or very fast ones there could be some other effects.

E. B. Bagley: Ever since I saw Stan Mason's lovely movie of rotating fibers in a shear field, bending when the stress gets large enough, I have been interested in the breakage of these things. I was looking at Takano's film, which you showed, to see any particle either bending or breaking, but I could not catch them from where I was sitting. Have you gone through those movies to see whether any fiber breakage occurs in that deformation field, or does it only occur in a screw extruder?

L. A. Goettler: We haven't done that. It does not appear that there is a lot of breakage, though. It could be that the flow was gentle enough, being rather slow and of a gradual convergence, that we are not seeing it.

E. B. Bagley: My only comment is that, of course, in Stan Mason's movies he also had a laminar flow. But when the particle rotates, it sees a compressive stress. So a particle can still buckle in laminar flow, and when the stress becomes high enough, it breaks. I would like to do an experiment like that which you showed, where I could actually measure the breaking stress of the fiber.

L. A. Goettler: Of course, these fibers in concentrated suspension are not free to buckle as if they were single. They are constrained by interactions with the neighboring fibers. Also, in this extensional field the fibers do not experience the periodic compressive force that they would see in a shear field.

G. C. Hawley: I am interested in the use of varying geometry, as you have shown, and also movable mold pieces to avoid weld-line problems in flow around inserts. Have you had any experience in that area?

L. A. Goettler: Not really. I know that the weld-line problem is a severe one in fiber-reinforced moldings. You could allow flow into the mold past the weld point before positioning the insert that would divide the flow.

G. C. Hawley: This is exactly what we used in flow of a mica-filled melt, when we had a problem with flow around a pin. There was some improvement, but not a lot. We had about 60 percent strength across the weld-line.

M. R. Kamal: I wonder if you picked up any effect of the packing pressure during the injection-molding process on the orientation distribution?

L. A. Goettler: I really have not seen any effect on the orientation distribution but there was some effect on the strength of the moldings.

M. R. Kamal: Some people have observed that instead of getting a random planar distribution, lets say normal to the direction of the flow, during the packing stage a rotation occurs that puts the fibers unidirectionally perpendicular to the flow.

L. A. Goettler: Don't forget, many of the experiments I reported were unusual in the sense that the material was packed first, and then continued flowing through an orifice in the mold after the compaction pressure was applied. It is different from the case you are talking about. However, even without the discharge flow, such a reorientation effect was not observed.

Deformation Design for Short-Fiber-Reinforced Thermoplastics

D. McCAMMOND *and* P. A. NORTH*

Department of Mechanical Engineering
University of Toronto
Toronto, Canada

Stiffness matrices are predicted, using the Halpin-Tsai laminate analogy, at different locations in 4 short glass-fiber-reinforced thermoplastic moldings, and the resulting anisotropy and inhomogeneity discussed, relative to quasi-isotropic values. The predictions are based on actual material structure as obtained from contact microradiographs. Considerable anisotropy and inhomogeneity are noted. The response of the materials to tensile, flexure, and shear loads is calculated and it is shown that this deviates to a lesser degree from a quasi-isotropic response. Finally the load deformation behavior in plate bending and twisting are predicted using both a quasi-isotropic model and the stiffness properties based on actual structure and compared with previously available experimental data. It is concluded that, in the absence of a predictive approach to fiber orientation in short-glass-fiber-reinforced thermoplastic moldings, the use of quasi-isotropic stiffness data provides an acceptable means of performing deformation design analysis. Based on the analysis of the moldings considered, the quasi-isotropic assumption could be expected to introduce errors of less than 20 percent in deformation predictions for planar moldings.

INTRODUCTION

The stiffness of fiber-reinforced materials, because of their anisotropic nature, must be defined by a matrix of stiffness (or compliance) coefficients. For those materials (laminates) which are manufactured from planar laminae, a theory has existed for many years which predicts the stiffness properties of the laminate given those properties of the laminae and their relative orientation. More recently (1), the stiffness properties of laminae, whose fiber-reinforcement geometry is well defined, can be predicted from a knowledge of the component fiber and matrix properties, plus their geometry.

In those components manufactured by injection or compression molding, no such precise lamination occurs and the length and orientation of the reinforcing fibers are strongly dependent on the molding process. In injection moldings, the fiber orientation is dependent on the flow characteristics of the melt as it fills the mold. For glass-reinforced thermoplastics, the fiber length has been shown to be almost independent of the fiber length of the raw material, being influenced mainly by the mechanical action of the injection screw and ram.

The laminate theory has been developed (2-4) and used with these less uniformly structured injection molded materials in those situations where a 2-D planar fiber orientation is realized. The material is divided into arbitrary laminae, in each of which the fiber length and orientation can be described by distribution functions (fiber-length distribution, FLD, and fiber-orientation distribution, FOD). The assumption is made that the FLD and the FOD are constant through the thickness of the lamina and in the limit model the structure of the material at a point. The error in this assumption can be minimized, compatible with increased computational complexity, by reducing the thickness of the imaginary laminae. Every lamina is then considered to be composed of plies, each containing matrix and uniaxially aligned fibers and with the fiber aligned in different directions in each ply. A stiffness matrix for a lamina is then assembled from the ply stiffness with the plies weighted in relation to the lamina FOD.

This predictive technique required a knowledge of the fiber volume fraction, fiber dimensions (diameter and FLD), and the FOD in addition to the fiber and matrix properties. The first two can be obtained by standard burn-off procedures and the FOD by the use of contact-radiography (5). In this procedure, thin slices (25 μm) are cut and contact microradiographs produced. The FOD is obtained by counting manually or by means of image analysis techniques. This procedure is time consuming and each slice only provides information at one point in what is a distinctly inhomogeneous mate-

* Currently with Atomic Energy of Canada Ltd., Sheridan Park, Mississauga, Ontario.

rial. In addition, for a truly predictive stiffness analysis, predictions of the FOD as a function of position must be made. Currently this is not possible, although from experience some qualitative predictions of general fiber-orientation patterns may be made. Finally, even if the stiffness field for the molded component were known, subsequent stress and deformation analysis would require the use of a finite element program with elements each capable of having different anisotropic stiffness matrices. This is current technology but would add to the complexity and therefore the cost of the design process ruling out its application to more simple components.

From the previous arguments, it can be seen that precise stiffness predictions for short-fiber-reinforced thermoplastic components is at worst not economically viable and at best complex and expensive. An investigation of less precise but more readily applicable techniques is therefore warranted.

An examination of the microradiographs of slices cut from moldings where it might have been expected that high degrees of fiber alignment could have occurred (e.g., end gated ASTM tensile bars) indicates a distribution around a favored direction. When considered in conjunction with the rapid decrease in stiffness with orientation in directions other than the fiber direction for fully aligned fiber reinforcement (*Fig. 1*), it is apparent that the stiffness in injection-molded short-fiber-reinforced components will never approach the high value which might be hoped for. Similarly, the low values indicated in the cross fiber directions will also not be approached. In practical situations, therefore, the range of anisotropy displayed will be substantially less than that predicted from ideally aligned fibers. It would be of interest to examine the magnitude of the stiffness anisotropy about the quasi-isotropic value since the use of 2-D quasi-isotropic material properties, with a clear indication of the limiting anisotropy range expected in practice, would be a powerful simplifying factor in deformation design with short-fiber-reinforced materials.

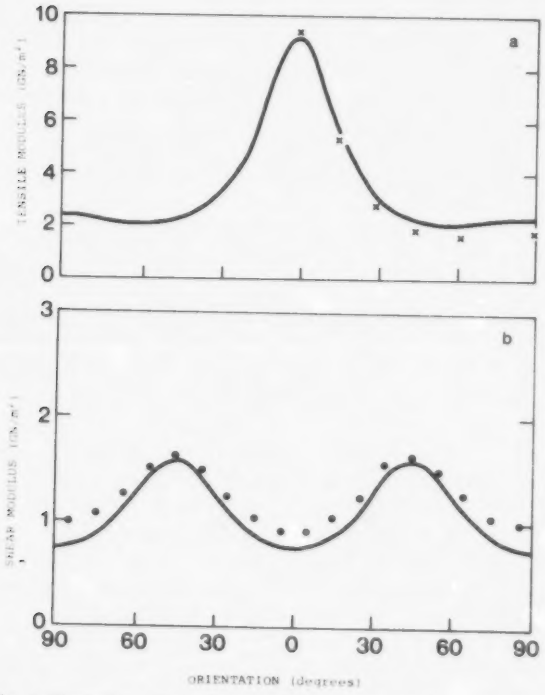

Fig. 1. Variation of tensile and shear moduli with orientation for fully aligned, continuous fiber, G.F.P.P. (Ref. 3).

——— *theory*
x *experiment, tensile*

THEORY

A summary of the theory used for the analytical predictions is presented, a more complete development can be obtained from *Refs 1-3* and *6*. Consider an arbitrary lamina in a short-fiber-reinforced material as being composed of n imaginary plies and that the FOD can be described by a discrete distribution function a^k for $1 \leqq k \leqq n$ where a^k is the fraction of the total number of fibers whose orientation lies between angles of $180(k - 1.5)/n$ and $180(k - 0.5)/n$ degrees. It follows that

$$\sum_{k=1}^{n} a^k = 1.0$$

The stiffness coefficients for each ply, Q_{ij}, are related to the anisotropic moduli and Poisson's ratios by

$$\begin{aligned} Q_{11} &= E_{11}/(1 - \upsilon_{12}\upsilon_{21}) \\ Q_{22} &= E_{22}/(1 - \upsilon_{12}\upsilon_{21}) \\ Q_{12} &= \upsilon_{21}E_{11}/(1 - \upsilon_{12}\upsilon_{21}) = \upsilon_{12}E_{22}/(1 - \upsilon_{12}\upsilon_{21}) \quad (1) \\ Q_{66} &= G_{12} \\ Q_{16} &= Q_{26} = 0 \end{aligned}$$

Equations 1 can be evaluated using the Halpin-Tsai equations (1).

$$\begin{aligned} E_{11} &= E_m(1 - V_F) + \eta_L E_F V_F \\ \upsilon_{12} &= \upsilon_m(1 - V_F) + \upsilon_F V_F \\ P_c &= P_m\left\{\frac{1 + \rho B V_F}{1 - B V_F}\right\} \end{aligned} \quad (2)$$

where

$$B = \left(\frac{P_F}{P_m} - 1\right)\Big/\left(\frac{P_F}{P_m} + \rho\right)$$

Here P_c is the ply composite modulus E_{22} or G_{12}, P_F the corresponding fiber modulus E_F or G_F, P_m the corresponding matrix modulus E_m or G_m, ρ a measure of the reinforcement (1), and υ_m and υ_F are the Poisson's ratios of the matrix and fibers, respectively. E_{11}, E_{22}, G_{12}, and υ_{12} are longitudinal and transverse Young's moduli, the shear modulus and Poisson's ratio, respectively, for each ply. η_L is a length correction factor (3) to allow for the discontinuous nature of the fibers.

Q_{ij} is the stiffness matrix of each ply with respect to the ply's fiber and cross fiber directions. If $\bar{Q}^k_{ij}$ is the stiffness matrix of the k^{th} ply referred to an arbitrary set of laminate axis then the transformation is given by the following equations (1):

$$\begin{aligned} \bar{Q}^k_{11} &= U_1 + U_2\cos(2\theta^k) + U_3\cos(4\theta^k) \\ \bar{Q}^k_{22} &= U_1 - U_2\cos(2\theta^k) + U_3\cos(4\theta^k) \end{aligned}$$

$$\bar{Q}_{12}^k = U_4 - U_3 \cos(4\theta^k)$$
$$\bar{Q}_{66}^k = U_5 - U_3 \cos(4\theta^k)$$
$$\bar{Q}_{16}^k = -\frac{1}{2} U_2 \sin(2\theta^k) - U_3 \sin(4\theta^k) \quad (3)$$
$$\bar{Q}_{26}^k = -\frac{1}{2} U_2 \sin(2\theta^k) + U_3 \sin(4\theta^k)$$

where

$$U_1 = \frac{1}{8}(3Q_{11} + 3Q_{22} + 2Q_{12} + 4Q_{66})$$
$$U_2 = \frac{1}{2}(Q_{11} - Q_{22})$$
$$U_3 = \frac{1}{8}(Q_{11} + Q_{22} - 2Q_{12} - 4Q_{66}) \quad (4)$$
$$U_4 = \frac{1}{8}(Q_{11} + Q_{22} + 6Q_{12} - 4Q_{66})$$
$$U_5 = \frac{1}{8}(Q_{11} + Q_{22} - 2Q_{12} + 4Q_{66})$$

Since the lamina is used to model the material at a particular point, the k plies all have the same position coordinates and can be assumed to all experience the same strain field. The stiffness matrix for the lamina can therefore be expressed as the weighted summation of the stiffness of the imaginary plies.

$$\bar{Q}_{ij} = \sum_{k=1}^{n} a^k \bar{Q}_{ij}^k \quad (5)$$

$\bar{Q}_{ij}$ describes the stiffness properties at a point in the material where the FOD is given by a^k and, if preferred, the engineering anisotropic moduli and Poisson's ratios may be extracted from compliance coefficients which are obtained by inverting the stiffness matrix.

Equations 1-4, together with measured FOD information, provide the vehicle for examining the bounds on the stiffness properties which might be expected to occur in practical component moldings.

In order to determine the properties of a quasi-isotropic (2-D random in the plane fiber orientation distribution), it is convenient to write *Eq 5* in its integral form

$$\bar{Q}_{ij} = \int_0^{\pi} a(\theta)\, \bar{Q}_{ij}^k(\theta)\, d\theta \quad (6)$$

where $\bar{Q}_{ij}^k(\theta)$ is still given by *Eq 3* but θ becomes a continuous rather than a discrete variable. Integration of *Eq 6* yields for the quasi-isotropic case,

$$\bar{Q}_{11} = \bar{Q}_{22} = U_1$$
$$\bar{Q}_{12} = U_4 \quad (7)$$
$$\bar{Q}_{66} = U_5$$

The moduli and Poisson's ratio of the quasi-isotropic material can be obtained from *Eq 7*,

$$E = \frac{1}{U_1}(U_1^2 - U_4^2)$$
$$\upsilon = \frac{U_4}{U_1} \quad (8)$$
$$G = U_5$$

ANALYSIS

The orientation of the fibers will be strongly dependent on the flow behavior of the melt entering the mold; four geometries with widely differing flow characteristics have been chosen for examination. The materials used in the study are as follows.

GFPP: Polypropylene containing 25.7 percent by weight of well coupled, short, 10 μm diameter, glass fibers (ICI "Propathene" HW 70 GR).

GFPA 66: Polyamide 66 containing 32 percent by weight of well coupled, short, 10 μm diameter, glass fibers (ICI "Maranyl" A 190).

GFPB TP: Poly (butylene terephthalate) containing 20 percent by weight of well coupled, short, 10 μm glass fibers (AKZO Plastics b.v. "Arnite" TV6 240).

The four molded components analyzed were:

(i) GFPA 66, ASTM tensile bar, *Fig 2*.
(ii) GFPP, edge gated disc, 100 mm diameter, 3 mm thick, *Fig. 2*.
(iii) GFPP, edge gated disc, 100 mm diameter, 6 mm thick, *Fig. 2*.
(iv) GFPBTP, flash gated 100 mm square plaque, 2 mm thick, *Fig. 2*.

The molded components have been produced, physically examined, and tested in a program of research conducted at the Cranfield Institute of Technology and the moldings have been described and some of the data presented in *Refs. 3-5*. The ASTM bar and the flash gated plaque have parallel flow patterns, which could be expected to produce a high degree of orientation in the direction of flow while in the edge gated discs the melt expands from the gate to fill a large cavity. The resulting anisotropies will be examined in terms of the variation with orientation of a tensile and shear modulus. These moduli can be most easily predicted from the compliance matrix $\bar{S}_{ij}$ as follows:

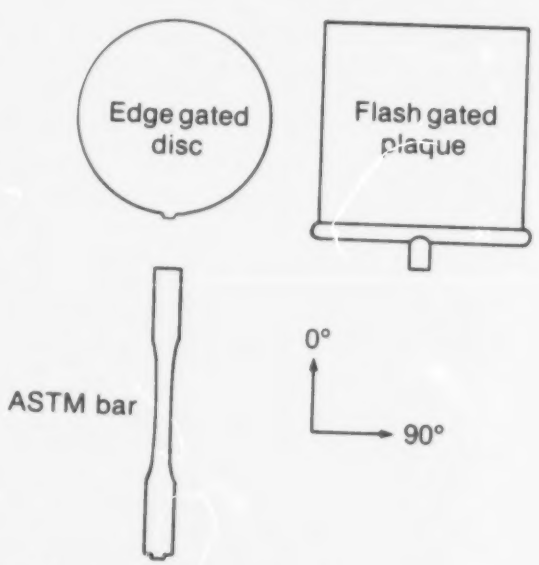

Fig. 2. Injection moldings considered.

$$E = \frac{1}{\bar{S}_{11}}$$
$$G = \frac{1}{\bar{S}_{66}} \qquad (9)$$

where

$$\bar{S}_{ij} = [\bar{Q}_{ij}]^{-1} \qquad (10)$$

Slices cut, parallel to the surface, from various thickness locations at the center of each component were analyzed, FOD's obtained, (5), and the values of tensile and shear modulus as a function of orientation were calculated for each slice. The data for four slices are presented in *Figs. 3-6*, slice 1 is from the surface and slice 4 is from the mid-depth of the molding. As expected, the ASTM

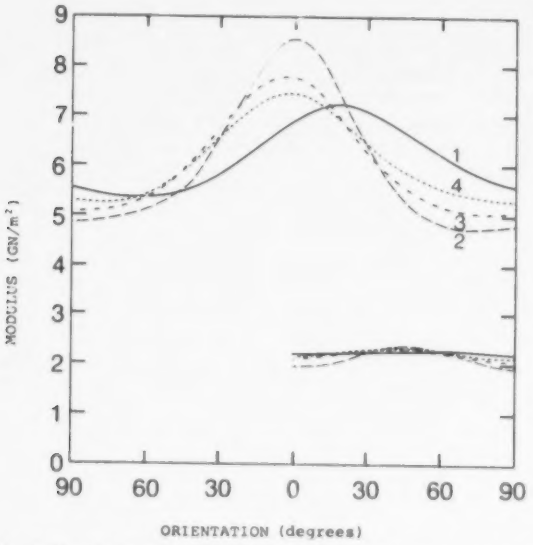

Fig. 3. Variation of tensile and shear moduli with orientation for slices cut from GFPA, ASTM bar. Slice 1 is from the surface, slice 4 from the mid thickness.

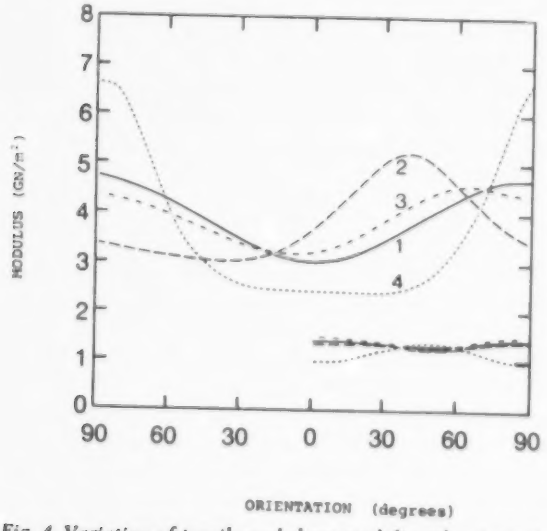

Fig. 4. Variation of tensile and shear moduli with orientation for slices cut from GRPP 3 mm thick edge gated disc. Slice 1 is from the surface, slice 4 is from the mid thickness.

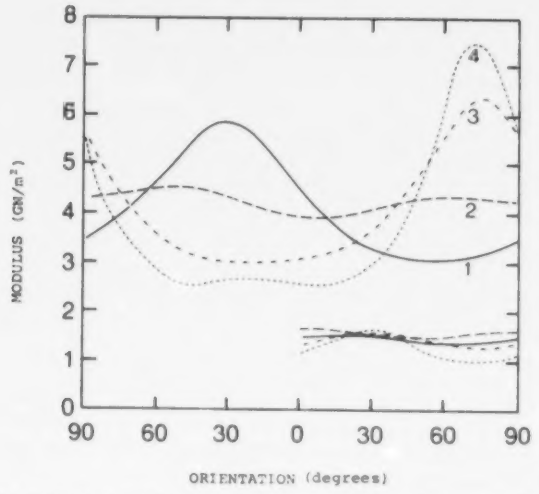

Fig. 5. Variation of tensile and shear moduli with orientation for slices cut from GRPP 6 mm thick edge gated disc. Slice 1 is from the surface, slice 4 is from the mid thickness.

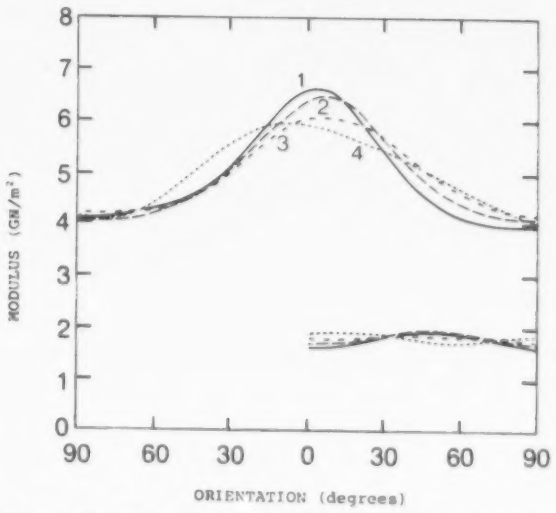

Fig. 6. Variation of tensile and shear moduli with orientation for slices cut from GFPBT flash gated plaque. Slice 1 is from the surface and slice 4 is for the mid thickness.

bar and the flash gated plaque displayed the greatest degree of consistency of anisotropy among the slices. However, even with these well-defined mold flow fields, variations of 25 to 40 degrees in the direction of maximum tensile moduli were noted and tensile anisotropy ratios, (max tensile modulus/min tensile modulus), which varied between 1.40 and 1.80, were obtained. Shear anisotropy did not exceed 1.2 for any of the slices.

The slices cut from the edge gated discs indicate that a complex flow field exists at the centre of the disc during the molding operation. The direction of anisotropy varies by 90 degrees between the surface and the mid-depth in both the 3 mm and 6 mm discs. The degree of fiber alignment is high in some slices, particularly those near the mid-depth. Tensile anisotropy ratios as high as 2.92 being predicted.

In spite of the high local anisotropy exhibited by this analysis, it is clear that the inhomogeneity of the anisot-

ropy means that the performance of the component to applied forces or moments may be much less anisotropic than that suggested by the analysis of some individual slices.

Tensile, flexural, and shear moduli for the molding calculated from the slice data are shown in *Figs. 7-10*, together with those predicted for 2-D random in the plane fiber distribution. Also shown in *Figs. 8* and *10* are experimental data from tensile and rail shear tests (3) and in *Fig. 9* experimental data from tensile tests (6). The upper and lower limits of the variation of tensile, shear, and flexural moduli from the quasi-isotropic values (2-D random in the plane fiber-orientation distribution) are tabulated below.

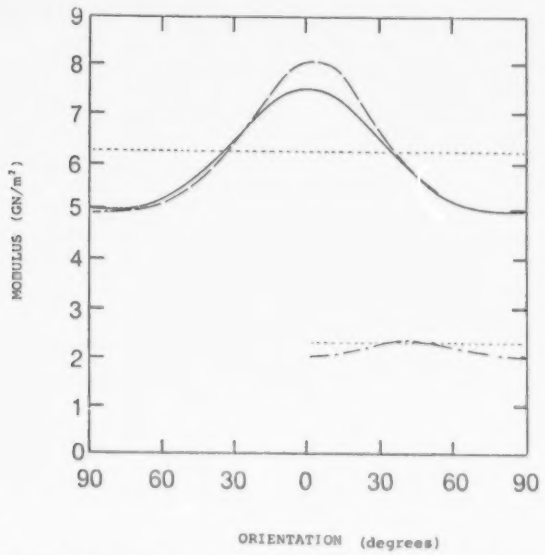

Fig. 7. Variation of tensile, flexure, and shear moduli with orientation for GFPA, ASTM bar.

tensile
flexure
shear
quasi-isotropic

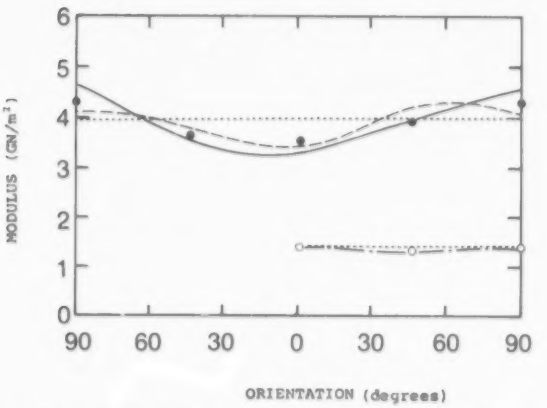

Fig. 8. Variation of tensile, flexure, and shear moduli with orientation for GFPP 3 mm thick edge gated disc.

tensile
flexure
shear
quasi-isotropic
experimental data, tensile
experimental data, shear

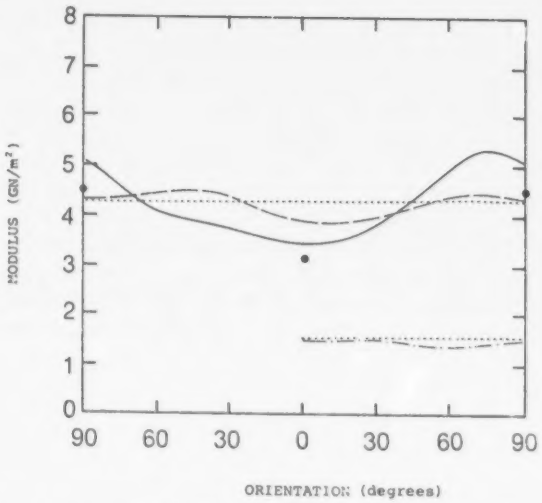

Fig. 9. Variation of tensile, flexure, and shear moduli with orientation for GFPP 6 mm thick edge gated disc.

tensile
flexure
shear
quasi-isotropic
experimental data, tensile

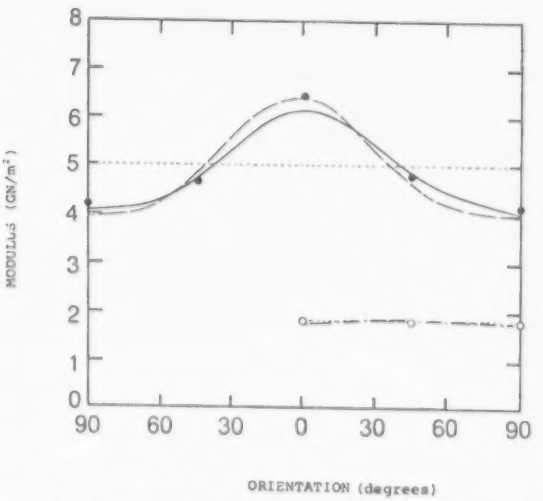

Fig. 10. Variation of tensile, flexure, and shear moduli with orientation for GFPBT flash gated plaque.

tensile
flexure
shear
quasi-isotropic
experimental data, tensile
experimental data, shear

Table 1 indicates that a range of +30 to −22 percent covers the tensile and flexural variations and +2 to −11 percent covers those for the shear modulus. It also illustrates clearly, in the case of the 6 mm disc, the necessity of obtaining (or predicting) the structure at all points in the component. For the 6 mm disc, at the centre of the disc, the structure is totally different at the core and at

Table 1. Maximum and Minimum Variation of Moduli from Quasi-isotropic Values

Molding	Tensile modulus		Flexural modulus		Shear modulus		Reinforcement factor
	maximum	minimum	maximum	minimum	maximum	minimum	
	quasi-isotropic	quasi-isotropic	quasi-isotropic	quasi-isotropic	quasi-isotropic	quasi-isotropic	$\frac{E}{E_m}$
ASTM bar	1.21	0.80	1.30	0.80	1.02	0.89	2.20
Flash gated plaque	1.23	0.80	1.27	0.78	1.00	0.94	1.90
3 mm disc	1.18	0.83	1.10	0.87	0.98	0.91	2.20
6 mm disc	1.25	0.80	1.04	0.90	0.99	0.87	2.40

the surface giving different anisotropy magnitudes and directions in flexure and tension. Since other parts of the discs would experience different flow patterns during mold filling, different structures would result with correspondingly different stiffness properties. However, it is unlikely that anything more consistently anisotropic than that in the ASTM bar and flash gated plaque would result and so the range of +30 to −22 percent on E and +2 to −11 percent on G might be considered as the expected error band which would result from the use of 2-D quasi-isotropic moduli values with these molding materials. This error band is clearly dependent on fiber modulus, fiber length, and volume fraction, and a larger error band could be expected with increases in the values of these parameters. Since deformations (unlike strength) are an integration of the stiffness at all points in a component, some further averaging could be expected and errors in deformation predictions due to the use of quasi-isotropic properties could be expected to be less than the error range suggested above.

In order to examine the performance of the quasi-isotropic assumption in the prediction of load/deformation relationships for practical components two simple tests are considered, namely 3 point plate bending and 4 point plate twisting (*Fig. 11*). Details of the testing methods and experimental data are given in *Refs.* 3 and 6. The resulting experimental load deflection relationships were linear and plots of the constants of proportionality against orientation of the plate are presented together with the exact and quasi-isotropic predictions in *Figs. 12-15*. The maximum deviations of experiment from theory are listed in *Table 2*.

The exact theory provided better qualitative and quantitative correlation for the GRPP 3 mm disc in bending and the GRPTB plaque in twisting. However, in the remaining two cases the quasi-isotropic theory is at least as good and is possibly better for the GRPP 6 mm disc in bending. The maximum deviations were 22 percent and 19 percent for the quasi-isotropic and exact theories respectively. The reinforcement factor achieved by addition of fibers to the matrices used in this study is given in *Table 1* and varies from 1.9 to 2.4 (based on the quasi-isotropic tensile modulus for the composite). The error of up to 20 percent introduced in deformation calculations by the use of the quasi-isotropic assumption must be viewed relative to this reinforcement value. That is, in all actual component produced from the GRP used in this study, an effective increase in stiffness by a factor of 2.2 ± 0.4 could be expected.

CONCLUSIONS

Extreme inhomogeneity was exhibited by some of the moldings examined in this study with localized anisotropy ratios varying from close to 1.0 up to 2.92. The preferred anisotropic directions also varied by as much as 90 degrees between different positions in the thickness at one location on the 2-D components considered. The averaging effect of integrating the through thickness stiffness values to obtain tensile, flexural, or shear moduli for planar components considered effectively reduced the anisotropy to values which varied from the 2-D quasi-anisotropic values by less than +30 to −22 percent for tension and flexure and by less than +2 to −11 percent for shear. The further integration of the component stiffness field which occurs during analysis of component load-deformation relationships will again reduce the anisotropy. Predictions of plate bending and twisting experiments using models based on (i) "exact" structure; and (ii) assumed random in the plane structure (quasi-isotropic) indicated only sightly improved correlation with the exact model with maximum errors of 19

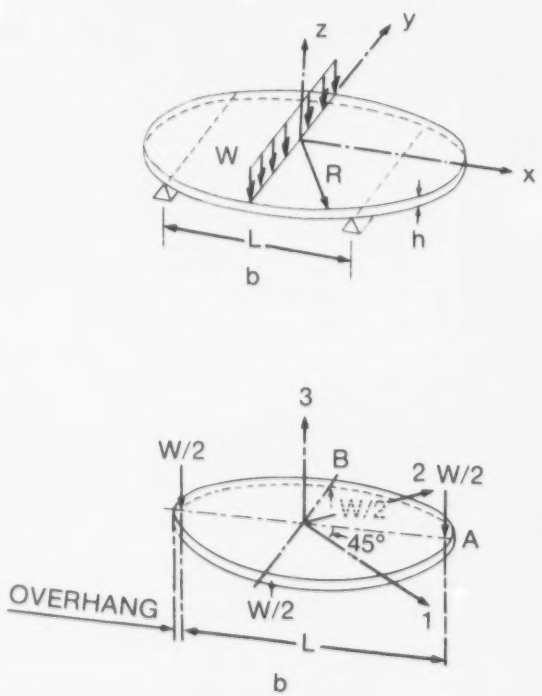

Fig. 11. Schematic of component tests.

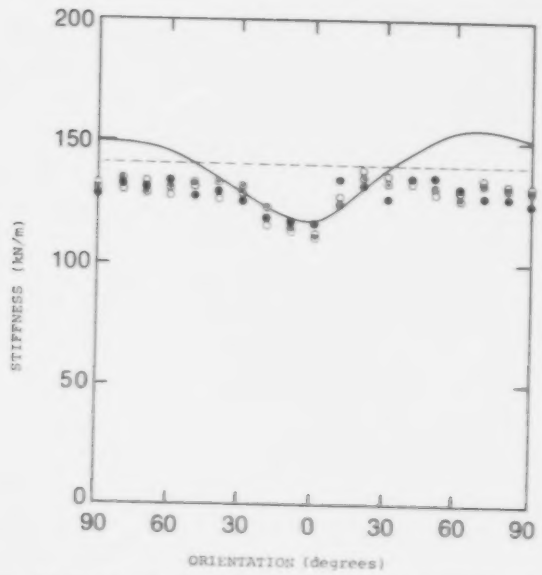

Fig. 12. Variation of stiffness in flexure with orientation for GFPP 3 mm thick edge gated disc.

exact theory
quasi-isotropic theory
experiment

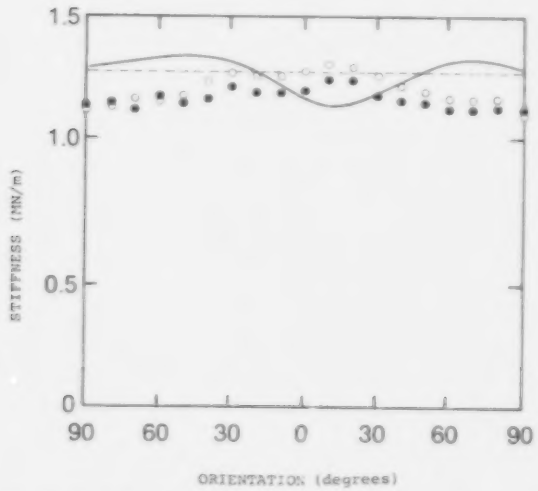

Fig. 13. Variation of stiffness in flexure with orientation for GFPP 6 mm thick edge gated disc.

exact theory
quasi-isotropic theory
experiment

percent and 22 percent, respectively. Since it is currently not possible to predict accurately what reinforcement structure will result in a molding, the assumption of quasi-isotropy, with the tremendous saving in analytical complexity, would appear to provide a suitable means of performing deformation design with short-glass-reinforced polymers. This study suggests that errors of less than 20 percent could be expected to be introduced by this assumption for the materials examined. This error could increase for materials with higher fiber modulus, length, or volume fraction.

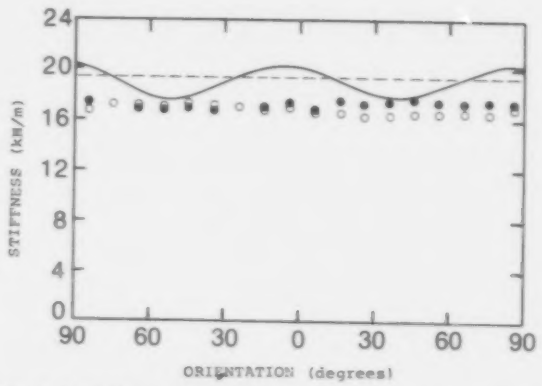

Fig. 14. Variation of stiffness in plate twisting with orientation for GFPP 3 mm thick edge gated disc.

exact theory
quasi-isotropic theory
experiment

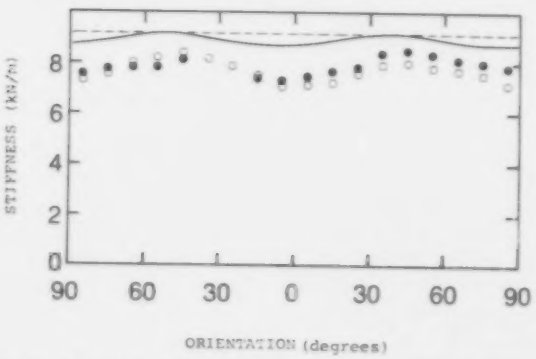

Fig. 15. Variation of stiffness in plate twisting with orientation for GFPBT flash gated plaque.

exact theory
quasi-isotropic theory
experiment

ACKNOWLEDGMENTS

The author would like to acknowledge the extensive contribution in the field of GRP of the current (and past) research team at Cranfield Institute of Technology in particular Professor Saunders and Drs. Darlington, McGinley, Smith, and Christie. The experimental and structural data cited in this paper was produced in their Laboratories. The financial support of the Research Council of Canada is gratefully acknowledged.

Table 2. Maximum Deviations of Experiment from Theory

	Plate bending		Plate twisting	
	GRPP 3 mm disc	GRPP 6 mm disc	GRPP 3 mm disc	GRPTB 2 mm plaque
Exact theory	−19%	−14%	−16%	−17%
Quasi-isotropic theory	−22%	−13%	−11%	−22%

NOMENCLATURE

- a = fiber distribution function
- E = tensile modulus
- G = shear modulus
- k, n = integers
- P = general modulus
- Q_{ij} = stiffness coefficients of ply with respect to fiber direction
- $\bar{Q}_{ij}$ = stiffness coefficients of ply with respect to global axis
- S_{ij} = compliance coefficients
- U = transformation invariants
- ν = Poisson's ratio
- θ = position coordinate
- ρ = reinforcement constant

Subscripts

- c = composite
- F = fiber
- m = matrix

REFERENCES

1. J. E. Ashton, J. C. Halpin, and P. H. Petit, "Primer on Composite Materials: Analysis," Technomic Publishing Co., Conn. (1969).
2. K. L. Jerina, J. C. Halpin, and J. Nicolais, *Ing. Chim. Ital.*, **9**, 194 (1973).
3. M. A. Christie, M. W. Darlington, D. McCammond, and G. R. Smith, *Fibre Sci. Technol.*, **12**, 167 (1979).
4. M. W. Darlington, P. L. McGinley, and G. R. Smith, *Plast. Rubber*, **2**, 51 (1977).
5. M. W. Darlington and P. L. McGinley, *J. Mater. Sci.*, **10**, 906 (1975).
6. G. R. Smith, M. W. Darlington, and D. McCammond, *J. Strain Anal.*, **13**, 221 (1978).

DISCUSSION

S. V. Hoa: Would you say that we would see the same isotropic behavior in compression?

D. McCammond: Yes, the only added problem that one has in compression, and this is less of a problem with short glass fibers than with long fibers, is that you can get buckling of the fiber within the resin and so at some point the compression behavior would deviate from the tension behavior. I think that is less of a problem with short glass fibers that it is with high-performance composites.

S. V. Hoa: Have you found that there is sometimes some difference between the moduli in tension and compression for this kind of material.

D. McCammond: No, not at small strains. By that I mean less than one percent.

R. Simha: Is it correct to say that I have a system in which the fibers are distributed with some orientation distribution and that I simulate the system by subdividing the system into layers, assigning for each layer a planar distribution, which varies then from layer i to layer $i + 1$? Is this what is being done? Now does this require some justification, is there some theorem which allows you rigorously to say that this is so? If I have an infinite number of layers, if I went to the limit, would this then be a mathematical identity? Is this then an approximation which becomes a better one the larger the number of layers into which I subdivide the system?

D. McCammond: Yes. Basically the infinite number of layers is when you take each fiber as being a layer, with a specific orientation of its own and then assign a proportion of the matrix to that particular fiber. Instead, which we have chosen to do is to consider ten-degree intervals, include everything into that ten-degree interval, and then assign a portion of the matrix in proportion to the number of fibers. So, yes, it is in layers, but each layer has, in physical space, the same position and depth.

J. M. Charrier: We have done calculations of this kind with mathematical distribution functions. Unfortunately, the mathematical distribution function does not necessarily fit exactly the experimental data. It is only an approximation. But then it is a direct integration not step by step or layer by layer.

D. McCammond: Yes. In effect an example of that is the quasi-isotropic case, when you are integrating a straight line.

J. M. Charrier: In previous analysis, that started to appear in mid-1960s, people had made a distinction between coupling of the lamina to make shear impossible. That makes a difference on the orientation effects. For instance, if you get the elastic constant as a function of the angle, it makes a difference if you do not consider two lamina with angle $\pm\theta$, coupled in a sense that there cannot be shear between the two. I could not quite tell if in your analysis you do consider this coupling preventing interlaminar shear or not. I sort of thought it was not taken into account. That would make a significant difference. But, of course, there are so many stages in the calculation, it is hard to trace deficiencies and what effect they have in the end.

D. McCammond: I believe that you are talking about interlaminar shear rather than coupling between axial and shear stresses? No, that was not considered.

S. V. Hoa: When you make up a laminate from many layers and have symmetric layers, half at the top and half at the bottom exactly the same, then the coupling disappears. But what if there is no symmetry? Symmetry may not always be present because you do not know how exactly the fibers are oriented in each layer. That is why it is difficult to neglect the coupling.

D. McCammond: You could do a more thorough analysis, the same type of analysis that one does with high-performance composites. Because of the lack of symmetry about the mid-plane, this would enable you to predict the coupling that would exist between applying an axial force and the bending or twisting resulting from that. So one could incorporate that if one wished. But it becomes much more complicated.

L. A. Goettler: You may have already said this. Reconciling your results, to what I was presenting earlier. It seems that it is probably more a function of the fiber length than anything else. You indicated the pres-

ence of a high degree of breakage in the injection-molding machine which would result in less isotropy. It seems that your results would likely be valid for a filled thermoplastic injection molding and may not be as valid, in fact, for long fiber thermosets.

D. McCammond: Yes. Clearly the anisotropy is going to increase as the fiber length and aspect ratio increase. I think that I mentioned that the length correction factor was of the order of 0.6 and 0.7. So if one has a longer fiber the aspect ratio goes up from 30, towards 60 and 70.

L. A. Goettler: You are referring to the length correction in terms of predicting the stiffness from a given distribution. But the fiber distribution itself would be different if the fiber would be longer.

D. McCammond: Do you think that you can get them more aligned?

L. A. Goettler: I think you would get a different one. For example, in the case of the edge-gated disk, more transverse orientation should be expected. More than what you have here, because one would have less shearing effect.

D. McCammond: Yes, this is possible.

L. A. Utracki: I don't quite understand how you sliced the specimens. I thought that slicing was vertical, in one plane. How do you account for the different out-of-the-plane orientation of fibers?

D. McCammond: A rectangular piece through thickness was removed first, and then a slice would be taken off the vertical face. Let us say the molding is a flat plate; the slice taken off the vertical side would simply indicate to you whether it was two-dimensional planar or not. Then there was a series of horizontal sections taken from what was left and it was these that showed the in-plane orientation.

Paper-Like Filled Polyethylene Films

V. G. ZBORIL *and* D. A. HARBOURNE

Du Pont Canada, Inc.
PO Box 5000
Kingston, Ontario
K7L 5A5

Filled high-density-polyethylene (HDPE) films for packaging applications have been developed. These films are of low permeability, are water and grease resistant, and can be heat-sealed like HDPE films but have stiffness, deadfold, cuttability, and appearance similar to those of paper. The films are produced in thicknesses of 10 to 100+ μm by the standard film blowing technique. The effect of the filler type, resin parameters, and film blowing process variables on the resultant filled film properties is discussed. The commercialization of filled films and the market acceptance of the products is also briefly elaborated upon.

INTRODUCTION

Plastic-based films and paper have earned their own place in the market determined by the price and performance of these two products. Paper has been used predominantly for printing (37 percent), packaging (bags and wrapping 23 percent), and tissue (15 percent). The greatest outlets for plastic films have been in customer and industrial packaging. A large segment of the packaging and wrapping end-use market can be served by either product but until recently the dominant material was plain or modified paper. As the cost of producing paper was expected to rise faster than that of plastic, there was a great incentive to develop paper-like films to take over. Paper is characterized by low price, low bulk density, high stiffness, high strength, low resistance to tear propagation, high permeability to liquids and gases, high fold retention, etc. It can also be easily cut, glued, and printed. It is now generally accepted that of all unmodified plastic films, those of plain high-density polyethylene (HDPE) or polypropylene (PP) have the best chance to compete economically and technically with paper. For many applications, however, such films are not sufficiently paper-like, eg., they will not run on machines designed to handle paper or, frequently, just do not appeal to people who have been conditioned to paper for many years, even though such films may be perfectly functional. Consequently, films have to be modified to achieve high stiffness, deadfold, ease of cutting and aesthetics (1). The properties of paper, HDPE, and PP films and an ideal film are compared in *Table 1*. One route to modify plastic films is to add inert fillers. The effect of fillers on polymer properties has been investigated by many authors (2-7) and many papers have been published on the subject. Almost all of them, however, pertain to bulk properties of such composites, when the filler particle size is negligible in comparison to the product size. Most of the information then is not applicable to filled films in which the filler particle size is of the same order as the film thickness. Also, many theories and conclusions are based on the results of tests which are irrelevant to films; Izod impact, for example. We have studied some of the important effects of the filler, resin, and process parameters on filled film properties and the results are presented here. The goal of our work was to develop a commercially successful filled-film candidate. Some of the work reported in this paper is covered by patents or patent applications in Canada and elsewhere.

EXPERIMENTAL

MATERIALS

Polymers

All the polyethylene resins used in this study were Sclair® ethylene homopolymers. Sclair 2907 is of narrow-molecular-weight distribution (Stress Exponent, SE = 1.3) and of MI = 5.0, Sclair 19A is of SE = 1.8 and MI = 0.73. Polypropylene was Shell 5520T.

Fillers

The fillers used and some of their characteristic properties are listed in *Table 2*.

®Du Pont Canada Inc. registered trademark for its polyethylene resins.

Table 1. Typical Properties of Films and Paper

Property	HDPE Film	PP Film	Paper	Ideal
Stiffness	Fair	Good	Excellent	High
Resistance to Tear	Good	Fair	Fair	High
Tear Balance	Poor	Fair	Good	Balanced
Bulk Density	Fair	Fair	Good	Low
Toughness	Excellent	Good	Fair	High
Cuttability	Poor	Fair	Excellent	Easy
Wet Strength	Excellent	Excellent	Poor	High
Permeability	Good	Good	Poor	Low
Fold Retention	Fair	Poor	Excellent	High

Table 2. Filler Characteristics

	Density g/ml	Particle Size (μm) % < 44	Mean	< 1, %	Particle Shape	Color	HPB/FDA*	Producer
$CaCO_3$ precipitated (USP dense)	2.65	Nil	3	30	Precipitate (irregular)	White	OK (USP)	Diamond Shamrock
$CaCO_3$ ground (OMYA BLR-3)	2.70	0.5	5	20	Angular	White	OK	Pluess-Staufer
Silica ground	2.60	0.6-1	10	5	Angular	White	?	Whittaker
Kaolin (hydrite 10)	2.58	Nil	0.6	>50	Hexagonal plates	Cream	?	Clark Georgia Kaolin
Wollastonite		0.5	6	8	Fibrous	White	HBP:OK	—
Talc cantal 325	2.70-2.80	0.4	10	7	Plates & fibres	White	No Status	Canada Talc
Talc, Montana beaver white 325	2.70-2.80	< 0.4	6	8	Plates	White	OK	United Sierra
Mica, wet ground (Alsibronz 12)	2.80-3.00	0.5	12	5	Plates	Brown	HPB:OK	Franklin Mineral
Fly ash	2.70	< 0.4	10	2	Spheres	Light brown	No Status	—
Diatomaceous earth (Celite 281)	2.40	1.0	6	low	Diatomite	White	?	Johns Manville

*HPB is Health Protection Branch of Health and Welfare Canada. FDA is Food and Drug Administration (USA). Both agencies regulate food packaging materials.

BLENDING

A Brabender Plasticorder fitted with Roller 6 head was used. The head was preheated to 190°C (oil) and then resin, additives, and filler were charged in that order. The total charge was approximately 50 ml of melt. It was found that the minimum conditions for satisfactory mixing in the mixer were 40 rpm, 8 minutes, at 190°C. Under conditions that were harsher than these minimum requirements, the blend performance slowly deteriorated. To prevent such degradation, the actual conditions were kept close to the minimum requirements, i.e., 40 rpm, 10 minutes, 190°C, the time being counted from the addition of the last component. After this time the head was opened, the blend removed and quenched between brass plates. The head was then thoroughly cleaned, reassembled, and used for the next blend. When reactive resin additives were used, the blending conditions were adjusted to match such reactivity.

PREPARATION OF FILLER CONCENTRATES

The filler concentrates were produced from dry blends of the filler with an appropriate resin. The dry blends were compounded in a W&H 53 mm twin-screw extruder fitted with a strand die. Three sections of the barrel were sufficient for good dispersion of most of our fillers. The screws had a feed section followed by kneading, reverse, normal, reverse, and normal sections. The blend was degassed in the second zone after the first reverse section. The maximum concentration of the filler was governed by the feeding characteristic of the dry blend which had to be free flowing and non-segregating in the hopper. Thus low-bulk-density fillers, such as mica, were used in 33-1/3 weight percent concentration as opposed to 50 weight percent achievable with compact fillers such as ground $CaCO_3$. The W&H extruder was dismantled and examined for wear after approximately 2500 kg of various concentrates had been produced and no signs of wear were present. Large lots of filler concentrate were made for us by an outside compounder. With due precautions, clean concentrates could be produced at both sources. Initially, however, decomposed resin remaining in the compounding equipment from previous runs was very effectively stripped by our products, resulting in contamination.

PREPARATION OF PLAQUES

The blend to be pressed into plaques was ground or broken into small pieces. A 0.76 mm thick 100 by 150 mm stainless steel mold was placed on a brass plate, sprayed with a release compound, and 15 to 20 g of the ground polymer blend were placed in the mold in a uniform layer.

Another brass plate coated with release agent was placed over the polymer and the assembly was then inserted into a laboratory press preheated to approximately 175°C. The press was then closed so that both brass plates were in light contact with the heated press platens. After melting the polymer for 5 minutes the press was closed further to give 89,000 N force and held for 5 minutes when the heaters were switched off and cooling water admitted. When the press temperature dropped to about 50°C, the mold was removed and quenched to room temperature. The plaque was removed and test dumbbells were cut, gaged, and used in an Instron for measurement of tensile properties. The conditions for pressing were chosen so that the resin charge was properly fused, without degradation, and the resin crystallinity was fully developed upon cooling.

TESTING

Plaques were tested for tensile properties using an elongation rate of 10 percent per minute at room temperature and 65 percent relative humidity (RH). The dumbbell samples were kept in the lab for at least 48 hours prior to testing. We found that conditioning for 1 to 7 days at 20 to 95 percent RH had no measurable effect on the test values. Films were tested according to the accepted ASTM standards: ASTM D-1922 for tear resistance, ASTM D-882 for tensile modulus and toughness (as tensile energy to break), ASTM E-252 for thick-

ness. The resins were tested according to ASTM D-1238 condition E for melt index, ASTM D-1505 for density. Stress exponent is defined as: SE = (ln MI (@ 6480 g− − ln MI (@ 2160 g))/ln3. Melt drawability was tested by extruding samples through a slit film die (1 mm kg 355 mm) into a water quench bath. The take-off speed was being increased until the molten web broke or severe unstability developed. The minimum film thickness attainable in stable operation is the measure of drawability. A 63.5 mm Egan extruder with a 24 to 1 L/D ratio mixing screw was used to feed the polymer melt into the die.

RESULTS AND DISCUSSION

CLASSIFICATION OF FILLERS

Particle size and shape are the most important parameters describing a filler. Various filler types and typical examples are shown in *Table 3*. All these fillers can be treated to increase adhesion to the polymeric matrix, to decrease water absorption, or for other reasons. Apart from the particle size and shape, purity, toxicity, density, color, availability, cost, and many other properties must also be considered.

EFFECT OF FILLERS ON SOLID STATE PROPERTIES OF PRESSED PLAQUES

Stiffness

The effect of various fillers on the tensile modulus is shown in *Fig. 1*. Within the range of fillers tested, only the filler particle shape affects the filler effectiveness in increasing the plaque stiffness. The higher the aspect ratio of the filler particle, the more effective the filler. From the lamellar fillers tested, their efficiency increased in the order delaminated clay < talc, dry ground mica < water ground mica. The effect of particle size or shape (spherical flyash, angular silica) was negligible.

Tensile toughness

This property was very sensitive to the addition of fillers. Similarly to other properties, the filler particle anisotropy had the most pronounced effect on the filler effectiveness. Some typical results are plotted in *Fig. 2*. It is interesting to note that the tensile toughness was controlled almost exclusively by the elongation at break (see *Fig. 3*). The tensile strength had only a minor effect. These correlations are quite different when toughness is measured by notched Izod impact method. A film toughness (by tear resistance or dart drop test), however, seems to correlate better with the plaque tensile toughness than with Izod impact toughness usually quoted in the literature. The literature data on various methods for improving toughness are, therefore, of limited usefulness in predicting properties of filled films.

Table 3. Particle Shape and Size of Typical Fillers.

Particle Shape	Size	Typical Filler
Irregular	Fine	Chalk
Irregular	Coarse	Ground $CaCO_3$
Fibrous	Fine	Asbestos
Fibrous	Coarse	Glass
Lamellar	Fine	Delaminated Clay
Lamellar	Coarse	Mica
Spherical	Fine	Fumed Alumina
Spherical	Coarse	Fly Ash
Lace Work	Coarse	Diatomaceous earth

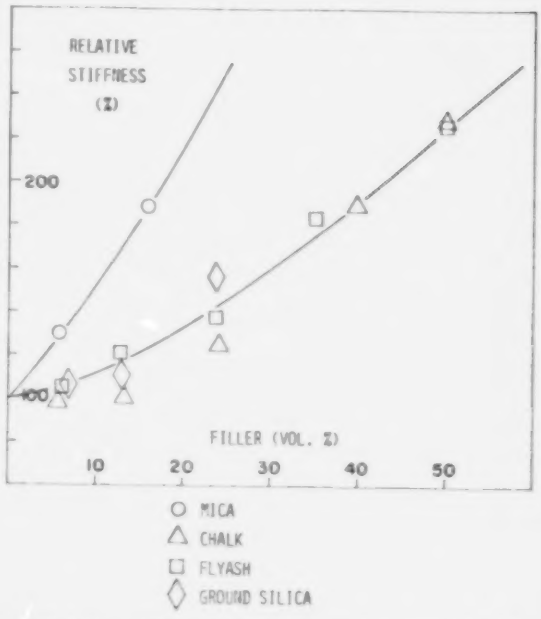

Fig. 1. Relative stiffness of pressed plaques (as tensile modulus) of Sclair 2907 filled with various fillers as a function of the filler content (volume percent).

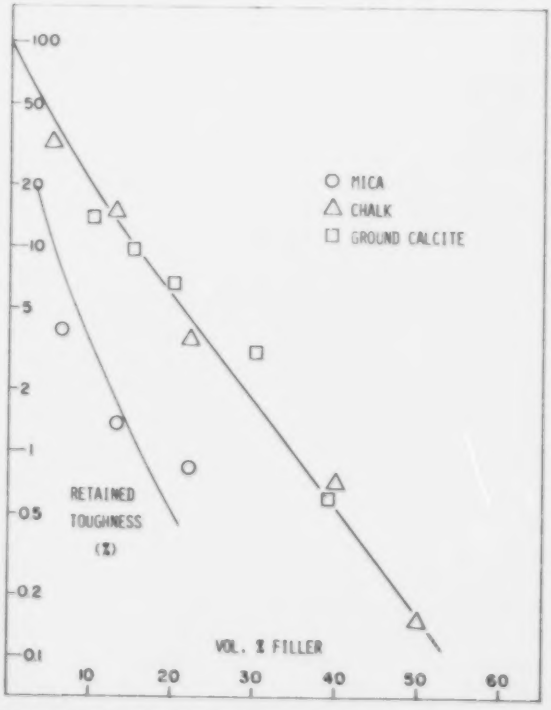

Fig. 2. Retained toughness as area under the stress-strain curve of plaques pressed from filled Sclair 2907 as a function of the filler content (volume percent).

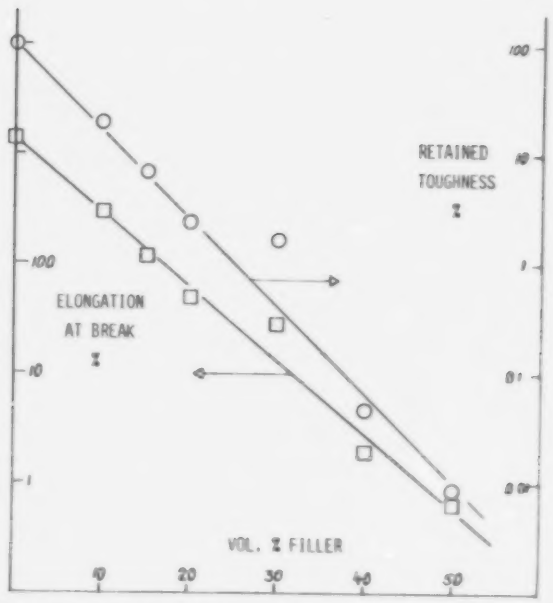

Fig. 3. Retained toughness and elongation at break of plaques pressed from Sclair 2907 filled with ground calcite as a function of the filler content (volume percent).

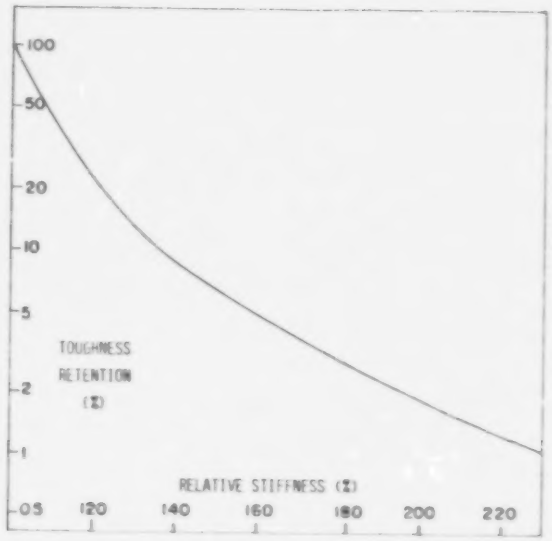

Fig. 4. Toughness retention of plaques pressed from Sclair 2907 filled with various fillers as a function of the relative stiffness (tensile modulus). Best fit to 90 experimental points.

Tensile Strength

We have not studied the effect of various fillers and filler treatments on tensile strengths to any great extent, since this property proved to be rather irrelevant in filled films (see *Tensile toughness*). The limited data we have recorded indicate that the tensile strength is enhanced by filler-matrix adhesion, by fillers having high aspect ratio particles and high specific surface area. All of these findings are in agreement with published data.

Toughness versus stiffness

The toughness of polyethylene filled with various fillers is plotted against stiffness in *Fig. 4*. It demonstrates that, for a given resin, toughness is a unique function of stiffness, regardless of the filler used. Treatment of the fillers, such as coupling agents or coating of various kinds, did increase the toughness of the composite but its stiffness decreased so that no superior performance was obtained. Similarly, addition of known toughness improvers such as various rubbers or accommodation resins (EVA for example), improved the toughness of the composites but lowered their stiffness with no real gain in their balance. We have tried most of the known, and some innovative, approaches to the production of tough and stiff filled polyethylene films with little success.

FILLED PE FILMS

Production methods

Three processes can be used for producing filled films: casting, blowing, and calendering. For economic reasons, blowing is preferred. It is also the most widely used process and practically the only one used in converting polyethylene to films. It is therefore imperative that if a new type of polyethylene film, such as filled film, is to be introduced on the market, the blowing process be used. This process requires that the polymer melt be drawn to low gages without breaking or pinholing and the melt tension (extensional viscosity) be high at the same time.

Drawability of filled HDPE melt

In our first attempts to produce thin filled HDPE films, we have failed to produce films thinner than about 50 μm. The resin was filled with 20 volume percent of ground calcite. Substitution of polypropylene for polyethylene further aggravated the situation. At a constant filler content, the largest effect on the melt drawability was the base resin melt index (see *Fig. 5*). The molecular-weight distribution had little effect. Manipulation of the film production parameters, such as the melt temperature, surprisingly changed the drawability surprisingly little. The filler particle shape is also an important parameter affecting drawability, which is worse when anisotropic fillers are used.

Processability of filled resins

As mentioned above, melt strength and melt drawability are required in the film blowing process. In unfilled PE, these two melt properties are not independent; melts exhibiting high extensional viscosity have poor drawability. Addition of fillers worsens the balance. We found that films thinner than about 50 μm cannot be blown from resins containing more than approximately 10 volume percent of irregular or 7 volume percent of platelet or fibrous fillers. More highly-loaded films would have to be calendered at much higher cost.

Melt drawability versus solid state properties

The relationship between the degree of modification (e.g. modulus) versus melt drawability is crucial (*Fig. 6*). It is obvious that only platelet or fibrous fillers are ac-

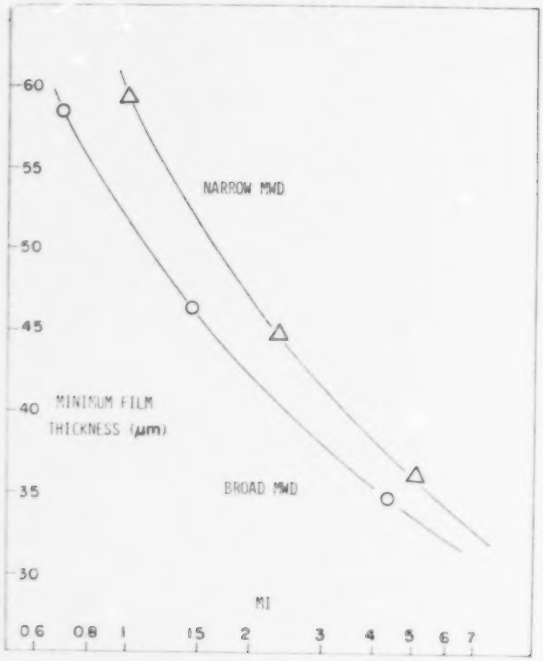

Fig. 5. Drawability (as minimum film thickness) of various Sclair ethylene homopolymers filled with 20 volume percent of ground calcite (Omya BLR) as a function of the resin melt index. Melt temperature 250°C.

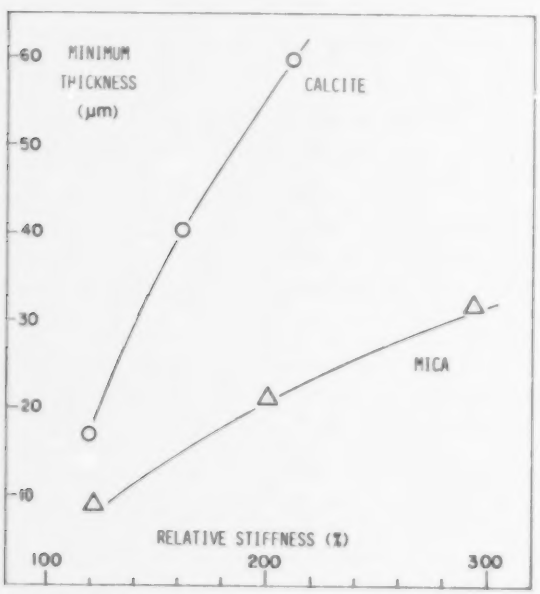

Fig. 6. Drawability (as minimum film thickness) of Sclair 2907 filled with mica (Alsibronz 10) or ground calcite (Omya BLR) as a function of the film relative stiffness (as tensile modulus).

ceptable. Fibrous fillers, however, were not used in further work, firstly because they are either suspected (glass fiber) or proven (asbestos) carcinogens and secondly, because they yield films of unbalanced (transverse versus machine direction) properties.

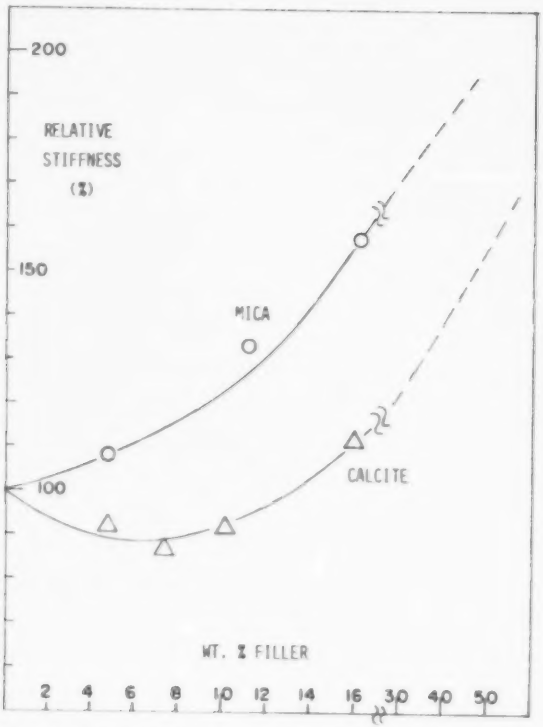

Fig. 7. Relative stiffness (as tensile modulus) of films blown from Sclair 19A filled with mica (Alsibronz 10) or ground calcite (Omya BLR) as a function of the filler content (weight percent).

Effect of Film Blowing Process

The tensile modulus of films blown from HDPE filled with wet-ground mica or ground $CaCO_3$ is plotted versus weight percent filler in *Fig. 7*. The difference between these two types of filler is amplified by the process, which tends to orient only the mica platelets, while the changed film morphology adversely affects the performance of both fillers. The balance of tear—important in cutting the films—is favourably modified by mica but not by $CaCO_3$ (*Table 4*). The desired combination of balanced tear, high stiffness, and low deadfold recovery angle could only be obtained in the mica-HDPE combination (*Table 5*). Polypropylene-based films, besides being difficult to make, have surprisingly poor deadfold.

Table 4. Tear Resistance (Elmendorf Tear, ASTM D-1922-67) of Sclair 19A Filled With Calcium Carbonate (OMYA BLR 3) or With Ground Mica (Alsibronz 12)

Filler Type	%	BUR*	Elmendorf Tear (G/μm) MD	TD	TD/MD
—	0	1.5	0.56	12.30	22.00
$CaCO_3$	8	1.5	0.53	12.60	23.70
Mica	8	1.5	0.57	3.70	6.43
—	0	4.0	0.53	1.40	2.61
$CaCO_3$	15	4.0	0.91	2.60	2.81
Mica	15	4.0	0.64	0.75	1.17
$CaCO_3$	8	4.0	0.75	1.90	2.47
Mica	8	4.0	0.80	1.40	1.82

*Blow-up ratio

Table 5. Characteristic Properties of Filled Films.

Sample	HDPE*	10% TiO_2 in HDPE	10% $CaCO_3$ in HDPE	10% Mica in HDPE	10% Mica in LDPE	10% Mica in PP
Nominal thickness, μm	43.00	50.00	50.00	43.00	50.00	41.00
Yield, m^2/kg	23.20	18.10	18.40	21.40	19.60	25.00
Density, g/ml	0.96	1.00	1.02	1.02	0.98	0.97
Tensile, MPa	33.80	22.10	20.00	16.50	21.40	14.50
Elongation, % (average of MD & TD)	1100	600	27	16	720	13
Elmendorf tear, MD	0.79	0.87	0.67	0.51	2.83	0.40
g/μm TD	2.17	1.65	1.42	0.71	4.05	0.40
Clark stiffness, cm_3	5.3	9.4	5.9	7.8	1.7	6.6
(Corrected to Gage)	(5.3)	(5.8)	(3.6)	(7.8)	(1.0)	(7.9)
Deadfold angle of recovery°	97	53	85	32	35	140

*Density = 0.96 g/ml; Melt flow index = 0.75 dg/min; Broad molecular weight distribution.
All percentages are by weight.

REFERENCES

1. V. M. Wolpert, "Synthetic and Plastic Paper," International Technoeconomic Survey, Wolpert & Jones Ltd., London, 1972.
2. Y. Sato, and Furukawa, J., *Rubber Chem. Technol.*, **36**, 1081 (1963).
3. L. E. Nielsen, *J. Appl. Polym. Sci.*, **10**, 97 (1966).
4. W. A. Zisman, *Ind. Eng. Chem.*, **57**, 26 (1965).
5. W. C. Jones, III and Fricke, A. L., *Modern Plastics*, **49**, 88 (1972).
6. W. F. Furter, *Can. J. Chem. Eng.*, **42**, 77 (1964).
7. W. M. Speri, and Jenkins, C. F., *Polym. Eng. Sci.*, **13**, 409 (1973).
8. E. Guth, *Kolloid Z.*, **74**, 266 (1936).

DISCUSSION

J. M. Charrier: I want to compliment you on the presentation. Has there been any work done to try to make slightly foamed film to achieve some of these properties? You mentioned bending stiffness as the parameter to improve. By increasing the thickness, one could improve the bending stiffness. Besides, the folding problem would also be resolved using a slightly foamed system. Would this be compatible with the thinness of the film?

V. G. Zboril: To some extent, yes. Unfortunately, it is incompatible with the basic characteristics of HDPE. The polyethylene which foams best is the high-pressure low-density polyethylene.

J. M. Charrier: Are you implying that it is impossible to foam the high-density polyethylene in thin films?

V. G. Zboril: We are not giving up yet.

J. M. Charrier: How about the film blowing process?

V. G. Zboril: You need a special design die. To some extent it works. We even tried laminates with foamed core and solid surfaces, a concept which from the mechanical point of view (not necessarily from the economic) makes sense.

G. C. Hawley: Two questions really. You mention the problem with the iron. Some of the micas do contain iron silicates, not free iron. Does the test you were talking about lump it together? Is the iron there, classified as being noxious?

V. G. Zboril: It is not necessarily as bad as I may have led you to believe. You have to prove that it does not migrate out. If you prove that, then it does not constitute a food additive and thus is outside the jurisdiction of the FDA. HPB works slightly differently in that they judge these things from case to case.

G. C. Hawley: The second question concerns the silanes. When I was working with silane-treated micas, this permissibility of the silane was always a question. We did a fair amount of work on this. The results were rather equivocal. Again, is this a case-by-case situation?

V. G. Zboril: In Canada, yes. In the USA, you have to prove that it does not migrate to food. FDA require extraction tests. If you prove that there is no extraction, then you are okay.

G. C. Hawley: One of the problems we found was that the very small amounts of silane are very difficult to detect. We went to the extent that we radio-labelled the silane and then did the extraction. The whole experiment took about a year of painstaking work to get a number which was marginal. Last question: I would like to get some comments on the effects on mica at these low levels on permeability of the film. Do you see any effect?

V. G. Zboril: Yes. The problem is interesting. The effect depends on two factors: the overlap of platelets, and the average film thickness. If you plot the improvement in barrier properties versus film thickness, there is a crossover. Below a certain thickness you are worse off. The reason in thin spots. If you go over this critical thickness then you start gaining. The critical thickness depends on the aspect ratio and the average flake size of the filler.

L. A. Utracki: Are these films you are talking about cast or blown?

V. G. Zboril: They are blown.

L. A. Utracki: In this case, you should have very good orientation of the platelets.

V. G. Zboril: That's correct. However, since the films are filled at 10 weight percent, the filler particles do not overlap to any great extent. One can improve the barrier properties by addition of aluminum flakes, but obviously the cost goes up.

P. Lepoutre: How is the opacity obtained?
V. G. Zboril: In this case, through addition of 2 percent of TiO_2.
P. Lepoutre: What is the film thickness?
V. G. Zboril: About 30 to 35 microns.
P. Lepoutre: What would be the advantage of adding mica to polymer? Paper used to be the cheapest filler. I am wondering if the better combination of stiffness and other properties might not be obtained by laminating, or extrusion coating, rather than adding mica.
V. G. Zboril: Yes, that is correct, I gave you a sort of average price of paper. Some special papers like parchment, coated papers, etc., are quite expensive. The price of our material is quite favorable.
P. Lepoutre: What would you expect to be the advantage of lamination or co-extrusion coating over the filled film substitution?
V. G. Zboril: The advantage of the filled film approach is the cost. It is usually made in a single-step operation, whereas paper coating requires more processing and, as a result, the price goes up.
M. Fenton: Did you say that your mica price was $1/L?
V. G. Zboril: Yes, about $300 per ton. This was water-ground 325 mesh grade.

Recent Developments in Sheet Molding Compound Technology

SEYMOUR NEWMAN *and* DONALD G. FESKO

Plastics, Paint and Vinyl Division
Ford Motor Company
Detroit, Michigan 48239

The molding of fiber-reinforced thermoset components is a complex process involving a highly exothermic chemical reaction, which takes place in the presence of flow and thermal gradients. The flow in turn is complicated by time- and temperature-dependent rheological characteristics. The industry has grown largely on the basis of empirical developments. However, numerous problems do remain which require increased understanding for solution. This report reviews work underway in numerous laboratories to characterize the flow and cure of sheet molding compounds and phenomena associated with these processes such as orientation, mechanical properties, residual internal stresses, mold fill, and surface defects.

INTRODUCTION

The term sheet molding compound (SMC) comprises a wide range of polyester pre-preg, thermosetting, molding materials reinforced generally with random short glass strands, although continuous glass strands may also be included. The system, based on styrene monomer as a crosslinking agent and unsaturated polyester resins, is both a fibrous and particulate reinforced composite since a typical composition is reinforced with E-glass, and calcium carbonate, as shown in *Table 1*. Small quantities of additives such as thickener (MgO), stearate lubricants, low-profile or shrink-control agents, initiators and accelerators, pigments, and other modifiers make up the total system. SMC is commonly fabricated into useful articles by compression molding but, with appropriate equipment, the material may also be injection molded.

After impregnating the loose glass fiber with a low-viscosity paste made up of the rest of the constituents, the sheet molding compound is set aside to thicken. A large increase in viscosity caused by MgO is attributed to the formation of high-molecular-weight polymer chains, which arise from salt formation and subsequent complexing of carboxylic acid groups with Mg ions.

Table 1. Typical SMC composition.

Resin:	% (by weight)
unsaturated polyester 10.5% low shrink additive 3.45% styrene monomer 13.4%	27.35
Filler ($CaCO_3$)	40.70
Thickener (MgO)	0.70
Initiator	0.25
Lubricant (zinc stearate)	1.00
Glass fibers (12-50mm)	30.00
	100.00

The stress-strain properties of SMC, particularly tensile modulus and strength, have been related (1) to the volume fraction of filler and glass fibers using mathematical relations established for composite materials. Such studies, however, are complicated because of the multiplicity of components present, the non-uniformity of dispersion of fillers and additives, fiber orientation due to flow, the presence of fibers as bundles, as well as the variability in interfacial adhesion and the defective structure introduced as a consequence of commercial processing.

It is not our intent, in this paper, to review in detail the mechanical properties of composites as applied to SMC but rather to focus our attention on process variables as they affect physical and mechanical properties. In particular, the thermal history and rheological behavior during processing represent the main areas we wish to address, since these are of most immediate concern to the fabricators of SMC products. Finally, an area which must also be addressed is the matter of surface characteristics of SMC parts used for high appearance applications. Few definitive fundamental studies have been directed toward this problem despite its great importance to commercial utilization.

THERMAL EFFECTS

Temperature profiles

During compression molding of relatively thick layers of highly filled polyesters (50 percent glass), the cure front has been shown to progress from the outer surface and move toward the center. This is readily ascertained by premature interruption of the cure cycle, which dis-

closes an uncured center region. Temperature-time curves at the outer surface, subsurface, and centerline of the material were measured in our laboratory by Mallick and Raghupathi (2). It is evident (*Fig. 1*) that the surface temperature in contact with the heated tool remains relatively uniform compared to the centerline, where the heat-up lags the surface but which ultimately experiences a large peak temperature due to the heat of reaction and the low thermal conductivity of the surrounding material.

Similar observations were subsequently made by Panter (3), who monitored the centerline temperature and cure in a traditional SMC material of 0.25 cm and 2.5 cm thickness. For the thin sheets at low mold temperatures (130°C), a uniform temperature rise leveling off at the mold temperature with no exothermic peak is observed (*Fig. 2*). Curing occurs more rapidly at higher mold temperatures and is accompanied by an exothermic peak. For the thicker sample, the cure reaction is delayed: but, once initiated, takes place rapidly and with exotherms as high as 50°C above the mold temperature.

The time to reach the exotherm peak, a measure of the time to cure, increases almost linearly with part thickness and depends also on the filler content and thermal characteristics of the composite material. The cure cycle can be shortened by elevating the mold temperature; but this approach is limited by the increasing magnitude of the peak exotherm temperature, which, under extreme conditions (~200°C), may result in burning and chemical degradation of the resin. For an analysis of the effect of preheating of SMC prior to molding or cure, see *Refs. 2* and *3*.

From model calculations, McGee (4) predicts that the center cures first and progresses toward the mold wall for thin samples regardless of filler content (see *Fig. 3*). For somewhat thicker samples, cure may begin at the mold wall or centerline, depending on filler content and, under certain conditions, may occur at both locations almost simultaneously. For thick, highly filled materials, cure begins at the mold wall, as experimentally shown in the studies quoted above.

Clearly, fillers play a significant role in the thermal properties of the resin system: fillers replace resin and thereby decrease the total amount of heat liberated in the crosslinking reaction and additionally act as a heat sink. Thus, increasing the filler content decreases the maximum centerline temperature (*Fig. 4*) and allows higher mold temperatures to be used.

Experimental time-temperature curves in the curing of polyester resins in heated molds has also been successfully modeled (5) by a chemical reaction rate which may be written in the form

$$dx/dt = k'[I](1 - x)^3 \exp(-a/RT) \qquad (1)$$

where $[I]$ is the initial initiator concentration (benzoyl peroxide) and x is the conversion of unsaturated bonds;

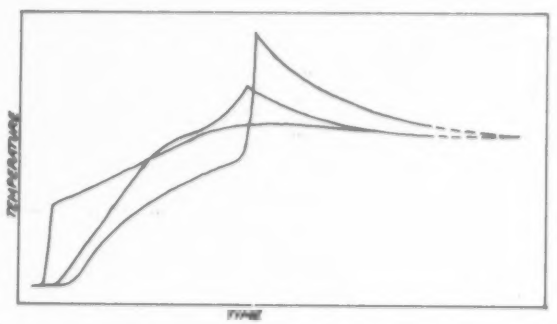

Fig. 1. Schematic representation of temperature-time curves during molding: (a) centerline, (b) outer surface, (c) layer below the outer surface. Plotted from data of Mallick and Raghupathi (2).

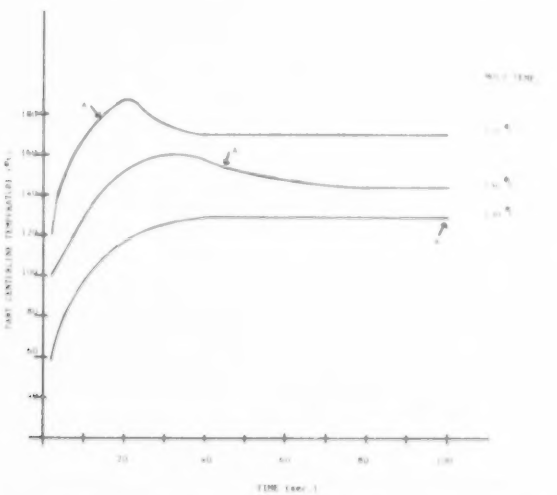

Fig. 2. Temperature versus time in 0.25 cm sheet. Points A correspond to about 50 percent cure. Plotted from data of Panter (3).

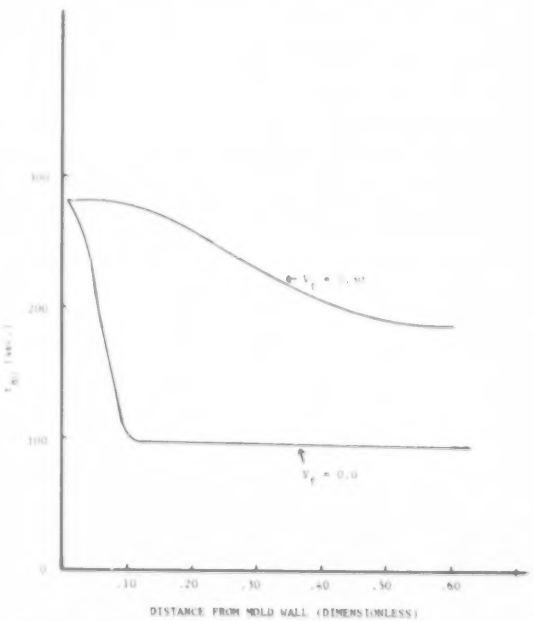

Fig. 3. Time to 80 percent of reaction versus distance from mold wall (dimensionless) for two levels of glass fiber content for a half mold thickness of 0.50 cm; wall temperature = 150°C. Plotted from data of McGee (4).

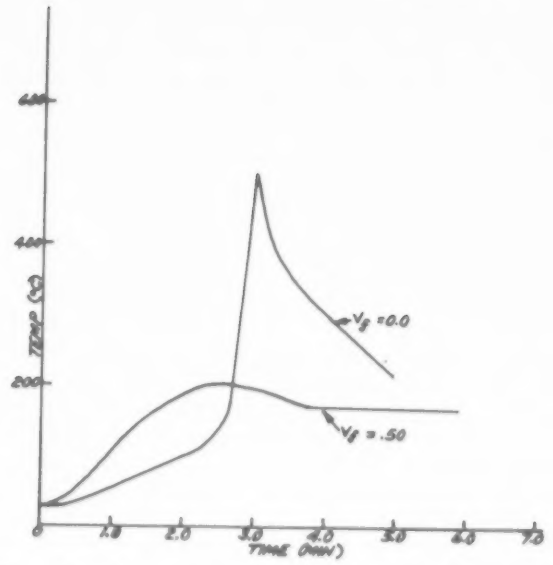

Fig. 4. Centerline temperature as a function of time for calcium carbonate/polyester at the indicated volume fractions. Wall temperature = 150°C; half-mold thickness = 0.75 cm. Plotted from data of McGee (4).

cobalt octoate was used as an accelerator (see *Fig. 5*). It is of interest to note in this study that deletion of the accelerator delays the reaction and enables the midplane temperature to rise by conduction before the reaction takes place. This, in turn, results in a higher peak temperature at the midplane.

In this connection, however, we feel that a more detailed representation of the reaction rate must be developed for a theoretical model to be of optimum use for industrial applications. (See, for example, *Ref. 6.*) Thus,

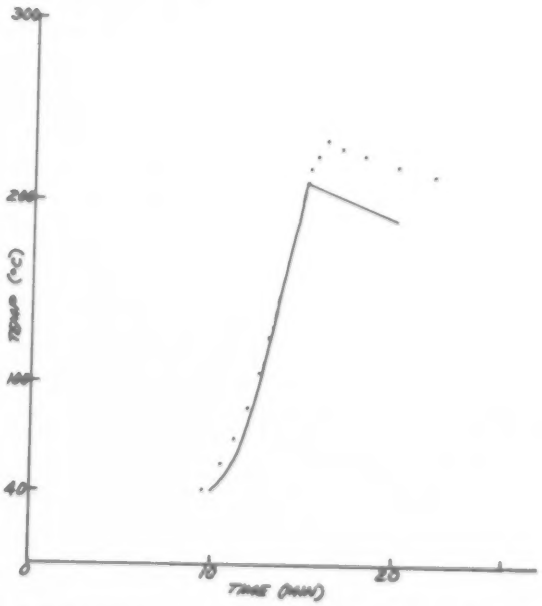

Fig. 5. Temperature-time curves near the centerline. Sold line is theoretical; points are experimental. Plotted from data of Rojas, et al. (5).

by incorporating the kinetics of catalyst decomposition, and, including the role of inhibitors in termination processes as well as of accelerators, one could more readily vary the type and concentration of these agents along with mold temperature to optimize systems for most efficient production. Also, a complete heat-transfer model should allow an evaluation of the usefulness of high thermal conductivity tooling inserts to speed cure in thick regions, e.g., bosses. Some studies of mold conductivity effects have been reported by Panter (3), Herman (7), and Barone and Caulk (8).

Interaction of Flow and Cure

A charge of SMC placed in a mold is subject to complex thermal history not only because of the heated mold surface and exothermic reactions of the SMC, but due also to complex flow of the material. Thus, in their pioneering studies with instrumented molds, Marker and Ford (9) point out that when disc-shaped stacked layers of SMC are placed in the mold, curing initiates at the edge of the mold and propagates towards the center. This is attributed to the fact that when a cold charge is placed in the mold, the surface layers are hot, whereas the bulk of the material between the press platens is essentially at its initial temperature. The resin viscosity at the surface falls rapidly due to breakdown of the network structure from thickening with MgO and before appreciable chemical crosslinking has progressed. This decrease in resin viscosity, in turn, accounts for a preferential flow of hot material from the surface to the periphery, and accounts for the observation that curing started at the edges of the disc

In a similar vein, Mallick and Raghupathi (2) investigated the effect of the number of layers (at a constant 0.5 inch total thickness) on the time to reach the exotherm peak at the mold center. The time to reach the exotherm peak increased with the number of layers because the hot surface layers flow to the mold edges, leaving a somewhat quenched mold surface to heat the underlayers. However, the peak exotherm temperature did not change appreciably with the number of layers. We attribute this observation to the fact that the material is heated largely adiabatically by the exothermic reaction only after first reaching a "kick-off" temperature.

In steady-state molding, Barone and Caulk (8) show that the flow effects described above lead to a steady-state convection of heat away from the charge region. Consequently, the mold develops a severe temperature gradient over its surface, especially in the rapid production of large, thin parts. This ultimately decreases the cure rate and increases the cure cycle time as suggested above. By a sophisticated thermal analysis, Barone and Caulk propose a new mold heating design which provides for a compensating non-uniform heating and results in a minimal variation of the mold surface temperature.

Mechanical properties

Mechanical and physical properties are primarily dependent on compositional variables, but are profoundly influenced by thermal history and rheology. From gen-

eral principles, it is well known that the degree of cure and network perfection has a strong influence on flexural strength and interlaminar shear strength, especially for thick section molding. Non-uniform cure can introduce planes of weakness in the interior section of a molding or in thick sections, e.g., bosses, and result in failure under thermal stresses or during certain loading conditions even in the absence of any apparent cracks or defects.

Mallick and Raghupathi demonstrated that a gradient of properties may be observed in thick section molding due to thermal history by cutting thick samples in half through the center plane and testing each half in flexure so that either the exposed center layer or outer skin is in tension. For short cure times (*Fig. 6*), the center has lower strength than the outer skin, indicating that the part was removed prior to the completion of cure. The slope of the curve increases rapidly at the time to reach the exotherm peak, indicating that the cure rate is near its maximum; thereafter, the flexural strength approaches its limiting value slowly but lagging the outer surface properties for a relatively long span of cure time.

Beyond these preliminary studies, little is known about the influence of the temperature profile and resultant gradients in the degree of crosslinking through the thickness of a molded specimen. This situation is further complicated by the existence of pressure gradients, which also exist during molding, as discussed later. Similarly, little is known about the degree of cure gradients in the radial direction as a function of cure time. Such analyses are, of course, masked by large variations in fiber orientation discussed elsewhere. Finally, it should be recognized that no studies have been performed on the relation between network topology and ultimate properties. For example, network topology can be varied by arranging the location of reactive double bonds along the polyester backbone.

Residual stresses

Thermal history and curing patterns not only affect strength properties through the thickness of a part, but may also lead to a complex pattern of residual stresses. Little effort has been devoted to this field, but considerable insight has been provided by Marker and Ford (9) using a circular tool with circular charges. See later discussion of *Fig. 10*. In this study, the fact that the center cured and underwent shrinkage after the perimeter implies that the perimeter is being pulled in by the center and is under compressive stress. Conversely, a radial tensile stress is being applied to the center by the perimeter. This was verified by cutting portions of the disc after the part was removed from the mold. After making this cut, it was found that the outer portion of the disc had expanded while the inner portion had contracted (see *Fig. 7*). Such complex residual stress patterns may be expected to lead, in general, to dimensional instability and warpage of complex shapes. This phenomenon must be further complicated by low profile agents, which modify the macroscopic shrinkage, but this factor has not yet been quantified.

Apart from these residual stresses, thermal stresses may also be anticipated:

a) Rapid cooling of the polymer results in internal stresses around the filler particle and glass due to different coefficients of thermal expansion of filler and matrix. This should become severe below the softening point or glass temperature of the matrix phase. See *Ref. 10*. Such effects have also been shown (11) to play an important role in determining the physical properties of epoxy composites especially with carbon fiber reinforcement, where the nature of the fiber-resin interface is apparently determined primarily by the compressive stresses exerted at the interface.

b) A temperature distribution in a molded part due to the thermal history during molding and non-uniform cooling thereafter likewise will lead to thermal stresses arising from constraints on thermal shrinkage, particularly as different portions of a specimen reach the glass temperature and prohibit stress relaxation (12). This is particularly likely to cause warpage in complex shapes. Few investigations of these residual stress effects on

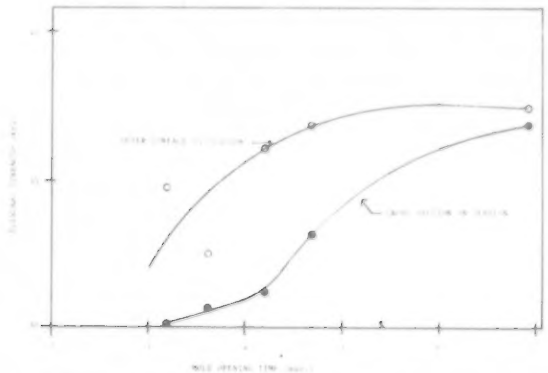

Fig. 6. Flexural strength variation indicating the extent of cure at the center and outer surface in a 0.5 in thickness part of a 50 percent glass-filled vinyl ester sheet. Plotted from data of Mallick and Raghupathi (2).

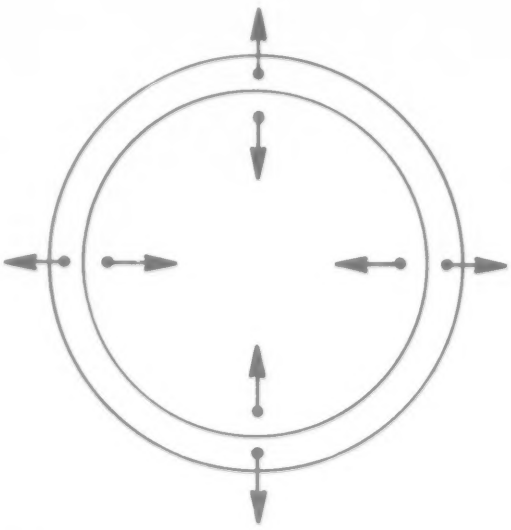

Fig. 7. ' ...stress pattern during cure according to Marker and Fo...

compression molded SMC have been carried out, particularly with regard to their effect on failure phenomena.

EFFECT OF RHEOLOGY

The flow of SMC under molding conditions is probably the least understood characteristic of the material and yet it is probably the single most important factor in determining part quality. Rheology determines the resulting fiber orientation and distribution, which profoundly affect mechanical properties, warpage, and waviness. It provides a means for release of entrapped air from the sheet and, therefore, influences the degree of porosity. Additionally, it determines which areas are preferentially heated by convection across the tool surface and, hence, the uniformity of cure. Numerous papers addressing the subject (9, 13-19) have appeared in recent years, indicating a growing interest. The extreme complexity of SMC rheology is probably responsible for the delay in applying research efforts to its study, but this arcane subject is slowly yielding to analysis.

Fiber orientation effects are probably the largest single factor causing strength variations in molding. Pye (20) has shown strength contours in a molded plaque due to fluctuations in fiber orientation as evidenced by X-ray radiography (see *Fig. 8*).

The effect of fiber orientation angle on both strength and modulus has been more recently documented by Watanabe and Yasuda (1). Techniques for experimentally determining the angle and degree of fiber orientation and incorporating these parameters into relationships to describe the resultant strength vector are being developed (21).

Owen, Thomas, and Found (13) in 1978 presented a convenient graphical method for predicting the flow front of fiber-filled fluids and resulting fiber orientation. The technique could be used easily to approximate how a mold would be filled by a given charge in compression molding or from a particular port in injection molding. The method consists of simply summing along radii from the center of charge mass, the original charge pattern plus a series of larger and larger circles concentric with the center of mass (see *Fig. 9*). Interestingly, this geometric method more accurately describes the flow front than many exercises in mathematical modeling. The authors also described other idiosyncracies of flow such as the formation of pseudo-knit lines caused by fiber orientation in shear zones and fiber orientation across flow fronts due to extensional flow, both of which significantly affect mechanical properties.

When Marker and Ford (9) published their results on the flow and cure of SMC in a circular compression mold in 1977, they reported several unexpected phenomena which profoundly affected molding behavior. In particular, they noted flow occurring primarily from the surface of the charge where the viscosity was reduced by being in direct contact with the hot tool surfaces. These authors used the technique of molding multicolored, layered charges to graphically display this behavior. This had many consequences, including non-uniform heat demand on the tooling and preferential heating of the material which flowed to the perimeter of the tool which, in turn, led to non-uniform curing. After mold closure, but before the onset of curing, the pressure distribution is determined by the SMC acting as a hydraulic fluid, and is initially uniform across the mold. Curing of convectively heated material starts at the outer edges and is accompanied by polymerization shrinkage which results in a pressure drop at the mold edges. (See *Fig. 10*). The pressure of the platen is then sustained by the charge in the center which expands as it heats but is restricted from flowing by the gelling perimeter. Then as the center cures and begins shrinking, the pressure shifts to the largely cured perimeter and the pressure over the original charge area drops.

Marker and Ford noted that because of this, most of the material went through the critical stages of gelation and cure at very low pressures. (It is thus not unex-

Fig. 8. Strength contour map of a plaque molding. Plotted from data of Pye (20). Charge placement is unknown.

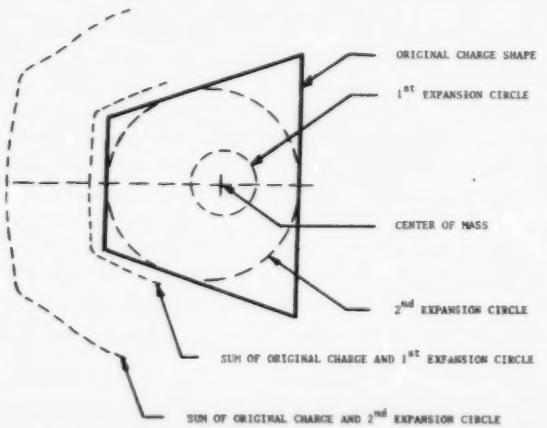
ORIGINAL CHARGE SHAPE
1st EXPANSION CIRCLE
CENTER OF MASS
2nd EXPANSION CIRCLE
SUM OF ORIGINAL CHARGE AND 1st EXPANSION CIRCLE
SUM OF ORIGINAL CHARGE AND 2nd EXPANSION CIRCLE

Fig. 9. Prediction of SMC flow in compression molding. Redrawn from Owen, Thomas, and Found (13).

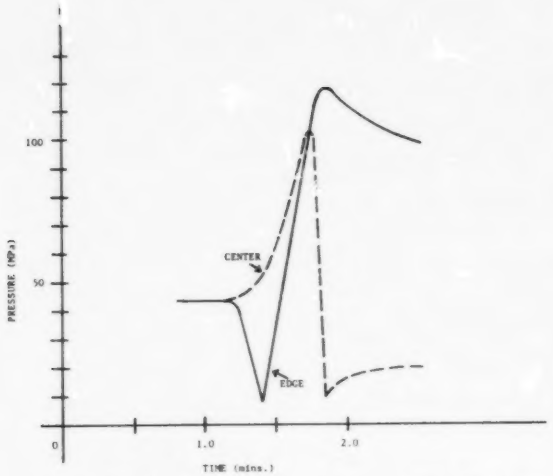

Fig. 10. Change of pressure at various radial positions during cure. Plotted from data of Marker and Ford (9).

pected that voids and porosity discussed later plague this type of molding.) This phenomenon has been also observed in our laboratory, and further, that the effect of surface flow could be dramatically reduced by preheating the charge to minimize the thermal gradients during press closure. In other instances (22), the behavior of surface material flowing preferentially was not observed, thus causing considerable consternation among researchers.

The resolution of the observed differences in flow lies in the geometry of flow and the constitutive relationship for SMC which describes its intrinsic flow behavior. Denton (22) used a rectangular charge pattern in a square mold which resulted in shear flow as the press closed. (See *Fig. 11.*) Marker and Ford used a circular charge in the center of a circular tool, which resulted in a combination of shear flow and elongation of material as the circumference of the charge increases during press closure. The resistance to elongation by the SMC is the factor that resulted in Marker's observations. Molding a square charge in a larger square mold is similar to the radial flow case.

Lee (12) is able to predict the behavior seen by Marker and Ford in the radial flow case for a binary

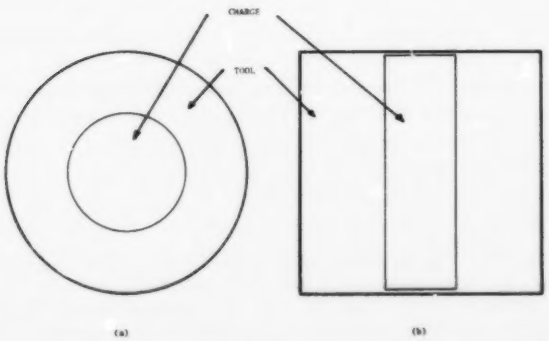

Fig. 11. Mold geometry and charge pattern for (a) Marker and Ford (9) and (b) Denton (22).

fluid system, both Newtonian and viscoelastic cases, where the lower viscosity fluid lies near the surfaces. This binary system represents a viscosity gradient. He develops a criterion for radial flow based on the dimensionless group:

$$\text{(Newtonian case), case, } S = \frac{\eta_{max} H^2}{\eta_{min} R^2} \qquad (2)$$

where η_{max} is the viscosity in the center region, η_{min} is the viscosity near the walls, H is the wall separation (charge thickness) and R is the radius of the charge. When S is small relative to unity, the maximum velocity occurs at mid-plane; and when S is large relative to unity, the maximum velocity occurs near the walls. This was developed for homogeneous fluids and, although viscoelasticity and the anisotropy existing for SMC will complicate the relationship, the behavior is expected to be qualitatively similar.

To treat the complexities of non-Newtonian squeeze flow, especially for anisotropic materials under nonisothermal and curing conditions, it is necessary to develop numerical techniques, and the flow problem must be solved iteratively on a computer. This analytical approach is being applied at at least two laboratories (21, 23) and accurate descriptions of the flow of SMC can probably be expected in the near future. Of course, besides the development of numerical techniques, parallel development of constitutive relations for SMC through experimental work must also take place. Quantitatively identifying the shear viscosity and the elongational viscosities as functions of temperature promises to be a major challenge.

When actual components are molded, the flow becomes even more complicated. Vertical walls adjacent to horizontal areas cause some regions to close at different rates than others. This will result in the jetting of some material past slower material. The region of shear that will occur between the two regions will cause a high degree of fiber orientation and a pseudo-knit line (13) will form. At this time, molders of SMC can only be aware of this situation and try to compensate for it in tool design. The ongoing development of numerical techniques, however, promises to model even this behavior.

The modeling of compression molding is not simply an academic challenge. Besides revealing phenomena that we may not even recognize other than erratic quality in the manufacturing environment, modeling will provide the tool to develop improved materials and processing techniques for better quality and higher productivity.

SURFACE DEFECTS

Molded SMC plaques or parts are subject to a wide variety of surface defects, which deteriorate the appearance of visible components and which are costly to repair. A catalog of some of these defects, whose origins are poorly understood, are listed in *Table 2.*

Of these, porosity is perhaps the most serious problem encountered by molders. These may be disclosed as voids or pits in the as-molded part but often appear to be sub-surface voids concealed by a thin skin and are re-

Table 2. Classification of surface defects.

Defect	Possible Contributing Factors	Reference
pinhole or pimple	coarse particles; particle agglomeration	(19)
long-range waviness or ripple	resin shrinkage; glass distribution	(19)
craters	poor zinc stearate dispersion	(19)
sink marks over ribs	fiber orientation; fiber length; filler loading; resin shrink	(19)
surface smoothness, show-through; short term waviness	resin shrinkage; fiber sizing (soluble vs. insoluble); strand dimensions; variations in glass concentration	(19)
porosity and voids leading to "volcano-like" defects or pop-up blisters in painted parts	surface or sub-surface voids due to trapped gases; flow and rheology during molding	(19, 24, 25)
dark areas leading to roughness and paint defects similar to above	styrene loss from the surface	(25)

vealed as defects as described in the *Table* only after painting and exposure to high temperature bake ovens.

Microscopic and infrared studies carried out by Cheaver (24) and by Pilkington Brothers Company as reported by Burns (19) indicate a complex surface morphology and composition gradient. Thus, what is postulated is:

- skin layer—2 μm thickness;
- surface layer rich in fine $CaCO_3$ particles—25 μm;
- subsurface layer of coarser $CaCO_3$ particles and agglomerates, deficient in glass—100 μm;
- layer rich in glass fibers—100 μm; and
- alternating layers of glass and $CaCO_3$, which make up the bulk of the composite.

Accompanying the above noted layering effect, it has been observed that a sharp gradient of low-profile additive and resin exists for several hundred micrometers below the surface with the maximum concentration of these constituents occurring at the surface. This is not surprising in light of the tendency of glass bundles to be excluded from the first 125 μm of the outer layer.

It is our impression that porosity and void regions may penetrate deeply into the thickness of the layer structure mentioned above and may, in fact, be visually estimated to be of the order of 100 to 1000 μm. (See also Cheever (24). Therefore, no clear relation has as ye. been established between surface composition and morphology and the occurrence of porosity.

Burns reports that the outermost skin layer is nonporous and, as mentioned previously, rich in resin and low profile additive. Under ideal conditions, this thin skin covers the porous layers below and functions as a sealing coat. Under turbulent flow conditions, however, this skin formation is disrupted, providing an opportunity for subsequent expansion of gases which erupt through the paint layer. In favor of this concept, it is generally acknowledged that a number of factors affecting flow do influence the frequency of occurrence of porosity, e.g., material rheology, flow path, thermal history, and material placement in the mold.

The likelihood that porosity can be attributed to styrene monomer is small in light of the fact that the styrene is well below its boiling point at typical molding temperatures (300°F) and pressures (nominally 100 atmospheres).

SMC sheet normally contains a substantial void content prior to molding which may be introduced at a number of stages in the process:

(a) mechanical mixing of polyester, styrene monomer and filler (SMC paste);
(b) incomplete wet-out of multi-filament strands of glass leaving voids;
(c) impregnation of the glass layer by the resin phase from both sides, which may trap air at the center of the SMC sheet as well as in the glass-fiber bundles;
(d) air trapped between stacked layers of sheet in the press prior to molding; and
(e) air trapped in the closed mold.

In our laboratory, Himebaugh and Newman (26) have attempted to measure the average void content at certain points of the process. Their methods have been based on (a) dissolution of uncured materials in methylene chloride and measurement of the volume of released air, and (b) expansion of trapped air in SMC sheet under vacuum. Some typical results are shown in *Table 3*.

It is evident that a substantial amount of air is, in fact, in the material prior to press closure. Some of this air must be trapped in the molded article; and, during primer and/or paint cure, expansion release of these gases at elevated temperatures (when the surface layers of the polymer composite are considerably softened) is not, therefore, unexpected. These methods, unfortunately, do not account for the void content near the surface, nor do they indicate the amount of air released and vented during fill-out of the mold. Nevertheless, it does suggest a source of expanding gases. It is acknowledged that voids or porous regions may also trap condensed vapors from solvents used in the primers. This mechanism is, however, also associated with void regions at the surface. It remains to establish a correlation of void content with defect frequency in painted parts. Two approaches for reducing the porosity problem may be envisioned: (a) reduction in the amount of trapped air; (b) control of the rheology so that air is consistently eliminated from the molding compound during flow and/or is kept away from the surface to be painted.

Table 3. Typical values of void content of SMC materials.

Material	Air content (ml/100g)
SMC paste	0-2
SMC sheet	5-15

REFERENCES

1. T. Watanabe and M. Yasuda, *Composites*, **13**, 54 and 59 (1982).
2. P. K. Mallick and N. Raghupathi, *Polym. Eng. Sci.*, **19**, 774 (1975).
3. M. R. Panter, SPI, 36th Annual Conference Reinforced Plastics/Composites Institute, **16F**, (Feb. 1981).
4. S. H. McGee, *Polym. Eng. Sci.*, **22**, 484 (1982).
5. A. J. Rojas, J. Borrajo and R. R. J. Williams, *Polym. Eng. Sci.*, **21**, 1122 (1981).
6. L. J. Lee, *Polym. Eng. Sci.*, **21**, 483 (1981).
7. E. A. Herman, SPI, 33rd Annual Conference Reinforced Plastics/Composites Institute, **14F**, (1978).
8. M. R. Barone and D. A. Caulk, *Polym. Eng. Sci.*, **21**, 1139 (1981).
9. L. Marker and B. Ford, SPI, 32nd Annual Technical Reinforced Plastics/Composites Institute, **16E**, (1977).
10. E. Alfthane, A. de Ruvo, and M. Ridgahl, *Int. J. Polym. Mater.*, **7**, 163 (1979).
11. C. H. Browning, priv. commun.
12. M. Rigdahl, *Int. J. Polym. Mater.*, **5**, 43 (1976).
13. M. J. Owen, D. H. Thomas, and M. S. Found, SPI, 33rd Annual Conference Reinforced Plastics/Composites Institute, **20B** (1978).
14. R. J. Silva-Nieto, B. C. Fisher, and A. W. Birkey, SPI, 34th Annual Conference Reinforced Plastics/Composites Institute, **7B** (1979)
15. G. Menges and H. Derek, 36th Annual Conference Reinforced Plastics/Composites Institute, **23C** (1981).
16. R. J. Silva-Nieto, B. C. Fisher, and A. W. Birley, *Polym. Eng. Sci.*, **21**, 499 (1981).
17. L. J. Lee, L. F. Marker and R. M. Griffith, *Polym. Compos.*, **2**, 209 (1981).
18. S. J. Lee, Ph.D. Thesis, Department of Chemical Engineering, University of Delaware, 1982.
19. R. Burns, "Polyester Molding Compounds," published by Marcel Dekker, Inc., New York, (1982).
20. K. F. Pye, Thesis, Nottingham University, 1967.
21. R. B. Pipes, Center for Composite Materials, University of Delaware, Newark, Delaware, priv. commun.
22. D. L. Denton, SPI, 36th Annual Conference Reinforced Plastics/Composites Institute, **16A** (1981).
23. C. L. Tucker, University of Illinois, Urbana, Illinois, priv. commun.
24. D. Cheever, *J. Coatings Technol.*, **50**, 36 (1978).
25. J. D. Gorsuch, R. M. Griffith and H. Shanoshi, SPI 33rd Annual Technical Conference, **9-F** (1978).
26. D. C. Himebaugh and S. Newman, SPI, 38th Annual Conference, Reinforced Plastics/Composites Institute, **9E**, (1983).

DISCUSSION

H. Ishida: Could you comment on the void content of BMC and TMC materials, where forced mixing is used. Also, could you discuss any recent advances in the thickening mechanism of MgO.

S. Newman: We have not studied BMC, but BMC also experiences these surface defects although probably to a lesser extent. I do not think that there is less air in these compounds, but rather a completely different flow mechanism during molding. Certainly, in blending BMC there are opportunities for incorporating air. TMC, which is made on a roll mill is a completely different material which we have not investigated.

The mechanism of thickening with MgO is quite complex and there is controversy over the exact chemical steps. The initial reaction appears to involve formation of a basic salt from MgO and carboxy functions. Secondary reactions must occur perhaps involving complex formation, however, to account for the large increases in viscosity (molecular weight). People have looked for alternate thickening methods, i.e. crosslinking with diisocyanates. This provides an alternate way of building molecular weight and thickening to the point where one can handle this material conveniently. This system, incidentally, is an example of an interpenetrating network.

S. V. Hoa: I wish to thank you for giving a very interesting overview of the problems. You showed the distribution of strength over whole areas of SMC. How did you measure this?

S. Newman: One can be simple minded about this; take a large part and cut it up into many small specimens lying in different directions at various locations. If you do this patiently, you can map out the strength contours of parts even of complex shape.

S. H. Hoa: How large were your specimens?

S. Newman: Part configuration often dictates small specimens. The resulting accuracy of the measurements may suffer somewhat, but property difference from one location to another are often so gross in regard to strength properties that even when the accuracy is poor we can still achieve good strength mapping. Strength is more sensitive to orientation and defects than is the modulus.

S. V. Hoa: Probably you can assume that properties from one sheet to another do not vary too much. In this way, you could cut up several sheets or parts and generate a statistically valid map.

S. Newman: Well, yes. But this is generally not necessary. You may have a sufficiently large area, so that if specimens are cut very closely to each other you can get a statistically valid representation from one single sheet or part.

J. M. Charrier: You talked about local strength measurements, but since the fibers are quite large this means that some may be chopped, some kept.

S. Newman: Yes, this may be a problem. If the fiber is 2.5 to 5 cm long and the specimen is shorter, then your results may be not representative. However, do not forget that in these specimens the fibers are planar. You do not have fibers lying up and down. So, if you cut samples 5 to 7 (cm) long, I do not think that you will run into much of a problem. Obviously, if the fiber is laying transverse to the long direction, you will be cutting it, but I do not think that this introduces a gross error in the measurements. You see, if the fiber is transverse, it does not contribute to strength very much, anyhow.

Actually, one of the biggest factors affecting the strength statistics is variation in glass concentration and the domain size for these variations. These domains appear to be on the order of 2 cm in diameter and so are large with respect to the sample size. This leads to a pronounced sample size effect that will be reflected on both the mean and deviation. The statistical theory to describe this has not been developed, so it is important to maintain constant sample size in the mapping.

M. R. Kamal: Knowing that your problems, defects, are related to entrapped air, what kind of ways can one devise to overcome this?

S. Newman: Well, I did mention that you can degas the paste. This provides some improvement but not much. There are other techniques for eliminating air during the process, e.g. by controlling the placement of the charge and resultant flow of the material. We are working in the direction of removing air from the sheet material but, I am sorry, this information is proprietary.

M. R. Kamal: I was wondering if you referred to the fact that for BMC and TMC you have to maximize the flow before curing of the surface film occurs. Probably temperature programming would greatly help.

S. Newman: Yes, this is one way.

GENERAL DISCUSSION

L. A. Utracki: Traditionally, at the end of each mini-symposium, we have a general discussion during which we would like to hear, as an *ad hoc* panel of experts, your views on plastics composites regarding: (i) the future areas of research and development, (ii) the role of our Institute, and on (iii) organization of the symposia. Also, this is the time to put the last unasked questions to the authors and a period for free comments and ideas.

S. Newman: Do you have problems getting speakers from the industry?

L. A. Utracki: Yes, very much so. A lot of commercial development is considered by the companies as proprietary information. It is very, very difficult to get speakers from the industry.

S. Newman: Frequently, the talk you would like to give to present a coherent story, you are not allowed to talk about. It has an inhibiting, debilitating effect. The only subject you can touch is an old work which still may be of interest to the general public. One just cannot talk about the current developments.

L. A. Utracki: This is another example of the chicken and the egg. Our Institute was created to help industry. We cannot do this if we do not know the methodology, the problems and the solutions the industry is looking for. If industry is unwilling to divulge this information, publicly, or not, we are in a very difficult position.

S. Newman: Maybe the way to do it is to talk through layers. Anything which comes out from large companies in the US has to pass through the legal staff. You cannot believe how complex the situation becomes. One has to deal with legally oriented people who have very little technical knowledge. What seems trivial and obvious to us may be considered of utmost importance to them. It is a very serious, practical problem in the industry.

E. B. Bagley: One method to overcome the isolation, accessible to government-sponsored institutes, is to build a basic research program which will be of interest to industry. Once you establish the expertise in an area a major part of your trouble is over. If you demonstrate that you can solve general problems in a given field (such as Halpin-Tsai equations which deal with the general science of composites), as opposite to techniques of manufacturing, you may start getting more industrial participation.

S. Newman: It is very important to involve industrial people in your work. In that way, problems will emerge and you will develop an interesting line of research, which otherwise you may never embark on. It is very important for all: universities, industry, and other research institutions, to interact as much as possible. It is important to talk as we have today. Various groups of people will become aware of the mutual problems, lines of interest and research. This has been an extremely stimulating meeting for everyone. Industrial researchers must keep abreast of academic developments in order to stay ahead of competition. They have to utilize and interpret the general information in their commercial environment. I have always felt that this interaction is fundamental for the health of both science and industry. It must go on in spite of all hurdles which we encounter. You have to insist, pursue this work.

R. Simha: We, from universities, would like to collaborate with industry; we do it, but we also need some help from industry, both intellectual and financial.

L. A. Utracki: Here, at the Institute, we are not concerned with the latter part, but we need more than a general direction in our work. To respond to Ed's comment, I think that the basic research as per your example may be more appropriate for the academic institution. We have the advantage over the universities of having full financial support and also rather well-equipped research and processing laboratories. We do not want to compete with academics and be limited to the basic general science. We would like, rather, to fill the gap between the academic and industrial lines of work. We want to go beyond fundamental development.

H. Ishida: This is a very old problem. Even if the industrial leaders are reluctant to talk about their work to the general public, frequently they are willing to do so in private, to academics with an established reputation. I have some experience in this area. One has to develop a certain expertise and see where the interests meet.

E. B. Bagley: One area which may be of interest is a well-instrumented processing laboratory. Many companies do not have the facility where the process can be adequately characterized. Now, there are big variations from one company to another. I am doing some work in this field on food rheology. There are a lot of problems in extrusion of food materials/instability of flow, reversal of output with screw speed, etc. If you go to many food companies, they dump stuff at one end of an extruder and collect at another without any idea what the pressure drops are, what type of flow they have in the die, and so on. People are trying to model this with thermoplastics flow equations, which does not make any sense at all. They do not have even remotely similar types of flow; they are trying to answer the wrong questions. The same occurs in other plastics processing areas. I have been appalled to see that even nowadays major plastics companies write their specifications in terms of melt index; later they are surprised to get funny results.

S. Newman: I accept your criticism. It is very valid. In fact, many companies have, for a long term, gotten along with astonishingly little knowledge of what they are doing. The need to develop this knowledge emerges when they get into a crisis. Then it is too late, they have neither time nor money to spend. This is disheartening to me, but we have to admit that a vast portion of industry is built on very little scientific knowledge but rather on entreprenerial initiative and empirical know-how.

R. Gauvin: I would like to hear some comments as to why it is frequently difficult not only to get speakers

from the industry, but also to have persons from industry participate in a meeting.

S. Newman: I do not think that this is true. There are many people who do appear. We have a number of industrial people right here: Lloyd Goettler, George Hawley, myself, and many others. You have to recognize the fact that many, many companies do not have people with the level of intellectual experience and academic training anywhere near as advanced as in academia. You are dealing with people having a different educational background, with people who may not appreciate what is being said, who will not know how to utilize the available information. I think that there is a serious lack of concern in our industry for the basic understanding. This has to be improved.

E. G. Bagley: I would like to add a couple of comments. I agree with you 100 percent. In many cases you can make things work in industry without even knowing why. I have done this myself. However, when the trouble starts, the problem is being solved over and over again, even in the same company. I saw this happen when I was consulting as a professor of Washington University. Frequently, the solution was difficult, expensive and each new division, each new material may have required that the same solution be re-invented.

S. Newman: I agree with you wholeheartedly. They failed to build their experience on a solid foundation and pay the price of inefficiency. Absolutely true.

V. G. Zboril: We are a small company by comparison with yours. We have, let us say, 50 graduates in research, who go on a project, solve the problem or not, and go off to do something else; these people do not have time to develop long-term expertise. They mostly rely on what they read in the literature, what is being done at the universities. You may not like to hear it, but I do not think that the universities are doing a good job in communicating. If you try to go into a new field by reading the papers, you will go gray first. The articles are not self-contained; there are chains of back references for many years. There are no up-to-date books, or monographs on plastics. I still admire writings of people like Ziegler or Flory—not too many of these today. The science is getting so specialized, so difficult to wade through, especially when one is urgently looking for some specific information. At Du Pont Canada, we try to invite speakers, two to three speakers a year, from very different fields, to talk to as wide a research audience as possible. We hope that in this way we may initiate more contacts.

S. Newman: Listening to the presentations today it seems that your approach is more from the phys-chem point of view. Only one paper, by D. McCammond, tried to rationalize the mechanical properties of the finished product. There has been very little discussion on mechnical properties of composites, on fatigue behavior, long-term performance, and so on. The whole area of these properties may become a focal point for a subsequent meeting.

M. R. Kamal: As a Canadian government laboratory you must ask yourself a question: what should be the priority subject for research in the composite field? Today the majority of contributions were on mica-filled systems, with a substantial emphasis on flow and processing. The question arises: are these the most pressing Canadian priorities in the composites field? The second comment, and I have to be defensive: Robert said the academics have limited resources and other duties besides industrial research. We have to teach and do more fundamental research; to advance the general knowledge, not necessarily to solve today's problems. Probably we should balance this, and some of our colleagues start earning their living by doing this. In answer to some of Seymor's comments, I must say that at McGill we are doing what he suggested. The industrial problems are quite familiar to us. For example, we are working extensively on cure kinetics, on flow and molding of thermosets. These are very complex, long-term, difficult systems for an academic to get into, but with the right cooperation and help from industry we are doing this, and like it. We spent some years cooperating with Du Pont Canada on the injection molding of thermoplastics, and similarly the experience was rewarding for them and ourselves. Right now we are trying to develop an integral model which will predict, on the basis of fiber-filled feed properties, the behavior of the finished articles. The companies never tackle these problems in their fundamental content, but rather try to solve a pressing need. However, if you do want to solve the general problem, it may require 100 to 200 man-years to solve it in a respectable way. To finish, I would like to go back to the first question and hear what are the important areas of research in the composite field which you feel IMRI should be involved in.

L. A. Utracki: First of all, let me respond to some of the comments. We received about 120 registrations for this symposium. Because of space limitations, we assigned only one place per organization. On the final approved list of 50 participants present in this room there are 22 attendees from industry. In addition, we have another group of people listening and watching the proceedings via a close-circuit TV system. I do not know how many of them are from industry. In short, we do have about 50 percent of the audience from industry, the rest being academics and governmental institutions including our own research staff. I do not think that it is difficult to attract the industrial audience; the problem is to secure the industrial speakers. This is the 6th symposium we have organized and getting industrial speakers has always been difficult. The prime goal for these meetings is to bring together people from industry, academia, and the governmental organizations, to break down the isolation which Mr. Zboril was complaining about, to provide an opportunity for direct contacts, to help us to learn where the expertise is in the three basic areas of the future industrial developments: polymer composites, polymer blends, and mathematical modeling. Finally, I would like to say that mica is one of the Canadian "specialties." This is why today, as well as a year ago, about one-half of presentations were on mica-filled plastics. It is true that today only Derek McCammond discussed the mechanical properties of composites; this was only to compensate for last year's concentration on

the subject. Unfortunately, the emphasis during each of these meetings cannot be very evenly distributed. On the other hand, the opposite approach: to focus on one single area of composites during each symposium also does not seem to be right. We have been trying to provide the audience with a cross-section of advances in the basic pertinent areas, starting with the thermodynamics, through flow rheology, processing, properties of the product, to some problems in economics. We can discuss the basic philosophy of these meetings, but so far we have attempted to provide the audience with a review of both the fundamental and the practical aspects of blends, composites or mathematical modeling. The narrow topics will bring the specialists to discuss the subject in their own language. We want to educate, to cross-pollinate the audience, to provide a more balanced view thatn one can obtain either by reading, or by participating in a big meeting with dozens of non-coordinated voluntary contributions. Finally, I would like to say that the discussion on the interactions between various research groups is very appropriate. However, as you remember, the debate started with a rather innocent question by Seymor Newman as to whether we have problems getting industrial speakers. We talked about audience; if you go to any large meeting, of the ACS, SPE, AIChE, etc., the majority of the audience is from industry, but frequently all the speakers are from academia. The audience is passive; they come to listen, especially to papers of a more direct industrial aspect, listen and depart to another room, another talk, like a flock of mute birds. To get speakers from industry is very difficult for all the reasons mentioned before and for some others as well. If you have any idea how we can bring more of them to these meetings, if you can help us to achieve this goal, it will be greatly appreciated.

G. C. Hawley: I find it very satisfying that at IMRI some work on mica-filled systems is being done. Mica in plastics began as a Canadian venture. It still relies heavily on the Canadian source of the material, which is very unique. A lot of work had been done around the world to use muscovite, which is a more common type of mica, as a replacement for phlogopite. So far there has been very little success in this direction. The Canadian phlogopite is rather unusual; it fortuitously delaminates very easily, therefore at low cost. I think that Ford's experience shows that it outperforms other materials.

S. Newman: During the course of this meeting we talked about a lot of advantages of mica. The fact that it is a very stiff platelet, with the modulus of about 25,000,000 psi, the fact that potentially it is a very efficient (with the right kind of coupling agent) additive giving a high modulus material. As a consequence of this high modulus, you will get high heat-distortion temperature, high yield stresses, and high stiffness. However, I do want to caution you, that the mica is very brittle. This dificiency, along with the fact that in some blends with polyolefins (especially polypropylene) some kinds of mica have a very poor adhesion, that there are severe problems with painting and finishing the mica composites imposes a severe limitation to the applications of mica. If some of these problems are resolved you will see much more intensive use of this filler.

G. C. Hawley: This is true, and that is why I would like to see more research being done at IMRI. There are problems with mica, e.g., the impact resistance is a severe limitation, surface smoothness may be another. These problems can be solved. In Quebec, we have the dying asbestos industry. There is a possibility to replace it with the mica industry, on a job-creating basis. I would like to see work done on systems with other polymers, of which we may have glut: PVC and LLDPE. There are a lot of problems to be solved. Many of these are rheological in nature. This is why I am so pleased to see IMRI being active in this area. If you look where mica is being used, you see today that mica is being excluded from the large market which cannot tolerate a porous or rough surface. This means that it is excluded for pipes, profiles, siding, and so on. Currently, the only way to overcome these difficulties is to post-form or finish the extrudates. This is an expensive proposition. Solving the surface finish problem could open a very large market. Again I think that this would be a very good area for IMRI to get involved in. Not all the problems associated with mica can be solved; some are inherent. A lot of problems have been very successfully dealt with at Ford, using an inexpensive coupling agent. Mica has a tremendous potential as a reinforcing agent. To realize this potential, a lot of good research must still be done.

S. V. Hoa: There is no question that IMRI should do work on mica, but not only on it. I would like to reinforce what S. Newman said about a need for research on mechanical properties of composites. Some of the companies in Canada do work in this field but from the user point of view. I think that there is a need to approach this from the manufacturer point of view—to produce the material with the desired mechanical performance. A lot of potential improvement for the aerospace and aviation industries, or even for the manufacturers of the corrosion-resistant vessels, can be achieved by tailoring, for example, the coefficient of thermal expansion, the low frequency dumping, the abrasion, and others.

R. Gauvin: We had numerous discussions with people from the aeronautics industry where, in most cases, epoxy with carbon-fiber composites is being used. As a result, we decided to start our activity on glass fiber-reinforced thermoset polyesters. We will try to correlate mechanical properties with the manufacturing process. We will work on resin transfer molding, later on using more complex methods of manufacturing pipes and cylinders. For the time being we have decided to stay out of high-performance composites, since there is a lot of effort being made at the universities and in the local aerospace industry. Also we do plan to use mica in resin transfer molding and RRIM technologies in the near future.

L. A. Utracki: The problem of processing desired mechanical properties is related to flow and flow-affected morphology. While in some cases the morphology in gross terms can be *a priori* imposed, namely by long-

fiber composites, in most plastics-processing operations like extrusion or injection molding it is very complex and extremely difficult to predict. In fact, the only way we can approach this problem is by mathematical modeling and computer simulation. As you know, this is another area of our activities which will be reviewed during the forthcoming mini-symposium on February 8, 1984. I invite you all to participate. With this I want to thank the speakers and the participants for this stimulating and fruitful meeting.

Call for Papers:

COMPOSITES: MATERIALS AND ENGINEERING

GENERAL INFORMATION

The International Symposium in Composites: Materials and Engineering is being held in conjunction with a celebration marking the founding of the Center for Composite Materials in 1974. The symposium will be held at the John M. Clayton Conference Center of the University of Delaware, Newark, Delaware starting Monday, September 24 and continuing through Friday, September 28, 1984. The meeting will be open to all interested persons. The Symposium will consist of keynote addresses from invited speakers, contributed papers, and poster sessions.

Dr. Anthony Kelly, Vice Chancellor, University Surrey (U.K.) and Professor Arthur B. Metzner, Department of Chemical Engineering, University of Delaware, (U.S.A.) are cochairmen of the organizing committee. Papers may be sent to: William Dick, 201 Spencer Laboratory, University of Delaware, Newark, DE 19716. Deadline for paper submission is February 1, 1984.

TECHNICAL PROGRAM

A balanced program of invited papers, contributed papers, and poster sessions will be presented. Contributed papers and poster sessions are requested in areas relevant to composite materials and engineering. Areas of particular interest include:

- Materials Modeling
- Computer-aided Design Techniques
- Processing Science and Technology
- Mechanical and Microstructural Characterization
- Durability
- Nondestructive Evaluation

INFORMATION FOR AUTHORS

Submission of original and review articles is encouraged. There is no limit on length. Three copies of the manuscript should be submitted, which should be typed, one side only, double space, with at least a 1-inch margin. Submission will be taken to imply that the paper has not been previously published, that it is not being considered elsewhere for publication, and that if accepted it will not be published elsewhere in the same form, in any language, without the consent of the editor or publisher. Authors must agree to transfer copyright to the publisher when an article is accepted for publication. Unless notified to the contrary by the authors, the publisher assumes that the act of submitting the article signifies the author's agreement to such copyright transfer to the publisher. The journal carries a voluntary page charge. Each manuscript should include:

A separate title page, headed by a concise, meaningful title (avoid abbreviations) for the paper. This page should provide:

- The name and affiliations of each contributing author at the time the paper was prepared.
- Indicate by asterisk any changes of address for each author since article preparation.
- Acknowledgment of any prior oral presentation and original source of the material.

A separate abstract page, consisting of a single paragraph of 100-200 words to include the title and the names and addresses of the authors. Define any abbreviations for substances or methods (such as ABS, SAXS, etc.).

A list of references, on a separate page at the end of the text, numbered in order of text citation. The references are to be abbreviated in the form used in Chemical Abstracts using the names of all authors preceded by initials; see Bibliographic Guide for Editors and Authors, American Chemical Society, Washington, D.C.

- Within the text, the reference citations are typed in parentheses in line with the main copy (no superscripts or subscripts), thus:

  According to Young, et al. (1) . . .

- In the list of references the general style is as follows:

For periodicals:

1. S. S. Young, J. L. White, E. S. Clark and Y. Oyanogi, Polym. Eng. Sci., 20, 798 (1980).

The journal name and volume are to be underlined and the year is placed in brackets. The issue number is given only when needed for identification. The article name is eliminated unless the reference is unclear without it.

For books: The title to be spelled out in full.

5. H.-G. Elias, "Macromolecules," Ch. 1, Vol. 2, Plenum Press, New York (1977). (Include the state when the city is not identifiable.)

A list of nomenclature, identifying symbols and abbreviations, commonly desirable at the end of the text. Footnotes are to be avoided.

Equations, numbered and typed in the appropriate place in the text. Where symbols cannot be typed, write them neatly in ink.

Tables, each typed on a separate page, with a heading, and numbered with arabic numerals that correspond to the order in which they are cited in the text. The tables should be inserted in the manuscript after the references and before the figures.

Figures, assembled at the end of the manuscript and preceded by a typed list of captions that explain them. Please also supply a set of original figures or sharp glossy photos thereof, on 8½ × 11 paper or attached to sheets of this size, one sheet for each figure. Each should be identified on the front edge or on the back (photographs) with the name of the first author and the figure number (e.g., Smith, Fig. 1). Originals are to be prepared with high contrast India ink and to bear uniformly stencilled notations. Line drawings and photos should be of a quality suitable for good photographic reproduction and retained legibility upon size reduction to one quarter. Manuscript transmittal letter should indicate if the figures need be returned.

Send manuscripts to:
Roger S. Porter, Editor
POLYMER COMPOSITES
c/o Polymer Science & Engineering
University of Massachusetts
Amherst, Massachusetts 01003

For information concerning publication dates page charges and reprint orders contact:
Editorial Department
Society of Plastics Engineers
14 Fairfield Drive
Brookfield Center, Connecticut 06805